CANADIAN THESES ON MICROFICHE

THÈSES CANADIENNES SUR MICROFICHE

National Library of Canada
Collections Development Branch

Canadian Theses on
Microfiche Service

Ottawa, Canada
K1A 0N4

Bibliothèque nationale du Canada
Direction du développement des collections

Service des thèses canadiennes
sur microfiche

NOTICE

The quality of this microfiche is heavily dependent upon the quality of the original thesis submitted for microfilming. Every effort has been made to ensure the highest quality of reproduction possible.

If pages are missing, contact the university which granted the degree.

Some pages may have indistinct print especially if the original pages were typed with a poor typewriter ribbon or if the university sent us an inferior photocopy.

Previously copyrighted materials (journal articles, published tests, etc.) are not filmed.

Reproduction in full or in part of this film is governed by the Canadian Copyright Act, R.S.C. 1970, c. C-30. Please read the authorization forms which accompany this thesis.

AVIS

La qualité de cette microfiche dépend grandement de la qualité de la thèse soumise au microfilmage. Nous avons tout fait pour assurer une qualité supérieure de reproduction.

S'il manque des pages, veuillez communiquer avec l'université qui a conféré le grade.

La qualité d'impression de certaines pages peut laisser à désirer, surtout si les pages originales ont été dactylographiées à l'aide d'un ruban usé ou si l'université nous a fait parvenir une photocopie de qualité inférieure.

Les documents qui font déjà l'objet d'un droit d'auteur (articles de revue, examens publiés, etc.) ne sont pas microfilmés.

La reproduction, même partielle, de ce microfilm est soumise à la Loi canadienne sur le droit d'auteur, SRC 1970, c. C-30. Veuillez prendre connaissance des formules d'autorisation qui accompagnent cette thèse.

THIS DISSERTATION
HAS BEEN MICROFILMED
EXACTLY AS RECEIVED

LA THÈSE A ÉTÉ
MICROFILMÉE TELLE QUE
NOUS L'AVONS REÇUE

Canada

NL 339 (r. 85/09)

TOWARDS A TURBULENCE MODEL FOR INDUSTRIAL HEAT EXCHANGER FLOWS

by

ARTHUR GORDON LAWRENCE HOLLOWAY

A thesis presented to the
University of Ottawa in partial
fulfillment of the requirements
for the degree of
MASTER OF APPLIED SCIENCE

in

MECHANICAL ENGINEERING

Ottawa, Ontario, 1984

UNIVERSITÉ D'OTTAWA
UNIVERSITY OF OTTAWA

Abstract

The equations governing turbulent flow in industrial heat exchangers are derived in detail. Simplified forms of these are derived separately for the tube-free, the near wall and the tube-filled regions. Three simplifications of the second-order turbulence model are used in the tube-free region, while a wall function method is used near the wall and the porous media approach is applied to the tube-filled region. Computations based on these models are tested versus experimental results in nearly homogeneous shear flow, two-dimensional channel flow, two-dimensional tube filled channel flow and recirculating flow.

ACKNOWLEDGEMENTS

I would like to thank Professor Stavros Tavoularis for his supervision, thorough editing and criticism of my dissertation. It has contributed immensely to its quality.

Special thanks are due to Liberato Carlucci with whom I had many valuable discussions and who lent needed support to my work.

The financial support provided by Atomic Energy of Canada through a University of Ottawa/Chalk River Nuclear Laboratories Fellowship has been very much appreciated.

Finally, I must thank my wife Patti for her understanding over the past two years.

NOMENCLATURE

$c_{(i)}$	i = 1, 20; μ, ℓ empirical constants for the turbulence model
$C_{(P)}$	specific heat at constant pressure
$C_{(T)}$	specific heat at constant temperature
C_{ij}	mean material derivative of Reynolds stress
C_i	mean material drivative of turbulent heat flux
$C_{(k)}$	mean material derivative of turbulent kinetic energy
$C_{(\epsilon)}$	mean material derivative of viscous dissipation rate
$C_{(g)}$	mean material derivative of mean square temperature fluctuation
D_{ij}	diffusion of Reynolds stress
D_i	diffusion of turbulent heat flux
$D_{(k)}$	diffusion of turbulent kinetic energy
$D_{(\epsilon)}$	diffusion of viscous dissipation rate
$D_{(g)}$	diffusion of mean square temperature fluctuation
e	specific internal energy
$F_{(1)i}$	force of the tubes on the fluid
$F_{(2)}$	heat flux from the tubes
$F_{(3)}$	production of turbulence by the tubes
g_i	gravitational acceleration
g	mean square temperature fluctuation
G_{ij}	buoyant generation of Reynolds stress
G_i	buoyant generation of turbulent heat flux

$G_{(k)}$	buoyant generation of turbulent kinetic energy
$G_{(\epsilon)}$	buoyant generation of viscous dissipation
$G_{(g)}$	buoyant generation of mean square temperature fluctuation
h	specific enthalpy
	irreversible work effects on the turbulent heat flux
$J_{(g)}$	irreversible work effects on the mean square temperature fluctuation
k	$\frac{1}{2}\overline{u_i u_i}$ mean turbulent kinetic energy
K_{ij}	$\overline{u_i u_j}/2k$ non-dimensional Reynolds stress tensor
l	$k^{c_{(l)}}/\epsilon_{(k)}$
L	integral length scale
m	dynamic viscosity fluctuation
n_i	unit area outward normal vector
P	thermodynamic pressure
p	pressure fluctuation
P_{ij}	shear production of Reynolds stress
P_i	gradient production of turbulent heat flux
$P_{(k)}$	shear production of turbulent kinetic energy
$P_{(\epsilon)}$	shear production of viscous dissipation
$P_{(g)}$	gradient production of mean square temperature fluctuation
$q_{(w)}$	heat flux to the wall
r	density fluctuation
R_i	reversible work effects on turbulent heat flux

$R_{(g)}$	reversible work effects on the mean square temperature
S	surface
$S_{(e)}$	production of viscous dissipation by vortex stretching
S_{ij}	fluid rate
t	time
T	temperature
$u_{(f)}$	wall friction velocity
u_i	velocity fluctuation
$\overline{u_i\theta}$	turbulent heat flux
$\overline{u_iu_j}$	turbulent momentum flux - Reynolds stress
$U_{(c)}$	centerline velocity
U_i	velocity
x_i	spatial position vector
V	volume

Greek Symbols

α	thermal diffusity
$\beta_{(P)}$	fluid thermal expansivity
$\beta_{(T)}$	fluid compressibility
δ_{ij}	Kronecker's delta
Δ	finite difference operator
$\Delta_{(i)}$	partial finite difference operator in the x_i direction
Δ_{ij}	pressure-strain correlation

Δ_i	pressure-fluctuating temperature gradient correlation
ϵ_{ij}	viscous destruction of Reynolds stress
ϵ_i	molecular destruction of the turbulent heat flux
$\epsilon_{(k)}$	viscous dissipation of turbulent kinetic energy
$\epsilon_{(\epsilon)}$	viscous dissipation of viscous dissipation
$\epsilon_{(g)}$	molecular destruction of the mean square temperature fluctuation
ζ	ratio of turbulent to mean time scales
θ	temperature fluctuation
κ	thermal conductivity
μ	dynamic viscosity
ν	kinematic viscosity
$\nu_{(t)}$	kinematic turbulent viscosity
κ_o	thermal conductivity fluctuation
ρ	density
$\tau_{(\omega)}$	wall shear stress
Ω_{ij}	vorticity

Others

γ	dynamic bulk viscosity
γ'	dynamic bulk viscosity fluctuation

Suffixes

$\overline{(\ldots)}$	time or ensemble average
$\underline{(\ldots)}$	volume average
$(\ldots)'$	difference between the variable on the current field and in a stagnant isothermal field
$(\ldots)_{(o)}$	initial value

Notes:

All vector components are rectangular cartesian and the Einstein summation convention is employed unless otherwise stated.

Bracketed indicies indicate that the variable is not a vector and hence the summation convention is not enforced.

Table of Contents

Table of Contents (Cont'd)

Table of Contents (Cont'd)

LIST OF FIGURES

CHAPTER I

INTRODUCTION

1.1 Historical Survey of Turbulence Modeling

The first concise description of the motion of fluids was presented by Euler (1755) who assumed that the velocity and density of a fluid could be treated as continuous field variables and that the acceleration of an elementary fluid volume was due to an internal pressure. This leads to the Euler equations which describe the motion of a fictitious fluid which has no tangential stresses. Such fluids do not exist although certain properties of real fluid flows can sometimes be approximated by those of this ideal fluid. Unfortunately, ideal fluid theory cannot predict tangential drag forces on solid structures, something which prevents the ideal fluid motion from being a completely satisfactory approximation. In addition, ideal fluid motion cannot become turbulent since it is unable to generate the vorticity which characterizes turbulent motions (Kelvin's Thereom).

It was not until the 19th century that a means of calculating the tangential stresses on fluid volumes and rigid boundaries became possible. The theory was first introduced by Navier (1822) and then later rationalized by Stokes and St. Venant (1843 and 1846); it assumes that tangential stresses are functions of the local strain of the fluid and are essentially added to the normal (pressure) stress of the ideal fluid. The result is the so-called Navier-Stokes equation

which is a second order non-linear partial differential equation for which a general solution has yet to be found or proven to exist (Ladyzhenskaya,1963). There have been, however, some solutions based on very restrictive assumptions and applicable to simple flows. The solution for vanishing velocity was in good agreement whith experiments and provided support for the postulated tangential stresses when compared to experimental results (Stokes,1845). Other known solutions include the case where the non-linear convective term may be neglected such as in Couette and Poiseuille flow, both these solutions agree very well to experimental data. All of these solutions describe laminar flows and are no way unique for a given geometry and boundary conditions. When flow is turbulent the Navier-Stokes equations may not be simplified at all, and hence it requires a general solution which is unavailable. Initially it was not obvious that the Navier-Stokes equations could predict turbulent flow because the shear stresses in a turbulent fluid are much greater than in a laminar one. An early hypothesis was that a turbulent fluid could be described by the Navier-Stokes equations if a higher "turbulent viscosity" were introduced (St. Venant, 1843 and Boussinesq, 1877).

Osborn Reynolds (1883) proved experimentally that laminar flows would become unstable and transform to a turbulent flow in a sudden but continuous manner as the ratio of inertial to viscous forces reached a critical value known as the critical Reynolds number. Also during the 19th century, the fact that fluid motion as seen by the naked eye was actually an average behavior of the molecular motion was becoming

recognized. Even laminar flows were mathematically complex although they appeared smooth and well behaved. Osbourne Reynolds (1894) viewed this turbulent motion in direct analogy to molecular motion, suggesting that it could be averaged and its mean behavior regarded as smooth and predictable. To acquire the equations of mean fluid motion he assumed that the Navier-Stokes equations could be applied to turbulent flow, averaged them over arbitrary space and time intervals and then decomposed the velocity and pressure into a mean motion and a turbulent motion, the averaging of the turbulent motion being zero. The result was the Reynolds equations, which were similar to the Navier-Stokes equations, but with an additional internal stress which is a result of the inertial-transfer by the turbulent motion about the mean motion. This is directly analogous to the viscous stress of the Navier Stokes equation which arises from the inertial transfer of the molecular motion about the continous motion. Reynolds equations clearly defined the idea of a turbulent motion and the need for a model of turbulent stress.

The first such models were the already existant ones of St. Venant (1843) and Boussinesq (1877). Boussinesq (1903) also formulated the turbulent equations of heat transport and suggested an isotropic heat diffusivity to relate the turbulent heat flux to the mean temperature gradients (Boussinesq, 1903). This was in direct analogy to the work of Navier and Stokes in their closure of the continuum equations. It was realized that like the molecular viscosity is a function of the local temperature (mean molecular kinetic energy) and mean free path,

the turbulent viscosity must be a function of the local turbulence temperature (mean turbulent kinetic energy) and transport length scale. Such a specification was not known and the turbulent transport coefficients were assumed to be constant.

Theories expressing the turbulent viscosity in terms of the local turbulent motion were developed by Taylor (1915), Prandtl (1925), and Von-Karman (1930) in direct analogy to the gradient transport of the kinetic theory of gases. These were the vorticity transport theory and the mixing length theories respectively. However, unlike the kinetic theory, which allows temperature to be transported, these models assumed that the local turbulence level was determined by the local mean velocity gradient. The models worked well for simple flows, such as mixing layers, where the transport length scale could be specified; but not in more complicated flows. It was recognized that, when the mean field does not vary linearly over considerable distances the gradient transport theory does not apply (Corrsin, 1974; Sreenivousan, Tavoularis and Corrsin, 1982), and that a single transport length scale cannot be defined since turbulent transport is continuous unlike molecular collisions. Taylor (1921) was the first to recognize that the transport length scale idea was not applicable to turbulence and presented a theory of turbulent diffusion, which led to the concept of an integral length scale as an analogy for the mean free path of molecular motion.

It was not until the mid 1920s that the hot wire measuring technique had been developed to a sufficient level of accuracy

e.g., (Taylor, 1935) that the turbulent fluctuations could be measured. The first case which was investigated in a complete way was isotropic turbulence (Taylor, 1935). Unfortunately, turbulent fluctuations are rarely isotropic and the theory of isotropic turbulence has limited practical application. Nevertheless, some very important facts about the statistical structure of the turbulent fluctuations emerged from such studies. Turbulent fluctuations are characterized by many scales, of which the very small scales which are associated with the change of turbulent energy into molecular energy and are nearly isotropic at high Reynolds number (Richardson, 1926; Kolmolgorov, 1941). In addition, the rate at which these small scales dissipate energy is controlled by the large scale turubulent fluctuations (Kolmolgorov, 1941). These facts, combined with the gradient transport assumption for diffusion allowed a closure of the mean turbulent kinetic energy equation which until that time had been prevented by the viscous dissipation term.

The result was the proposition of Kolmogrov (1942) and Prandtl (1945) that there exists an isotropic turbulent viscosity and a transport length scale. Unlike the earlier turbulent viscosity transport models these allowed the mean squared turbulent velocity to be determined not by the local mean velocity deformation but from a transport equation. The model of Prandtl still required that the length be determined by the mean flow geometry and be supplied intuitively. Kolmolgorov's model allowed a transport equation for turbulent frequency which when combined with the mean squared turbulent velocity

allowed the calculation of the local length scale. This was the first 2-equation model of turbulence. Unfortunately, the computational techniques of the 1940s were still insufficient to solve these equation sets for two and three dimensional flow fields and the potential of this method could not be realized.

Chou (1945) was the first to abandon the idea of an isotropic turbulent viscosity and make use of the fact that equations may be formulated for the Reynolds stresses, although it was known since Taylor's investigation of isotropic turbulence (1935) that such equations require knowledge of higher order statistical moments. Chou proposed transport equations for the Reynolds Stress (2nd order moments) and the 3rd order moments while neglecting the 4th order moments, however the resulting set of equations was unsolvable for a general flow.

Rotta (1951) and later Davidov (1960) further explored Chou's initiative but proposed closure of the Reynolds stress equation without a transport equation for the 3rd order moments or statistics involving pressure. These terms were modelled in terms of lower order statistics using the gradient diffusion and the return to isotropy hypotheses with the intuitive hope that this higher level of closure would introduce less error into the mean field solution than would be incurred by modelling Reynolds stresses themselves in this way. Rotta's solution technique was as far ahead of the computing facilities of his time as was Kolmogorov's and as a result the study did not progress at that

time. Following the development of digital computers, two variations on Kolmogorov's two equation solution scheme were put forward by Harlow and Nakayama (1968) and by Spalding (1969). In each study Kolmogorov's turbulent frequency was replaced with a different variable. These were the rate of turbulent kinetic energy dissipation, and the square of the fluctuating vorticity respectively. The development of these models was complete by the mid 1970s and since then, the so called k-ϵ model of Harlow and Nakayama (1968) has received wide application.

The availability of digitial computers also led to renewed interest in the work of Rotta by Daly and Harlow (1970) and Hanjalic and Launder (1972). These investigators performed calculations for simple shear flows using a transport equation for each of Reynold's stresses and the dissipation rate of turbulent kinetic energy and found good predictions for the mean velocity and turbulence statistics even for cases where the isotropic viscosity models had failed. The ability to carry these calculations to more complicated problems is not yet possible although they appear to have better potential than the two equation models.

In 1971 Launder proposed the first of the "Algebraic Stress Models" which retained only the two transport equations for k and ϵ, but eliminated the idea of an isotropic turbulent viscosity. This was done by ignoring the transport terms of Rotta's model and then deriving an algebraic relation for the Reynolds stresses which is based on the balance of its production and destruction terms. The result was essent-ally a two equation model of turbulence with a non-isotropic turbulent viscosity. Even with this crude assumption the method was more

general than the two equation isotropic viscosity method.

Another algebraic stress, non-isotropic viscosity model was introduced by Rodi (1976). This model suggested the transport of the Reynolds Stresses could be eliminated from Rotta's model by assuming that it is proportional to the transport of the turbulent kinetic energy.

The modelling of the turbulent heat transfer equations has also developed in a similar manner.

All of the above models contain constants which must be evaluated by comparison to experimental data. Although the algebraic and Reynolds stress closure models perform better than the two-equation models these constants are not universal as it was hoped and they must be adapted to give correct predictions in different flows. This phenomenological type of turbulence modelling has been pursued more rigourously by Lumley (1969, 1978 and 1980) who has tried to develop mathematically and physically consistent models with greater generality. At present the only turbulence models which may be practically applied to general two and three dimensional flows are the two equation isotropic viscosity models.

The simple and elegant closure of the continuum equation has not been matched in the anologous attempt to close Reynolds equations. Currently the equation set for the turbulent effect on the mean flow is much more complicated than the equations of the mean flow. The differences between the molecular and turbulent fluctuations which are responsible for this failure are the nonisotropy of the fluctuations, and the existence of a transport length scale comparable to the mean

flow dimensions. It seems possible that the original idea of Reynolds was misconceived and that the problem of turbulent motion cannot be solved by direct analogy to the treatment of molecular motions. If a truely practical and general solution technique is to be formulated for turbulent motion it may have to come from an alternative approach, such as the direct numerical solution of the general Navier-Stokes equations. This has been performed for low Reynolds number homogeneous, isotropic turbulent flow by Orszag and Patterson (1972) and, later by several others. However, as the Reynolds number is increased the spread of turbulent scales become so large that their full representation by far exceeds the capacity of todays computers. More attractive approachs are "Large Eddy Simulation" (for a review see Rogallo and Moin, 1984) or "Sub-Grid Scale Modelling" (Deardoff, 1970) where the smallest turbulent scales, which are the most statistically predictable and universal, are modelled while the large scale motions are calculated deterministically from their boundary conditions. The first technique has performed well in simple flows such as a turbulent channel (Moin and Kim, 1982) but required a time dependent solution at 500,000 spatial grid points. Such methods impractical for engineering analyses where the governing constraint is economics.

1.2 Objectives and Scope of the Present Research

Accurate predictions of turbulent flows are essential for the design of heat transfer equipment, since turbulence produces high mixing rates and thin thermal boundary layers. A general solution procedure cannot be the goal of an engineering analysis, at least at

present; instead it would be desirable to develop a technique which may be used with confidence over a somewhat limited range of problems. The present analysis will be focused on the calculation of the shell side flow of shell and tube heat exchangers which require a multidimensional approach.

Currently heat exchanger design is based on very simple techniques such as the Log Mean Temperature Difference method (Rohsenow and Hartnett, 1973). Such calculations require experimental tests to ensure that the assumptions of uniform distribution are satisfied. The goal of a multidimensional calculation proceedure is to allow accurate calculation of overall heat transfer and pressure drop without resorting to an experimental analysis. This would permit the evaluation of new or custom designs before their actual construction. In addition, the local velocity, temperature and pressure provided by such a solution would be valuable for predicting tube vibration, thermal stresses and corrosion or fouling.

Momentum, heat and passive contaminants are transported in turbulent flow by mean convection, molecular diffusion and turbulent diffusion in addition to sources and sinks. All of these mechanisms may be important in some flows, but in many cases some can be neglected. The objective of this investigation is to determine what methods could and should be used in calculating flows where turbulent transport is important. Rather than try to prescribe a method which is valid everywhere in the heat exchanger, the practical approach of separating the geometry into three different regions, which are treated separately, has been chosen.

These regions are the near-wall ,the tube-free and the tube filled regions. Isothermal versions of each examined turbulence model are chosen for each of these regions and their predictions of momentum transport in simple flows are compared to experimental results.

As a means of evaluating the turbulence models for the tube-free region, calculations were performed in uniformly sheared turbulence, a two-dimensional channel flow and a fully recirculating confined flow. The uniformly sheared turbulence was selected because it emphasizes the important relation betwen mean shear and turbulent shear stress. The two-dimensional channel flow is also a shear flow, but one in which diffusion is important. The recirculating confined flow represents a test where the mean streamlines undergo significant variations of curvature, and hence, tests a turbulence models sensitivity to inertial effects. The two-dimensional channel also provided a considerable test for the near wall turbulence models because of the importance of the wall shear stress. As a basis of evaluating the turbulence model for the tube-filled region a two-dimensional tube-filled channel was selected. This flow has a near uniform volume averaged velocity profile which allowed careful evaluation of the turbulent kinetic energy production by the tubes.

These tests have exposed the relative merits of each of the proposed models and served as a base of experience for their predictive capability.

CHAPTER II

MATHEMATICAL DESCRIPTION OF TURBULENT FLOW

2.1 Instantaneous Field Equations

The instantaneous field variables such as velocity, temperature and pressure vary in time and space at rates ranging from the very large to the very small. The small scales are still orders of magnitude larger than those on which molecular motions occur. Therefore, the turbulence phenomenon is sufficiently uncorrelated with molecular motions that the continuum equations describe it accurately.

The most common heat transfer mediums used in industrial heat exchange equipment are Newtonian fluids such as air and water. For this reason and for simplicity, the analysis will be restricted to an Eulerian description of Newtonian fluids with respect to an inertial frame of reference. The analysis begins with the closed set of the exact continuum equations for momentum, mass and thermal energy transport (Whitaker, 1976)

$$\frac{\partial}{\partial t}(\rho U_i) + \frac{\partial}{\partial x_j}(\rho U_i U_j) = -\frac{\partial}{\partial x_i}P + \frac{\partial}{\partial x_i}\left[\left(\kappa - \tfrac{2}{3}\mu\right)\frac{\partial}{\partial x_j}U_j\right]$$

$$+ \frac{\partial}{\partial x_j}\left[\mu\left(\frac{\partial}{\partial x_j}U_i + \frac{\partial}{\partial x_i}U_j\right)\right] + \rho g_i \qquad (2.1)$$

$$\frac{\partial}{\partial t}(\rho e) + \frac{\partial}{\partial x_j}(\rho e U_j) = \frac{\partial}{\partial x_j}(\kappa \frac{\partial}{\partial x_j} T) - P \frac{\partial}{\partial x_j} U_j \qquad (2.2)$$
$$+ \mu \frac{\partial}{\partial x_j} U_i (\frac{\partial}{\partial x_j} U_i + \frac{\partial}{\partial x_i} U_j) + (\lambda - \tfrac{2}{3}\mu)(\frac{\partial}{\partial x_j} U_j)^2$$

$$\frac{\partial}{\partial t} \rho + \frac{\partial}{\partial x_j}(\rho U_j) = 0 \qquad (2.3)$$

$$\rho = f_n(P,T) \quad e = f_n(P,T) \quad \kappa = f_n(P,T) \qquad (2.4)$$
$$\lambda = f_n(P,T) \quad \mu = f_n(P,T)$$

These equations describe all Newtonian fluid behaviour in the absence of non-gravitational body forces and radiative heat transfer. They are valid for both laminar and turbulent flows.

This investigation makes use of order of magnitude analysis to simplify the governing equations. Application of this technique to equation (2.1) will result in an over estimation of the gravitational influence on momentum, the reason for this being that all terms on the right hand side of the equation are not independent. In order to determine which factors actually are independent, each field variable will be decomposed into two components, the second of which corresponds to a fluid flow without any momentum or heat flux. The new variables are

$$U_i = U_i' + U_i'', \quad P = P' + P'', \quad T = T' + T'', \qquad (2.5)$$
$$e = e' + e'', \quad \rho = \rho' + \rho'', \quad \kappa = \kappa' + \kappa'', \quad \mu = \mu' + \mu'', \quad \lambda = \lambda' + \lambda''$$

The double primed variables must also satisfy equations (2.1) to (2.4) and this invokes the following relations;

$$-\frac{\partial}{\partial x_i} P'' \Big\} - \rho'' g_i = 0 \qquad \mu'' = f_n(P'', T'')$$

$$T'' = \text{a constant} \qquad \nu'' = f_n(P'', T'') \qquad (2.6)$$

$$\rho'' = f_n(P'', T'') \qquad \kappa'' = f_n(P'', T'')$$

Substitution of equations (2.6) into equations (2.1) to (2.4) and then using relations (2.5) between the double primed and unprimed variables, the equations for the instantaneous field variables become

$$\frac{\partial}{\partial t}(\rho U_i) + \frac{\partial}{\partial x_j}(\rho U_i U_j) = -\frac{\partial}{\partial x_i} P' + \frac{\partial}{\partial x_i}\left[\left(\nu - \frac{2}{3}\mu\right)\frac{\partial}{\partial x_j} U_j\right] + \frac{\partial}{\partial x_j}\left[\mu\left(\frac{\partial}{\partial x_j} U_i + \frac{\partial}{\partial x_i} U_j\right)\right] + (\rho - \rho'') g_i \qquad (2.7)$$

$$\frac{\partial}{\partial t}(\rho e) + \frac{\partial}{\partial x_i}(\rho e U_j) = \frac{\partial}{\partial x_j}\left(\kappa \frac{\partial}{\partial x_j} T\right) - P \frac{\partial}{\partial x_j} U_j + \mu \frac{\partial}{\partial x_j} U_i \left(\frac{\partial}{\partial x_j} U_i + \frac{\partial}{\partial x_i} U_j\right) + \left(\nu - \frac{2}{3}\mu\right)\left(\frac{\partial}{\partial x_j} U_j\right)^2 \qquad (2.8)$$

$$\frac{\partial}{\partial t} \rho + \frac{\partial}{\partial x_j}(\rho U_j) = 0 \qquad (2.9)$$

Only the momentum equation has been modified, it now displays the correct influence of gravity on momentum, $(\rho - \rho'')g_i$, equations (2.6) show that ρ'' will be constrained only after boundary conditions have been specified for P'' and T''. It is recommended that these be representative

of the ρ and T boundary conditions so that $(\rho - \rho'')$ will be as small as possible. In further work $(\rho - \rho')$ will be referred to as ρ'.

2.2 Mean Field Variables

2.2.1 Reynolds Decomposition

The dependent variables of the closed set of equations (2.7) to (2.9) are U_i, P', e, and T. Practically only the mean boundary conditions are known, and hence only the mean values of the field variables should be expected to be predictable. What is surprising is that the difference between the mean velocity field and the instantaneous velocity field should be so much greater than the corresponding difference at the boundaries. These mean values are solutions to the mean field equations, which are determined by averaging the instantaneous field equations. The mean variable may be defined as (Hinze, 1975)

$$\overline{A} = \lim_{N \to \infty} \frac{1}{N} \sum_{i=1}^{N} A_{(i)} \tag{2.10}$$

where $A_{(i)}$ is the value of A at the i^{th} realization. An alternate definition, which is popular in engineering, is due to Reynolds (1894)

$$\overline{A} = \frac{1}{\Delta t} \int_{t-\frac{\Delta t}{2}}^{t+\frac{\Delta t}{2}} A \, dt \tag{2.11}$$

where the time increment, Δt, must be carefully selected such that the second derivative of A be very nearly zero over the averaging interval. Although quite different, these methods have similar operator

properties so that $\overline{A}$ will be used for both. The properties of the average are commonly referred to as the Reynolds conditions and are as follows if $A = \overline{A} + a$ and $B = \overline{B} + b$, the lower case letters representing the fluctuation about the mean, then (Hinze, 1975)

$$
\begin{aligned}
&\text{(i)}\ \overline{a} = 0,\ \overline{b} = 0 \\
&\text{(ii)}\ \overline{\overline{A} + a} = \overline{\overline{A}} + \overline{a} = \overline{A} \\
&\text{(iii)}\ \overline{\overline{A}\overline{B}} = \overline{\overline{A}}\,\overline{\overline{B}} = \overline{A}\,\overline{B} \\
&\text{(iv)}\ \overline{\overline{A}b} = \overline{A}\,\overline{b} = 0 \\
&\text{(v)}\ \overline{AB} = \overline{A}\,\overline{B} + \overline{ab} \\
&\text{(vi)}\ \overline{\frac{\partial}{\partial x_i} A} = \frac{\partial}{\partial x_i} \overline{A} \\
&\text{(vii)}\ \overline{\frac{\partial}{\partial t} A} = \frac{\partial}{\partial t} \overline{A}
\end{aligned}
\tag{2.12}
$$

2.2.2 Mean Momentum Equation

Averaging the momentum equation results in

$$
\overline{\frac{\partial}{\partial t}(\rho U_i)} + \overline{\frac{\partial}{\partial x_j}(\rho U_i U_j)} = -\overline{\frac{\partial}{\partial x_i} P'} + \overline{\rho' g_i}
$$

$$
-\overline{\frac{\partial}{\partial x_i}\left[\left(\lambda - \tfrac{2}{3}\mu\right)\frac{\partial}{\partial x_j} U_j\right]} + \overline{\frac{\partial}{\partial x_j}\left[\mu\left(\frac{\partial}{\partial x_j} U_i + \frac{\partial}{\partial x_i} U_j\right)\right]} \tag{2.13}
$$

Presupposing that the variable U_1 is composed of the sum of a mean and a fluctuating portion (whose average = 0), $\overline{U}_1 + u_1$, allows for the explicit appearance of the mean velocity in the mean momentum equation. Defining similar expressions for the remaining variables of the equation: $\rho' = \overline{\rho}' + r$, $P' = \overline{P}' + p$, $\mu = \overline{\mu} + m$, $\lambda = \lambda + l$ and substituting into equation (2.13) gives

$$\overline{\frac{\partial}{\partial t}\left[(\bar{\rho}+r)(\bar{\rho}+r)\right]} + \overline{\frac{\partial}{\partial x_j}\left[(\bar{\rho}+r)(\bar{U}_i+u_i)(\bar{U}_j+u_j)\right]}$$

$$= -\overline{\frac{\partial}{\partial x_i}(\bar{P}+P')} + \overline{(\bar{\rho}'g_i + r g_i)}$$

$$-\overline{\frac{\partial}{\partial x_i}\left[\left(\bar{\mu}+\lambda-\tfrac{2}{3}\bar{\mu}-\tfrac{2}{3}m\right)\frac{\partial}{\partial x_j}(\bar{U}_j+u_j)\right]} \qquad (2.14)$$

$$+\overline{\frac{\partial}{\partial x_j}\left\{(\bar{\mu}+m)\left[\frac{\partial}{\partial x_j}(\bar{U}_i+u_i)+\frac{\partial}{\partial x_i}(\bar{U}_j+u_j)\right]\right\}}$$

Applying the properties of the average, equation (2.14) simplifies to

$$\frac{\partial}{\partial t}(\bar{\rho}\bar{U}_i + \overline{r u_i}) + \frac{\partial}{\partial x_j}(\bar{\rho}\bar{U}_i\bar{U}_j + \bar{\rho}\,\overline{u_i u_j} + \overline{r u_i}\,\bar{U}_j + \overline{r u_j}\,\bar{U}_i$$

$$+ \overline{r u_i u_j}) = -\frac{\partial}{\partial x_i}\bar{P}' + \overline{\rho'}\,g_i + \frac{\partial}{\partial x_i}\left[(\bar{\mu}-\tfrac{2}{3}\bar{\mu})\frac{\partial}{\partial x_j}\bar{U}_j\right. \qquad (2.15)$$

$$\left. + \overline{(\lambda-\tfrac{2}{3}m)\frac{\partial u_j}{\partial x_j}}\right] + \frac{\partial}{\partial x_j}\left[\bar{\mu}\left(\frac{\partial}{\partial x_j}\bar{U}_i + \frac{\partial}{\partial x_i}\bar{U}_j\right) + \overline{m\left(\frac{\partial u_i}{\partial x_j}+\frac{\partial u_j}{\partial x_i}\right)}\right]$$

In the subsequent development, the effects of the fluctuating-velocity fluctuating-density covariance is ignored because density fluctuations are poorly correlated with velocity fluctuations at low Mach numbers (Hinze, 1975). The fluctuating-viscosity fluctuating-velocity-gradient correlation will be ignored since fluid viscosity is a property of the fluid and therefore not directly dependent on the fluid deformation, although some coupling does occur through viscosity's dependence on temperature. Removing these terms gives the result

$$\frac{\partial}{\partial t}(\bar{\rho}\bar{U}_i) + \frac{\partial}{\partial x_j}(\bar{\rho}\bar{U}_i\bar{U}_j + \bar{\rho}\overline{u_i u_j}) = -\frac{\partial}{\partial x_i}\overline{P'}$$

$$+ \overline{\rho' g_i} + \frac{\partial}{\partial x_i}\left[(\bar{\lambda} - \tfrac{2}{3}\bar{\mu})\frac{\partial}{\partial x_j}\bar{U}_j\right] + \frac{\partial}{\partial x_j}\left[\bar{\mu}\left(\frac{\partial}{\partial x_j}\bar{U}_i + \frac{\partial}{\partial x_i}\bar{U}_j\right)\right] \quad (2.16)$$

It is only the second portion of the second term which makes the mean momentum equation different from the instantaneous momentum equation. If the same process were applied to a linear differential equation the average equation would be of identical form to the exact equation. Hence, a fluctuating boundary condition would only produce a proportional fluctuation in the exact field variables. For fluid flow, however, very small boundary fluctuations will completely change the character of the flow due to the presence of the quasi-linear terms.

2.2.3 Mean Thermal Energy Equation

The thermal energy equation may be expressed in terms of enthalpy with the relation $h = e + P/\rho$ as (Whitaker, 1976)

$$\frac{\partial}{\partial t}(\rho h) + \frac{\partial}{\partial x_j}(\rho h \bar{U}_j) = \frac{\partial}{\partial x_j}\left(k\frac{\partial}{\partial x_j}T\right) + \frac{\partial}{\partial t}P$$

$$+ \bar{U}_j\frac{\partial}{\partial x_j}P + \mu\left[\frac{\partial}{\partial x_j}U_i\left(\frac{\partial}{\partial x_j}U_i + \frac{\partial}{\partial x_i}U_j\right)\right] \quad (2.17)$$

$$+ (\lambda - \tfrac{2}{3}\mu)\left(\frac{\partial}{\partial x_j}U_j\right)^2$$

where the continuity equation has been used to eliminate

$$\frac{P}{\rho}\left[\frac{\partial}{\partial t}\rho + \frac{\partial}{\partial x_j}(\rho U_j)\right] = 0 \quad (2.18)$$

Equation (2.17) may be expressed in terms of temperature rather than enthalpy. Substituting (Whitaker, 1976)

$$\frac{\partial}{\partial t} h + U_j \frac{\partial}{\partial x_j} h = \left(\frac{\partial h}{\partial P}\right)_{(T)} \left(\frac{\partial}{\partial t} P + U_j \frac{\partial}{\partial x_j} P\right) + \left(\frac{\partial h}{\partial T}\right)_{(P)} \left(\frac{\partial}{\partial t} T + U_j \frac{\partial}{\partial x_j} T\right) \tag{2.19}$$

into equation (2.16), one gets

$$C_{(P)} \left[\frac{\partial}{\partial t}(\rho T) + \frac{\partial}{\partial x_j}(\rho T U_j)\right] = \frac{\partial}{\partial x_j}\left(\kappa \frac{\partial}{\partial x_j} T\right) + (1 - C_{(T)})\left(\frac{\partial}{\partial t} P + U_j \frac{\partial}{\partial x_j} P\right) + \tag{2.20}$$

$$\mu \left[\frac{\partial}{\partial x_j} U_i \left(\frac{\partial}{\partial x_j} U_i + \frac{\partial}{\partial x_i} U_j\right)\right] + \left(\tau - \tfrac{2}{3}\mu\right)\left(\frac{\partial}{\partial x_j} U_j\right)^2$$

where $C_{(T)}$ and $C_{(P)}$ are the differential coefficients $\left(\frac{\partial h}{\partial P}\right)_{(T)}$ and $\left(\frac{\partial h}{\partial T}\right)_{(P)}$, respectively.

This is an instantaneous field equation for temperature. It may be averaged and with the substitutions:

$$\rho = \overline{\rho} + r \,,\; U_i = \overline{U}_i + u_i \,,\; T = \overline{T} + \theta \,,\; \kappa = \overline{\kappa} + o$$
$$P = \overline{P} + p \,,\; C_{(P)} = \overline{C}_{(P)} + c_{(P)} \,,\; C_{(T)} = \overline{C}_{(T)} + c_{(T)} \,, \tag{2.21}$$
$$\mu = \overline{\mu} + m \,,\; \tau = \overline{\tau} + s$$

(in the fluids under consideration $C_{(P)}$ and $C_{(T)}$ are relatively weak functions of pressure and temperature, and therefore $c_{(P)} = c_{(T)} \approx 0$) equation (2.20) becomes

$$\bar{C}_{(p)}\left\{\frac{\partial}{\partial t}(\bar{\rho}\bar{T}+\overline{\rho\theta})+\frac{\partial}{\partial x_j}\left[(\bar{\rho}\bar{T}+\overline{\rho\theta})\bar{U}_j+\overline{\rho u_j}\,\bar{T}\right.\right.$$

$$\left.\left.+\bar{\rho}\,\overline{u_j\theta}+\overline{\rho\theta u_j}\right]\right\}=\frac{\partial}{\partial x_j}\left(\bar{K}\frac{\partial}{\partial x_j}\bar{T}+\overline{\rho\frac{\partial\theta}{\partial x_j}}\right)$$

$$+\left(1-\bar{\rho}\,\bar{C}_{(r)}\right)\left(\frac{\partial}{\partial t}\bar{P}+\bar{U}_j\frac{\partial}{\partial x_j}\bar{P}+\overline{u_j\frac{\partial P}{\partial x_j}}\right)$$

$$-\bar{C}_{(r)}\left[\overline{r\left(\frac{\partial P}{\partial t}+\bar{U}_j\frac{\partial P}{\partial x_j}+u_j\frac{\partial}{\partial x_j}P+u_j\frac{\partial P}{\partial x_j}\right)}\right]$$

$$+\bar{\mu}\left[\frac{\partial}{\partial x_j}\bar{U}_i\left(\frac{\partial}{\partial x_j}\bar{U}_i+\frac{\partial}{\partial x_i}\bar{U}_j\right)+\overline{\frac{\partial u_i}{\partial x_j}\left(\frac{\partial u_i}{\partial x_j}+\frac{\partial u_j}{\partial x_i}\right)}\right] \tag{2.22}$$

$$+\left(\bar{\lambda}-\tfrac{2}{3}\bar{\mu}\right)\left[\left(\frac{\partial}{\partial x_j}\bar{U}_j\right)^2+\overline{\left(\frac{\partial u_j}{\partial x_j}\right)^2}\right]+\overline{m\left[\frac{\partial}{\partial x_j}\bar{U}_i\left(\frac{\partial u_i}{\partial x_j}\right.\right.}$$

$$\overline{\left.\left.+\frac{\partial u_j}{\partial x_i}\right)+\frac{\partial u_i}{\partial x_j}\left(\frac{\partial u_i}{\partial x_j}+\frac{\partial u_j}{\partial x_i}\right)+\frac{\partial u_i}{\partial x_j}\left(\frac{\partial}{\partial x_j}\bar{U}_i+\frac{\partial}{\partial x_i}\bar{U}_j\right)\right]}$$

$$+\overline{\left(\lambda-\tfrac{2}{3}m\right)\left[2\frac{\partial u_i}{\partial x_j}\frac{\partial}{\partial x_i}\bar{U}_i+\left(\frac{\partial u_j}{\partial x_j}\right)^2\right]}$$

For low Mach numbers the density-velocity covariance may be ignored. When density fluctuations are small compared to density and largely due to temperature changes, then the density-pressure covariances may be ignored. The transport properties m and λ are not dependent on the velocity or temperature gradients and hence these covariances are zero. The effect of the density-temperature covariance on the transport of mean temperature is often ignored

since it is small when compared to $\bar{\rho}\,\bar{T}$ which is also convected by the mean flow. The velocity- temperature covariance on the other hand is not a mean convection phenomenon but a diffusive one. When compared to molecular diffusion it is large and therefore retained. With these considerations the average temperature equation becomes

$$\bar{C}_{(p)}\left[\frac{\partial}{\partial t}(\bar{\rho}\bar{T}) + \frac{\partial}{\partial x_j}(\bar{\rho}\bar{T}\bar{U}_j + \bar{\rho}\,\overline{u_j\theta})\right] = \frac{\partial}{\partial x_j}\left(\bar{\kappa}\frac{\partial}{\partial x_j}\bar{T}\right) \tag{2.23}$$

$$+ (1-\bar{\rho}\,\bar{C}_{(T)})\left(\frac{\partial}{\partial t}\bar{P} + \bar{U}_j\frac{\partial}{\partial x_j}\bar{P} + \overline{u_j\frac{\partial P}{\partial x_j}}\right) + \bar{\mu}\frac{\partial}{\partial x_j}\bar{U}_i\left(\frac{\partial}{\partial x_j}\bar{U}_i + \frac{\partial}{\partial x_i}\bar{U}_j\right) + \left(\bar{\kappa}-\tfrac{2}{3}\bar{\mu}\right)\left(\frac{\partial}{\partial x_j}\bar{U}_j\right)^2 + \bar{\mu}\,\overline{\frac{\partial u_i}{\partial x}\left(\frac{\partial u_i}{\partial x_j}+\frac{\partial u_j}{\partial x_i}\right)}$$

$$+ \left(\bar{\kappa}-\tfrac{2}{3}\bar{\mu}\right)\overline{\left(\frac{\partial u_j}{\partial x_j}\right)^2}$$

2.2.4 Mean Continuity Equation

The mass conservation equation may also be averaged and making similar substitutions for the mean field variables

$$\frac{\partial}{\partial t}\bar{\rho} + \frac{\partial}{\partial x_j}\left(\bar{\rho}\,\bar{U}_j + \overline{\rho u_j}\right) = 0 \tag{2.24}$$

for low Mach Numbers this becomes (Hinze, 1975)

$$\frac{\partial}{\partial t}\bar{\rho} + \frac{\partial}{\partial x_j}\left(\bar{\rho}\,\bar{U}_j\right) = 0 \tag{2.25}$$

2.3 Fluctuating Field Equations

Each of the indeterminate variables of the mean field equations are the average products of the fluctuating components of two field variables. If the fluctuarting components were known, then this

average product could be uniquely determined. The equations for the fluctuating components of the field variables may be determined by subtracting the mean field equations from the instantaneous field equations. Decomposing each field variable into a mean and a fluctuating portion, as done in the derivation of the mean field equations; produces an explicit equation for the fluctuating portion of that field variable. The solution of these equations requires the fluctuating portion of the boundary conditions, which as mentioned, are unknown.

If the fluctuating portion of all thermodynamic and fluid properties is ignored with the exception of the body force term in the momentum equation and the mean properties assumed constant, then the fluctuating field equations are deduced:

$$\frac{\partial u_i}{\partial t} + \bar{U}_j \frac{\partial u_i}{\partial x_j} = -u_j \frac{\partial}{\partial x_j} \bar{U}_i - \frac{1}{\bar{\rho}} \frac{\partial P}{\partial x_i} + \frac{\rho}{\bar{\rho}} g_i + \bar{\nu} \frac{\partial}{\partial x_j} \left(\frac{\partial u_i}{\partial x_j} + \frac{\partial u_j}{\partial x_i} \right) - \frac{\partial}{\partial x_j} \left(u_i u_j - \overline{u_i u_j} \right) \tag{2.26}$$

$$\frac{\partial \theta}{\partial t} + \bar{U}_j \frac{\partial \theta}{\partial x_j} - u_j \frac{\partial}{\partial x_j} \bar{T} - \frac{\partial}{\partial x_j} \left(u_j \theta - \overline{u_j \theta} \right) + \alpha \frac{\partial^2 \theta}{\partial x_j \partial x_j} + \left(1/\bar{\rho} \bar{C}_{(P)} - \bar{C}_{(T)} / \bar{C}_{(P)} \right) \left(\frac{\partial P}{\partial t} + \bar{U}_j \frac{\partial P}{\partial x_j} + u_j \frac{\partial}{\partial x_j} \bar{P} + u_j \frac{\partial P}{\partial x_j} - \overline{u_j \frac{\partial P}{\partial x_j}} \right) + \left(\bar{\nu} / \bar{C}_{(P)} \right) \Big[2 \frac{\partial u_i}{\partial x_j} \left(\frac{\partial}{\partial x_j} \bar{U}_i + \frac{\partial}{\partial x_i} \bar{U}_j \right) + \frac{\partial u_i}{\partial x_j} \left(\frac{\partial u_i}{\partial x_j} + \frac{\partial u_j}{\partial x_i} \right) - \frac{\partial u_j}{\partial x_j} \left(\frac{\partial u_i}{\partial x_j} + \frac{\partial u_j}{\partial x_i} \right) \Big] \tag{2.27}$$

$$\frac{\partial u_i}{\partial x_i} = 0 \tag{2.28}$$

The above simplifications are necessary to obtain expressions for the unknown correlations and luckily do not circumvent the basic mechanisms of turbulence. In the formulation of turbulence models these fluctuating field equations are used extensively.

2.4 Overview of Turbulence Modelling

The problem is now one of too many variables and not enough equations. The variables which as yet cannot be determined are $\overline{u_i u_j}$, $\overline{u_i \theta}$, $\overline{u_j \frac{\partial p}{\partial x_j}}$, $\overline{\frac{\partial u_i}{\partial x_j}\frac{\partial u_j}{\partial x_i}}$ and $\overline{\frac{\partial u_i}{\partial x_j}\frac{\partial u_j}{\partial x_i}}$. The last three of these are source terms arising from irreversible and reversible work and in most flows have little effect on the mean field. The first two correlations, however, greatly enhance the apparent diffusion of the flow. They represent the fluctuating momentum and fluctuating heat per unit mass convected by the fluctuating velocity. The $\overline{u_i u_j}$ variable is an inertial term and hence may be regarded as a stress per unit mass per unit volume by D'Alembert's principle. They were originally formulated by Osborn Reynolds (1894) and have become widely known as "Reynolds stresses".

The instantaneous equations, together with boundary conditions, represent a closed system, that can in principle, be solved for the variables of interest provided that a unique solution exists. However, the boundary conditions are only approximately known and the instantaneous solutions are very sensitive to the boundary condition choice. The average solutions are not nearly so sensitive and so the boundary conditions may be prescribed with suitable accuracy. The set

of averaged equations are not closed since they include unknown correlations, so that further independent constraints must be supplied to close the equation set. This is an analogous situation to the one which is encountered in going from a molecular description of a fluid flow to a continuous one. Guidance in solving the present problem can be acquired from studying the successful solution of the molecular problem.

Two approaches are taken in closing the continuum field equations; one is to study the molecular velocity distributions and hence determine their statistical properties while the other approach is to establish a general relation between an unknown correlation and the continuous field variables by experimentally known constraints of the continuous motion. It is the latter approach which is used in the field of turbulence modelling.

The unknown variables of the mean field equations must be expressed as functions of the mean-field dependent-variables, $\bar{U}_j$, $\bar{T}$, $\bar{P}$ their space and time derivatives, the space and time derivatives of the unknown variables and the thermodynamic state to obtain closure. For example the Reynolds stress would be of the functional form

$$\overline{u_i u_j} = (f_n)_{ij}\left(\bar{U}_m, \bar{T}, \bar{P}, \frac{\partial}{\partial x_n}\bar{U}_p, \frac{\partial}{\partial x_n}\bar{T}, \frac{\partial}{\partial x_n}\bar{P}, \frac{d}{dt}\overline{u_i u_j}, \frac{\partial}{\partial x_s}\overline{u_m u_n}, \bar{\mu}, \bar{\kappa}\right) \qquad (2.29)$$

In the classic approach to constituent relations, the following requirements are invoked (Aris, 1962; Slattery, 1981)

1) the principle of determinism, "The stress in a body is determined by the history of the motion that the body has undergone."

2) the principle of local action, "The motion of the material outside of an arbitrarily small neighbourhood of a material point may be ignored in determining the stress at this material point."

3) the principle of material frame indifference, "The response of a material is the same for all observers."

These constraints have led to successful constituent relations for both liquids and gases.

The first of these principles is applicable to turbulence modelling but the second and third are not. Normally the second principle could be used to eliminate the dependence of $\overline{u_i u_j}$ on its space and time derivatives, however, experiments have shown that unlike molecular transport, turbulent motions affect points in the fluid at distances of the same order as the mean flow dimensions, and hence, not arbitrarily small.

The principle of material frame indifference is usually used to eliminate the vorticity and absolute velocity dependence from equation (2.29). This technique has been supported by Speziale (1979) and other authors but partially refuted by Lumley (1970, 1983) and experimental results from flows with streamline curvature so that it may only be used to eliminate the absolute velocity dependence.

The principle of determinism does not further restrict equation (2.28). There is, however, a general agreement that the turbulent stresses are determined only by the mean deformation of the flow; i.e. $\frac{\partial}{\partial x_n}\overline{U}_m$ and its own space and material derivatives. This reduces equation (2.29) to the form

$$\overline{u_i u_j} = (f_n)_{ij}\left(\frac{d}{dt}\overline{u_i u_j}, \frac{\partial}{\partial x_n}\overline{u_p u_q}, \frac{\partial}{\partial x_n}\overline{U}_m, \bar{\mu}\right) \qquad (2.30)$$

This expression is immensely more complicated than the usual expression for the molecular stress

$$\overline{T}_{ij} = (f_n)_{ij}\left(\frac{\partial}{\partial x_n}\overline{U}_m + \frac{\partial}{\partial x_m}\overline{U}_n, P, T\right) \qquad (2.31)$$

Equation (2.30) is necessarily a differential equation and hence the value of $\overline{u_i u_j}$ at any point is dependent on the value of mean velocity at all other points. Differential equations for the unknown variables may be derived from fluctuating field equations of section 2.3. Unfortunately these too contain further unknown variables and the problem becomes increasingly complicated. Nevertheless this is currently the most successful approach and the one which will be reviewed in the subsequent sections.

2.5 Reynolds Stress Equation

An equation may be formulated for each of the Reynolds stresses as follows (Hinze, 1975): multiply the u_i equation by u_j, multiply the u_j equation by u_i, add the two equations and average the results.

The resulting equations are

$$\frac{\partial}{\partial t}\overline{u_i u_j} + \overline{U}_k \frac{\partial}{\partial x_k}\overline{u_i u_j} = -\left(\overline{u_i u_k}\frac{\partial}{\partial x_k}\overline{U}_j + \overline{u_j u_k}\frac{\partial}{\partial x_k}\overline{U}_i\right)$$

mean material derivative — shear production

$$+ \frac{1}{\rho}\left(\overline{\tau u_j}\,g_i + \overline{\tau u_i}\,g_j\right) + \overline{p/\rho\left(\frac{\partial u_i}{\partial x_j} + \frac{\partial u_j}{\partial x_i}\right)}$$

bouyancy generation — pressure redistribution

$$+ \frac{\partial}{\partial x_k}\left[-\overline{u_i u_j u_k} + \nu\frac{\partial}{\partial x_k}\overline{u_i u_j} - \frac{1}{\rho}\left(\overline{p u_j}\,\delta_{ik} + \overline{p u_i}\,\delta_{jk}\right)\right] \qquad (2.32)$$

turbulent and molecular diffusion

$$- 2\nu\,\overline{\frac{\partial u_i}{\partial x_j}\frac{\partial u_i}{\partial x_i}}$$

molecular dissipation

or in the more compact form

$$C_{ij} = P_{ij} + G_{ij} + \Delta_{ij} + D_{ij} - \epsilon_{ij}$$

2.6 Turbulent Heat Flux Equation

An equation for the variable $\overline{u_i\theta}$ may be obtained by (Hinze, 1975): multiplying the u_i equation by θ, the θ equation by u_i,

adding the two equations and averaging the result. The equation is

$$\frac{\partial}{\partial t}\overline{u_i\theta} + \bar{U}_j\frac{\partial}{\partial x_j}\overline{u_i\theta} = -\left(\overline{u_iu_j}\frac{\partial}{\partial x_j}\bar{T} + \overline{u_j\theta}\frac{\partial}{\partial x_j}\bar{U}_i\right)$$

mean material derivative — gradient production

$$+ \frac{1}{\bar{T}}\overline{T\theta}\,g_i + \overline{p/\bar{\rho}\,\frac{\partial\theta}{\partial x_i}}$$

bouyancy generation — pressure scrambling

$$+ \frac{\partial}{\partial x_j}\left[-\overline{u_iu_j\theta} - \frac{1}{\bar{\rho}}\overline{p\theta}\,\delta_{ij} + (\bar{\nu}+\bar{\alpha})\frac{\partial}{\partial x_j}\overline{u_i\theta} - \bar{\nu}\,\overline{u_i\frac{\partial\theta}{\partial x_j}} - \bar{\alpha}\overline{\theta\frac{\partial u_i}{\partial x_j}}\right]$$

turbulent and molecular diffusion

$$- (\alpha + \nu)\overline{\frac{\partial u_i}{\partial x_j}\frac{\partial\theta}{\partial x_j}} \qquad (2.33)$$

molecular destruction

$$+ \left(1/\bar{\rho}\,\bar{C}_{(p)} - C_{(T)}/C_{(p)}\right)\left(\overline{u_i\frac{\partial p}{\partial t}} + \overline{u_iu_j\frac{\partial p}{\partial x_j}} + \bar{U}_j\overline{u_i\frac{\partial p}{\partial x_j}} + \overline{u_iu_j}\frac{\partial}{\partial x_j}\bar{P}\right)$$

reversible work effects

$$+ \frac{\bar{\nu}}{\bar{C}_{(p)}}\left[\overline{u_i\frac{\partial u_k}{\partial x_j}\left(\frac{\partial u_k}{\partial x_j} + \frac{\partial u_j}{\partial x_k}\right)} + \frac{\partial}{\partial x_j}\bar{U}_k\left(\overline{u_i\frac{\partial u_k}{\partial x_j}} + \overline{u_i\frac{\partial u_j}{\partial x_k}}\right)\right.$$

$$\left. + \overline{u_i\frac{\partial u_k}{\partial x_j}}\left(\frac{\partial}{\partial x_j}\bar{U}_k + \frac{\partial}{\partial x_k}\bar{U}_j\right)\right]$$

irreversible work effects

or in the more compact form

$$C_i = P_i + G_i + \Delta_i + D_i - \epsilon_i + R_i + d_i$$

2.7 Scaling Parameters

The unknowns in the Reynolds Stress and turbulent heat flux equations can be modelled in terms of mean field variables, mean turbulence parameters $\overline{u_i u_j}$, $\overline{u_i \theta}$ or neglected. The tools used in this analysis are those of dimensional and order of magnitude analysis. To carry out these analyses, the characteristic amplitudes and times of velocity and temperature must be determined. Some obvious scales are: the square root of the mean turbulent kinetic energy; the root-mean-squared temperature and the ratio of the turbulent kinetic energy to its dissipation rate. These quantities will be obtained from an equation for each.

2.7.1 Mean Turbulent Kinetic Energy Equation

The turbulent kinetic energy equation may be derived by contracting the $\overline{u_i u_j}$ equation and multiplying by one-half. The result is

$$\frac{\partial}{\partial t} k + \bar{U}_j \frac{\partial}{\partial x_j} k = -\overline{u_i u_j} \frac{\partial}{\partial x_j} \bar{U}_i + \frac{1}{\rho} \overline{\tau u_i} g_i$$

$$+ \frac{\partial}{\partial x_j}\left(-\overline{u_j k} + \bar{\nu} \frac{\partial}{\partial x_j} k - \frac{1}{\rho} \overline{p u_i} \delta_{ij} \right) \qquad (2.34)$$

$$- \bar{\nu} \overline{\frac{\partial u_i}{\partial x_j} \frac{\partial u_i}{\partial x_j}}$$

or more compactly as

$$C_{(k)} = P_{(k)} + G_{(k)} + D_{(k)} - \epsilon_{(k)}$$

2.7.2 Mean Turbulent Kinetic Energy Dissipation Rate Equation

The equation for the dissipation rate of the mean turbulent kinetic energy is formed by (Hanjalic and Launder, 1972) differentiating the u_i equation with respect to x_k and multiplying this by $2\bar{\nu}\frac{\partial u_i}{\partial x_k}$. The result is

$$\frac{\partial}{\partial t}\epsilon + \bar{U}_j\frac{\partial}{\partial x_j}\epsilon = -4\bar{\nu}\,\overline{\frac{\partial u_j}{\partial x_k}\frac{\partial u_i}{\partial x_j}\frac{\partial u_i}{\partial x_k}}$$

mean material derivative — fluctuating vortex stretching

$$-4\bar{\nu}\left(\overline{\frac{\partial u_i}{\partial x_j}\frac{\partial u_i}{\partial x_k}} + \overline{\frac{\partial u_j}{\partial x_i}\frac{\partial u_k}{\partial x_i}}\right)\frac{\partial}{\partial x_k}\bar{U}_j - 4\bar{\nu}\,\overline{u_j\frac{\partial u_i}{\partial x_k}\frac{\partial^2}{\partial x_k\partial x_j}}\bar{U}_i$$

shear production

$$+\frac{4\bar{\nu}}{\bar{\rho}}g_i\,\overline{\frac{\partial \rho}{\partial x_k}\frac{\partial u_i}{\partial x_k}}$$

buoyancy production

$$+\frac{\partial}{\partial x_k}\left(-2\bar{\nu}\,\overline{u_k\frac{\partial u_i}{\partial x_j}\frac{\partial u_i}{\partial x_j}} - \frac{4\bar{\nu}}{\bar{\rho}}\overline{\frac{\partial p}{\partial x_i}\frac{\partial u_k}{\partial x_i}} + 2\bar{\nu}\frac{\partial \epsilon}{\partial x_k}\right) \qquad (2.35)$$

turbulent and molecular diffusion

$$-4\bar{\nu}^2\,\overline{\frac{\partial^2 u_i}{\partial x_k\partial x_j}\frac{\partial^2 u_i}{\partial x_k\partial x_j}}$$

molecular destruction

or more compactly as

$$C_{(\epsilon)} = S_{(\epsilon)} + P_{(\epsilon)} + G_{1(\epsilon)} + D_{(\epsilon)} - \epsilon_{(\epsilon)}$$

2.7.3 Mean Square Fluctuating Temperature Equation

The equation for the mean square fluctuating temperature is obtained by multiplying the fluctuating temperature equation by 2θ and averaging the results (Corrsin, 1951). This equation is

$$\frac{\partial}{\partial t}\overline{g} + \bar{U}_j \frac{\partial}{\partial x_j}\overline{g} = -2\overline{u_j\theta}\frac{\partial}{\partial x_j}\bar{T}$$

mean material derivative — gradient production

$$+ \frac{\partial}{\partial x_j}\left(-\overline{u_j g} + \bar{\alpha}\frac{\partial}{\partial x_j}\overline{g}\right) - 2\bar{\alpha}\,\overline{\frac{\partial\theta}{\partial x_j}\frac{\partial\theta}{\partial x_j}}$$

turbulent and molecular diffusion — molecular destruction

$$+ 2\left(1/\bar{\rho}\bar{C}_{(p)} + \bar{C}_{(T)}/\bar{C}_{(p)}\right)\left(\overline{\theta\frac{\partial p}{\partial t}} + \overline{u_j\theta\frac{\partial p}{\partial x_j}} + \bar{U}_j\overline{\theta\frac{\partial p}{\partial x_j}} + \overline{u_j\theta}\frac{\partial}{\partial x_j}\bar{P}\right) \qquad (2.36)$$

reversible work effects

$$+ \frac{2\bar{\nu}}{\bar{C}_{(p)}}\left[\frac{\partial}{\partial x_j}\bar{U}_k\overline{\theta\left(\frac{\partial u_k}{\partial x_j} + \frac{\partial u_j}{\partial x_k}\right)} + \left(\frac{\partial}{\partial x_j}\bar{U}_k + \frac{\partial}{\partial x_k}\bar{U}_j\right)\overline{\theta\frac{\partial u_k}{\partial x_j}} + \overline{\theta\frac{\partial u_k}{\partial x_j}\left(\frac{\partial u_k}{\partial x_j} + \frac{\partial u_j}{\partial x_k}\right)}\right]$$

irreversible work effects

or in the more compact form

$$C_{(g)} = P_{(g)} + D_{(g)} - \epsilon_{(g)} + R_{(g)} + J_{(g)}$$

2.8 Closure

The mean turbulent kinetic energy, mean turbulent kinetic energy dissipation rate and mean square fluctuating temperature equations introduce 200 more unknowns which must be approximated in a similar manner to the unknown terms in the Reynolds stress and the turbulent heat flux equations. Though unsolvable, these equations are exact transport equations for mean turbulent quantities within the constraint of constant mean thermodynamic and fluid properties. They apply to all regions of a heat exchanger.

CHAPTER III

MODELLING TURBULENT FLOW IN A HEAT EXCHANGER

3.1 Separation of a Heat Exchanger into Three Regions

To reduce the number of unknowns, an order of magnitude analysis is applied to the general equations within three distinct regions of a heat exchanger. Terms considered to have negligible effects are omitted. The cross-section of a hypothetical heat exchanger is shown in Figure 1. It is divided into 3 characteristic regions:

a) tube-free regions

b) near-wall regions, and

c) tube-filled regions.

These were chosen because they each represent limiting cases which provide an opportunity to reduce the complexity of the solution. In the tube-free region, the Reynolds number is high enough to neglect viscous effects, furthermore the velocity gradients are gradual enough so that a relatively course computational grid is sufficient hence, permitting a multidimensional numerical solution. In the near-wall region, approximations similar to those in plane boundary layers, can be made. The tube-filled region approaches the behaviour of a porous medium in the limit of a large number of closely spaced tubes and it is treated in this simple way for the sake of understanding heat transfer and pressure drop in tube bundles.

Approximate forms of the field equations will be closed with modelling approximations for each region.

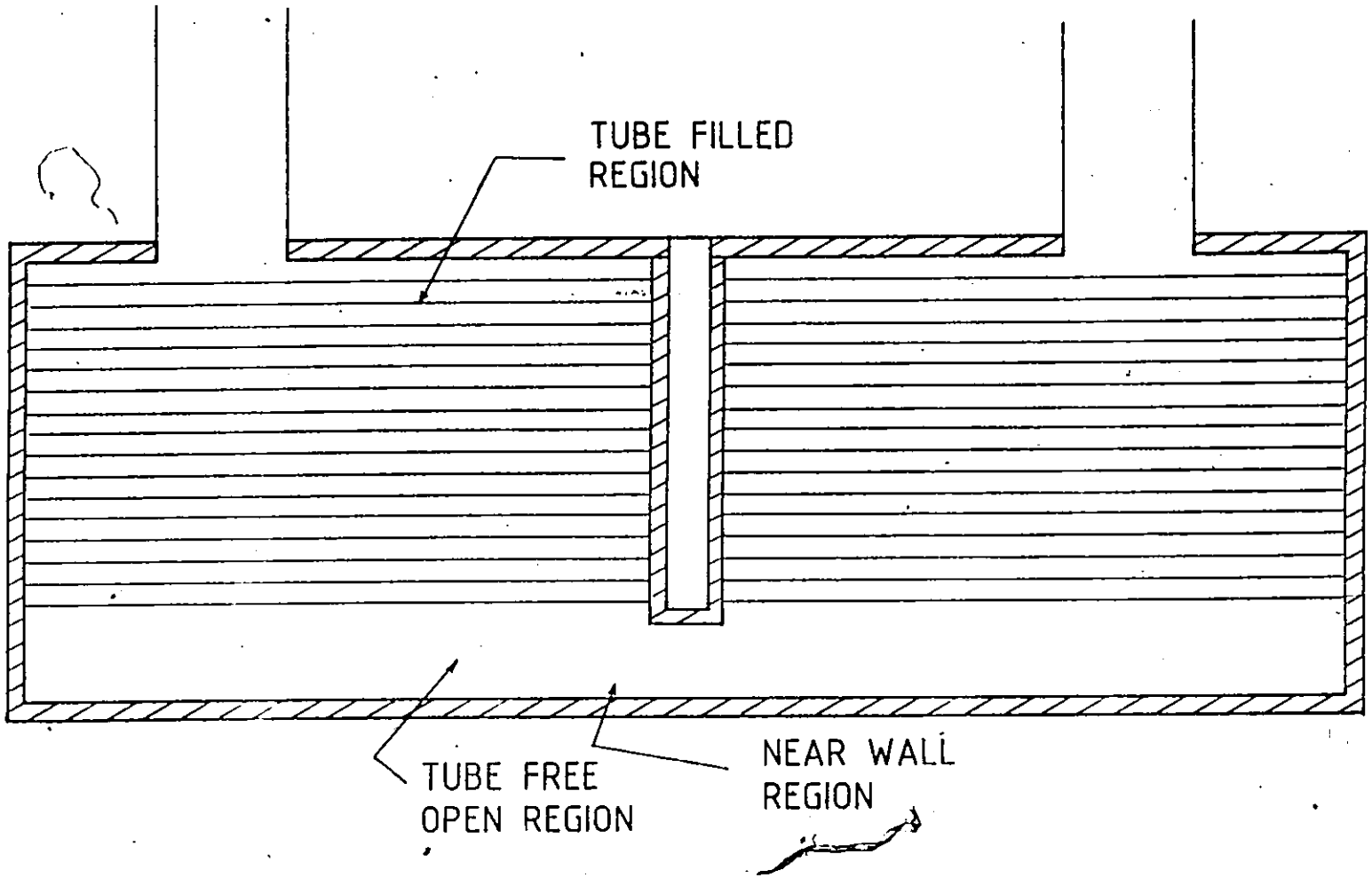

FIGURE 1: Regions of a Heat Exchanger

3.2 Tube-Free or Open Region

The governing equations which were derived in Chapter 2 are very complicated, however, they contain terms which are negligible in the open region of a shell and tube heat exchanger. To identify these simplifications an order of magnitude analysis is performed. First, the different variables in equations (2.16), (2.23), (2.32), (2.33), (2.34), (2.35) and (2.36) are grouped together into the minimum number of dimensionless ratios using the Buckingham Pi thereom. Then, the orders of magnitude of these ratios are estimated by a survey of typical industrial heat exchanger geometries and operating conditions. The results are

$$
\begin{aligned}
&\lambda_{(k)}/|\Delta x_i| = \Theta(10^{-3}) && \bar{\rho} C_{(T)} = \Theta(10^{0})\\
&\overline{\rho'}/\bar{\rho} = \Theta(10^{-2}) && \bar{C}_{(P)} \Delta\bar{T} / |\bar{U}_i|^2 = \Theta(10^{5})\\
&\bar{\mu}/\bar{\rho}\,|\Delta x_i|\,|\bar{U}_i| = \Theta(10^{-6}) && r/\bar{\rho} = \Theta(10^{-2})\\
&\Delta\bar{\mu}/\bar{\rho}\,|\Delta x_i|\,|\bar{U}_i| = \Theta(10^{-8}) && \lambda_{(g)}/|\Delta x_i| = \Theta(10^{-3})\\
&\bar{\mathcal{K}}/\bar{\rho}\,|\Delta x_i|\,|\bar{U}_i| = \Theta(10^{-6}) && \Theta/\Delta\bar{T} = \Theta(10^{0})\\
&\Delta\bar{\mathcal{K}}/\bar{\rho}\,|\Delta x_i|\,|\bar{U}_i| = \Theta(10^{-8}) && |u_i|/|\bar{U}_i| = \Theta(10^{0})\\
&\bar{\mathcal{K}}\,\Delta\bar{T}/\bar{\rho}\,|\bar{U}_i|^3|\Delta x_i| = \Theta(10^{-2}) && |g_i||\Delta x_i|/|\bar{U}_i|^2 = \Theta(10^{0})\\
&\Delta\bar{\mathcal{K}}\,\Delta\bar{T}/\bar{\rho}\,|\bar{U}_i|^3|\Delta x_i| = \Theta(10^{-4}) && \left(\frac{\partial}{\partial x_i}\bar{U}_i\right)|\Delta x_i|/|\bar{U}_i| = \Theta(10^{-1/2})\\
&\Delta\bar{P}/\bar{\rho}\,|\bar{U}_i|^2 = \Theta(10^{0}) && \left(\frac{\partial w}{\partial x_i}\right)|\Delta x_i|/|\bar{U}_i| = \Theta(0)\\
&\Delta\overline{P'}/\bar{\rho}\,|\bar{U}_i|^2 = \Theta(10^{0}) && P/\bar{\rho}\,|\bar{U}_i|^2 = \Theta(10^{0})
\end{aligned}
\qquad (3.1)
$$

where $\lambda_{(k)}$ and $\lambda_{(g)}$ represent the Taylor and Corrsin microscales and $|u_i|$, $|\bar{U}_i|$ and $|\Delta x_i|$ represent absolute value of the fluctuating velocity, mean velocity and mean spatial vectors respectively. This order of magnitude approximation will eliminate the need for modelling many indeterminate variables.

3.2.1 Mean Field Equations

Applying the order of magnitude estimates for the open region to the mean momentum, mean temperature and mean continuity equations indcates the they may be simplified to the forms

$$\frac{\partial}{\partial t}(\bar{\rho}\bar{U}_i) + \frac{\partial}{\partial x_j}(\bar{\rho}\bar{U}_i\bar{U}_j) = -\frac{\partial}{\partial x_i}\bar{P}' + \frac{\partial}{\partial x_j}(-\bar{\rho}\overline{u_i u_j}) + \overline{\rho'}\,g_i \quad (3.2)$$

$$\frac{\partial}{\partial t}(\bar{\rho}\bar{T}) + \frac{\partial}{\partial x_j}(\bar{\rho}\bar{T}\bar{U}_j) = \frac{\partial}{\partial x_j}(-\bar{\rho}\,\overline{u_j\theta}) \quad (3.3)$$

$$\frac{\partial}{\partial t}\bar{\rho} + \frac{\partial}{\partial x_j}(\bar{\rho}\bar{U}_j) = 0 \quad (3.4)$$

The only indeterminate unknowns in these equations are the Reynolds stress and the turbulent heat flux. The following sections will deal with the development of models which may be used in the open region to eliminate these unknowns.

3.2.2 The Reynolds Stress and Heat Flux Closure

3.2.2a Reynolds Stress Equation

The order of magnitude analysis has reduced equation (2.31) for Reynolds stress to

$$C_{ij} = P_{ij} + G_{ij} + \Delta_{ij} + D_{ij} - \epsilon_{ij} \quad (3.5)$$

where the diffusion tensor has been simplified to the form

$$D_{ij} \equiv \frac{\partial}{\partial x_k}\left[-\overline{u_i u_j u_k} - \frac{1}{\rho}\left(\overline{p u_j}\,\delta_{ik} + \overline{p u_i}\,\delta_{jk}\right)\right]$$

The remaining tensors whose components are indeterminate variables are G_{ij}, A_{ij}, D_{ij} and ϵ_{ij}.

The G_{ij} tensor represents the buoyancy production and has the components

$$G_{ij} = \frac{1}{\rho}\left(\overline{\rho u_j} g_i + \overline{\rho u_i} g_j\right) \qquad (3.6)$$

Although r is a function of temperature and pressure, the pressure dependence is very weak for a nearly incompressible fluid or where pressure variation is moderate. For small variations of pressure and temperature,

$$r = \left(\frac{\partial r}{\partial T}\right)_{(P)} \theta + \left(\frac{\partial r}{\partial P}\right)_{(T)} P \qquad (3.7)$$

or $$\frac{r}{\rho} = \beta_{(P)}\theta + \beta_{(T)} P$$

Neglecting its dependence on pressure, H_{ij} becomes

$$G_{ij} = \beta_{(P)}\left[\overline{u_j\theta}\, g_i + \overline{u_i\theta}\, g_j\right] \qquad (3.8)$$

which is a function of the determinate variable u_j.

The A_{ij} tensor is responsible for redistribution of energy among the components and contains the indeterminate variables $\overline{p\left(\frac{\partial u_i}{\partial x_j} + \frac{\partial u_j}{\partial x_i}\right)}$. An equation for the pressure fluctuation can be derived by differentiating the u_i equation with respect to the x_i

coordinate. The exact form with constant properties is

$$\frac{\partial^2}{\partial x_j \partial x_j} P/\bar{\rho} = 2 \frac{\partial}{\partial x_i} \bar{U}_j \frac{\partial u_i}{\partial x_j} - \left(\frac{\partial u_j}{\partial x_i} \frac{\partial u_i}{\partial x_j} - \overline{\frac{\partial u_j}{\partial x_i} \frac{\partial u_i}{\partial x_j}} \right) + \frac{\partial}{\partial x_j} \frac{\Gamma}{\bar{\rho}} g_j \tag{3.9}$$

The solution of this equation can be obtained in integral form using Green's Theorem, it is

$$P/\bar{\rho} = \frac{1}{4\pi} \int_V \left[2 \frac{\partial}{\partial x_i} \bar{U}_j \frac{\partial u_i}{\partial x_j} + \left(\frac{\partial u_j}{\partial x_i} \frac{\partial u_i}{\partial x_j} - \frac{\partial u_j}{\partial x_i} \frac{\partial u_i}{\partial x_j} \right) - \frac{\partial}{\partial x_j} \frac{\Gamma}{\bar{\rho}} g_j \right]^* \left(\frac{1}{r} + \frac{1}{r^*} \right) dV + \frac{1}{4\pi} \int_S \left(\frac{\partial P}{\partial x_i} n_i \right)^* \left(\frac{1}{r} + \frac{1}{r^*} \right) dS \tag{3.10}$$

where the star superscript indicates that the quantity is to be evaluated at the point q* (Figure 2).

The surface integral which is proportional to the normal pressure gradient at the wall may be neglected (Irwin, 1975) as it amounts to the hydrostatic force. The remaining solution contains two portions; one proportional to 1/r and the other to 1/r*. As the region of interest is moved away from the wall, 1/r* tends to zero so that this second portion may be attributed to a wall effect.

If both sides of the solution for p at the point q are multiplied by $(\partial u_i/\partial x_j + \partial u_j/\partial x_i)$ evaluated at the point q and averaged, then equations are obtained for the indeterminate variables $p(\partial u_i/\partial x_j + \partial u_j/\partial x_i)$ (Chou, 1945). Noticing that the integral for p is evaluated at the point q* while the term $(\partial u_i/\partial x_j + \partial u_j/\partial x_i)$ is evaluated at the point q, one infers that this

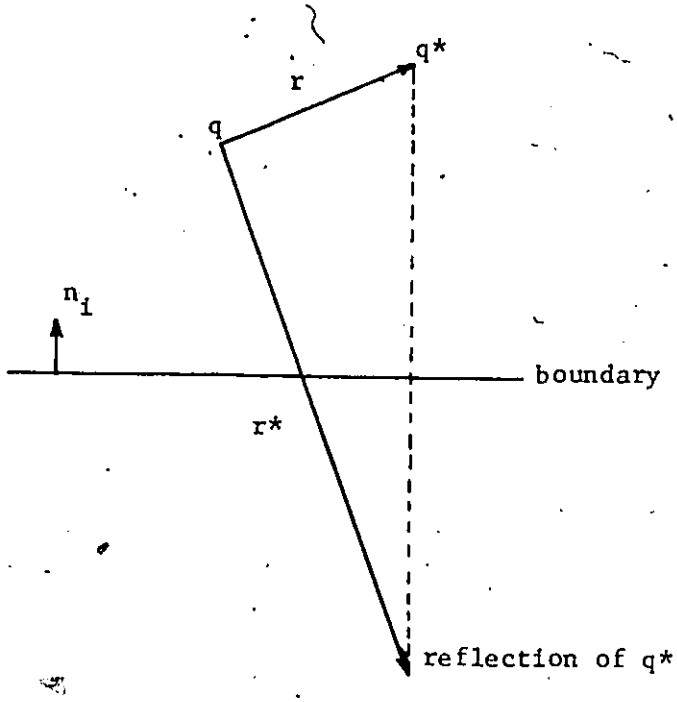

FIGURE 2: Region for the Integral Solution of Poisson's Equation

latter term behaves as a constant with respect to the integral. The resulting equation is

$$\overline{\frac{\rho}{\rho}\left(\frac{\partial u_i}{\partial x_j}+\frac{\partial u_j}{\partial x_i}\right)} = \frac{1}{4\pi}\int_V \Bigg\{ \overline{\left(2\frac{\partial}{\partial x_\ell}\bar{U}_k \frac{\partial u_\ell}{\partial x_k}\right)^*\left(\frac{\partial u_i}{\partial x_j}+\frac{\partial u_j}{\partial x_i}\right)}$$

$$+ \overline{\left(\frac{\partial u_k}{\partial x_\ell}\frac{\partial u_\ell}{\partial x_k} - \frac{\partial u_k}{\partial x_\ell}\frac{\partial u_\ell}{\partial x_k}\right)^*\left(\frac{\partial u_i}{\partial x_j}+\frac{\partial u_j}{\partial x_i}\right)} \qquad (3.11)$$

$$- g_k \overline{\left(\frac{\partial}{\partial x_k}\frac{\rho}{\bar{\rho}}\right)^*\left(\frac{\partial u_i}{\partial x_j}+\frac{\partial u_j}{\partial x_i}\right)} \Bigg\}\left(\frac{1}{r}+\frac{1}{r^*}\right) dV$$

The three terms of equation (3.11) represent the mean field contribution, the fluctuating field contribution and the bouyancy contribution, respectively. In modelling these expressions the $1/r$ portion which is proportional to $1/r$ will be treated first.

Each of the integrals for the open region accounts for a different effect on the Reynolds Stresses. The model attempts to simulate each of them with a tensor whose components are functions of the determinate mean turbulent variables ($\overline{u_i u_j}$, $\overline{u_i \theta}$). A great deal of attention has been paid to the modelling of the pressure-strain correlation because its redistributive effect on the normal components of Reynolds stress can be dominant, as is the case in a simple shear layer.

The mean field contribution is usually referred to as the rapid term (Lumley, 1978). It was first suggested by Rotta (1951) that the mean velocity gradient undergoes little change over the effective

region of integration and hence may be taken outside the integral. He further suggested that the remaining integral, which is a fourth order tensor, satisfy the phenomenological constraints of symmetry of indicies and incompressibility. Launder, Reece and Rodi (1976) implemented these arguments and suggested that the above integral is a linear combination of Reynolds stresses. The resulting model for the mean velocity contribution is

$$-\frac{1}{2\pi}\int_V \overline{\left(\frac{\partial}{\partial x_\ell}\bar{U}_k\frac{\partial u_\ell}{\partial x_k}\right)^*\left(\frac{\partial u_i}{\partial x_j}+\frac{\partial u_j}{\partial x_i}\right)}\frac{1}{r}\,dV = -\frac{C+8}{11}\left(P_{ij}-\frac{2}{3}\delta_{ij}P\right)$$

$$-\frac{30C-2}{55}\left(\frac{\partial}{\partial x_j}\bar{U}_i+\frac{\partial}{\partial x_i}\bar{U}_j\right)-\frac{8C-2}{11}\left(\mathcal{D}_{ij}-\frac{2}{3}P\delta_{ij}\right) \quad (3.12)$$

where $$\mathcal{D}_{ij} = -\left(\overline{u_i u_k}\frac{\partial}{\partial x_j}\bar{U}_k+\overline{u_j u_k}\frac{\partial}{\partial x_i}\bar{U}_k\right)$$

The same expression has been proposed by Naot, Shavit and Wolfstein (1973). Which, however, derived the expression on the basis of a postulated statistical structure for the turbulent fluctuations. This expression has not been overly successful because the constants must be adjusted for practically every flow to which it is applied (Leslie, 1980). A somewhat more universal expression can be made by retaining the first term only (Launder, Reece and Rodi, 1976) of equation (3.12), at the expense of course of physical relevance, as

$$\frac{1}{2\pi}\int_V \left(\frac{\partial}{\partial x_k}\bar{U}_k\,\overline{\frac{\partial u_k}{\partial x_l}}\right)^*\left(\frac{\partial u_i}{\partial x_j}+\frac{\partial u_j}{\partial x_i}\right)\frac{1}{r}\,dV = -c_{(1)}\left(P_{ij}-\tfrac{2}{3}P\delta_{ij}\right) \quad (3.13)$$

By comparison to data for homogeneous shear flow the value of $c_{(1)}$ is chosen as 0.6.

The contribution from the fluctuating field is represented by the second term of equation (3.9). Rotta (1951) interpreted this term as the effect of pressure in increasing the isotropy of Reynolds stresses and suggested the form

$$\frac{1}{4\pi}\int_V \left(\overline{\frac{\partial u_k}{\partial x_l}\frac{\partial u_i}{\partial x_k}}-\overline{\frac{\partial u_k}{\partial x_l}\frac{\partial u_l}{\partial x_k}}\right)^*\left(\frac{\partial u_i}{\partial x_j}+\frac{\partial u_j}{\partial x_i}\right)\frac{1}{r}\,dV = -c_{(2)}\frac{\epsilon}{k}\left(\overline{u_iu_j}-\tfrac{2}{3}k\delta_{ij}\right) \quad (3.14)$$

Although this form has been critisized by Lumley and Newman (1977) who suggest that non-linear terms are also necessary, it is still in in common use (Launder, Reece and Rodi, 1976; Rodi, 1980). The value $c_{(2)}=1.8$ appears compatible with experiments in nearly homogeneous shear flow.

The final term of equation (3.11) is the buoyancy contribution. Launder (1975) was the first to suggest a model for this term by interpreting equation (3.13) for the mean field contribution as tending to make turbulent production more isotropic. The buoyancy effect also produces turbulence and so it was suggested that it is the total turbulent production which tends to become more isotropic as a result of the pressure strain correlation. The result is a model for the buoyancy term which is analogous to equation (3.13)

$$-\frac{1}{4\pi}\int g_k\left(\frac{2}{\partial x_k}\frac{r_i}{r}\right)^*\left(\frac{2u_i}{\partial x_j}+\frac{2u_j}{\partial x_i}\right)\frac{1}{r}\,dV = C_{(3)}\left(G_{ij}-\tfrac{2}{3}G\delta_{ij}\right) \qquad (3.15)$$

The constant $C_{(3)}$ would be equal to $C_{(1)}$ if Launder's hypothesis were correct. Studies by Gibson and Launder (1978) support this, and hence $C_{(3)} = C_{(2)} = 0.6$.

Combining equations (3.13), (3.14) and (3.15) gives the popular model for the pressure-strain correlation as (Rodi, 1980):

$$\overline{p/\rho\left(\frac{2u_i}{\partial x_j}+\frac{2u_j}{\partial x_i}\right)} = -C_{(1)}\left(P_{ij}-\tfrac{2}{3}P\delta_{ij}\right) - C_{(2)}\frac{\epsilon_{(H)}}{k}\left(\overline{u_iu_j}-\tfrac{2}{3}k\delta_{ij}\right) + C_{(3)}\left(G_{ij}-\tfrac{2}{3}G\delta_{ij}\right) \qquad (3.16)$$

The treatment of the near wall effect is similar to that of the first portion. A proposal based on the previous analysis (ignoring buoyancy) (Launder, Reece and Rodi, 1976) has produced the following result

$$\overline{p/\rho\left(\frac{2u_i}{\partial x_j}+\frac{2u_j}{\partial x_i}\right)}_{(wall)} = \left[0.33\,\frac{\epsilon_{(H)}}{k}\left(\overline{u_iu_j}-\tfrac{2}{3}k\delta_{ij}\right) + 0.039\left(P_{ij}-\tfrac{2}{3}P\delta_{ij}\right)\right]f \qquad (3.17)$$

Alternatively, other investigators (Shir, 1973; Gibson and Launder, 1978) have formed expressions by only requiring that the tensor be traceless and that it extract energy from the component

normal to the wall and add it to the streamwise component. This formula is

$$\overline{p/\rho\left(\frac{\partial u_i}{\partial x_j}+\frac{\partial u_j}{\partial x_i}\right)_{wall}} = \Big[c_{(4)}\frac{\epsilon_{(k)}}{k}\left(\overline{u_k u_m}\, n_k n_m \delta_{ij} - \tfrac{3}{2}\overline{u_k u_i}\, n_k n_j - \tfrac{3}{2}\overline{u_k u_j}\, n_k n_i\right) + c_{(5)}\frac{\epsilon_{(k)}}{k}\left(\psi_{km} n_k n_m \delta_{ij} - \tfrac{3}{2}\psi_{ik} n_k n_j - \tfrac{3}{2}\psi_{jk} n_k n_i\right) + c_{(6)}\frac{\epsilon_{(k)}}{k}\left(\phi_{km} n_k n_m \delta_{ij} - \tfrac{3}{2}\phi_{ik} n_k n_j - \tfrac{3}{2}\phi_{jk} n_k n_i\right)\Big] f \tag{3.18}$$

where $\psi_{km} = -c_{(1)}\left(P_{ij} - \frac{2}{3}P\delta_{ij}\right)$

$\phi_{km} = c_{(3)}\left(G_{km} - \frac{2}{3}G\delta_{km}\right)$

The variable f, appearing in Equations (3.17) and (3.18), is used to ensure that the effect of the wall fades as it becomes more remote. The function f is designated as (Launder, Reece and Rodi, 1976)

$$f = 0.38\, k^{3/2}/\epsilon_{(k)}\, n_i x_i \tag{3.19}$$

In the open region, the near wall effect will be neglected.

The open region approximation of D_{ij} contains indeterminate components of the form $\overline{u_i u_j u_k}$ and $\overline{pu_i}$. This term diffuses the $\overline{u_i u_j}$ correlation and is assumed proportional to the gradient of $\overline{u_i u_j}$. By analogy to molecular transport

$$\overline{u_i u_j u_k} - \frac{1}{\rho}\left(\overline{pu_j}\,\delta_{ik} + \overline{pu_i}\,\delta_{jk}\right) = TTT_{ijklmn}\frac{\partial}{\partial x_n}\overline{u_l u_m} \tag{3.20}$$

The problem then becomes one of specifying $\overline{\Pi}_{ijklmn}$. To resolve this, further investigation into the components of D_{ij} and their governing equations is necessary. The first term may be approximated by constructing its corresponding transport equation

$$\frac{\partial}{\partial t}\overline{u_iu_ju_k} + \bar{U}_k\frac{\partial}{\partial x_k}\overline{u_iu_ju_k} = -\left(\overline{u_ju_ku_k}\frac{\partial}{\partial x_k}\bar{U}_i + \overline{u_iu_ku_k}\frac{\partial}{\partial x_k}\bar{U}_j + \overline{u_iu_ju_k}\frac{\partial}{\partial x_k}\bar{U}_k\right) + \left(\overline{u_iu_j}\frac{\partial}{\partial x_k}\overline{u_iu_k} + \overline{u_ku_i}\frac{\partial}{\partial x_k}\overline{u_ju_k} + \overline{u_iu_j}\frac{\partial}{\partial x_k}\overline{u_ku_k}\right) - \frac{\partial}{\partial x_k}\overline{u_iu_ju_ku_l} + \frac{1}{\bar{\rho}}\left(\overline{u_ju_k\frac{\partial p}{\partial x_i}} + \overline{u_ku_i\frac{\partial p}{\partial x_j}} + \overline{u_iu_j\frac{\partial p}{\partial x_k}}\right) + \bar{\nu}\left(\overline{u_ju_k\frac{\partial^2 u_i}{\partial x_k\partial x_k}} + \overline{u_iu_k\frac{\partial^2 u_j}{\partial x_k\partial x_k}} + \overline{u_iu_j\frac{\partial^2 u_k}{\partial x_k\partial x_k}}\right) + \left(\overline{u_ju_k\rho}/\bar{\rho}\,g_i + \overline{u_iu_k\rho}/\bar{\rho}\,g_j + \overline{u_iu_j\rho}/\bar{\rho}\,g_k\right) \tag{3.21}$$

This equation was obtained by multiplying the u_iu_j equation by u_k and adding to this the product of the u_k equation and u_iu_j, and then averaging the result. Equation (3.21) has introduced many further unknowns. It is simplified by neglecting the convective transport of $\overline{u_iu_ju_k}$, its molecular diffusion and dissipation and any correlation involving pressure. With the assumption that the $\overline{u_iu_ju_ku_l}$ correlation is gaussian, Hanjalic and Launder (1972) have obtained

$$-\overline{u_iu_ju_k} = c_{(7)}\frac{k}{\epsilon_{(u)}}\left(\overline{u_iu_k}\frac{\partial}{\partial x_k}\overline{u_ju_l} + \overline{u_ju_k}\frac{\partial}{\partial x_k}\overline{u_ku_i} + \overline{u_ku_k}\frac{\partial}{\partial x_k}\overline{u_iu_j}\right) \tag{3.22}$$

A similar analysis to that for $\overline{p/\bar{\rho}\left(\frac{\partial u_i}{\partial x_j} + \frac{\partial u_j}{\partial x_i}\right)}$ may be carried out for the exact equation for $\overline{pu_j}$. However, even equation (3.22) is considered too complicated and the whole expression is further simplified to the form (Rodi, 1980)

$$-\overline{u_iu_ju_k}' - \frac{1}{\bar{\rho}}\left(\overline{pu_j}\,\delta_{ik} + \overline{pu_i}\,\delta_{jk}\right) = c_{(7)}\frac{k}{\epsilon_{(u)}}u_ku_k\frac{\partial}{\partial x_k}\overline{u_iu_j} \tag{3.23}$$

This formula was suggested directly by Daly and Harlow (1970) and has been found to be nearly as accurate as Equation (3.22) (Launder, Reece and Rodi, 1976). This last assumption implies that only the gradients of $\overline{u_i u_j}$ are important in determining the diffusion of $\overline{u_i u_j}$. Consequently, D_{ij} is modelled as

$$D_{ij} = c_{(7)} \frac{\partial}{\partial x_k} \left(\frac{k}{\epsilon_{(k)}} \overline{u_k u_\ell} \frac{\partial}{\partial x_\ell} \overline{u_i u_j} \right) \qquad (3.24)$$

In view of the strong assumptions used to derive a gradient diffusion model from the transport equations for $\overline{u_i u_j u_k}$, future models for the diffusion of higher correlations will be derived by analogy to (3.24). Corrsin (1974) has shown the gradient diffusion model to be inaccurate for inhomogeneous flows but it is hoped that this error introduced by it at this level will have an insignificant effect on the mean field variables. The basis of this belief is that it is now just one of a number of other important mechanisms contributing to the determination of $\overline{u_i u_j}$. The value of $c_{(7)}$ has been chosen as 0.22 by Launder, Reece and Rodi (1976).

ϵ_{ij} is the last tensor whose components must be estimated. In high Reynolds number flows, such as occur in the open region, the process of turbulent kinetic energy dissipation is very nearly isotropic (Kolmolgorov, 1942; Monin and Yaglom, 1981), so that (Hanjalic and Launder, 1972)

$$\epsilon_{ij} = \frac{2}{3} \epsilon_{(k)} \delta_{ij} \qquad (3.25)$$

which may be used as an approximation since $\epsilon_{\omega j}$ is determined from a proper transport equation.

3.2.2b Turbulent Heat Flux Equation

The mean turbulent heat flux equation in the open region becomes

$$C_i = P_i + G_i + A_i + D_i - \epsilon_i \qquad (3.26)$$

where the diffusion vector has been simplified to

$$D_i = \frac{\partial}{\partial x_k}\left(-\overline{u_i u_j \theta} - \frac{1}{\rho}\overline{p\theta}\,\delta_{ik}\right)$$

Equation (3.26) contains four vectors, G_i, A_i, D_i and ϵ_i, whose components are indeterminate.

G_i may be expressed as

$$G_i = \beta_{(\theta)}\, g\, g_i \qquad (3.27)$$

by analogy to G_{ij}.

The vector ϵ_i is responsible for the destruction of the $\overline{u_i\theta}$ correlation and has components proportional to $\overline{\frac{\partial u_i}{\partial x_j}\frac{\partial \theta}{\partial x_j}}$. This term can be neglected, considering that at high Reynolds number the dissipation is locally isotropic (Gibson and Launder, 1978).

The vector Δ_i is somewhat similar to the Δ_{ij} tensor modelled in the Reynolds Stress equation and is approached in an analogous manner. Multiplying the integral form of p shown in Equation (3.10) by $\partial\theta/\partial x_k$ and averaging one gets

$$\overline{p/\rho \frac{\partial\theta}{\partial x_k}} = \frac{1}{4\pi}\int_V \Big[\Big(2\frac{\partial}{\partial x_i}\bar{U}_j\frac{\partial u_i}{\partial x_j}\Big)^* \frac{\partial\theta}{\partial x_k} + \overline{\Big(\frac{\partial u_j}{\partial x_i}\frac{\partial u_i}{\partial x_j} - \overline{\frac{\partial u_j}{\partial x_i}\frac{\partial u_i}{\partial x_j}}\Big)^* \frac{\partial\theta}{\partial x_k}} - g_i\overline{\Big(\frac{\partial}{\partial x_i}\frac{r}{\rho}\Big)^* \frac{\partial\theta}{\partial x_k}}\Big]\Big(\frac{1}{r}+\frac{1}{r^*}\Big)dV \qquad (3.28)$$

This is approximated by direct analogy to the Δ_{ij} term of Reynolds Stress equation (Gibson and Launder, 1978). The expression is

$$\Delta_i = \Big(-C_{(8)}P_i - C_{(9)}\frac{\epsilon_{(u)}}{k}\overline{u_i\theta} - C_{(10)}G_i\Big) + \Big(-C_{(11)}C_{(8)}P_* n_i n_k - C_{(12)}C_{(9)}\frac{\epsilon_{(u)}}{k}\overline{u_k\theta}\, n_i n_k - C_{(12)}C_{(10)}G_i n_i n_k\Big) f \qquad (3.29)$$

where $f = 0.38\, k^{3/2}/\epsilon\, n_i x_i$. In the open region f is taken as zero. The constants $C_{(8)}$, $C_{(9)}$, $C_{(10)}$, $C_{(11)}$, $C_{(12)}$ and $C_{(13)}$ were selected by Gibson and Launder (1978) to be 0.33, 3.0, 0.0, 0.0, 0.5 and 0.0 by comparison to experimental data for near equilibrium buoyant flows.

The last vector needing approximation is D_i. Its indeterminate

components are proportional to $\overline{u_i u_j \theta}$ and $\overline{p\theta}$. This is a diffusion term and is therefore treated with the gradient transport model by analogy to D_{ij} with the result (Sha and Launder, 1979)

$$D_i = C_{(14)} \frac{\partial}{\partial x_k} \left(\frac{k}{\epsilon_{(k)}} \overline{u_k u_l} \frac{\partial}{\partial x_l} \overline{u_i \theta} \right) \tag{3.30}$$

The constant $C_{(14)}$ has been chosen as 0.2 by Sha and Launder (1979).

3.2.2c Mean Turbulent Kinetic Energy Equation

The turbulent kinetic energy equation for the open region

$$C_{(k)} = P_{(k)} + G_{(k)} + D_{(k)} - \epsilon_{(k)} \tag{3.31}$$

contains two terms with indeterminate components, $G_{(k)}$ and $D_{(k)}$, which have already been approximated as for the Reynolds stress equations. By contraction

$$G_{(k)} = \frac{1}{2} G_{ij} = \beta_{(p)} \overline{u_i \theta} g_i \tag{3.32}$$

similarly,

$$D_{(k)} = \frac{1}{2} D_{ii} = C_{(1)} \frac{\partial}{\partial x_k} \left(\frac{k}{\epsilon_{(k)}} \overline{u_k u_l} \frac{\partial}{\partial x_l} k \right) \tag{3.33}$$

3.2.2d Mean Turbulent Kinetic Energy Dissipation Rate Equation

The open region form of the mean turbulent kinetic energy dissipation rate equation is

$$C_{(\epsilon)} = S_{(\epsilon)} + G_{(\epsilon)} + D_{(\epsilon)} - \epsilon_{(\epsilon)} \qquad (3.34)$$

where $D_{(\epsilon)}$ has been simplified to

$$D_{(\epsilon)} \equiv \frac{\partial}{\partial x_k}\left(-2\nu\,\overline{u_k \frac{\partial u_i}{\partial x_j}\frac{\partial u_i}{\partial x_j}} - \frac{4\nu}{\rho}\overline{\frac{\partial p}{\partial x_i}\frac{\partial u_k}{\partial x_i}}\right)$$

contains four terms that are composed of the indeterminate variables $S_{(\epsilon)}$, $G_{(\epsilon)}$ $D_{(\epsilon)}$ and $\epsilon_{(\epsilon)}$.

$D_{(\epsilon)}$ is a diffusion term and is modelled by the gradient transport analogy as (Sha and Launder, 1979)

$$D_{(\epsilon)} = C_{(15)} \frac{\partial}{\partial x_k}\left(\frac{k}{\epsilon_{(k)}}\,\overline{u_k u_\ell}\,\frac{\partial \epsilon_{(k)}}{\partial x_\ell}\right) \qquad (3.35)$$

The constant $c_{(15)}$ has been found to be 0.15 by the computer optimization in a number of flows (Launder, Reece and Rodi, 1976).

The closure of the remaining terms of the $\epsilon_{(k)}$ equation is based on the two hypotheses of Kolmolgorov (1942). First, that the turbulent fluctuations contributing to the dissipation of turbulent kinetic energy are isotropic at high Reynolds numbers and hence only isotropic contributions to $\epsilon_{(k)}$ need be considered, thus the $G_{(\epsilon)}$ term resulting from bouyancy effects and zero in isotropic turbulence, can be neglected. Second, that the dissipation rate should be completely determined by the turbulent kinetic energy and its length or time

scale. The $S_{(\epsilon)}$ and $\epsilon_{(\epsilon)}$ terms represent both production and destruction of the dissipation rate. The most common approach (Sha and Launder, 1979; Rodi, 1980) is to assume that the production and destruction of the turbulent energy dissipation is proportional to the production and destruction of the turbulent kinetic energy

$$S_{(\epsilon)} \sim P_{(\epsilon)} + G_{(\epsilon)} \quad \text{and} \quad \epsilon_{(\epsilon)} \sim \epsilon_{(k)} \tag{3.36}$$

where the constant of proportionality is of the order $\epsilon_{(k)}/k$.

This gives

$$\left(S_{(\epsilon)} - \epsilon_{(\epsilon)}\right) = \frac{\epsilon_{(k)}}{k}\left(C_{(16)} P_{(k)} + C_{(17)} G_{(k)} - C_{(18)} \epsilon_{(k)}\right) \tag{3.37}$$

where $C_{(16)}$=1.44, $C_{(17)}$=1.44 and $C_{(18)}$=1.92 (Gibson and Launder, 1976).

3.2.2e Mean Square Fluctuating Temperature Equation

The mean-square temperature fluctuation equation for the open region is

$$C_{(g)} = P_{(g)} + D_{(g)} - \epsilon_{(g)} \tag{3.38}$$

where the diffusion term, $D_{(g)}$, has been simplified to the form

$$D_{(g)} = \frac{\partial}{\partial x_j}\left(-\overline{u_j g}\right)$$

The unknown correlation in $\epsilon_{(g)}$ is $\overline{\frac{\partial g}{\partial x_j}\frac{\partial g}{\partial x_j}}$ which represents the destruction of g by molecular conduction. It is assumed proportional

to the dissipation of turbulent kinetic energy (Launder, 1974). then becomes

$$\epsilon_{(g)} = \frac{2}{c_{(19)}} \alpha \, g/k \, \epsilon_{(k)} \tag{3.39}$$

The value $c_{(19)} = 0.8$ is recommended by Gibson and Launder (1978) to obtain agreement with buoyant shear flows.

Term $D_{(g)}$ contains average products of the form $\overline{u_j g}$. This term represents diffusion and is modelled with the gradient transport assumption as

$$D_{(g)} = c_{(20)} \frac{\partial}{\partial x_k} \left(\frac{k}{\epsilon_{(k)}} \overline{u_k u_l} \frac{\partial}{\partial x_l} g \right) \tag{3.40}$$

where $c_{(20)}$ is taken as 0.15 by Sha and Launder (1979).

The above analysis has provided a closed set of eight equations known as the Reynolds Stress Modal (RSM) for the variables $\overline{U}_i$, $\overline{P}$, $\overline{T}$, $\overline{u_i u_j}$, $\overline{u_i \theta}$, k, g and $\epsilon_{(k)}$ provided that the necessary thermodynamic and fluid properties are known. Although only the variables $\overline{U}_i$, $\overline{T}$, and $\overline{P}$ are of direct interest, the other variables are necessary to close the three primary mean field equations.

The above set of equations has been formulated in three dimensional form, however, its numerical solution for fully three dimensional problems over large domains would be very costly and impractical. The general formulation can be simplified in particular cases which permit a numerical solution.

3.2.3 Simplifications of the Reynolds Stress and Heat Flux Closure

3.2.3a Equilibrium Algebraic Stress Model (EASM)

The equations for the tensors $\overline{u_i u_j}$, $\overline{u_j \phi}$ are all partial differential equations. A significant simplification could be achieved by reducing them to algebraic forms. One way is to neglect all derivatives (Launder, 1971), which implies that the variable is nearly constant along mean material lines. Mathematically, this is expressed for the Reynolds Stress equations as

$$C_{ij} - D_{ij} = 0 \tag{3.41}$$

What remains is the balance of the sources and the sinks of the variable

$$P_{ij} + G_{ij} + \Delta_{ij} - \epsilon_{ij} = 0 \tag{3.42}$$

Expressing these tensors in the determinate variables gives the following semi-explicit equation for the Reynolds stresses

$$\overline{u_i u_j} = \frac{2}{3} k + \frac{k}{\epsilon_{(k)}} \left[\left(\frac{1 - c_{(1)}}{c_{(2)}} \right) \left(P_{ij} - \frac{2}{3} P_{(k)} \delta_{ij} \right) \right. \tag{3.43}$$

$$\left. + \left(\frac{1 + c_{(3)}}{c_{(2)}} \right) \left(G_{ij} - \frac{2}{3} G_{(k)} \delta_{ij} \right) \right]$$

If the approximation is applied to the three normal components of the Reynolds stress tensor and the equations are added, one gets

$$\frac{\partial}{\partial t} k + \bar{U}_j \frac{\partial}{\partial x_j} k - c_{(7)} \frac{\partial}{\partial x_j} \left(\frac{k}{\epsilon_{(k)}} \overline{u_j u_\ell} \frac{\partial}{\partial x_\ell} k \right) = 0 \qquad (3.44)$$

which implies that,

$$P_{(k)} + G_{(k)} = \epsilon_{(k)} \qquad (3.45)$$

or that the turbulent kinetic energy is in local statistical equilibrium. This condition is approximately satisfied in some regions of boundary layers, but not generally in open regions for which equation (3.43) is to be used. The solution of equation (3.44) for weak diffusion produces nearly constant values of k along the mean material lines of the flow; for this reason, it will not be used to find k. Expression (3.43) will, however, be used to calculate all the Reynolds stresses while differential equation (3.31) will be used to calculate k. This inconsistency is justified by the assumption that the Reynolds stresses are weak functions of their net transport rates.

Making a similar assumption for the $\overline{u_i \theta}$ equations

$$C_i - D_i = 0 \qquad (3.46)$$

one gets the result

$$P_i + G_i + \Delta_i = 0 \qquad (3.47)$$

A semi-explicit expression for $\overline{u_i\theta}$ from equation (3.47) is

$$\overline{u_i\theta} = \frac{k}{\epsilon_{(k)}}\left[\left(\frac{1-c_{(8)}}{c_{(7)}}\right)P_i + \left(\frac{1-c_{(10)}}{c_{(7)}}\right)G_i\right] \qquad (3.48)$$

Equations (3.47) and (3.48) form a closed set of equations for $\overline{u_iu_j}$ and $\overline{u_i\theta}$, which consists of algebraic equations for the components of $\overline{u_iu_j}$ and $\overline{u_i\theta}$ very much simpler than the full second order closure. Although these equations were obtained by neglecting derivative terms without fully adequate justification, it appears that the model still reflects some crucial mechanisms of the physical process.

3.2.3b Proportional Transport Algebraic Stress Model (PTASM)

A more realistic means of approximating the differential terms of the $\overline{u_iu_j}$ and $\overline{u_i\theta}$ equations is based on the assumption that the net transport of these variables is proportional to the transport of one or more determinate variables for which a differential equation is being solved. For the $\overline{u_iu_j}$ equations, a suitable expression in terms of k and $\epsilon_{(k)}$ is (Rodi, 1976)

$$C_{ij} - D_{ij} = \frac{\overline{u_iu_j}}{k}\left(C_{(k)} - D_{(k)}\right)$$

or (3.49)

$$P_{ij} + G_{ij} + \Delta_{ij} - \epsilon_{ij} = \frac{\overline{u_iu_j}}{k}\left(P_{(k)} + G_{(k)} - \epsilon_{(k)}\right)$$

The implications of this approximations are made more visible by considering the most restrictive form.

$$C_{ij} = \overline{u_i u_j}/k \; C_{(k)} \tag{3.50}$$

The product rule of differentiation gives exactly

$$\frac{\partial}{\partial t}\left(\frac{\overline{u_i u_j}}{k}\right) + \bar{U}_m \frac{\partial}{\partial x_m}\left(\frac{\overline{u_i u_j}}{k}\right) = 0 \tag{3.51}$$

which implies that the mean material rate of change of $\overline{u_i u_j}/k$ is zero. The resulting expression for $\overline{u_i u_j}$ is

$$\overline{u_i u_j} = \tfrac{2}{3} k \delta_{ij} + \frac{k}{\epsilon_{(k)}}\left[\frac{(1-C_{(1)})\left(P_{ij} - \tfrac{2}{3} P_{(k)}\delta_{ij}\right)}{\left(P_{(k)} + G_{(k)}\right)/\epsilon_{(k)}}\right.$$

$$\left. + \frac{(1+C_{(3)})\left(G_{ij} - \tfrac{2}{3} G \delta_{ij}\right)}{+ \left(C_{(2)} - N\right)}\right] \tag{3.52}$$

A similar approximation for the $\overline{u_i \theta}$ equations is (Gibson, 1978)

$$\frac{\partial}{\partial t}\left(\frac{\overline{u_i \theta}}{\sqrt{k}\sqrt{g}}\right) + \bar{U}_m \frac{\partial}{\partial x_m}\left(\frac{\overline{u_i \theta}}{\sqrt{k}\sqrt{g}}\right) = 0 \tag{3.53}$$

which lends support to the expression

$$\left(C_i - D_i\right) = \frac{\overline{u_i \theta}}{2g}\left(C_{(g)} - D_{(g)}\right) + \frac{\overline{u_i \theta}}{2k}\left(C_{(k)} + D_{(k)}\right) \tag{3.54}$$

or

$$P_i + G_i + \Delta_i = \frac{\overline{u_i\theta}}{2g}\left(P_{(g)} - \epsilon_{(g)}\right) + \frac{\overline{u_i\theta}}{2k}\left(P_{(k)} + G_{(k)} - \epsilon_{(k)}\right)$$

In semi-explicit form, this becomes

$$\overline{u_i\theta} = \left[\frac{(1-C_{(8)})P_i + (1-C_{10})G_i}{C_{(9)}\frac{\epsilon_{(k)}}{k} + \frac{P_{(g)} - \epsilon_{(g)}}{2g} + \frac{P_{(k)} + G_{(k)} - \epsilon_{(k)}}{2k}}\right] \quad (3.55)$$

Equations (3.50) and (3.53) form a closed set of equations, which are similar in complexity and form to the EASM. However, the PTASM was acquired with a more realistic assumption and, presumably, it describes better the physical mechanism of turbulence.

3.2.1c Isotropic Equilibrium Algebraic Stress Model (IEASM)

The EASM was acquired by the local balance of the sources and sinks of the variable and resulted in an equation for $\overline{u_iu_j}$, which, expressed in terms of the degree of isotropy tensor, $a_{ij} = \overline{u_iu_j} - 2/3\ k\delta_{ij}$, is

$$a_{ij} = \frac{k}{\epsilon}\left[\left(\frac{1-C_{(1)}}{C_{(2)}}\right)\left(a_{ik}\frac{\partial}{\partial x_k}\bar{U}_j + a_{jk}\frac{\partial}{\partial x_k}\bar{U}_i + \frac{2}{3}k\left(\frac{\partial}{\partial x_i}\bar{U}_j + \frac{\partial}{\partial x_j}\bar{U}_i\right)\right) + \frac{2}{3}\left(a_{ik}\frac{\partial}{\partial x_k}\bar{U}_i\right)\delta_{ij} + \left(\frac{1+C_{(1)}}{C_{(2)}}\right)\left(\beta_{(p)}\overline{u_j\theta}\,g_i\right. \quad (3.56)$$

$$\left. + \beta_{(p)}\overline{u_i\theta}\,g_j - \frac{2}{3}\overline{u_k\theta}\,g_k\delta_{ij}\right)\Bigg]$$

If the turbulence were nearly isotropic, $a_{ij}a_{ij} \to 0$, then Equation (3.56) would become

$$a_{ij} = -\frac{2}{3}\left(\frac{1-C_{(1)}}{C_{(2)}}\right)\frac{k^2}{\epsilon_{(k)}}\left(\frac{\partial}{\partial x_i}\bar{U}_j + \frac{\partial}{\partial x_j}\bar{U}_i\right)$$
$$+ \left(\frac{1+C_{(3)}}{C_{(2)}}\right)\left(\beta_{(p)}\overline{u_j\theta}\, g_i + \beta_{(p)}\overline{u_i\theta}\, g_j - \frac{2}{3}\overline{u_k\theta}\, g_k \delta_{ij}\right) \tag{3.57}$$

In the nearly isotropic turbulence approximation, the heat flux vector is usually assumed to be unimportant, and therefore neglected for simplicity to give

$$\overline{u_i u_j} = \frac{2}{3}k\delta_{ij} - \frac{2}{3}\left(\frac{1-C_{(1)}}{C_{(2)}}\right)\frac{k^2}{\epsilon_{(k)}}\left(\frac{\partial}{\partial x_i}\bar{U}_j + \frac{\partial}{\partial x_j}\bar{U}_i\right) \tag{3.58}$$

which is similar to the popular k-ϵ turbulence model (Harlow and Nakayama, 1968). This model is often expressed in terms of an eddy viscosity as

$$\overline{u_i u_j} = \frac{2}{3}k\delta_{ij} - \nu_{(t)}\left(\frac{\partial}{\partial x_i}\bar{U}_j + \frac{\partial}{\partial x_j}\bar{U}_i\right) \tag{3.59}$$

where $\nu_{(t)} = C_{(\mu)}\frac{k^2}{\epsilon_{(k)}}$. A crude extrapolation to non-isotropic flow can be made by adjusting the value of $C_{(\mu)}$ to agree with the data.

Turning now to the EASM formulae for $\overline{u_i\theta}$, expressed in terms of the degree of anisotropy tensor a_{ij} it becomes

$$\overline{u_i\theta} = \frac{k}{\epsilon_{(k)}}\left[-\left(\frac{1-C_{(8)}}{C_{(9)}}\right)\left(a_{ij}\frac{\partial}{\partial x_j}\bar{T} + \frac{2}{3}k\frac{\partial}{\partial x_i}\bar{T} + \overline{u_j\theta}\frac{\partial}{\partial x_j}\bar{U}_i\right) + \left(\frac{1-C_{(10)}}{C_{(9)}}\right)\beta_{(p)}g\, g_i\right] \tag{3.60}$$

Again taking the limit as $a_{ij}\,a_{ij} \to 0$ in equation (3.60), one gets

$$\overline{u_i\theta} = -\frac{k}{\epsilon_{(k)}}\left[-\left(\frac{1-C_{(8)}}{C_{(9)}}\right)\left(\frac{2}{3}k\frac{\partial}{\partial x_i}\overline{T} + \overline{u_j\theta}\frac{\partial}{\partial x_j}\overline{U}_i\right) + \left(\frac{1-C_{(10)}}{C_{(9)}}\right)\beta_{(P)}\,g\,g_i\right] \tag{3.61}$$

Neglecting the buoyant contribution for simplicity, the result is

$$\overline{u_i\theta} = -\frac{2}{3}\left(\frac{1-C_{(8)}}{C_{(9)}}\right)\frac{k^2}{\epsilon_{(k)}}\frac{\partial}{\partial x_i}\overline{T} \tag{3.62}$$

When expressed in terms of the turbulent diffusivity this becomes

$$\overline{u_i\theta} = -\Gamma_{(t)}\frac{\partial}{\partial x_i}\overline{T} \tag{3.63}$$

where $\Gamma_{(t)} = \sigma_{(T)}\,C_{(\mu)}\frac{k^2}{\epsilon_{(k)}}$ and the turbulent Prandtl number $\sigma_{(T)}=0.7$. This is an identical result to that given by the $k-\epsilon$ model.

The formulae (3.48) and (3.62) are less general than either the EASM and PTASM expressions which allow for anisotropic conditions, the most common state of turbulence in general flows, and the dependence of strain rates on Reynolds stresses which are not in the same plane. The isotropic assumption has, however, provided simplification which makes a numerical solution manageable. The concept of eddy viscosity preceded the development given here by approximately 140 years (St. Venant, 1843). It was first treated as a constant throughout the flow field although the fact that it was neither homogeneous nor isotropic has long been

recognized. The problem was to specify it accurately as a function of space and direction. Turbulent kinematic viscosity has units of $L^2 s^{-1}$ which can be achieved by the product of a length and a velocity (i.e., $\nu_{(t)} \propto VL$). The velocity scale is generally chosen as the square root of the turbulent kinetic energy, however, there is no obvious choice for the length scale. A suitable choice for length scale is $k^{3/2}/\epsilon_{(x)}$ representing the distance travelled by a particle having a unit of turbulent kinetic energy before its energy is dissipated.

3.2.3d Other Algebraic Relations for $\overline{u_i u_j}$ and $\overline{u_i \theta}$

Another resolution of the turbulence closure problem is Prandtl's "mixing length" hypothesis (1945) developed by direct analogy to the kinetic theory of gases. It requires the specification of a "mixing length", which, in the open regions of a heat exchanger, depends on a constantly changing geometry and is impractical.

3.3 Near-Wall Region

The near-wall region is characterized by steep mean velocity gradients, low mean velocities and the increased significance of molecular action. The first characteristic makes numerical solution of the governing equations impractical because of the number of grid points required to obtain the necessary accuracy. However, the near-wall region is a thin shear layer whose properties are not very senstive to the open region flow, which allows significant simplification of the exact equations. In addition, few heat exchangers are designed to transfer heat through the shell wall so the accuracy of these

calculations is not critical. The analysis of the near-wall region will attempt to obtain simple algebraic or ordinary differential equations for the unknown variables in this region. These will serve to relate the last near wall point of the computational grid to the wall, and hence remove the need for a fine computational mesh in this region.

For the purpose of this analysis the near wall region has been divided into a viscous region and a fully turbulent region. In reality the separation is not so distinct and a buffer region also exists (Hinze, 1975), but this will be ignored for simplicity as will any variation in mean fluid or thermodynamic properties.

The viscous and fully turbulent regions are illustrated in Figure 3. The domination of the flow by viscous effects is assumed to extend until the turbulent Reynolds number, $R_{(t)} = \frac{k^{1/2} x_2}{\bar{\nu}}$, has reached a value of about 20 (Chieng and Launder, 1980), corresponding to dimensionless distances from the wall, $x_1^* < 20 \bar{\nu} k^{*-1/2}$.

The turbulence models recommended for the open region only require boundary conditions for $\bar{U}_i$, $\bar{T}$, k, q, $\epsilon_{(k)}$ and $\epsilon_{(q)}$. It is fortunate that the distributions of $\epsilon_{(k)}$ and $\epsilon_{(q)}$ are known empirically in both regions since their equations cannot be simplified significantly. The remaining four equations will be analyzed to provide information about the distribution of $\bar{U}_i$, $\bar{T}$, k and q. Unfortunately, these equations contain other unknowns such as $\overline{u_i u_j}$, $\overline{u_i k}$, $\overline{u_i \theta}$ and $\overline{u_i q}$. To obtain these from their balance equations would require a very complicated model for those correlations which involve pressure. For this reason these variables will be estimated from experimental investigations in boundary layers.

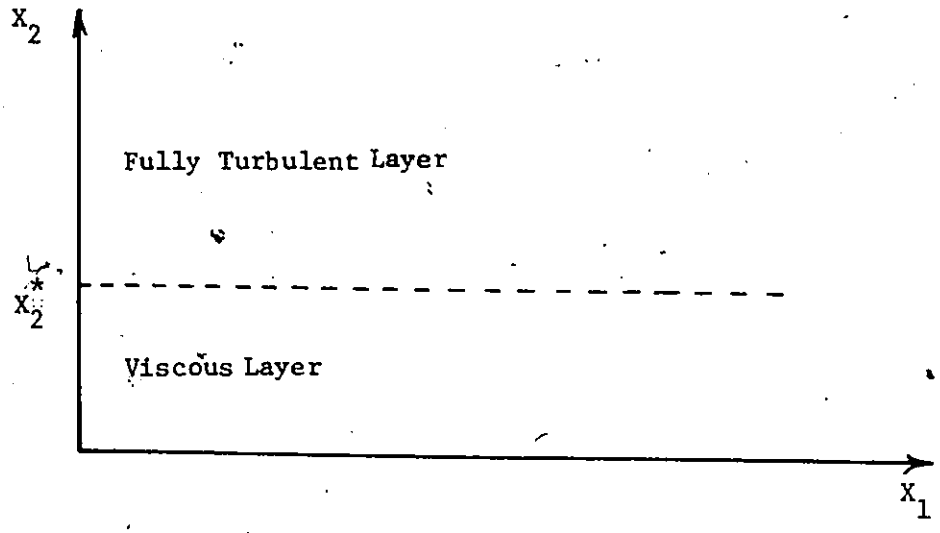

FIGURE 3: Structure of the Near Wall Region

It is assumed that the mean flow in the near wall region always lies in a plane, and hence can be analyzed with only 2 cartesion coordinates, and that the boundary layer thickness is small when compared with the local radius of curvature. This simplifies the problem to a two dimensional rectilinear one.

3.3a The Viscous Layer

An order of magnitude analysis similar to the one employed in Section 3.2 has been performed here using the following scales which are suitable to the viscous sublayer of a boundary layer.

$$\lambda_{(1)} / \Delta \bar{x}_2 = \Theta(10^{-1})$$
$$\mu / \rho \bar{U}_1 \Delta \bar{x}_2 = \Theta(10^{1})$$
$$\bar{U}_2 / \bar{U}_1 = \Theta(10^{-3})$$
$$\Delta_{(2)} \bar{P} / \rho \bar{U}_1^2 = \Theta(10^{-3})$$
$$\lambda_{(3)} / \Delta \bar{x}_2 = \Theta(10^{-1})$$
$$\Delta_{(1)} \bar{T} / \Delta_{(2)} \bar{T} = \Theta(10^{-2})$$
$$|u_i| / \bar{U}_1 = \Theta(10^{-1})$$

$$\Delta \bar{x}_1 / \Delta \bar{x}_2 = \Theta(10^{3})$$
$$\rho C_{(P)} = \Theta(10^{0})$$
$$\Theta / \Delta_{(2)} \bar{T} = \Theta(10^{-1})$$
$$\Delta_{(1)} \bar{P} / \rho \bar{U}_1^2 = \Theta(10^{0}) \quad (3.64)$$
$$\bar{U}_1^2 / C_{(P)} \Delta_{(2)} \bar{T} = \Theta(10^{-1})$$
$$k \Delta_{(2)} \bar{T} / \rho \bar{U}_1^3 \Delta \bar{x}_2 = \Theta(10^{7})$$

The viscous region approximation for the mean velocity equation in the streamwise direction is

$$d^2 \bar{U}_1 / d x_2^2 = 0 \quad (3.65)$$

which with the no slip boundary condition, gives the solution

$$\bar{U}_1 - \bar{U}_{(w)} = \left(\frac{\tau_{(w)}}{\mu} \right) x_2 \quad (3.66)$$

The simplified equation for the mean temperature is

$$d^2\overline{T} / dx_2^2 = 0 \tag{3.67}$$

In order for temperature to satisfy the wall condition it must be of the form

$$\overline{T} - \overline{T}_{(w)} = \left(q_{(w)} / k\right) x_2 \tag{3.68}$$

The simplified mean turbulent kinetic energy equation for the viscous region is

$$d^2k / dx_2^2 = \epsilon_{(k)} / \overline{\nu} \tag{3.69}$$

In the viscous region it has been observed experimentally that $\epsilon_{(k)}$ is constant (Jones and Launder, 1973). Hence, the first derivative of k vanishes at the wall. Since the wall is considered rigid, k also vanishes at the wall. The expression for k which satisfies equation (3.69) and the boundary conditions is

$$k = \left(\frac{\epsilon^*_{(k)}}{\overline{\nu}}\right) x_2^2 \tag{3.70}$$

where the star indicates the level of the variable at y*.

The simplified equation for the mean square fluctuating temperature in the viscous region is

$$d^2g / dx_2^2 = \frac{1}{\alpha}\, \epsilon_{(g)} \tag{3.71}$$

In analogy to the viscous energy dissipation the conductive thermal dissipation will be assumed constant in this region. The boundary conditions for g are not as constraining as these for the kinetic energy. The constant level of $\epsilon_{(g)} (= \mu \overline{\frac{\partial \theta}{\partial x_i} \frac{\partial \theta}{\partial x_i}})$ requires that θ vary linearly in the viscous region. If in addition to this the boundary temperature fluctuation is assumed to be zero, then the solution of equation (3.71) is

$$g = \left(\frac{1}{\alpha} \epsilon^*_{(g)} \right) x_2^2 \tag{3.72}$$

3.3b The Fully Turbulent Portion

The scales which will be used to simplify the equations for the fully turbulent portion are

$$\begin{aligned}
&\lambda_{(u)} / \Delta x_2 = \Theta(10^{-2}) && \lambda_{(g)} / \Delta x_2 = \Theta(10^{-2}) \\
&\bar{U}_2 / \bar{U}_1 = \Theta(10^{-2}) && |u_i| / \bar{U}_1 = \Theta(10^{0}) \\
&\mu / \rho \bar{U}_1 \Delta x_2 = \Theta(10^{-3}) && \Delta_{(1)} \bar{T} / \Delta_{(2)} \bar{T} = \Theta(10^{-2}) \\
&\kappa \Delta_{(2)} \bar{T} / \rho \bar{U}_1^3 \Delta x_2 = \Theta(10^{1}) && \bar{U}_1^2 / C_{(f)} \Delta_2 \bar{T} = \Theta(10^{6}) \\
&\Delta_{(2)} \bar{P} / \rho \bar{U}_1^2 = \Theta(10^{-2}) && \Delta x_1 / \Delta x_2 = \Theta(10^{2}) \\
&\Delta_{(1)} \bar{P} / \rho \bar{U}_1^2 = \Theta(10^{0}) && \theta / \Delta_{(2)} \bar{T} = \Theta(10^{0}) \\
&\rho C_{(f)} = \Theta(10^{0})
\end{aligned} \tag{3.73}$$

The equation for the mean velocity in the fully turbulent region reduces to

$$\frac{d}{dx_2} \overline{u_1 u_2} = 0 \tag{3.74}$$

At the beginning of the turbulent region the turbulent shear stress must be equal to the viscous shear stress which is equal to the wall shear stress. This limits the solution of the equation (3.74) to

$$-\overline{u_1 u_2} = \frac{\tau_{(\omega)}}{\rho} \tag{3.75}$$

It does not, however, restrict $\bar{U}_1$. Experimental investigations (Hinze, 1975) of boundary layers demonstrate that

$$-\overline{u_1 u_2} = \varkappa \sqrt{\frac{\tau_{(\omega)}}{\rho}}\; x_2 \left| \frac{\partial \bar{U}_1}{\partial x_2} \right| \tag{3.76}$$

where $\varkappa$ is the Von-Karman constant, about 0.42. This specifies that the turbulent shear stress is proportional to the distance from the wall. Substituting equation (3.76) into equation (3.75) and integrating over the fully turbulent region one gets

$$\bar{U}_1 - \bar{U}_1^* = \sqrt{\frac{\tau_{(\omega)}}{\rho}} \Big/ \varkappa \; \ln\left(x_2 / x_2^*\right) \tag{3.77}$$

The unknown variable $\bar{U}_1^*$ may be eliminated from equation (3.77) by using equation (3.66) for $\bar{U}_1^*$ to give

$$\frac{\bar{U}_1 - \bar{U}_{(\omega)}}{\sqrt{\frac{\tau_{(\omega)}}{\rho}}} = \frac{1}{\varkappa} \ln\left(x_2 / x_2^*\right) + \left(\sqrt{\frac{\tau_{(\omega)}}{\rho}}\; \frac{\rho}{\mu}\right) x_2^* \tag{3.78}$$

The mean temperature equation for the fully turbulent region reduces to

$$\frac{d}{dx_2}\,\overline{u_2\theta} = 0 \tag{3.79}$$

The turbulent heat flux must equal the heat flux in the viscous region which is also equal to the wall heat flux. This restricts the solution of equation (3.79) to

$$-\overline{u_2\theta} = \frac{q_{(w)}}{\rho C_{(p)}} \tag{3.80}$$

The turbulent heat flux has been found experimentally to be of the form (Hinze, 1975)

$$-\overline{u_2\theta} = \frac{\varkappa}{\sigma_{(T)}}\sqrt{\frac{\tau_{(w)}}{\rho}}\; x_2\; \frac{d}{dx_2}\overline{T} \tag{3.81}$$

for boundary layer flows where $\sigma_{(T)}$ is the turbulent Prandtl number. Substituting equation (3.81) into equation (3.8) and then integrating over the turbulent region one gets the result

$$\overline{T} - \overline{T}^* = \frac{q_{(w)}}{\rho C_{(p)}}\,\frac{\sigma_{(T)}}{\varkappa\sqrt{\tau_{(w)}/\rho}}\,\ln\left(x_2/x_2^*\right) \tag{3.82}$$

The unknown T* may be eliminated in favour of T_w by using equation (3.68). The resulting expression is

$$\frac{\overline{T} - \overline{T}_{(w)}}{q_{(w)}\,\sigma_{(T)}/\rho C_{(p)}\sqrt{\tau_{(w)}/\rho}} = \frac{1}{\varkappa}\ln\left(\frac{x_2}{x_2^*}\right) + \frac{1}{\alpha\sigma_{(T)}}\sqrt{\frac{\tau_{(w)}}{\rho}} \tag{3.83}$$

The equation for the mean turbulent kinetic energy is simplified into the form

$$\overline{u_1 u_2} \frac{d}{dx_2} \bar{U}_1 + \frac{d}{dx_2} \overline{u_2 k} + \epsilon_{(k)} = 0 \qquad (3.84)$$

Using equation (3.75) shows that $\overline{u_1 u_2} = \frac{\tau_{(w)}}{\rho}$, which may be integrated over the fully turbulent region to give

$$\frac{\tau_{(w)}}{\rho}\left(\bar{U}_1 - \bar{U}_1^*\right) + \left(\overline{u_2 k} - \overline{u_2 k}^*\right) + \int_{x_2^*}^{x_2} \epsilon_{(k)}\, dx_2 = 0 \qquad (3.85)$$

The turbulent diffusion term in equation (3.85) is eliminated with the expression

$$\overline{u_2 k} = -\left(\frac{\varkappa}{\sigma_{(k)}} \sqrt{\frac{\tau_{(w)}}{\rho}}\, x_2\right) \frac{dk}{dx_2} \qquad (3.86)$$

In addition, it is known experimentally that in the fully turbulent region (Spalding, 1967)

$$\epsilon_{(k)} = \frac{k^{3/2}}{C_{(l)} x_2} \qquad (3.87)$$

where $C_{(l)}$ is a universal constant equal to 2.55. Equations (3.86) and (3.87) may be substituted into equation (3.84) to give an ordinary integro-differential equation for k

$$\frac{dk}{dx_2} - \frac{\sigma_{(k)}}{\varkappa} \sqrt{\frac{\tau_{(w)}}{\rho}}\, \frac{1}{x_2}\left(\bar{U}_1 - \bar{U}_1^*\right) - \frac{1}{x_2}\left(x_2 \frac{dk}{dx_2}\right)^* - \left(\frac{\sigma_{(k)} C_{(l)}}{\varkappa x_2} \Big/ \sqrt{\frac{\tau_{(w)}}{\rho}}\right) \int_{x_2^*}^{x_2} k^{3/2} \frac{dx_2}{x_2} \qquad (3.88)$$

This is usually simplified by making various assumptions concerning the variation of k over the control volume so that the integral may be eliminated (Chieng and Launder, 1976).

The simplified equation for g is

$$2\overline{u_2\theta}\,\frac{d}{dx_2}\overline{T} + \frac{d}{dx_2}\overline{u_2 g} + \epsilon_{(g)} = 0 \qquad (3.89)$$

Equation (3.80) indicates that $\overline{u_2\theta} = \frac{q_{(w)}}{\rho C_{(p)}}$. This allows integration of equation (3.89) over the turbulent region which gives

$$\frac{2q_{(w)}}{\rho C_{(p)}}\left(\overline{T} - \overline{T}^*\right) + \left(\overline{u_2 g} - \overline{u_2 g}^*\right) + \int_{x_2^*}^{x_2} \epsilon_{(g)}\, dx_2 \qquad (3.90)$$

The turbulent diffusion of g may be eliminated by assuming

$$\overline{u_2 g} = -\frac{\nu}{\sigma_{(g)}}\sqrt{\frac{\tau_{(w)}}{\rho}}\; x_2\, \frac{d}{dx_2} g \qquad (3.91)$$

where $\sigma_{(g)}$ is the turbulent Prandtl number for fluctuating temperature. The conductive destruction is eliminated by assuming that it is proportional to the viscous dissipation

$$\epsilon_{(g)} = \frac{g}{k}\,\frac{1}{c_2}\,k^{3/2}/x_2 \qquad (3.92)$$

Equations (3.91) and (3.92) may be substituted into equation (3.90) to give the ordinary integro-differential equation for

$$\frac{d}{dx_2} g - \frac{\sigma_{(g)}}{\nu}\sqrt{\frac{\tau_{(w)}}{\rho}}\,\frac{1}{x_2}\left(\overline{T} - \overline{T}^*\right) - \frac{1}{x_2}\left(x_2 \frac{d}{dx_2} g\right)^* - \left(\frac{\sigma_{(g)}}{\nu}\,\frac{c_{(p)}}{x_2}\right)\Big/\sqrt{\frac{\tau_{(w)}}{\rho}}\int_{x_2^*}^{x_2} g\, k^{1/2}\,\frac{dx_2}{x_2} \qquad (3.93)$$

This equation may be further simplified by making assumptions concerning the variation of η and k which will eliminate the integral.

3.4 Tube Filled Region

The governing equations for fluid flow have been simplified by an order of magnitude analysis for the special case of the tube filled region. The characteristic dimensionless groups for this purpose are

$$\lambda_{(k)}/|\Delta x_i| = \Theta(10^{-3}) \qquad \Delta\overline{P'}/\bar{\rho}|\bar{U}_i|^2 = \Theta(10^{0})$$
$$\lambda_{(\eta)}/|\Delta x_i| = \Theta(10^{-2}) \qquad P/\bar{\rho}|\bar{U}_i|^2 = \Theta(10^{0})$$
$$|g_i||\Delta x_i|/|\bar{U}_i|^2 = \Theta(10^{-2}) \qquad |u_i|/|\bar{U}_i| = \Theta(10^{0})$$
$$\overline{\rho'}/\bar{\rho} = \Theta(10^{-3}) \qquad \theta/\Delta\overline{T} = \Theta(10^{0})$$
$$r/\bar{\rho} = \Theta(10^{-2}) \qquad \Delta\left(\frac{\partial}{\partial x_i}\bar{U}_i\right)|\Delta x_i|/|\bar{U}_i| = \Theta(10^{-2})$$
$$\bar{\mathcal{H}}/\bar{\rho}|\bar{U}_i||\Delta x_i| = \Theta(10^{-3}) \qquad \Delta\left(\frac{\partial u_i}{\partial x_i}\right)|\Delta x_i|/|\bar{U}_i| = \Theta(0) \quad (3.94)$$
$$\Delta\bar{\mathcal{H}}/\bar{\rho}|\bar{U}_i||\Delta x_i| = \Theta(10^{-5}) \qquad \bar{\mu}/\bar{\rho}|\bar{U}_i||\Delta x_i| = \Theta(10^{-3})$$
$$\bar{C}_{(\rho)}\Delta\overline{T} = \qquad \Delta\bar{\mu}/\bar{\rho}|\bar{U}_i||\Delta x_i| = \Theta(10^{-5})$$
$$\bar{\rho}\bar{C}_{(\eta)} = \Theta(10^{0}) \qquad K\Delta\overline{T}/\bar{\rho}|\bar{U}_i|^3/|\Delta x_i| = \Theta(10^{1})$$
$$\Delta\bar{P}/\bar{\rho}|\bar{U}_i|^2 = \Theta(10^{0}) \qquad \Delta K\Delta\overline{T}/\bar{\rho}|\bar{U}_i|^3/|\Delta x_i| = \Theta(10^{1})$$

3.4.1 Mean Field Equations

The simplified mean field equations of the tube filled region are:

mean momentum

$$\frac{\partial}{\partial t}(\bar{\rho}\bar{U}_i) + \frac{\partial}{\partial x_j}(\bar{\rho}\bar{U}_i\bar{U}_j) = -\frac{\partial}{\partial x_i}\overline{P'}$$
$$+ \frac{\partial}{\partial x_j}\left[\bar{\mu}\left(\frac{\partial}{\partial x_j}\bar{U}_i + \frac{\partial}{\partial x_i}\bar{U}_j\right)\right] \quad (3.95)$$
$$+ \frac{\partial}{\partial x_j}\left(-\bar{\rho}\overline{u_i u_j}\right)$$

mean temperature

$$C_{(p)}\left[\frac{\partial}{\partial t}\left(\bar{\rho}\,\overline{T}\right)+\frac{\partial}{\partial x_j}\left(\bar{\rho}\,\overline{T}\,\overline{U}_j\right)\right]=$$

$$\frac{\partial}{\partial x_j}\left(\kappa\,\frac{\partial}{\partial x_j}\overline{T}\right)+C_{(p)}\frac{\partial}{\partial x_j}\left(-\bar{\rho}\,\overline{u_j\theta}\right) \tag{3.96}$$

mean mass conservation

$$\frac{\partial}{\partial t}\bar{\rho}+\frac{\partial}{\partial x_j}\left(\bar{\rho}\,\overline{U}_j\right)=0 \tag{3.97}$$

Although somewhat simpler than the general form, due to the absence of the buoyancy, divergence and work terms, the above equations are still too complicated to permit a simple analytical solution. An alternative would be a numerical solution, however, this would require a grid density far beyond practical limits due to the very steep mean velocity gradients. A simpler approach is to take advantage of the fact that this region is approaching a "porous medium" (Patankar and Spalding, 1974).

This concept is based on an averaging of the local dependent variables over small volumes in space in an attempt to smooth the variable functions. The volume average is defined as (Slattery, 1981),

$$\underline{A}=\frac{1}{V}\int_{V(f)}A\,dV \tag{3.98}$$

where the underbar denotes a volume averaged variable. V is the sum

of both the fluid and solid volumes, and $V_{(f)}$ is the fluid volume. An example of an averaging volume is shown in Figure 4.

This averaging procedure applied to the mean variables of the tube-filled region produces the volume-averaged variables

$$\underline{\bar{U}}_i = \frac{1}{V}\int_{V_{(f)}} \bar{U}_i \, dV$$

$$\underline{\bar{T}} = \frac{1}{V}\int_{V_{(f)}} \bar{T} \, dV \qquad (3.99)$$

$$\underline{\bar{P}} = \frac{1}{V}\int_{V_{(f)}} \bar{P} \, dV$$

Averaging of the mean continuity equation gives

$$\frac{1}{V}\int_{V_{(f)}} \left[\frac{\partial}{\partial t}\bar{\rho} + \frac{\partial}{\partial x_j}(\bar{\rho}\bar{U}_j) \right] dV = 0 \qquad (3.100)$$

Interchanging the order of averaging and differentiation, as (Slattery, 1981)

$$\frac{\partial}{\partial x_i}\underline{A} = \frac{\partial}{\partial x_i}\underline{A} + \frac{1}{V}\int_{S_{(fs)}} A n_i \, dS \qquad (3.101)$$

where $S_{(fs)}$ is the fluid-solid interface, the continuity equation becomes

$$\frac{\partial}{\partial t}\underline{\bar{\rho}} + \frac{\partial}{\partial x_j}(\underline{\bar{\rho}\bar{U}_j}) + \frac{1}{V}\int_{S_{(fs)}} \bar{\rho}\bar{U}_j n_j \, dS \qquad (3.102)$$

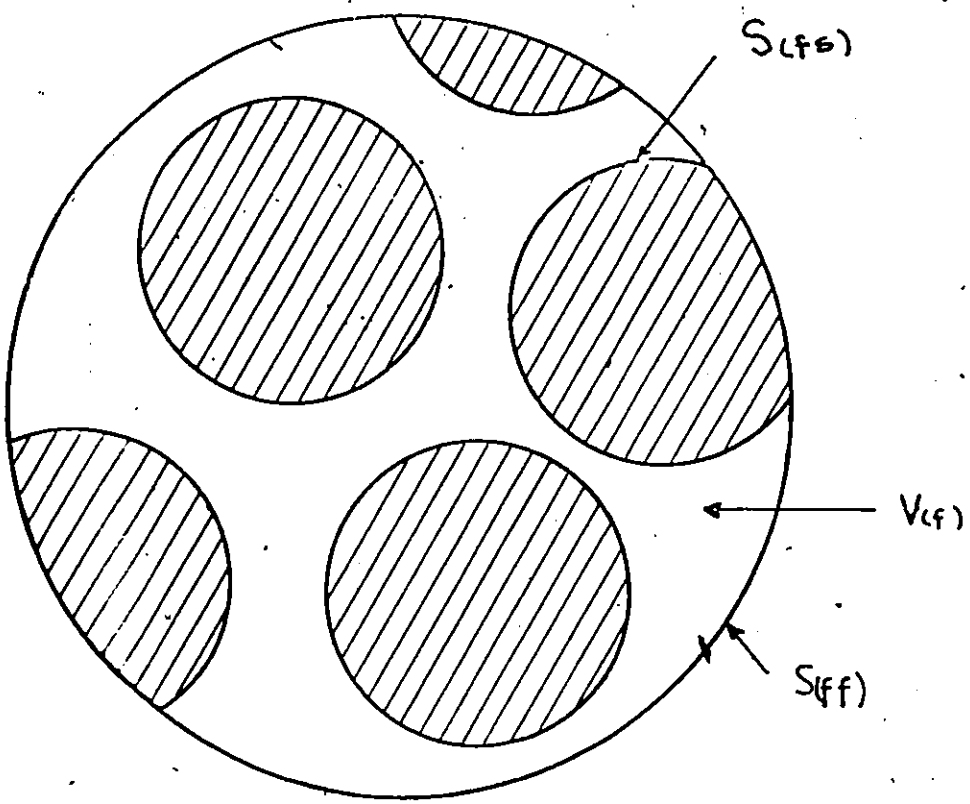

FIGURE 4: Averaging Volume for a Porous Medium

The no-penetration boundary condition for the velocity at the fluid-solid interface causes the surface integral to vanish and Equation (3.102) reduces to

$$\frac{\partial}{\partial t}\bar{\rho} + \frac{\partial}{\partial x_j}(\bar{\rho}\bar{U}_j) = 0 \qquad (3.103)$$

A similar treatment of the mean momentum and mean temperature equations, where $C_{(p)}$, $\bar{\mu}$ and k are constant, yields

$$\frac{\partial}{\partial t}(\bar{\rho}\bar{U}_i) + \frac{\partial}{\partial x_j}(\bar{\rho}\bar{U}_i\bar{U}_j) = -\frac{\partial}{\partial x_i}\bar{P}$$

$$+ \frac{\partial}{\partial x_j}\left[\bar{\mu}\left(\frac{\partial}{\partial x_j}\bar{U}_i + \frac{\partial}{\partial x_i}\bar{U}_j\right)\right] + \frac{\partial}{\partial x_j}(-\bar{\rho}\overline{u_i u_j}) \qquad (3.104)$$

$$+ \frac{1}{V}\int_{S_{(fs)}}\left[-\bar{P}n_i + \bar{\mu}\left(\frac{\partial}{\partial x_j}\bar{U}_i + \frac{\partial}{\partial x_i}\bar{U}_j\right)n_j\right]ds$$

and

$$\bar{C}_{(p)}\left[\frac{\partial}{\partial t}(\bar{\rho}\bar{T}) + \frac{\partial}{\partial x_j}(\bar{\rho}\bar{T}\bar{U}_j)\right] = \frac{\partial}{\partial x_j}\left(k\frac{\partial}{\partial x_j}\bar{T}\right)$$

$$+ \bar{C}_{(p)}\frac{\partial}{\partial x_j}(-\bar{\rho}\overline{u_j\theta}) + \frac{1}{V}\int_{S_{(fs)}} k\frac{\partial}{\partial x_j}\bar{T}\,n_j\,ds \qquad (3.105)$$

$$+ \frac{\partial}{\partial x_j}\left(\frac{k}{V}\int_{S_{(ss)}}\bar{T}n_j ds\right)$$

Equations (3.104) and (3.105), as expected, contain the indeterminate Reynolds stress and the turbulence heat flux. In addition to these unknowns, the averaging has introduced ten new unknowns and three

surface integrals. To eliminate the new unknowns the following assumptions may be made in the application of the porous media concept

i) $\underline{\bar{\rho}\,\bar{U}_i} = \underline{\bar{\rho}}\,\underline{\bar{U}_i}$

ii) $\underline{\bar{\rho}\,\bar{T}} = \underline{\bar{\rho}}\,\underline{\bar{T}}$

iii) $\underline{\bar{\rho}\,\overline{u_i u_j}} = \underline{\bar{\rho}}\,\underline{\overline{u_i u_j}}$

iv) $\underline{\bar{\rho}\,\overline{u_i e}} = \underline{\bar{\rho}}\,\underline{\overline{u_i e}}$

v) $\underline{\bar{\rho}\,\bar{U}_i \bar{U}_j} = \underline{\bar{\rho}}\,\underline{\bar{U}_i}\,\underline{\bar{U}_j}$ (3.106)

vi) $\underline{\bar{\rho}\,\bar{T}\,\bar{U}_j} = \underline{\bar{\rho}}\,\underline{\bar{T}}\,\underline{\bar{U}_j}$

vii) $\frac{\partial}{\partial x_j}\left[\bar{\mu}\left(\frac{\partial}{\partial x_j}\bar{U}_i + \frac{\partial}{\partial x_i}\bar{U}_j\right)\right] << \frac{\partial}{\partial x_j}\left(-\underline{\bar{\rho}\,\overline{u_i u_j}}\right)$

viii) $\frac{\partial}{\partial x_j}\left[\bar{k}\frac{\partial}{\partial x_j}\bar{T} + \frac{\bar{k}}{V_{(s)}}\int_{S(fs)} \bar{T}\, n_j\, dS\right] << \frac{\partial}{\partial x_j}\left(-\bar{c}_{(p)}\,\underline{\bar{\rho}\,\overline{u_j e}}\right)$

Assumptions i) to iv) are justified when the density changes at relatively slow rates over the averaging volume. Assumptions v) and vi) are less justified since they require that both U_j and T have uniform profiles across the flow paths of the tube bundle to be valid. The last two assumptions require that the flow be fully turbulent and that the surface temperature of the tubes vary slowly. These two assumptions are always satisfied in industrial tube bundle flows.

To evaluate the two remaining surface integrals, it is necessary to solve for the local distributions of $\bar{P}$, $\bar{U}_i$ and $\bar{T}$. As a practical alternative, the integrals

$$F_{(1)\,i} = \frac{1}{V} \int_{S(fs)} \left[-\bar{P} n_i + \bar{\mu} \left(\frac{\partial}{\partial x_j} \bar{U}_i + \frac{\partial}{\partial x_i} \bar{U}_j \right) n_j \right] ds$$

$$F_{(2)} = \frac{1}{V} \int_{S(fs)} \bar{k} \frac{\partial}{\partial x_j} \bar{T} n_j \, ds \qquad (3.107)$$

will be approximated by empirical functions. The functions $(F_1)_i$ and $F_{(2)}$ represent the momentum and heat transferred to the tubes, respectively. Simplifications (3.106) and (3.107) reduce equations (3.103), (3.104) and (3.105) to

$$\frac{\partial}{\partial t} \bar{\rho} + \frac{\partial}{\partial x_i} (\bar{\rho} \bar{U}_i) = 0 \qquad (3.108)$$

$$\frac{\partial}{\partial t} (\bar{\rho} \bar{U}_i) + \frac{\partial}{\partial x_j} (\bar{\rho} \bar{U}_i \bar{U}_j) = -\frac{\partial}{\partial x_i} \bar{P} + \frac{\partial}{\partial x_j} (-\bar{\rho} \overline{u_i u_j}) + F_{(3)i} \qquad (3.109)$$

$$\bar{C}_{(p)} \left[\frac{\partial}{\partial t} (\bar{\rho} \bar{T}) + \frac{\partial}{\partial x_j} (\bar{\rho} \bar{T} \bar{U}_j) \right] = \bar{C}_{(p)} \frac{\partial}{\partial x_j} (-\bar{\rho} \overline{u_j \theta}) + F_{(2)} \qquad (3.110)$$

These equations also contain volume averaged Reynolds Stress Tensor and turbulent heat flux vector. A suitable closure method must be found for these quantities.

3.4.2 A Turbulence Model

An analysis of the turbulence data in tube filled regions shows that it is not in a state of equilibrium (Currie, 198), although the non-equilibrium character is essentially confined to the entrance region of the bundle. In that region the mean turbulent kinetic energy rises rapidly due to the mean shear production, but further downstream a production/dissipation balance is attained.

A simple turbulence model for $\overline{u_i u_j}$ and $\overline{u_i \theta}$, is the isotropic equilibrium algebraic stress model which provides equations for k and $\epsilon_{(k)}$. A comparison of the conditions in the tube filled region to those of the open region shows that the open region models may not be applicable to the tube filled region. For example the strong viscous effects near the tube wall, invalidate the earlier models of production and dissipation of $\epsilon_{(k)}$ which assumed local isotropy of the small scales and an inertial spectral subrange. Nevertheless, considering the crudeness of volume averaging, local isotropy and inertial subrange assumptions might be approximately satisfied, within much of the tube-filled region. Thus open region models for the unknown terms of the equation will be applied to the tube filled region, with the only exception being that the molecular diffusion terms will be retained to allow for possible interaction of k and $\epsilon_{(k)}$ with the tubes.

Volume averaging the modelled k equation and interchanging the order of averaging and differentiation gives

$$\frac{\partial}{\partial t}\underline{k} + \frac{\partial}{\partial x_j}(\underline{k}\bar{U}_j) = -\underline{\overline{u_i u_j}\frac{\partial}{\partial x_j}\bar{U}_i} - \underline{\epsilon_{(k)}}$$

$$+ c_{(7)}\frac{\partial}{\partial x_m}\left(\underline{\frac{k}{\epsilon_{(k)}}\overline{u_m u_\ell}\frac{\partial}{\partial x_\ell}k}\right) + \bar{\nu}\frac{\partial}{\partial x_\ell}\underline{k} \qquad (3.111)$$

$$+ \frac{1}{V_{(s)}}\int_{S_{(s)}} \bar{\nu}\frac{\partial}{\partial x_\ell} k\, n_\ell\, dS .$$

Assumptions similar to (3.106) concerning the material derivative and diffusion terms may be made in (3.111). These are

$$\text{i)}\quad \underline{k\bar{U}_j} = \underline{k}\,\underline{\bar{U}_j}$$

$$\text{ii)}\quad \frac{\partial}{\partial x_\ell}\left(\bar{\nu}\frac{\partial}{\partial x_\ell}\underline{k}\right) << \underline{c_{(7)}\frac{\partial}{\partial x_m}\left(\frac{k}{\epsilon_{(k)}}\overline{u_m u_\ell}\frac{\partial}{\partial x_\ell}k\right)} \qquad (3.112)$$

$$\text{iii)}\quad \underline{c_{(7)}\frac{k}{\epsilon_{(k)}}\overline{u_m u_\ell}\frac{\partial}{\partial x_\ell}k} = \underline{c_{(7)}}\,\underline{k}\left(\underline{\epsilon_{(k)}}\right)^{-1}\underline{\overline{u_m u_\ell}}\,\underline{\frac{\partial}{\partial x_\ell}k}$$

The surface integral represents the interaction of turbulent kinetic energy with the tubes. This integral is zero, however, because in the viscous sublayer turbulent kinetic energy varies quadraticly (Jones and Launder, 1973). The production term of Equation (3.111) requires special treatment. It would be unrealistic to equate

$$\underline{-\overline{u_i u_j}\frac{\partial}{\partial x_j}\bar{U}_i} \qquad \text{with} \qquad \underline{-\overline{u_i u_j}\frac{\partial}{\partial x_j}\bar{U}_i} \qquad (3.113)$$

because this would ignore much of the production in the tube filled region. As a solution to this problem the production may be formulated as the sum of two portions

$$-\overline{u_i u_j}\frac{\partial}{\partial x_j}\bar{U}_i = -\overline{u_i u_j}\frac{\partial}{\partial x_j}\bar{U}_i + F_{(3)} \qquad (3.114)$$

The first term accounts for the production caused by the volume averaged mean velocity gradients, and the second for the production due to the local velocity gradients around the tubes. The $F_{(3)}$ term may be prescribed as an empirical function of the volume average variables. With these modifications the k equations becomes

$$\frac{\partial}{\partial t}k + \frac{\partial}{\partial x_j}\left(k\bar{U}_j\right) = \left(-\overline{u_i u_j}\frac{\partial}{\partial x_j}\bar{U}_i + F_{(3)}\right) - \epsilon_{(k)} + C_{(7)}\frac{\partial}{\partial x_m}\left(k\,\epsilon_{(k)}^{-1}\,\overline{u_m u_\ell}\frac{\partial}{\partial x_\ell}k\right) \qquad (3.115)$$

The equation for $\epsilon_{(k)}$ may be volume-averaged and with simplifications analogous to (3.112) it becomes

$$\frac{\partial}{\partial t}\epsilon_{(k)} + \frac{\partial}{\partial x_j}\left(\epsilon_{(k)}\bar{U}_j\right) = C_{(16)}\frac{\epsilon_{(k)}}{k}\left(-\overline{u_i u_j}\frac{\partial}{\partial x_j}\bar{U}_i\right) - C_{(18)}\epsilon^2 k^{-1} + C_{(15)}\frac{\partial}{\partial x_m}\left(k\,\epsilon_{(k)}^{-1}\,\overline{u_m u_\ell}\frac{\partial}{\partial x_\ell}\epsilon\right) + F_{(4)} \qquad (3.116)$$

where

$$F_{(4)} = \frac{1}{V}\int_{S_{(fs)}} \nu\frac{\partial}{\partial x_j}\epsilon_{(k)}\,n_j\,dS$$

The production and dissipation will be treated in a manner which is similar to that used in the $\underline{k}$ equation

$$c_{(16)} \frac{\epsilon_{(k)}}{k} \left(-\overline{u_i u_j} \frac{\partial}{\partial x_j} \overline{U}_i \right) = \underline{c_{(16)}} \; \underline{\epsilon_{(k)}} \underline{k}^{-1} \left(-\underline{\overline{u_i u_j}} \frac{\partial}{\partial x_j} \underline{\overline{U}_i} + F_{(3)} \right) \tag{3.117}$$

$$c_{(18)} \underline{\epsilon_{(k)}^2 k^{-1}} = \underline{c_{(18)}} \; \underline{\epsilon_{(k)}}^2 \underline{k}^{-1}$$

These simplifications reduce the $\epsilon_{(k)}$ equation into the following form

$$\frac{\partial}{\partial t} \underline{\epsilon_{(k)}} + \frac{\partial}{\partial x_j} \left(\underline{\epsilon_{(k)}} \, \underline{\overline{U}_j} \right) = \underline{c_{(16)}} \; \underline{\epsilon_{(k)}} \; \underline{k}^{-1} \left[-\underline{\overline{u_i u_j}} \frac{\partial}{\partial x_j} \underline{\overline{U}_i} + F_{(3)} \right] - \underline{c_{(18)}} \; \underline{\epsilon_{(k)}}^2 \; \underline{k}^{-1} + \underline{c_{(15)}} \frac{\partial}{\partial x_m} \left[\underline{k} \; \underline{\epsilon_{(k)}^{-1}} \; \underline{\overline{u_m u_n}} \frac{\partial}{\partial x_n} \underline{\epsilon_{(k)}} \right] \tag{3.118}$$

The IEASM formulations for the Reynolds Stress tensor and the turbulent heat flux vector may be volume averaged to give the approximate results

$$\underline{\overline{u_i u_j}} = - \underline{\nu_{(t)}} \left(\frac{\partial}{\partial x_j} \underline{\overline{U}_i} + \frac{\partial}{\partial x_i} \underline{\overline{U}_j} \right) + \frac{2}{3} \underline{k} \, \delta_{ij} \tag{3.119}$$

$$\underline{\overline{u_i \theta}} = - \underline{\Gamma_{(t)}} \; \frac{\partial}{\partial x_i} \underline{\overline{T}} \tag{3.120}$$

which is consistent with assumptions (3.106) and (3.112) and the empirical assertion that most of the diffusion occurs in regions where $\nu_{(t)}$ and $\Gamma_{(t)}$ have a modest slope.

3.5 Closure

The purpose of this investigation was to select turbulence models for use in industrial heat exchangers. This was done by an analysis of the fundamental equations of fluid mechanics. These equations were simplified by order of magnitude analyses for the three characteristic regions of a heat exchanger:

- tube free
- near wall region
- tube filled region.

In the open region the turbulence model must be sufficiently general to provide confidence in parametric optimization. Thus, a full Reynolds stress model was derived for this region. Although this method is impractical for numerical calculations, it provided a guide for deriving more usable models, namely a) the equilibrium algebraic stress model (EASM), b) the proportional transport algebraic stress model (PTASM), and c) the isotropic equilbrium algebraic stress model (IEASM). These models are respectively based on the assumptions that

a) there is negligible transport of the Reynolds stresses,

b) the net transport of Reynolds stress is proportional to the net transport of the turbulent kinetic energy, and

c) there is a nearly isotropic turbulent state with little transport of the Reynolds Stresses.

The simplest of these models is the third one, however, a comparison with experimental data is necessary to determine which gives the best compromise between accuracy and simplicity.

In the near wall region the Reynolds Stresses and turbulent heat fluxes can be modelled with empirical functions. The resulting equations are simple enough to allow analytic or one-dimensional numerical solution.

The tube-filled region was modelled using the porous-medium approach. A feature of the flow in this region is its non-equilibrium turbulence state near the boundaries of the tube bundle. The simplest turbulence model that reflects these characteristics is the nearly isotropic equilibrium model. When this model is expressed in porous media form, three additional empirical functions are introduced, which must be specified by further modelling.

The turbulence models proposed for the three regions contain a number of uncertain assumptions and a great deal of empiricism. For this reason, the predictive ability of these models will be compared to experimental data collected in a few simple shear flows.

CHAPTER IV

COMPUTATIONS OF UNIFORMLY SHEARED TURBULENCE

4.1 Introduction

In Chapter III, three turbulence models have been developed for possible use in the open region of heat exchangers: a) the Equilibrium Algebraic Stress Model (EASM), b) the Proportional Transport Algebraic Stress Model (PTASM), and c) the Isotropic Equilibrium Albegraic Stress Model (IEASM).

In this chapter, these models will be tested in the simplest turbulent shear flow, that with a undirectional mean velocity and a constant mean gradient in a transverse direction; in such a flow, the mean velocity is defined as,

$$\bar{U}_i = (\bar{U}_1, 0, 0) \qquad (4.1)$$

where $\bar{U}_1 = Ax_2 + \bar{U}_{(c)}$, A and $\bar{U}_{(c)}$ = constant

and is shown in Figure 5. The advantage of this shear flow is that it allows the study of the turbulent shear stress and its relation to the mean shear strain in the absence of other complicating effects such as boundaries and inhomogeneity. This type of flow has been investigated experimentally by several researchers, most notably by Rose (1966, 1967), Champagne, Harris and Corrsin (1980), Mulhearn and Luxton (1970, 1975), Tavoularis and Corrsin (1981) and Karnik and Tavoularis (1983). The latter study will be used for comparison with the present predictions.

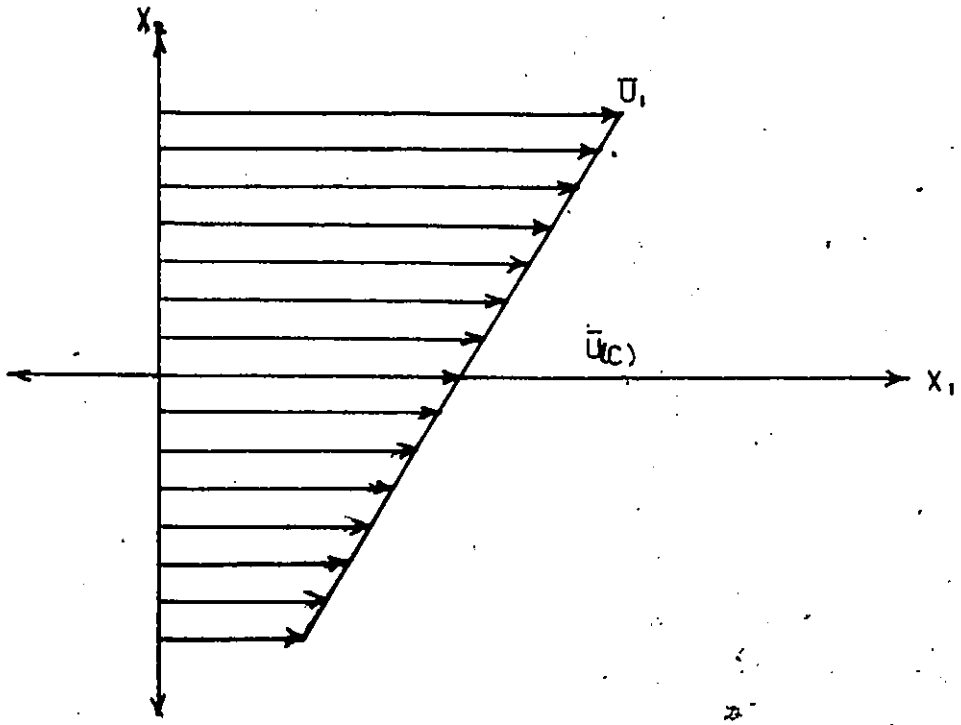

FIGURE 5: Uniform Shear Flow

Predictions of turbulent kinetic energy, integral length scale and Reynolds stress tensor are made using each turbulence model. These are then compared to one another and to the experimental measurements of Karnik and Tavoularis (1983) and to those in Karnik's M.A.Sc. thesis (1983).

4.2 Governing Equations

The mean velocity described in Section 4.1 for a fluid with constant properties is coupled to the other flow parameters through the dynamic equations of motion. The three turbulence models which will be analyzed here have four transport equations in common; a) mean mass; b) mean momentum c) mean turbulent kinetic energy and d) mean turbulent kinetic energy dissipation rate. These four equations will be simplified for this uniform shear flow and then each individual model will be dealt with separately.

4.2.1 Transport Equations

The mean mass conservation equation for the open region simplifies to the trivial case, 0=0.

The mean momentum equation for the open region reduces to

$$\frac{\partial}{\partial x_i}\overline{P} = \frac{\partial}{\partial x_j}\left(\rho\overline{u_i u_j}\right) \qquad (4.2)$$

Further simplification is achieved by the flow symmetry about the x_1-x_2 plane and all planes parallel to it. This requires that

$$\overline{u_1 u_3} = 0 \,, \quad \overline{u_2 u_3} = 0 \quad \text{and} \quad \frac{\partial}{\partial x_3}\left(\overline{\cdots}\right) = 0 \qquad (4.3)$$

Using the fact that Karnik's data shows negligible transverse variation of $\overline{u_i u_j}$ one may simplify equation (4.2) to

$$\begin{aligned} \frac{1}{\rho}\frac{\partial}{\partial x_1}\overline{P} &= \frac{d}{dx_1}\overline{u_1^2} \\ \frac{1}{\rho}\frac{\partial}{\partial x_2}\overline{P} &= \frac{d}{dx_1}\overline{u_1 u_2} \\ \frac{1}{\rho}\frac{\partial}{\partial x_3}\overline{P} &= 0 \end{aligned} \qquad (4.4)$$

The modelled mean turbulent kinetic energy equation for the open region is reduced to

$$\overline{U}_1 \frac{d}{dx_1} k = -\overline{u_1 u_2}\frac{d}{dx_2}\overline{U}_1 - \epsilon_{(k)} + C_{(7)}\left[\frac{\partial}{\partial x_j}\left(\frac{k}{\epsilon_{(k)}}\overline{u_i u_j}\frac{\partial}{\partial x_j}k\right)\right] \qquad (4.5)$$

When the convection rate is large, streamwise diffusion may be ignored. Ignoring the cross-steam diffusion as the data would suggest results in an anomaly. The production rate $-\overline{u_1 u_2}\, d\overline{U}_1/dx_2$ is homogeneous in the x_2 -direction, but the convection rate is not, since $U_1 = Ax_2 + \overline{U}_{(c)}$. If, however, $\overline{U}_1/\overline{U}_{(c)}$ is nearly one in the region of interest then the dependence of convection on x_2 is a second order one. In the experiment of Karnik (1983), the value of $\overline{U}_1/\overline{U}_{(c)}$ varied from 0.75 to 1.5.

If the convection rate is assumed proportional to $\bar{U}_{(c)}$ and diffusion ignored, then it would be possible for k to be only a function of x_1, if this is true initially, since there is no other explicit appearance of x_2 or x_3 in equation (4.5). The remaining turbulence equations, as will be shown, are only functions of x_2 or x_3 if k and $\epsilon_{(k)}$ are functions of x_2 or x_3.

It has been assumed by Tavoularis (1984) that diffusion is negligible, and the same will be done here. The neglect of diffusion prevents the interaction of mean streamlines, and hence, they may be treated individually. This does not remove the problem arising from the fact that the convection is dependent on x_2 and production is not. Tavoularis (1984) has suggested that the dissipation is a function of x_2 to maintain the required balance.

All calculations will be performed along the channel centreline where the convection rate equals $\bar{U}_{(c)}$ and all turbulence parameters will be assumed to be functions of x_1 only. Equation (4.5) now becomes

$$\bar{U}_{(c)} \frac{d}{dx_1} k = -\overline{u_1 u_2} \frac{d}{dx_2} \bar{U}_1 - \epsilon_{(k)} \qquad (4.6)$$

Following a procedure analogous to that for the k equation, one may reduce the modelled mean turbulent kinetic energy dissipation rate for the open region to the form

$$\bar{U}_{(c)} \frac{d}{dx_1} \epsilon_{(k)} = c_{(1\epsilon)} \frac{\epsilon_{(k)}}{k} \left(-\overline{u_1 u_2} \frac{d}{dx_2} \bar{U}_1 \right) - c_{(2\epsilon)} \frac{\epsilon_{(k)}^2}{k} \qquad (4.7)$$

Equations (4.6) and (4.7) must be solved simultaneously with an equation for $\overline{u_1 u_2}$. Some insight into their solution, and the implications of the modelling assumptions made to obtain the $\epsilon_{(k)}$ equation can be achieved in the following way.

In the development of the $\epsilon_{(k)}$ equation it was assumed that its production and dissipation were proportional to the production and dissipation of k (see Section 3.1). Rewriting equations (4.6) and (4.7) with $P_{(k)} = -\overline{u_1 u_2}\ d\bar{U}_1/dx_2$

$$\bar{U}_{(c)} \frac{d}{dx_1} k = P_{(k)} - \epsilon_{(k)} \qquad (4.8)$$

$$\bar{U}_{(c)} \frac{d}{dx_1} \epsilon_{(k)} = C_{(16)} \frac{\epsilon_{(k)}}{k} P_{(k)} - C_{(18)} \frac{\epsilon_{(k)}^2}{k} \qquad (4.9)$$

If $\epsilon_{(k)}$ is eliminated from these equations in favour of the ratio $l = \frac{k^{C_{(16)}}}{\epsilon_{(k)}}$, then equation (4.8) becomes

$$\bar{U}_{(c)} \frac{d}{dx_1} k = P_{(k)} - \frac{k^{C_{(16)}}}{l} \qquad (4.10)$$

and equation (4.9) becomes

$$\bar{U}_{(c)} \left(k^{C_{(16)}} l^{-1} \right) = C_{(16)} \frac{k^{C_{(16)}-1}}{l} P_{(k)} - C_{(18)} \frac{k^{2C_{(16)}-1}}{l^2} \qquad (4.11)$$

Expanding the left hand side and rearranging the right hand side gives the result

$$\bar{U}_{(c)}\left(c_{(16)}\ell^{-1}k^{c_{(16)}-1}\frac{d}{dx_1}k-\frac{k^{c_{(16)}}}{\ell^2}\frac{d}{dx_1}\ell\right)=$$

$$c_{(16)}\frac{k^{c_{(16)}-1}}{\ell}\left(P_{(k)}-\frac{k^{c_{(16)}}}{\ell}\right)+\left(c_{(16)}-c_{(18)}\right)\frac{k^{2c_{(16)}-1}}{\ell^2} \qquad (4.12)$$

Using equation (4.10) to eliminate $\left(P_{(k)}-\frac{k^{c_{(16)}}}{\ell}\right)$ from equation (4.12) gives the relation

$$\bar{U}_{(c)}\frac{d}{dx_1}\ell=\left(c_{(18)}-c_{(16)}\right)k^{c_{(16)}-1} \qquad (4.13)$$

This equation may be integrated to obtain

$$\ell=\frac{\left(c_{(18)}-c_{(16)}\right)}{\bar{U}_{(c)}}\int k^{c_{(16)}-1}\,dx_1+\ell_{(0)} \qquad (4.14)$$

Now substituting equation (4.14) into equation (4.10) gives the result

$$\bar{U}_{(c)}\frac{d}{dx_1}k=P_{(k)}-\frac{k^{c_{(16)}}}{\frac{\left(c_{(18)}-c_{(16)}\right)}{\bar{U}_{(c)}}\int k^{c_{(16)}-1}\,dx_1+\ell_{(0)}} \qquad (4.15)$$

In this flow, equation (4.14) imples that ℓ grows indefinitely if $c_{(18)}$ is greater than $c_{(16)}$ and vice-versa, because the integrand is always positive.

The definition of a ratio of the form $\ell = \frac{k^{c_{(16)}}}{\epsilon_{(k)}}$ is not new and has been expressed more generally by Spalding (1982) as $\ell^n = k^m / z$, where z represents a few different parameters, by Spalding (1982). Specific reference to the case where n=1, m=3/2 and ℓ is a constant length scale has been made by Spalding and Launder (1974). However, the implications of $c_{(16)} \neq c_{(18)}$ have not been discussed in earlier references. Equation (4.15) clearly shows that the growth of ℓ, which represents a dissipation length scale if $c_{(16)}=1.5$, is directly proportional to ($c_{(18)} - c_{(16)}$).

The dissipation length scale ℓ has been found experimentally by Townsend (1976) to be approximately ($k^{1.5}-c_{(16)}/1.06$) times the integral length scale of turbulence in homogeneous flows.

4.2.2 Algebraic Expressions for Reynolds Stresses

Algebraic relations for $\overline{u_i u_j}$ are provided by three models: a) EASM, b) PTASM, and c) IEASM. For convenience in the analysis, the equations will be formulated in terms of the non-dimensional Reynolds Stress tenor $K_{ij}(=2\overline{u_i u_j}/k)$. For this reason $\overline{u_i u_j}$ will be replaced by it in all formulae.

Each model results in an expression which depends on k, $\epsilon_{(k)}$ and P_{ij}. In this flow, P_{ij} simplifies to

$$P_{ij} = \begin{pmatrix} -4k\,K_{12}\,d\bar{U}_1/dx_2 & -2k\,K_{22}\,d\bar{U}_1/dx_2 & 0 \\ -2k\,K_{22}\,d\bar{U}_1/dx_2 & 0 & 0 \\ 0 & 0 & 0 \end{pmatrix} \quad (4.16)$$

4.2.2a EASM

The relation for K_{ij} provided by the EASM for isothermal flow is

$$K_{ij} = \left(\frac{1-C_{(1)}}{C_{(2)}}\right)\frac{P_{ij}}{\epsilon_{(k)}} + \frac{1}{2}\left(\frac{C_{(1)}+C_{(2)}-1}{C_{(2)}}\right)\delta_{ij} \qquad (4.17)$$

After substituting equation (4.16) into equation (4,17) the components of K_{ij} are found as

$$K_{11} = \frac{1}{3}\left[2\left(\frac{1-C_{(1)}}{C_{(2)}}\right) + \left(\frac{C_{(1)}+C_{(2)}-1}{C_{(2)}}\right)\right]$$

$$K_{12} = -\frac{1}{3}\left(\frac{1-C_{(1)}}{C_{(2)}}\right)\left(\frac{C_{(1)}+C_{(2)}-1}{C_{(2)}}\right)\zeta$$

$$K_{13} = 0$$

$$K_{22} = \frac{1}{3}\left(\frac{C_{(1)}+C_{(2)}-1}{C_{(2)}}\right) \qquad (4.18)$$

$$K_{23} = 0$$

$$K_{33} = \frac{1}{3}\left(\frac{C_{(1)}+C_{(2)}-1}{C_{(2)}}\right)$$

where ζ is $k\,d\bar{U}_1/dx_2/\epsilon_{(k)}$.

These relations are plotted versus ζ in Figure 6a. The value for K_{12} becomes unrealistic when ζ is large, since Schwarz's inequality requires that $|K_{12}| \leq 1$.

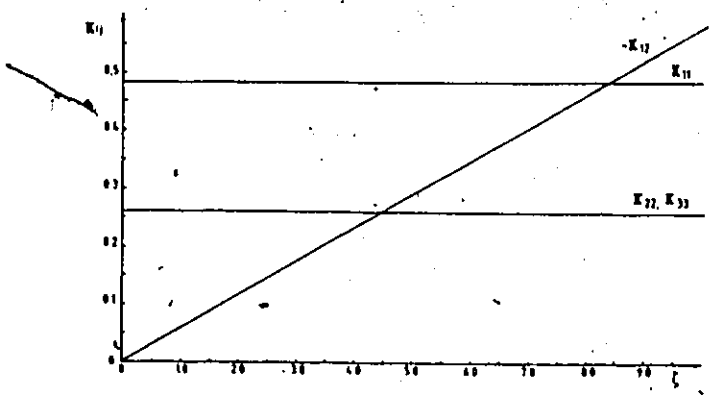

(a)

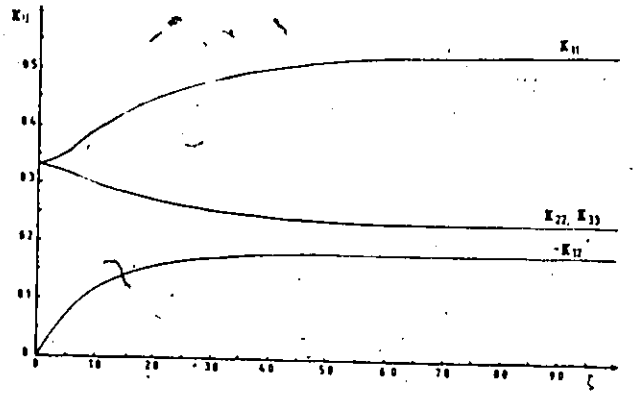

(b)

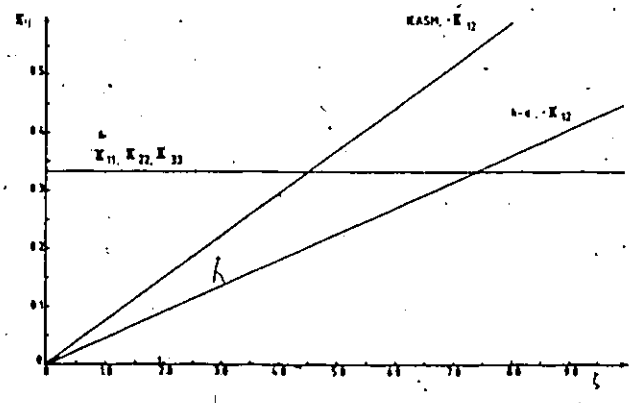

(c)

FIGURE 6: Variation of the Dimensionless Reynolds Stress with the Ratio of Turbulent to Mean Time Scale for (a) EASM, (b) PTASM, (c) IEASM and k-ε Model

4.2.2b PTASM

The expression for K_{ij} provided by the PTASM for isothermal flow is

$$K_{ij} = \frac{1}{3}\delta_{ij} + \left[\frac{2(1-c_{(1)})(P_{ij} - \frac{2}{3}P_{(k)}\delta_{ij})}{P_{(k)} + G_{1(k)} + (c_{(2)}-1)\epsilon_{(k)}}\right] \tag{4.19}$$

Substituting P_{ij} for this flow, one gets the equations for the components of K_{ij} as

$$K_{11} = \frac{1}{3} + \left[\frac{(6-4c_{(1)})(-K_{12})\zeta + (c_{(2)}-1)}{2(-K_{12})\zeta + (c_{(2)}-1)}\right]$$

$$K_{12}^3 - \left[(c_{(2)}-1)/\zeta\right] K_{12}^2 + \left[\left(\frac{c_{(2)}-1}{2\zeta}\right)^2 - \frac{c_{(1)}(1-c_{(1)})}{6}\right] K_{12} + \left[\frac{(1-c_{(1)})(c_{(2)}-1)}{12\zeta}\right] = 0 \tag{4.20}$$

$$K_{13} = 0$$

$$K_{22} = \frac{1}{3}\left[\frac{2c_{(1)}(-K_{12})\zeta + (c_{(2)}-1)}{2(-K_{12})\zeta + (c_{(2)}-1)}\right]$$

$$K_{23} = 0$$

$$K_{33} = \frac{1}{3}\left[\frac{2c_{(1)}(-K_{12})\zeta + (c_{(2)}-1)}{2(-K_{12})\zeta + (c_{(2)}-1)}\right]$$

The above relations have been plotted in Figure 6b. This model's asymptotic prediction for $-K_{12}$ is realistic, since it is bounded by 0.2.

4.2.2c **IEASM and k-ε Model**

The expression for K_{ij} provided by the IEASM is for isothermal flow

$$K_{ij} = \frac{1}{3}\delta_{ij} - \frac{1}{3}\left(\frac{1-c_{(1)}}{c_{(2)}}\right)\frac{k}{\epsilon_{(4)}}\left(\frac{\partial}{\partial x_j}\bar{U}_i + \frac{\partial}{\partial x_i}\bar{U}_j\right) \qquad (4.21)$$

For this flow the components of K_{ij} are

$$\begin{aligned} K_{11} &= \frac{1}{3} \\ K_{12} &= -\frac{1}{3}\left(\frac{1-c_1}{c_2}\right)\xi \\ K_{13} &= 0 \\ K_{22} &= \frac{1}{3} \\ K_{23} &= 0 \\ K_{33} &= \frac{1}{3} \end{aligned} \qquad (4.22)$$

To permit use of this model in non-isotropic flows, the constants $c_{(1)}$ and $c_{(2)}$ have been adjusted such that $K_{12} = 0.045\xi$ (Rodi, 1980). With this adjustment of constants, the IEASM becomes the k-ε model of turbulence.

The relations between K_{ij} and ξ for these variations is shown in Figure 6c.

This model also produces values for K_{12} which are unrealistic when ζ is large.

4.3 Solution of the Equations

4.3.1 General Solution Procedure

The simultaneous solution of equations (4.10, 4.13 and 4.18b or 4.20b or 4.22b) is required to obtain k, ℓ, and K_{ij} for each of the models of Section 4.2.2. It is apparent that the components of K_{ij} depend only on the variable ζ which may be more clearly recognized if $\epsilon_{(k)}$ is expressed as $k^{3/2}/(1.06L)$ where L is the integral length scale. Then becomes $(d\bar{U}_1/dx_2)/(k^{\frac{1}{2}}/1.06L)$ which represents the ratio of turbulent field time scale to the mean field time scale.

When ζ is small, namely when the mean field time scale is large compared to the turbulent time scale the turbulent field is able to adjust to the mean field which results in similarity of the flow (Townsend, 1976). The other limit when the mean field time scale is short compared to the turbulent time scale, has been the subject of a different approximation, known as the Rapid Distortion Theory (Townsend 1979).

It is possible to derive an equation for ζ from Equations (4.8) and (4.9), the product rule of differentiation requires that

$$\bar{U}_{(c)} \frac{d}{dx_1}\left(k \epsilon_{(k)}^{-1}\right) = \frac{1}{\epsilon_{(k)}} \bar{U}_{(c)} \frac{d}{dx_1} k - \frac{k}{\epsilon_{(k)}^2} \bar{U}_{(c)} \frac{d}{dx_1} \epsilon_{(k)} \quad (4.23)$$

Using this relation in conjunction with Equations (4.8) and (4.9) the equation for ζ becomes

$$\bar{U}_{(c)} \frac{d}{dx_1} \zeta = \left[2(C_{(2)}-1) K_{12} \, d\bar{U}_1/dx_2 \right] \zeta + \left[(C_{(1)}-1) \, d\bar{U}_1/dx_2 \right] \quad (4.24)$$

This shows that ζ depends only on K_{12} which in turn depends only on ζ.

For the EASM and the IEASM, K_{12} is a linear function of ζ and may be substituted to give the expression

$$\bar{U}_{(c)} \frac{d}{dx_1} \zeta = \left[2(C_{(2)}-1) \frac{d}{dx_2} \bar{U}_1 B \right] \zeta^2 + \left[(C_{(1)}-1) \frac{d}{dx_2} \bar{U}_1 \right] \quad (4.25)$$

where

$$B \equiv \begin{cases} -\frac{1}{3} \left(\frac{1-C_{(1)}}{C_{(2)}} \right) \left(\frac{C_{(1)} + C_{(2)} - 1}{C_{(2)}} \right) & , \text{EASM} \\ -0.45 & , k-\epsilon_{(H)} \text{ model} \\ -\frac{1}{3} \left(\frac{1-C_{(1)}}{C_{(2)}} \right) & , \text{IEASM} \end{cases}$$

Equation (4.25) may be separated and integrated to give the result

$$\zeta = \frac{a \left[e^{2abx_1} - \left(\frac{1 - \frac{b}{a} \zeta_{(0)}}{1 + \frac{b}{a} \zeta_{(0)}} \right) \right]}{b \left[e^{2abx_1} + \left(\frac{1 - \frac{b}{a} \zeta_{(0)}}{1 + \frac{b}{a} \zeta_{(0)}} \right) \right]} \quad (4.26)$$

where

$$a^2 \equiv \frac{(C_{1\epsilon}-1)}{\bar{U}_{(\epsilon)}} \frac{d}{dx_2} \bar{U}_1$$

and

$$b^2 = \frac{2(-B)(C_{(\epsilon)}-1)}{\bar{U}_{(\epsilon)}} \frac{d}{dx_2} \bar{U}_1$$

The variable $\zeta_{(0)}$ is the initial condition for ζ, which may be calculated from the initial condition for k and L as

$$\zeta_{(0)} = \frac{d\bar{U}_1/dx_2}{(k_{(0)}^{1/2}/1.06 L_{(0)})} \qquad (4.27)$$

The PTASM provides a complicated expression for K_{12} in terms of ζ which requires the solution of a cubic algebraic equation. Although the solution of the cubic form is known, it does not lead to a solvable differential equation for ζ. It is preferable to solve equation (4.24) and the PTASM expression for K_{12} numerically. This may be done using the improved Euler finite difference method for equation (4.25) while solving equation (4.21) for K_{12} at each step using the standard cubic equation solution formula.

It is also desirable to solve for the development of the mean turbulent kinetic energy. This requires the simultaneous solution of equations (4.10) and (4.13) for k and ℓ respectively and an expression for K_{12} depending on the model. A solution in closed form is not available and a numerical solution is necessary. Since both differential equations are of first order, the improved Euler method may be used to solve them. This solution method requires the initial conditions k_o and ℓ_o .

An analytical solution can be obtained when $d\bar{U}_1/dx_2$ is exactly zero which would correspond to the case of decaying grid turbulence. Then equation (4.10) becomes

$$\frac{d}{dx_1} k = - \frac{k^{C_{(16)}}}{\ell \bar{U}_{(c)}} \tag{4.28}$$

This may be combined with equation (4.13) to give the expression

$$\frac{1}{\ell} \frac{d\ell}{dx_1} = - (C_{(18)} - C_{(16)}) \frac{1}{k} \frac{d}{dx_1} k \tag{4.29}$$

which can be separated and integrated to give the result

$$\ell = \ell_{(o)} \, k_{(o)}^{(C_{(18)} - C_{(16)})} \, k^{-(C_{(18)} - C_{(16)})} \tag{4.30}$$

Substituting this expression into equation (4.10) and integrating gives

$$k = \left[\frac{(C_{(18)} - 1)(X_1 - X_{(o)})}{\bar{U}_{(c)} \ell_{(o)} k_{(o)}^{C_{18} - C_{16}}} + k_{(o)}^{1 - C_{(18)}} \right]^{\frac{1}{1 - C_{(18)}}} \tag{4.31}$$

Hence, k decays roughly to the -1 power for the standard value of $c_{(18)}$. By the use of equations (4.30) and (4.31) an expression for ℓ may be isolated

$$\ell = \left[\frac{(c_{(18)}-1)(x_1 - x_{(0)})}{\bar{U}_{(c)}\, \ell_{(0)}^{\frac{1-c_{(18)}}{c_{(18)}-c_{(16)}}}\, k_{(0)}^{1-c_{(16)}}} + \ell_{(0)}^{\frac{c_{(18)}-1}{c_{(18)}-c_{(16)}}} \right]^{\frac{c_{(18)}-c_{(16)}}{c_{(18)}-1}} \qquad (4.32)$$

This shows that ℓ grows downstream roughly to the $\frac{1}{2}$ power for standard values of $c_{(18)}$ and $c_{(16)}$ equal to 1.92 and 1.44 respectively.

An expression for $\epsilon_{(k)}$ may be found by combining equations (4.31) and (4.32) as

$$\epsilon_{(k)} = \frac{k_{(0)}}{\ell_{(0)}^{c_{(16)}-c_{(18)}}} \left[\frac{(c_{(18)}-1)(x_1 - x_{(0)})}{\bar{U}_{(c)}\, \ell_{(0)}\, k_{(0)}^{c_{(18)}-c_{(16)}}} + k_{(0)}^{1-c_{(18)}} \right]^{\frac{1+c_{(18)}}{1-c_{(18)}}} \qquad (4.33)$$

which indicates that $\epsilon_{(k)}$ decays faster than k, which means that the turbulent time scale

$$\frac{k}{\epsilon} = \frac{\ell_{(0)}}{k_{(0)}^{c_{(16)}-c_{(18)}}} \left[\frac{(c_{(18)}-1)(x_1 - x_{(0)})}{\bar{U}_{(c)}\, \ell_{(0)}\, k_{(0)}^{c_{(18)}-c_{(16)}}} + k_{(0)}^{1-c_{(18)}} \right]^{\frac{c_{(18)}}{c_{(18)}-1}} \qquad (4.34)$$

grows indefinitely in the downstream direction and becomes infinite when x_1 is infinite. The mean field time scale is, however, zero throughout and hence ζ is zero even as x_1 approaches infinity.

4.3.2 Asymptotic Solution

Most of the equations governing K_{ij}, k and ℓ for all x have complicated analytic or numerical solutions. However, as x approaches infinity the solutions are simplified. The range of x for which asymptotic solutions apply is not known a priori.

The three algebraic models give K_{12} as a linear function of (EASM and IEASM) or as a constant (PTASM for large ζ). All proportionality coefficients are negative. As a result, equation (4.24) does has an assymptoptic solution, which may be obtained by letting $d\zeta/dx_1$ approach zero, as

$$\zeta = \frac{C_{(1)} - 1}{2(C_{(1)}-1)(-K_{12})} \qquad (4.35)$$

Using results from Figure 6 for K_{12} and $c_{(1)}$ and $c_{(2)}$ values of 0.6 and 1.8, one may obtain ζ for each model by an iterative procedure. The values of $\zeta_{(\infty)}$ for the EASM, PTASM and IEASM models are 4.08, 6.14 and 3.76 respectively, implying that the ratio of turbulent to mean time scale reaches a constant value of about 5 far downstream of the origin. Consequently all three models predict asymptotic values for K_{ij}

$$K_{ij} = \begin{pmatrix} 0.491 & 0.245 & 0.0 \\ 0.245 & 0.259 & 0.0 \\ 0.0 & 0.0 & 0.259 \end{pmatrix}, \quad \zeta_{(\infty)} = 4.26 \qquad (4.36a)$$

PTASM

$$K_{ij} = \begin{pmatrix} 0.530 & 0.184 & 0.0 \\ 0.184 & 0.237 & 0.0 \\ 0.0 & 0.0 & 0.237 \end{pmatrix}, \quad \zeta_{(\infty)} = 5.66 \qquad (4.36b)$$

IEASM

$$K_{ij} = \begin{pmatrix} 0.333 & 0.278 & 0.0 \\ 0.278 & 0.333 & 0.0 \\ 0.0 & 0.0 & 0.333 \end{pmatrix}, \quad \zeta_{(\infty)} = 3.76 \qquad (4.36c)$$

k-ε model

$$K_{ij} = \begin{pmatrix} 0.333 & 0.217 & 0.0 \\ 0.217 & 0.330 & 0.0 \\ 0.0 & 0.0 & 0.333 \end{pmatrix}, \quad \zeta_{(\infty)} = 4.82 \qquad (4.36d)$$

To obtain the asymptotic form of the mean turbulent kinetic energy, one can use the asymptotic form of equation (4.14)

$$\ell = \frac{(c_{(8)} - c_{(6)})}{\bar{U}_{(1)}} \int k^{c_{(6)}-1} \, dx_1 \qquad (4.37)$$

which reduces equation (4.10) to

$$\frac{d}{dx_1} k = \frac{P_{(k)}}{\bar{U}_{(1)}} - \frac{k^{c_{(6)}}}{(c_{(8)} - c_{(6)}) \int k^{c_{(6)}-1} \, dx_1} \qquad (4.38)$$

where $P_{(k)} = -2kK_{12} d\bar{U}_1/dx_2$. Since K_{12} is asymptotically constant, $P_{(k)}$ is proportional to k in this flow at large distances downstream and equation (4.38) is satisfied when

$$k = k_{(r)}\, e^{a(x_1 - x_{(r)})}$$

and

$$a \equiv \frac{2(c_{(18)} - c_{(16)})(-\overline{uv})}{(c_{(18)} - 1)\,\bar{U}_{(r)}} \frac{d}{dx_2}\bar{U}_1 \qquad (4.39)$$

where $k_{(r)}$ is the value of k at $x_{(r)}$, the beginning of the asymptotic region. Expression (4.39) is not valid when $d\bar{U}_1/dx_2$ is identically zero, in which case equation (4.38) is only balanced by equation (4.39) for certain values of $\bar{U}_1$, $c_{(16)}$ and $c_{(18)}$.

Equation (4.37) then requires that

$$\ell = \left[\frac{c_{(18)} - 1}{c_{(16)} - 1} \frac{k_{(r)}^{\,c_{(16)}-1}}{2(-\overline{uv})\, d\bar{U}_1/dx_2}\right] e^{a(c_{(16)}-1)(x_1 - x_{(r)})} \qquad (4.40)$$

From the definition, $\ell = \frac{k^{c_{(16)}}}{\epsilon_{(k)}}$ it follows that

$$\epsilon_{(k)} = \left[\frac{2(c_{(16)} - 1)}{c_{(18)} - 1} \frac{d}{dx_2}\bar{U}_1 (-\overline{uv}) k_{(r)}\right] e^{a(x_1 - x_{(r)})} \qquad (4.41)$$

This shows that the turbulent kinetic energy, dissipation length scale and dissipation rate grow exponentially far downstream, provided that

$$\frac{c_{(18)} - 1}{c_{(18)} - c_{(16)}} > 0 \qquad (4.42)$$

which is the case for the commonly used values $c_{(16)} = 1.44$ and $c_{(18)} = 1.92$.

Tavoularis (1984) has also deduced exponential expressions for k and L for the asymptotic region of this flow. Starting with equation (4.6) he used the experimental observations that

$$K_{ij} = \text{constant} \tag{4.43a}$$

$$\bar{U}_{(c)}(dk/dx)/P = \text{constant} \tag{4.43b}$$

which also implies that

$$\frac{\epsilon_{(k)}}{k} = \text{constant} \tag{4.43c}$$

His resulting expressions for k and L are

$$k = k_{(r)}\, e^{2(x_1 - x_{(r)})/b}$$

$$L = L_{(r)}\, e^{2(x_1 - x_{(r)})/b} \tag{4.44}$$

where

$$b = \left[- \frac{\overline{IK}_{12}}{\bar{U}_{(c)}} \frac{d}{dx_2} \bar{U}_1 - \frac{\epsilon_{(k)}}{\bar{U}_{(c)}\, k} \right]^{-1}$$

These are very similar to equations (4.37) and (4.38).

4.4 Comparison with Experimental Results and Discussion

In the experiment performed by Karnik and Tavoularis (1983), the shear was generated by flowing air through a set of channels whose flow rate was individually controlled in the transverse direction. To obtain homogeneity of the turbulence scales, the air was then passed through a flow separator. All measurements were made with hot wire anenometers.

The mean velocity field showed little variation in either depth or the downstream direction and varied linearly in the transverse direction excluding regions close to the walls. The transverse variation of turbulence parameters was significant when grids were not used, however, this variation may be insufficient to cause a diffusive effect on the net transport. When grids were installed, the transverse variation of turbulence parameters was significantly reduced.

Two grid sizes were used, 25.4 mm and 50.8 mm. Both produced transversely homogeneous turbulence. The data obtained with the 25.4 mm grid will be used for comparison to predictions. This was chosen because the data show acceptable homogeneity, a production-dissipation imbalance of turbulent kinetic energy and distinct initial values of the components of the Reynolds stress tensor.

Closely behind the grid, the relative magnitudes of Reynolds stresses were distorted from their asymptotic values, but further downstream a quasi-universal self-similar state was again reached. Although different values of the mean shear could be obtained by adjusting the fan speed, this variation did not produce any unexpected

changes of the physical processes. Thus, it seems sufficient to examine one representative case, that with $\bar{U}_1 = (18.4x_1 + 6)ms^{-1}$.

The measured development of turbulent kinetic energy is shown in Figure 7. For this flow the kinetic energy decreases close to the grid, but further downstream it attains an exponential rise which continues until the end of the test section. The integral length scale grows monotonically downstream, as shown in Figure 7. The non-dimensional Reynolds stress, $K_{ij} = \overline{u_i u_j}/2k$, developed downstream as shown in Figure 8. It is remarkable that for almost all the existing realizations of homogeneous shear flows the components of K_{ij} approached quasi-universal asymptotic values (Karnik and Tavoularis), which were

$$K_{ij} = \begin{pmatrix} 0.54 & -0.16 & 0.0 \\ -0.16 & 0.21 & 0.0 \\ 0.0 & 0.0 & 0.26 \end{pmatrix} \qquad (4.45)$$

The governing equations for UST have been solved for the flow described above with initial conditions, $k = 0.18\ m\ s^{-1}$ and $L = 0.019$ m at $x = 1.83$ m. The solutions to each model for the variables k, L, K_{ij} and ζ are shown in Figures 7 and 8.

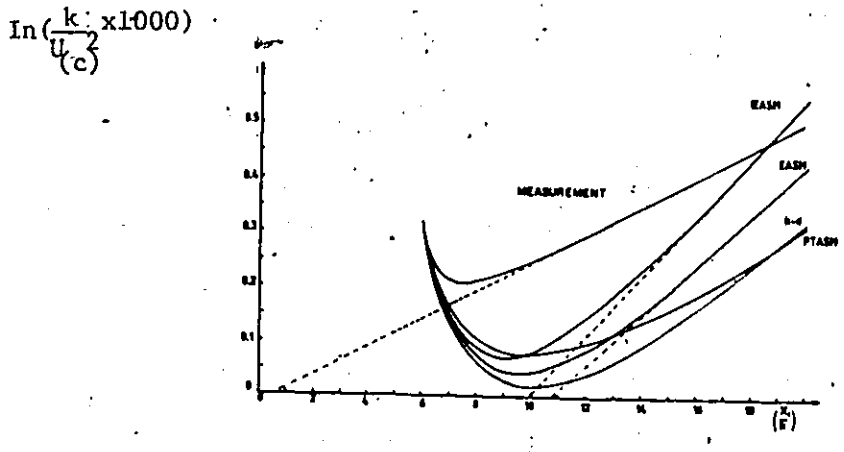

(a)

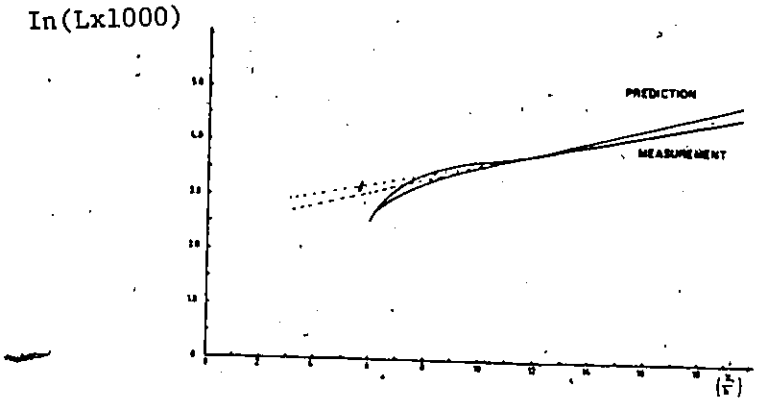

(b)

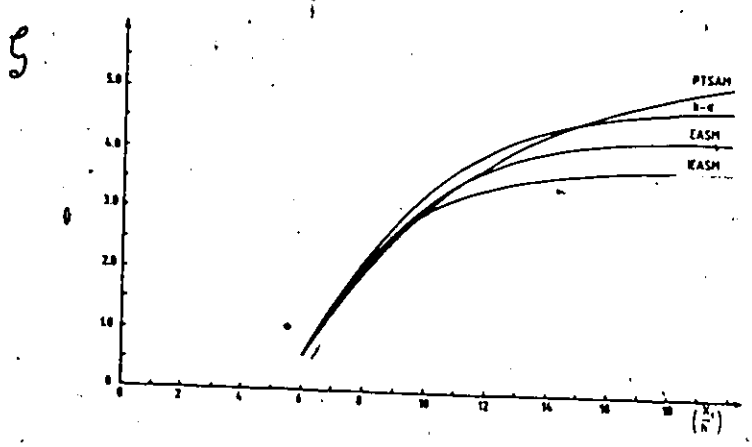

(c)

FIGURE 7: Downstream Development of (a) Turbulent Kinetic Energy, (b) Integral Length Scale, (c) Turbulent to Mean Time Scale Ratio; Measurements by Karnik and Tavoularis (1983)

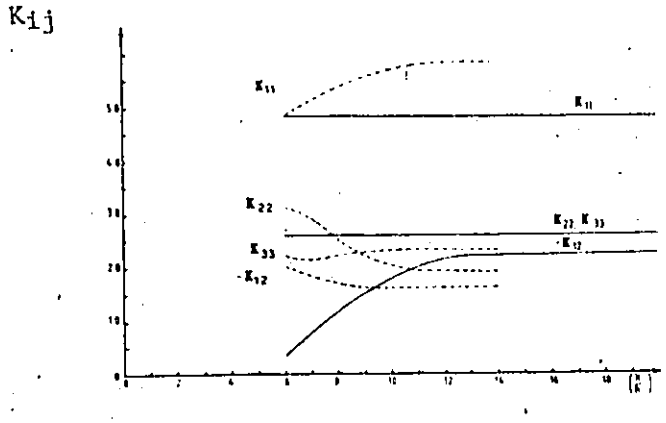

(a)

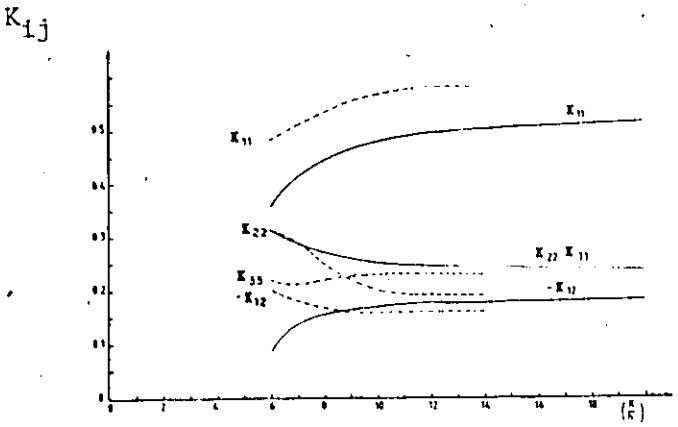

(b)

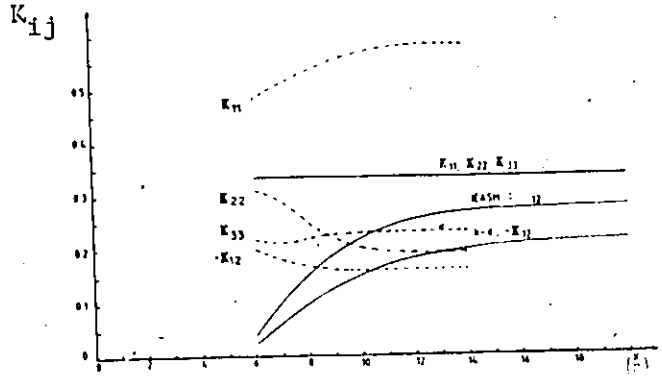

(c)

FIGURE 8: Downstream Development of the Dimensionless Reynolds Stress in Uniformly Sheared Turbulence for (a) EASM, (b) PTASM, (c) IEASM and k-ε Model; Broken Lines are Measurements by Karnik and Tavoularis (1983)

4.4a EASM

The EASM was based on the assumption that the production and dissipation of Reynolds stresses were in balance, a condition which was not satisfied anywhere in this flow. The asymptotic values of the predictions show fair agreement with the data. The major discrepancies are that the model implies equality of K_{22} and K_{33}, while the data consistently shows that $K_{33} > K_{22}$.

This inability of the model to predict a difference between K_{22} and K_{33} can be traced to the pressure strain correlation and would be present even if full transport equations were used. Expanding the open region approximation of the $\overline{u_i u_j}$ equation for this flow gives the expressions

$$\bar{U}_1 \frac{d}{dx_1}\overline{u_1^2} = -\frac{2}{\rho}\overline{u_1 u_2}\frac{d}{dx_2}\bar{U}_1 + \frac{2}{\rho}\overline{p\frac{\partial u_1}{\partial x_1}} - \frac{2}{3}\epsilon_{(k)} \qquad (4.46)$$

$$\bar{U}_1 \frac{d}{dx_1}\overline{u_2^2} = \frac{2}{\rho}\overline{p\frac{\partial u_2}{\partial x_2}} - \frac{2}{3}\epsilon_{(k)} \qquad (4.47)$$

$$\bar{U}_1 \frac{d}{dx_1}\overline{u_3^2} = \frac{2}{\rho}\overline{p\frac{\partial u_3}{\partial x_3}} - \frac{2}{3}\epsilon_{(k)} \qquad (4.48)$$

This shows that neither $\overline{u_2^2}$ or $\overline{u_3^2}$ have any direct production by the mean field and as a result, their only source is the pressure strain correlation, which acts as an energy redistribution term. The general

pressure-strain model (neglecting the wall influence introduced in Section 3.1) can be rewritten in terms of strain and vorticity so that its physical meaning will be better understood as

$$\overline{p/\rho\left(\frac{\partial u_i}{\partial x_j}+\frac{\partial u_j}{\partial x_i}\right)} = (a+c)\left(\overline{u_iu_k}\,\bar{S}_{jk}+\overline{u_ju_k}\,\bar{S}_{ik}\right) + (a-c)\left(\overline{u_iu_k}\,\bar{\Omega}_{jk}+\overline{u_ju_k}\,\bar{\Omega}_{ik}\right) - \tfrac{2}{3}(a+c)\left(\overline{u_ku_k}\,\bar{S}_{ki}\right)\delta_{ij} - 2bk\,\bar{S}_{ij} + c_2\frac{\epsilon_{(k)}}{k}\left(\overline{u_iu_j}-\tfrac{2}{3}k\right)\delta_{ij} \tag{4.49}$$

where $\bar{S}_{ij}=\frac{1}{2}\left(\frac{\partial}{\partial x_j}\bar{U}_i+\frac{\partial}{\partial x_i}\bar{U}_j\right)$, $\bar{\Omega}_{ij}=\frac{1}{2}\left(\frac{\partial}{\partial x_i}\bar{U}_j+\frac{\partial}{\partial x_j}\bar{U}_i\right)$

$a=\frac{c+8}{11}$ $\quad b=\frac{30c-2}{55}$ $\quad c=\frac{8c-2}{11}$

Simplifying this expression for UST gives

$$2\overline{p/\rho\frac{\partial u_1}{\partial x_1}} = \frac{a+c}{3}\overline{u_1u_2}\,\bar{S}_{12}+(a-c)\overline{u_1u_2}\,\bar{\Omega}_{12} - 4c_2\frac{\epsilon_{(k)}}{k}\left(\overline{u_1^2}-\tfrac{2}{3}k\right) \tag{4.50a}$$

$$2\overline{p/\rho\frac{\partial u_2}{\partial x_2}} = \frac{a+c}{3}\overline{u_1u_2}\,\bar{S}_{12}-(a-c)\overline{u_1u_2}\,\bar{\Omega}_{12} - 4c_2\frac{\epsilon_{(k)}}{k}\left(\overline{u_2^2}-\tfrac{2}{3}k\right) \tag{4.50b}$$

$$2\overline{p/\rho\frac{\partial u_3}{\partial x_3}} = -\tfrac{2}{3}(a+c)\overline{u_1u_2}\,\bar{S}_{12}-4c_2\frac{\epsilon_{(k)}}{k}\left(\overline{u_3^2}-\tfrac{2}{3}k\right) \tag{4.50c}$$

Since $(-\overline{u_1u_2}\,d\bar{U}_1/dx_2) > 0$ it becomes clear that the mean strain transfers equal amounts of energy from the $\overline{u_1^2}$ and $\overline{u_2^2}$ components to $\overline{u_3^2}$ component, while the mean vorticity transfers energy from the $\overline{u_1^2}$

component and places it in the $\overline{u_2^2}$ component. As a result the source of the $\overline{u_3^2}$ component is greater than that of the $\overline{u_2^2}$ component resulting in the inequality of $\overline{u_2^2}$ and $\overline{u_2^3}$. Using this expression and the constants provided in Section 3 (for other USTs) gives the asymptotic values for K_{ij} as

$$K_{ij} = \begin{pmatrix} 0.474 & -0.183 & 0.0 \\ -0.183 & 0.223 & 0.0 \\ 0.0 & 0.0 & 0.302 \end{pmatrix} \qquad (4.51)$$

In order to simulate different UST flows, the constants a, b, and c had to be adjusted significantly and as a result its use was discontinued by its originators (Launder, Reece and Rodi, 1976). However, by setting b and c equal to zero the more universal model used in the PTASM was achieved at the expense of the incorrect prediction, $K_{22} = K_{33}$. This changes equations (4.50) to

$$2\overline{P/\rho \frac{\partial u_1}{\partial x_1}} = a\overline{u_1 u_2}\left(\tfrac{1}{3}\overline{S}_{12} + \overline{\Omega}_{12}\right) - 4c_{(k)}\frac{\epsilon_{(k)}}{k}\left(\overline{u_1^2} - \tfrac{2}{3}k\right) \qquad (4.52a)$$

$$2\overline{P/\rho \frac{\partial u_2}{\partial x_2}} = a\overline{u_1 u_2}\left(\tfrac{1}{3}\overline{S}_{12} - \overline{\Omega}_{12}\right) - 4c_{(k)}\frac{\epsilon_{(k)}}{k}\left(\overline{u_2^2} - \tfrac{2}{3}k\right) \qquad (4.52b)$$

$$2\overline{P/\rho \frac{\partial u_3}{\partial x_3}} = -\tfrac{2}{3}a\overline{u_1 u_2}\,\overline{S}_{12} - 4c_{(k)}\frac{\epsilon_{(k)}}{k}\left(\overline{u_3^2} - \tfrac{2}{3}k\right) \qquad (4.52c)$$

In this flow $\overline{S}_{12} = \overline{\Omega}_{12}$ and hence the sources of $\overline{u_2^2}$ and $\overline{u_3^2}$ are equal.

The predicted development of K_{12} is different from the data since it increases from its initial level while the data indicate a decrease. Far downstream, K_{12} is predicted to reach a constant level, but one which is larger than the measured value.

The predicted development of k is rather poor compared to the data, first decreasing below the measurements and then rising at too fast a rate farther downstream. This is connected with the over estimation of K_{12} , since the production of k is proportional to K_{12} . The length scale is well predicted throughout, demonstrating its insensitivity to K_{12} variation.

4.4b PTASM

This model is based on the assumption that K_{ij} is constant, a condition which is only satisfied asymtotically.

In the asymptotic region the predictions of K_{ij} agree well with the data, reflecting proper specification of the constants which were chosen so that this would be the case. The measured inequality of K_{22} and K_{33} cannot be predicted.

Predicted development of the normal components of K_{ij} , agrees qualitatively with the data except for the equality of K_{22} and K_{33} . The development of K_{12} is poorly predicted since it shows a trend opposite to that of the data.

The predicted development of k is in poor agreement with the data, however, in the fully developed region, the prediction of k has approximately the same slope as the as the data which can be attributed to the fact that the K_{12} prediction is comparable to the measurements in this region.

4.4c IEASM and k-ϵ

The IEASM model is based on the assumption that the turbulence stress tensor is nearly isotropic, a condition which is not satisfied in this flow. The predicted normal components of K_{ij} are equal constants which are considerably different from the predictions.

The K_{12} component develops at a slower rate and to too high an asymptotic value when compared to the data. This is caused by a lack of an initial condition for K_{12} and from K_{22} being much higher than that measured.

Due to the improperly predicted development of K_{12}, k also develops differently than the data indicates, although it seems better than the EASM and PTASM in the initial; it has a steeper slope in the exponential region than was measured.

The k-ϵ model is a version of the IEASM with properly adjusted values of $c_{(1)}$ and $c_{(2)}$. It has exactly the same deficiences as the true IEASM with the exception that, in the asymtotic region, K_{12} and hence the predicted slopes of k and L are more accurate. However, this has been achieved by ignoring the behaviour of the normal stresses; if one permits variation of these stresses, the constants would need to be readjusted.

4.5 Closure

The development of K_{ij}, k and L may be separated into two portions: a) the initial stage where K_{ij} is changing, and b) the asymptotic stage where K_{ij} is constant and k and L are growing exponentially.

In the initial stage the values of K_{ij}, k and L cannot be accurately calculated unless transport equations are used for the K_{ij} components with appropriate initial conditions. In the asymptotic stage, the logarithmic slope of k and L can be calculated accurately only if K_{12} has the correct asymptotic value. None of the models investigated in this section did well in the initial stage, although the PTASM model was the best.

In the asymptotic stage, all models would accurately predict K_{12}, k and L with the right choise of constants. In this flow the normal components of K_{ij} are of little importance to the mean momentum transport or the production of k. In view of this, a constant value of K_{12}, combined with the k and $\epsilon_{(k)}$ equation would be acceptable. If, however, the flow was not in the asymptotic stage, then K_{12} would be variable and some error would be introduced. Equation (4.26) for ζ indicates that for large values of $(d\overline{U_1}/dx_2)/U_{(\epsilon)}$, ζ approaches an asymptote more quickly and hence so does K_{12}. This would seem to indicate that for increasingly large ratios of mean shear to velocity the initial conditions for K_{ij} become less important and the PTASM predictions improved.

The equation for k used here has no modelling approximations, but the equation for $\epsilon_{(k)}$ has been modelled extensively. This model predicts a constant value of K_{ij} and exponential growth of k and L in agreement with experiment.

CHAPTER V

TWO-DIMENSIONAL TURBULENT CHANNEL FLOW

5.1 Introduction

In this chapter, the Proportional Transport Algebraic Stress Model and the k-ε version of the Isotropic Equilibrium Algebraic Stress Model are used to compute a two-dimensional turbulent channel flow, which is somewhat more complex than the uniformly sheared flow. The added complications arise from the influence of the solid walls and the fact that turbulence is produced mostly near the walls and dissipated mostly in the channel core. Thus, both the near wall treatment and the diffusion rate predictions may be tested. In turbulent channel flow the mean velocity profile is entirely determined by the turbulent shear stress, as opposed to molecular and turbulent normal stresses. This shear stress varies considerably over the channel and hence, emphasizes the different stress strain rate relationships.

In turbulent channel flow, the wall affects the turbulent shear stress well into the channel core. This case provides a good test for the near wall pressure strain correction formula, the purpose of which is to predict this effect. The two formulae for the near wall correction introduced in Section 3.1 were tested in conjunction with the PTASM to determine which one performed best compared with measurements as well as the extent of the influence of the wall effect.

The PTASM and k-ϵ model predictions are compared to one another, the Reynolds Stress Model (RSM) prediction of Lauder, Reece and Rodi (1975) and the experimental data of Laufer (1951) and Comte-Bellot (1965).

5.2 The Governing Equations

5.2.1 General Form

Consider a two-dimensional channel flow which is assumed to be steady and statistically homogeneous in the x_3 direction. This requires that $\bar{U}_3$ and all time derivatives and x_3 derivatives of mean quantities be zero. By symmetry, one can infer that $\overline{u_1 u_3} = \overline{u_2 u_3} = 0$. The flow is also assumed isothermal and incompressible with constant properties.

The mean continuity, mean momentum, mean turbulent kinetic energy and mean turbulent kinetic energy dissipation rate equations are simplified as follows

$$\bar{U}_1 \frac{\partial}{\partial x_1}\bar{U}_1 + \bar{U}_2 \frac{\partial}{\partial x_2}\bar{U}_1 = -\frac{1}{\rho}\frac{\partial}{\partial x_1}\bar{P} + \nu\left(\frac{\partial^2}{\partial x_1^2}\bar{U}_1 + \frac{\partial}{\partial x_2^2}\bar{U}_1\right) - \frac{\partial}{\partial x_1}\overline{u_1^2} - \frac{\partial}{\partial x_2}\overline{u_1 u_2} \tag{5.1}$$

$$\bar{U}_1 \frac{\partial}{\partial x_1}\bar{U}_2 + \bar{U}_2 \frac{\partial}{\partial x_2}\bar{U}_2 = -\frac{1}{\rho}\frac{\partial}{\partial x_2}\bar{P} + \nu\left(\frac{\partial^2}{\partial x_1^2}\bar{U}_2 + \frac{\partial^2}{\partial x^2}\bar{U}_2\right) - \frac{\partial}{\partial x_1}\overline{u_1 u_2} - \frac{\partial}{\partial x_2}\overline{u_2^2} \tag{5.2}$$

$$\frac{\partial}{\partial x_1}\bar{U}_1 + \frac{\partial}{\partial x_2}\bar{U}_2 = 0 \tag{5.3}$$

$$\bar{U}_1 \frac{\partial}{\partial x_1}k + \bar{U}_2 \frac{\partial}{\partial x_2}k = -\left[\overline{u_1^2}\frac{\partial}{\partial x_1}\bar{U}_1 + \overline{u_1 u_2}\left(\frac{\partial}{\partial x_2}\bar{U}_1 + \frac{\partial}{\partial x_1}\bar{U}_2\right) + \overline{u_2^2}\frac{\partial}{\partial x_2}\bar{U}_2\right]$$
$$- \epsilon_{(k)} + c_{(7)}\left[\frac{\partial}{\partial x_1}\left(\frac{k}{\epsilon_{(k)}}\overline{u_1^2}\frac{\partial}{\partial x_1}k + \frac{k}{\epsilon_{(k)}}\overline{u_1 u_2}\frac{\partial}{\partial x_2}k\right) + \frac{\partial}{\partial x_2}\left(\frac{k}{\epsilon_{(k)}}\overline{u_1 u_2}\frac{\partial}{\partial x_1}k\right.\right.$$
$$\left.\left. + \frac{k}{\epsilon_{(k)}}\overline{u_2^2}\frac{\partial}{\partial x_2}k\right)\right] \tag{5.4}$$

$$\bar{U}_1 \frac{\partial}{\partial x_1}\epsilon_{(k)} + \bar{U}_2 \frac{\partial}{\partial x_2}\epsilon_{(k)} = -c_{(1)}\frac{\epsilon_{(k)}}{k}\left[\overline{u_1^2}\frac{\partial}{\partial x_1}\bar{U}_1 + \overline{u_1 u_2}\left(\frac{\partial}{\partial x_2}\bar{U}_1\right.\right.$$
$$\left.\left. + \frac{\partial}{\partial x_1}\bar{U}_2\right) + \overline{u_2^2}\frac{\partial}{\partial x_2}\bar{U}_2\right] - c_{(1)}\frac{\epsilon_{(k)}}{k} + c_{(5)}\left[\frac{\partial}{\partial x_1}\left(\frac{k}{\epsilon_{(k)}}\overline{u_1^2}\frac{\partial}{\partial x_1}\epsilon_{(k)}\right.\right.$$
$$\left.\left. + \frac{k}{\epsilon_{(k)}}\overline{u_1 u_2}\frac{\partial}{\partial x_2}\epsilon_{(k)}\right) + \frac{\partial}{\partial x_2}\left(\frac{k}{\epsilon_{(k)}}\overline{u_1 u_2}\frac{\partial}{\partial x_1}\epsilon_{(k)} + \frac{k}{\epsilon_{(k)}}\overline{u_2^2}\frac{\partial}{\partial x_2}\epsilon_{(k)}\right)\right] \tag{5.5}$$

To test the near wall correction portion of the pressure strain correlation, the near wall correction formulae of Section 3.1 have been added to the PTASM model. The resulting model and the k-ε version of the IEASM simplified for this flow are

PTASM

$$\left(-\frac{\partial}{\partial x_1}\bar{U}_1\right)\left(\overline{u_1^2}\right)^2 + \left[-\overline{u_1u_2}\left(\frac{\partial}{\partial x_2}\bar{U}_1 + \frac{\partial}{\partial x_1}\bar{U}_2\right) - \overline{u_2^2}\frac{\partial}{\partial x_2}\bar{U}_1 + \left(2-\tfrac{4}{3}C_{(1)}\right)\frac{\partial}{\partial x_1}\bar{U}_1 + (C_{(2)}-1)\epsilon_{(K)}\right]\overline{u_1^2} + k\left[\left(2-\tfrac{4}{3}C_{(1)}\right)\overline{u_1u_2}\frac{\partial}{\partial x_2}\bar{U}_1 + \tfrac{2}{3}C_1\,\overline{u_1u_2}\frac{\partial}{\partial x_1}\bar{U}_2 + \tfrac{2}{3}C_{(1)}\overline{u_2^2}\frac{\partial}{\partial x_2}\bar{U}_2 - \tfrac{2}{3}(C_{(2)}-1)\epsilon_{(K)} - 2\,\overline{P/\rho\left(\frac{\partial u_1}{\partial x_1}\right)_{(wall)}}\right] = 0 \tag{5.6}$$

$$\left(-\frac{\partial}{\partial x_2}\bar{U}_1 - \frac{\partial}{\partial x_1}\bar{U}_2\right)\left(\overline{u_1u_2}\right)^2 + \left[-\overline{u_1^2}\frac{\partial}{\partial x_1}\bar{U}_1 - \overline{u_2^2}\frac{\partial}{\partial x_2}\bar{U}_2 + (C_{(3)}-1)\epsilon_{(K)}\right]\overline{u_1u_2} + k\left[(1-C_{(1)})\left(\overline{u_1^2}\frac{\partial}{\partial x_1}\bar{U}_2 + \overline{u_2^2}\frac{\partial}{\partial x_2}\bar{U}_1\right) + \overline{P/\rho\left(\frac{\partial u_1}{\partial x_2} + \frac{\partial u_2}{\partial x_1}\right)_{(wall)}}\right] = 0 \tag{5.7}$$

$$\left(-\frac{\partial}{\partial x_2}\bar{U}_2\right)\left(\overline{u_2^2}\right) + \left[-\overline{u_1^2}\frac{\partial}{\partial x_1}\bar{U}_1 - \overline{u_1u_2}\left(\frac{\partial}{\partial x_2}\bar{U}_1 + \frac{\partial}{\partial x_1}\bar{U}_2\right) + \left(2-\tfrac{4}{3}C_{(1)}\right)k\frac{\partial}{\partial x_2}\bar{U}_2 + (C_{(2)}-1)\epsilon_{(K)}\right]\overline{u_2^2} + k\left[\tfrac{2}{3}C_{(1)}\overline{u_1^2}\frac{\partial}{\partial x_1}\bar{U}_1 + \left(2-\tfrac{4}{3}C_{(1)}\right)\overline{u_1u_2}\frac{\partial}{\partial x_1}\bar{U}_2 + \tfrac{2}{3}C_{(1)}\overline{u_1u_2}\frac{\partial}{\partial x_2}\bar{U}_1 - \tfrac{2}{3}(C_{(2)}-1)\epsilon_{(K)} - 2\,\overline{P/\rho\left(\frac{\partial u_2}{\partial x_2}\right)_{(wall)}}\right] = 0 \tag{5.8}$$

$$\overline{u_3^2} = 2k - \left(\overline{u_1^2} + \overline{u_2^2}\right) \tag{5.9}$$

k-ε model

$$\overline{u_1^2} = \tfrac{2}{3}k - C_{(\mu)}\frac{k^2}{\epsilon_{(K)}}\left(2\frac{\partial}{\partial x_1}\bar{U}_1\right) \tag{5.10}$$

$$\overline{u_1 u_2} = -C_{(\mu)} \frac{k^2}{\epsilon_{(\mu)}} \left(\frac{\partial}{\partial x_2} \bar{U}_1 + \frac{\partial}{\partial x_1} \bar{U}_2 \right) \tag{5.11}$$

$$\overline{u_2^2} = \frac{2}{3} k - C_{(\mu)} \frac{k^2}{\epsilon_{(\mu)}} \left(2 \frac{\partial}{\partial x_2} \bar{U}_2 \right) \tag{5.12}$$

$$\overline{u_3^2} = \frac{2}{3} k \tag{5.13}$$

where: Shir (1973) wall correction

$$2\overline{p/\rho \left(\frac{\partial u_1}{\partial x_1} \right)}_{(wall)} = \left[C_{(4)} \frac{\epsilon_{(k)}}{k} \overline{u_1^2} - C_{(2)} C_{(5)} \left(P_{22} - \frac{2}{3} P_{(k)} \right) \right] f$$

$$\overline{p/\rho \left(\frac{\partial u_1}{\partial x_2} + \frac{\partial u_2}{\partial x_1} \right)}_{(wall)} = \left[C_{(3)} \frac{\epsilon_{(k)}}{k} \left(-\overline{u_1 u_2} \right) + \frac{2}{3} C_{(1)} C_{(5)} P_{12} \right] f$$

$$2\overline{p/\rho \left(\frac{\partial u_1}{\partial x_3} \right)}_{(wall)} = \left[C_{(3)} \frac{\epsilon_{(k)}}{k} \left(-2 \overline{u_3^2} \right) + 2 C_{(3)} C_{(5)} \left(P_{22} - \frac{2}{3} P_{(k)} \right) \right] f$$

Launder, Reece and Rodi (1976) wall correction

$$2\overline{p/\rho \frac{\partial u_1}{\partial x_1}}_{(wall)} = \left[0.125 \frac{\epsilon_{(k)}}{k} \left(\overline{u_1^2} - \frac{2}{3} k \right) + 0.015 \left(P_{11} - D_{11} \right) \right] f$$

$$\overline{p/\rho \left(\frac{\partial u_1}{\partial x_2} + \frac{\partial u_2}{\partial x_1} \right)}_{(wall)} = \left[0.125 \frac{\epsilon_{(k)}}{k} \overline{u_1 u_2} + 0.015 \left(P_{12} - D_{12} \right) \right] f$$

$$2\overline{p/\rho \frac{\partial u_2}{\partial x_2}}_{(wall)} = \left[0.125 \frac{\epsilon_{(k)}}{k} \left(\overline{u_2^2} - \frac{2}{3} k \right) + 0.015 \left(P_{22} - D_{22} \right) \right] f$$

and

$$P_{11} = -2 \left(\overline{u_1^2} \frac{\partial}{\partial x_1} \bar{U}_1 + \overline{u_1 u_2} \frac{\partial}{\partial x_2} \bar{U}_1 \right) \qquad D_{11} = -2 \left(\overline{u_1^2} \frac{\partial}{\partial x_1} \bar{U}_1 + \overline{u_1 u_2} \frac{\partial}{\partial x_1} \bar{U}_2 \right)$$

$$P_{12} = -\left(\overline{u_1^2} \frac{\partial}{\partial x_1} \bar{U}_2 + \overline{u_2^2} \frac{\partial}{\partial x_2} \bar{U}_1 \right) \qquad D_{12} = -\left(\overline{u_1^2} \frac{\partial}{\partial x_2} \bar{U}_1 + \overline{u_2^2} \frac{\partial}{\partial x_1} \bar{U}_2 \right)$$

$$P_{22} = -2 \left(\overline{u_1 u_2} \frac{\partial}{\partial x_1} \bar{U}_2 + \overline{u_2^2} \frac{\partial}{\partial x_2} \bar{U}_2 \right) \qquad D_{22} = -2 \left(\overline{u_1 u_2} \frac{\partial}{\partial x_2} \bar{U}_1 + \overline{u_2^2} \frac{\partial}{\partial x_2} \bar{U}_2 \right)$$

$$f = \frac{k^{3/2}}{\epsilon_{(k)}} \left(\frac{1}{x_2} + \frac{1}{2\omega - x_2} \right)$$

The algebraic formulae for Reynolds stresses have the quadratic form

$$ay^2 + by + c = 0 \tag{5.14}$$

When $a \neq 0$, this equation has, in general, two roots

$$y = -\frac{b}{2a} \pm \sqrt{\left(\frac{b}{2a}\right)^2 - \frac{c}{a}} \qquad (5.15)$$

Determination of the correct root for each of the components will be based on the following criteria:

a) the normal stresses $\overline{u_1^2}$ and $\overline{u_2^2}$ must be positive, and

b) the turbulent shear stress $\overline{u_1 u_2}$ must have a sign opposite to that of the local mean shear.

These criteria imply that

$$\overline{u_1^2} = -b_{(1)}/2a_{(1)} + \sqrt{\left(\frac{b_{(1)}}{2a_{(1)}}\right)^2 - \frac{c_{(1)}}{a_{(1)}}}$$

$$\overline{u_1 u_2} = -b_{(2)}/2a_{(2)} + \sqrt{\left(\frac{b_{(2)}}{2a_{(2)}}\right)^2 - \frac{c_{(2)}}{a_{(2)}}}, \quad a_{(2)} > 0 \qquad (5.16)$$

$$\overline{u_1 u_2} = -b_{(2)}/2a_{(2)} - \sqrt{\left(\frac{b_{(2)}}{2a_{(2)}}\right)^2 - \frac{c_{(2)}}{a_{(2)}}}, \quad a_{(2)} < 0$$

$$\overline{u_2^2} = -b_{(3)}/2a_{(3)} + \sqrt{\left(\frac{b_{(2)}}{2a_{(2)}}\right)^2 - \frac{c_{(3)}}{a_{(3)}}}$$

Since the coefficients $a_{(1)}$, $b_{(1)}$, and $c_{(1)}$ depend on the values of Reynolds stresses, an iterative procedure is employed to solve for $\overline{u_1^2}$, $\overline{u_1 u_2}$ and $\overline{u_2^2}$.

Equations (5.3) are generally applicable in two dimensional flow except when a = 0. In this case the solutions become:

$$\begin{aligned} \overline{u_1^2} &= - b_{(1)}/c_{(1)} \\ \overline{u_1 u_2} &= - b_{(2)}/c_{(2)} \\ \overline{u_2^2} &= - b_{(3)}/c_{(3)} \end{aligned} \qquad (5.17)$$

To smooth the transition between the equation sets (5.16) and (5.17) the following forms are used for small $a_{(1)}$, $a_{(2)}$ and $a_{(3)}$

$$\begin{aligned} \overline{u_1^2} &= - c_{(1)}/(a_{(1)} \overline{u_1^2}^* + b_{(1)}) \\ \overline{u_1 u_2} &= - c_{(2)}/(a_{(2)} \overline{u_1 u_2}^* + b_{(2)}) \\ \overline{u_2^2} &= - c_{(3)}/(a_{(3)} \overline{u_2^2}^* + b_{(3)}) \end{aligned} \qquad (5.18)$$

where the star denotes the value of the quantity resulting from the last iteration of the solution sequence.

5.2.2 Fully Developed Region

At sufficiently long distances from the channel inlet, the mean and turbulence field reach a state which is commonly known as "fully developed", where the streamwise gradient of all statistical parameters is zero. The governing equations for such fully developed regions of two-dimensional flows are simplified as follows

$$\frac{1}{\rho} \frac{\partial}{\partial x_2} \bar{P} = - \frac{d}{dx_2} \overline{u_2^2} \qquad (5.19)$$

$$\frac{1}{\rho} \frac{\partial}{\partial x_1} \bar{P} = - \frac{d}{dx_2} \overline{u_1 u_2} + \nu \frac{d^2}{dx^2} \bar{U}_1 \qquad (5.20)$$

$$\frac{\partial}{\partial x_2} \bar{U}_2 = 0 \qquad (5.21)$$

$$c_{(7)} \frac{d}{dx_2}\left(\frac{k}{\epsilon_{(k)}} \overline{u_2^2} \frac{d}{dx_2} k\right) = \overline{u_1 u_2} \frac{d}{dx_2} \bar{U}_1 + \epsilon_{(k)} \tag{5.22}$$

$$c_{(5)} \frac{d}{dx_2}\left(\frac{k}{\epsilon_{(k)}} \overline{u_2^2} \frac{d}{dx_2} \epsilon_{(k)}\right) = c_{(6)} \frac{\epsilon_{(k)}}{k} \overline{u_1 u_2} \frac{d}{dx_2} \bar{U}_1 + c_{(8)} \frac{\epsilon_{(k)}^2}{k} \tag{5.23}$$

PTASM

$$\overline{u_1^2} = \tfrac{2}{3} k \left[\frac{(3-2c_{(1)})(\overline{u_1 u_2}\, d\bar{U}_1/dx_2) + 2P/\rho \overline{\frac{\partial u_1}{\partial x_1}}_{(wall)} + (c_{(3)}-1)\epsilon_{(k)}}{-\overline{u_1 u_2}\, d\bar{U}_1/dx_2 + (c_{(2)}-1)\epsilon_{(k)}}\right] \tag{5.24}$$

$$(\overline{u_1 u_2})^2 + \left[(c_{(2)}-1)\epsilon_{(k)}/(d\bar{U}_1/dx_2)\right]\overline{u_1 u_2} + \left[(1-c_{(1)})\overline{u_2^2} k\, d\bar{U}_1/dx_2 + P/\rho\left(\overline{\frac{\partial u_1}{\partial x_2}} + \overline{\frac{\partial u_2}{\partial x_1}}\right)_{(wall)}\right] = 0 \tag{5.25}$$

$$\overline{u_2^2} = \tfrac{2}{3} k \left[\frac{c_{(1)}(-\overline{u_1 u_2}\, d\bar{U}_1/dx_2) + 2P/\rho \overline{\frac{\partial u_2}{\partial x_2}}_{(wall)} + (c_{(3)}-1)\epsilon_{(k)}}{-\overline{u_1 u_2}\, d\bar{U}_1/dx_2 + (c_{(2)}-1)\epsilon_{(k)}}\right] \tag{5.26}$$

$$\overline{u_3^2} = 2k - (\overline{u_1^2} + \overline{u_2^2}) \tag{5.27}$$

k-ε model

$$\overline{u_1^2} = \tfrac{2}{3} k \tag{5.28}$$

$$\overline{u_2^2} = \tfrac{2}{3} k \tag{5.29}$$

$$\overline{u_1 u_2} = -c_{(4)} \frac{k^2}{\epsilon_{(k)}} \frac{d}{dx_2} \bar{U}_1 \tag{5.30}$$

$$\overline{u_3^2} = \tfrac{2}{3} k \tag{5.31}$$

where: $2P/\rho \overline{\frac{\partial u_1}{\partial x_1}}_{(wall)}$, $P/\rho \left(\overline{\frac{\partial u_1}{\partial x_2}} + \overline{\frac{\partial u_2}{\partial x_1}}\right)_{(wall)}$, $2\overline{P/\rho \frac{\partial u_2}{\partial x_2}}_{(wall)}$

and f are as per p.119.

$$P_{11} \equiv -2\overline{u_1 u_2} \frac{d}{dx_2} \bar{U}_1 \qquad D_{11} \equiv 0$$

$$P_{12} \equiv -\left(\overline{u_2^2} \frac{d}{dx_2} \bar{U}_1\right) \qquad D_{12} \equiv \overline{u_1^2} \frac{d}{dx_2} \bar{U}_1$$

$$P_{22} \equiv 0 \qquad D_{22} \equiv -2\overline{u_1 u_2} \frac{d}{dx_2} \bar{U}_1$$

The mean momentum equation expresses the static balance of the mean normal stress ($\frac{1}{\rho}\frac{\partial}{\partial x_1}\bar{P}$), the turbulent shear stress ($\frac{d}{dx_2}\overline{u_1 u_2}$) and the viscous shear stress ($\nu \frac{d^2}{dx_2^2}\bar{U}_1$). The turbulent shear stress must

be related to the mean shear strain ($\frac{1}{2}d\bar{U}_1/dx_2$). The $\overline{u_1^2}$, $\overline{u_1u_2}$, $\overline{u^2}$, k and $\epsilon_{(k)}$ equations provide such a relationship.

Using equation (5.7) for $\overline{u_1u_2}$, it is possible to compute the non-dimensional turbulent shear stress ($-\overline{u_1u_2}/k$) which is plotted versus the mean shear strain-rate ($\frac{1}{2}d\bar{U}/dx_2$) which for various levels of $k/\epsilon_{(k)}$ in Figure 9. The corresponding relation provided by the $k-\epsilon$ model is

$$-\overline{u_1u_2} = 0.09 \frac{k}{\epsilon_{(k)}} \frac{d}{dx_2} \bar{U}_1 \qquad (5.32)$$

which is also plotted Figure 9. The non-linear PTASM predicts a finite non-dimensional shear stress at high strain rates unlike the $k-\epsilon$ model The former also predicts a considerably higher shear-stress at low strain rates.

5.3 Finite Control Volume Formulation and Solution Proceedure

The closed set of equations (5.1) to (5.13) must be solved simultaneously for the unknown $\bar{U}_1$, $\bar{U}_2$, and $\bar{P}$ fields. The solution of the partial differential equations requires their integration over the space of interest. To economize on the numerical solution procedure, equations (5.1) to (5.5) are usually written in the form

$$\frac{\partial}{\partial x_1}\left(\rho\phi\bar{U}_1 - \Gamma_{(\phi)}\frac{\partial}{\partial x_1}\phi\right) + \frac{\partial}{\partial x_2}\left(\rho\phi\bar{U}_2 - \Gamma_{(\phi)}\frac{\partial}{\partial x_2}\phi\right) = S_{\phi 1} \qquad (5.33)$$

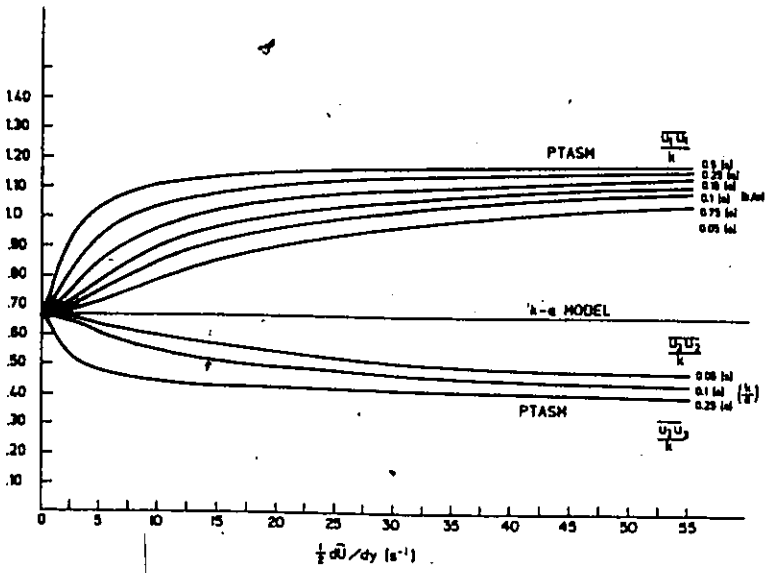

(a)

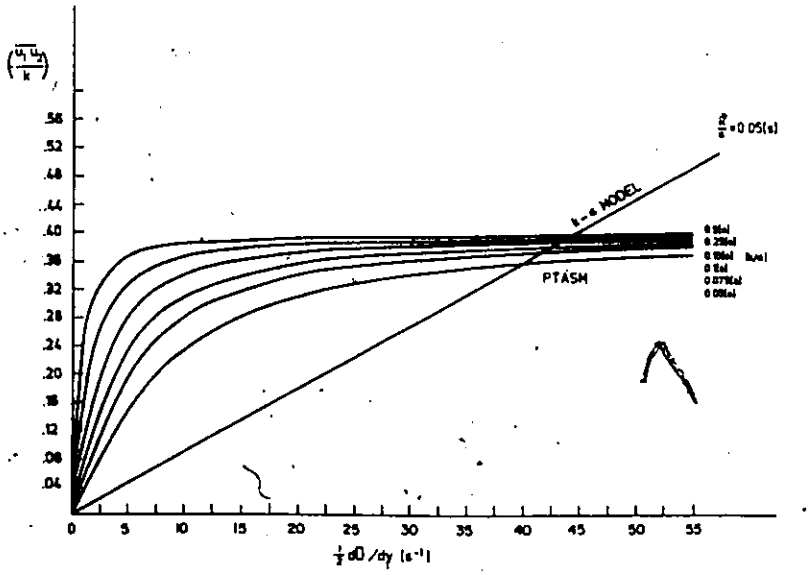

(b)

FIGURE 9: Non-Dimensional Stress-Strain Relationships for Fully Developed Channel Flow (a) Normal Components and (b) Shear Component

where ϕ represents a transported quantity such as $\bar{U}_1$, $\bar{U}_2$, k or $\epsilon_{(k)}$, while the source term $S_{(\phi)}$ and diffusivity coefficient $\Gamma_{(\phi)}$ would need to be adjusted so that the particular equation is correct. This equation for ϕ could be integrated over the region of interest if the variable functions were known a priori. However, this is not the case, and so approximate forms of the variable functions are postulated and the integration performed. To achieve suitable accuracy, this is done over small interconnecting subregions (control volumes), applying the approximate solution to each control volume separately. The equations for the scalar variables such as $\bar{P}$, k, and $\epsilon_{(k)}$, are integrated over the control volume indicated in Figure 10, while the control volumes for integrating the components of the velocity vector, $\bar{U}_1$ and $\bar{U}_2$, are staggered to the scalar control volume. This is done to ensure a unique pressure field (Patankar,1980). Integrating equation (5.23) for ϕ over one of these control volumes one gets

$$\int_S \left(\rho \phi \bar{U}_1 - \Gamma_{(\phi)} \frac{\partial}{\partial x_1} \phi\right) n_1 \, ds + \int_S \left(\rho \phi \bar{U}_2 - \Gamma_{(\phi)} \frac{\partial}{\partial x_2} \phi\right) n_2 \, ds = \int_V S_{(\phi)} \, dV \qquad (5.34)$$

The value of ϕ in the control volume is assumed to be represented by that at the central node; the flux across the control volume boundary is based on interpolation of these nodal values. The result of this integration is an algebraic equation for each control volume

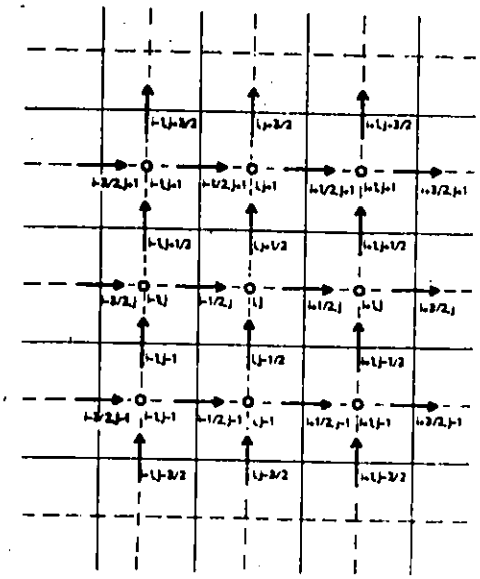

(a)

o scaler node; $\bar{U}_1$ node, $\bar{U}_2$ node

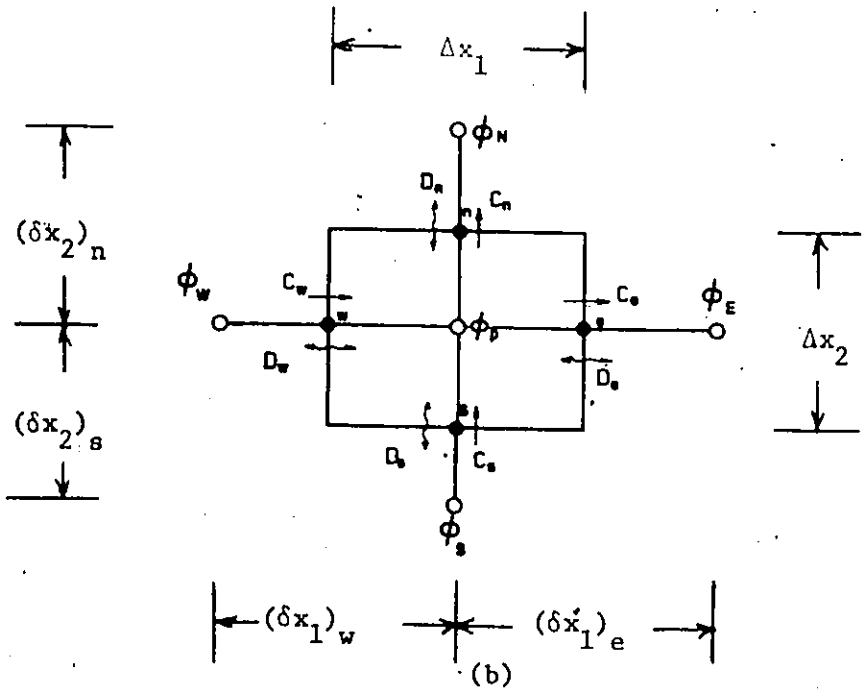

(b)

FIGURE 10: Computational Grid Arrangement (a) Relation Between Nodes, and (b) a General Computational Molecule

whose center is $\overline{P}$ and whose neighbours are N, E, W and S (see Figure 15).

$$(a_{(N)} + a_{(S)} + a_{(W)} + a_{(E)})\,\phi_{(P)} = a_{(N)}\,\phi_{(N)} + a_{(S)}\,\phi_{(S)} + a_{(W)}\,\phi_{(W)} + a_{(E)}\,\phi_{(E)} + S_{(\phi)} * V \qquad (5.35)$$

The coefficients $a_{(N)}$, $a_{(S)}$, $a_{(W)}$ and $a_{(E)}$ represent the influence of the neighbouring nodes through convective and diffusive transport, their exact form is dependent on the interpolation scheme used to evaluate the flux of ϕ through each control volume surface. The computations performed here are based on the hybrid interpolation scheme (for example see Patankar, 1980). The development of the coefficients, $a_{(N)}$, $a_{(S)}$, $a_{(E)}$ and $a_{(W)}$, when only convection and molecular diffusion are present, is lengthy and well documented by Patankar (1980) and Warnica (1981), he results are

$$a_{(E)} = \mathcal{D}_{(e)}\, f\{P_{(e)}\} + [\![-\mathcal{F}_{(e)}, 0]\!] \qquad (5.36)$$

$$a_{(W)} = \mathcal{D}_{(w)}\, f\{P_{(w)}\} + [\![\mathcal{F}_{(w)}, 0]\!] \qquad (5.37)$$

$$a_{(N)} = \mathcal{D}_{(n)}\, f\{P_{(n)}\} + [\![-\mathcal{F}_{(n)}, 0]\!] \qquad (5.38)$$

$$a_{(S)} = \mathcal{D}_{(s)}\, f\{P_{(s)}\} + [\![\mathcal{F}_{(s)}, 0]\!] \qquad (5.39)$$

where $\mathcal{F}$ and $\mathcal{D}$ represent the coefficients of convective and diffusive flux and are

$$\mathcal{F}_{(e)} = (\rho \bar{U}_1)_{(e)} \Delta x_2 \qquad \mathcal{D}_{(e)} = \Gamma_{(e)} \Delta x_2 / (\delta x_1)_{(e)}$$

$$\mathcal{F}_{(w)} = (\rho \bar{U}_1)_{(w)} \Delta x_2 \qquad \mathcal{D}_{(w)} = \Gamma_{(w)} \Delta x_2 / (\delta x_1)_{(w)}$$

$$\mathcal{F}_{(n)} = (\rho \bar{U}_2)_{(n)} \Delta x_1 \qquad \mathcal{D}_{(n)} = \Gamma_{(n)} \Delta x / (\delta x_2)_{(n)} \qquad (5.40)$$

$$\mathcal{F}_{(s)} = (\rho \bar{U}_2)_{(s)} \Delta x_1 \qquad \mathcal{D}_{(s)} = \Gamma_{(s)} \Delta x_1 / (\delta x_2)_{(s)}$$

$\mathcal{P}$ is the Peclet number and is defined as the ratio $\mathcal{F}/\mathcal{D}$. The variable is representative of the specific interpolation scheme used and for the hybrid scheme is

$$f\{\mathcal{P}\} = \max [0, 1 - 0.5|\mathcal{P}|] \qquad (5.41)$$

The source term $S_{(\phi)}$ is different for each variable

$$\begin{aligned} S_{(\bar{U}_1)} &= -(\bar{P}_{(e)} - \bar{P}_{(w)}) \\ S_{(\bar{U}_2)} &= -(\bar{P}_{(n)} - \bar{P}_{(s)}) \\ S_{(k)} &= \int_V P_{(k)}\, dV \\ S_{(\epsilon)} &= C_{f(b)} \int_V \frac{\epsilon_{(k)}}{k} P_{(k)}\, dV \end{aligned} \qquad (5.42)$$

Such terms are often expanded into a Taylor series with only the linear terms retained as $S_{(\phi)}\Big|_n = S_{(\phi)}\Big|_{n-1} + \frac{\partial}{\partial \phi} S_{(\phi)}\Big|_{n-1} [\phi|_n - \phi|_{n-1}]$ or $S_{(\phi)} = Su + Sp\,\phi|_n$ with n being the current iteration level. The resulting set of simultaneous algebraic equations are solved by the SIMPLE algorithm (Patankar,1980) which is modified as shown in Figure 11 to include the calculation of the Reynolds stresses. The standard coefficients and sources, (5.39) to (5.42) are modified to include the effect of Reynolds stresses.

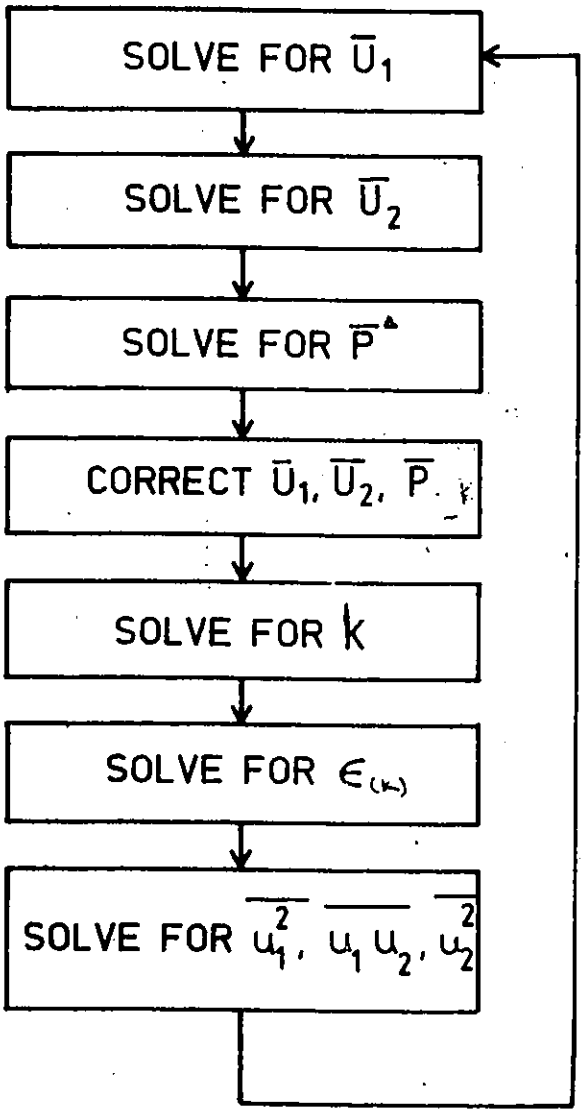

FIGURE 11: The Solution Algorithm

5.3.1 Mean Streamwise Momentum Equation

The streamwise momentum equation may be rewritten as

$$\frac{\partial}{\partial x_1}\left(\rho \bar{U}_1^2 - \mu \frac{\partial}{\partial x_1}\bar{U}_1\right) + \frac{\partial}{\partial x_2}\left(\rho \bar{U}_1 \bar{U}_2 - \mu \frac{\partial}{\partial x_2}\bar{U}_1\right)$$

$$= -\frac{\partial}{\partial x_1}\bar{P} - \left[\frac{\partial}{\partial x_1}(\rho \overline{u_1^2}) + \frac{\partial}{\partial x_2}(\rho \overline{u_1 u_2})\right] \qquad (5.44)$$

The last two terms on the right hand side represent the average turbulent convection. Integration of these terms over the $\bar{U}_1$ control volume (see Figure 9) gives

$$-\int_V \frac{\partial}{\partial x_1}(\rho \overline{u_1^2})\, dV - \int_V \frac{\partial}{\partial x_2}(\rho \overline{u_1 u_2})\, dV \qquad (5.45)$$

Using Gauss's thereom, this may be changed to the surface integral

$$-\left(\int_{S(e)} \rho \overline{u_1^2}\, dS - \int_{S(w)} \rho \overline{u_1^2}\, dS\right)$$

$$-\left(\int_{S(n)} \rho \overline{u_1 u_2}\, dS - \int_{S(s)} \rho \overline{u_1 u_2}\, dS\right) \qquad (5.46)$$

where S is the area of the control volume surface on the side indicated by the subscripts.

In evaluating the above surface integrals, the Reynolds Stresses are assumed to be uniform over the control volume faces and equal to the value at the center of that face, which may be interpolated from the nodal values. The $\overline{u_1 u_2}$ component is not directly available on these surfaces; one obtains $\overline{u_1 u_2}$ by linear interpolation between nodal values, but this method is computationally unstable (Launder and Samaraveera, 1979). This can be seen clearly if $\overline{u_1 u_2}$ is calculated from the linear formula

$$\overline{u_1 u_2} = -A \frac{\partial}{\partial x_2} \bar{U}_1 \qquad (5.47)$$

which is approximately true in fully developed channel flow at moderate strain levels (see Figure 9). Calculating $\overline{u_1 u_2}$ at the scalar node from $\partial \bar{U}_1 / \partial x_2$ at this node (obtained by linear interpolation) and then linearly interpolating $\overline{u_1 u_2}$ to the north and south faces of the $\bar{U}_1$ control volume gives the following expression for the $\bar{U}_1$ control volume

$$\left(-\int_S \overline{u_1 u_2} n_2 \, ds\right)_{(i-1/2,\, j)} = \frac{\Delta x_1}{\Delta x_2} \frac{A}{16} \left\{ \bar{U}_{1(i-3/2, j+2)} + \bar{U}_{1(i+1/2, j+2)} \right.$$
$$+ \bar{U}_{1(i+1/2, j-2)} + \bar{U}_{1(i-3/2, j-2)} \Big) + 2 \left(\bar{U}_{1(i-1/2, j+2)} \right. \qquad (5.48)$$
$$\left. \left. + \bar{U}_{1(i-1/2, j-2)} \right) - 2 \left(\bar{U}_{1(i-3/2, j)} + 2 \bar{U}_{1(i-1/2, j)} + \bar{U}_{1(i+1/2, j)} \right) \right\}$$

where the indices are defined in Figure 12.

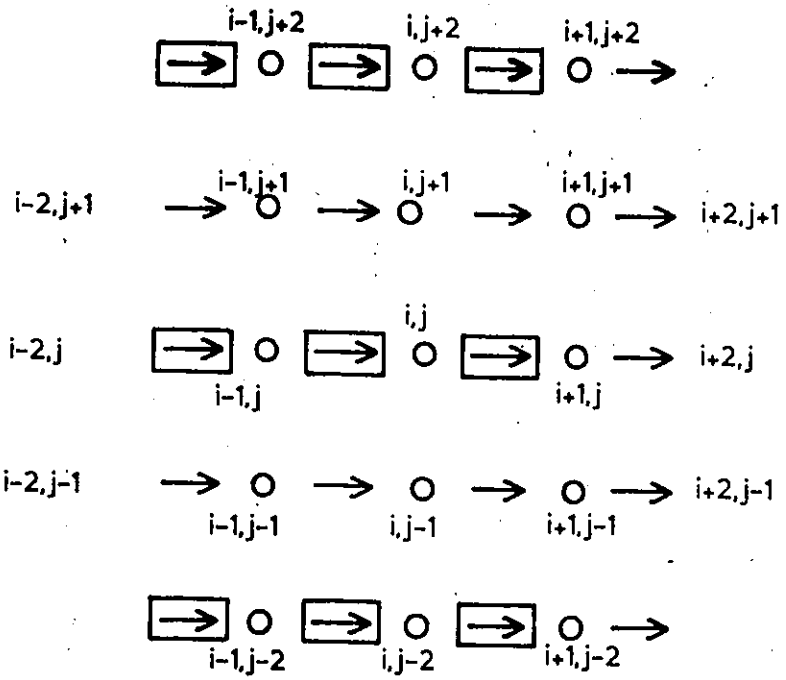

FIGURE 12: Unstable Computational Pattern for the Turbulent Shear Stress; the Outlined Lined Nodes are those Involved in the Computation

Expression (5.48) does not require that $\int_s \overline{u_1 u_2}\, n_2\, ds$ depend on the adjacent values of $\bar{U}_1$ in the x_2 direction. If the flow is dominated by $\int_s \overline{u_1 u_2}\, n_2\, ds$ then the result will be a zig-zag velocity field. This problem can be overcome by calculating $\overline{u_1 u_2}$ at the scalar nodes using $\partial \bar{U}_1/\partial x_2$ and $\partial \bar{U}_2/\partial x_1$ as before ($\overline{u_1 u_2}$ is not generally a linear function of strain) and then dividing by $(\partial \bar{U}_1/\partial x_2 + \partial \bar{U}_2/\partial x_1)$. This ratio (similar to a turbulent viscosity) is then linearly interpolated to obtain values at the north and south faces of the $\bar{U}_1$ $(i-\frac{1}{2}, j)$ control volume. The interpolated ratio is then multiplied by $(\partial \bar{U}_1/\partial x_2 + \partial \bar{U}_2/\partial x_1)$ at the north and south faces to obtain $\overline{u_1 u_2}$. The integral $\left(\int_s \overline{u_1 u_2}\, n_2\, ds\right)_{(i+\frac{1}{2},j)}$ will depend on the adjacent values of $\bar{U}_1$.

The normal component of the stress, $\int_s \overline{u_1^2}\, n_1\, ds$, is added to the source term $S_{\phi 1}$. The shear stress, $\int_s \overline{u_1 u_2}\, n_2\, ds$, is combined with the diffusion coefficients $\mathfrak{D}_{(n)}$ and $\mathfrak{D}_{(s)}$ which contribute to the coefficients $a_{(n)}$ and $a_{(s)}$.

5.3.2 Mean Transverse Momentum Equation

The treatment of the mean turbulent convection in the $\bar{U}_2$ equation is analogous to that in the $\bar{U}_1$ equation. The $\bar{U}_2$ equation is first arranged in the form

$$\frac{\partial}{\partial x_1}\left(\rho \bar{U}_2 \bar{U}_1 - \mu \frac{\partial}{\partial x_1} \bar{U}_2\right) + \frac{\partial}{\partial x_2}\left(\rho \bar{U}_2^2 - \mu \frac{\partial}{\partial x_2} \bar{U}_2\right)$$

$$= -\frac{\partial}{\partial x_2} \bar{P} - \left[\frac{\partial}{\partial x_1}\left(\rho \overline{u_1 u_2}\right) + \frac{\partial}{\partial x_2}\left(\rho \overline{u_2^2}\right)\right] \qquad (5.49)$$

Integrating this equation over the $\bar{U}_2$ vector control volume (see Figure 9) results in an expression for the Reynolds stress contribution

$$-\left(\int_{S(e)} \rho \overline{u_1 u_2}\, ds - \int_{S(w)} \rho \overline{u_1 u_2}\, ds\right) - \left(\int_{S(n)} \rho \overline{u_2^2}\, ds - \int_{S(s)} \rho \overline{u_2^2}\, ds\right) \quad (5.50)$$

These integrals are then discretized in a similar manner to those in the $\bar{U}_1$ equation with the shear stress combined with the $\mathfrak{D}_{(n)}$ and $\mathfrak{D}_{(s)}$ coefficients and the normal stress with Su.

5.3.3 Mean Turbulent Kinetic Energy Equation

Equation (5.4) for the mean turbulent kinetic energy may be rewritten by noting that the molecular diffusion and the diagonal components of turbulent diffusion can be combined with the mean convection on the right hand side to give:

$$\begin{aligned}
&\frac{\partial}{\partial x_1}\left(\rho k \bar{U}_1 - \mu \frac{\partial}{\partial x_1} k - c_{(7)} \frac{k}{\epsilon_{(k)}} \rho \overline{u_1^2} \frac{\partial}{\partial x_1} k\right) \\
&+ \frac{\partial}{\partial x_2}\left(\rho k \bar{U}_2 - \mu \frac{\partial}{\partial x_2} k - c_{(7)} \frac{k}{\epsilon} \rho \overline{u_2^2} \frac{\partial}{\partial x_2} k\right) \\
&= c_{(7)} \frac{\partial}{\partial x_1}\left(\frac{k}{\epsilon_{(k)}} \rho \overline{u_1 u_2} \frac{\partial}{\partial x_2} k\right) + c_{(7)} \frac{\partial}{\partial x_2}\left(\frac{k}{\epsilon_{(k)}} \rho \overline{u_1 u_2} \frac{\partial}{\partial x_1} k\right) \quad (5.51) \\
&+ \rho P_{(k)} - \rho \epsilon_{(k)}
\end{aligned}$$

This is obviously valid from an algebraic viewpoint, it is also suitable for computational purposes. Since $\overline{u_1^2}$ and $\overline{u_2^2}$ are positive definite, this form will result in an implicit representation

with all coefficients positive in the finite control volume equations (Launder and Samaraveera, 1979). The $\overline{u_1 u_2}$ stress may be positive or negative and therefore may not be treated in this way, because k is always positive (Patankar, 1980). If $\overline{u_1 u_2}$ is negative, it is placed implicitly in the equation on the left hand side as a coefficient of $k_{(p)}$ (Sp term). If it is positive it is placed on the right hand side of the equation (Su term). The production of k in this formulation differs from the k-ϵ formulation in that $P_{(k)}$ may be positive or negative, if it is negative it is included in the Sp term, if it is positive it is included in the Su term. An example of where the turbulent "production" term might be negative is during a severe acceleration of flow such as in a sudden contraction or in asymetric channel flow (Eskinazi and Erian, 1969).

The mean turbulent kinetic energy dissipation represents a sink at all times since $\epsilon_{(k)}$ is always positive; it must therefore be placed into the Sp term. Turbulent kinetic energy is a scalar and hence integration of equation (5.51) is done over the scalar control volume of Figure 9.

5.3.4 Mean Turbulent Kinetic Energy Dissipation Rate Equation

The $\epsilon_{(k)}$ equation is very similar to the k equation and hence it is treated in an analogous manner. The equation is first rearranged to the form

$$\frac{\partial}{\partial x_1}\left(\rho \epsilon_{(k)} \bar{U}_1 - \mu \frac{\partial}{\partial x_1}\epsilon_{(k)} - C_{(15)} \frac{k}{\epsilon_{(k)}} \rho \overline{u_1^2} \frac{\partial}{\partial x_1}\epsilon_{(k)}\right)$$
$$+ \frac{\partial}{\partial x_2}\left(\rho \epsilon_{(k)} \bar{U}_2 - \mu \frac{\partial}{\partial x_2}\epsilon_{(k)} - C_{(15)} \frac{k}{\epsilon_{(k)}} \rho \overline{u_2^2} \frac{\partial}{\partial x_2}\epsilon_{(k)}\right) \qquad (5.52)$$
$$= \frac{\partial}{\partial x_1}\left(C_{(15)} \frac{k}{\epsilon_{(k)}} \rho \overline{u_1 u_2} \frac{\partial}{\partial x_2}\epsilon_{(k)}\right) + \frac{\partial}{\partial x_2}\left(C_{(15)} \frac{k}{\epsilon_{(k)}} \rho \overline{u_1 u_2} \frac{\partial}{\partial x_1}\epsilon_{(k)}\right)$$
$$+ C_{(16)} \frac{\epsilon_{(k)}}{k} \rho P_{(k)} - C_{(18)} \rho \epsilon_{(k)}^2 / k$$

The molecular diffusion, diagonal and non-diagonal turbulent diffusion and production are treated in a manner identical to those in the k equation. Since $\epsilon_{(k)}$ is a scaler variable, it is integrated over the scaler control volume of Figure 9.

5.4 Geometry and Computational Grid Specification

The geometry for which computations were performed corresponds to the experimental set up of Laufer (1951), which was 7.01 m long, 0.127 m high and 1.52 m deep. The Reynolds number, which is based on the channel half width and the bulk velocity, was 61,600.

A good cross-stream computational grid for the channel should have the following characteristics:

a) small grid spacing in the near wall region where the velocity gradients are large,

b) large grid spacing in the center of the channel where velocity gradients are small.

A simple grid satisfying these requirements exhibits an abrupt transition from a uniform fine spacing to a uniform coarse spacing. This method, however, produces a very slow rate of convergence due to the widely different shear stresses on either side of the step change. A smooth transition between the fine and course regions can be achieved by using elementary functions to define the grid spacing. A particularly suitable function for defining the distance of the grid line j from the origin of x_2 is

$$x_2(j) = m\ e^{nj} + b \qquad (5.53)$$

The constants m and b are specified by assigning values to $x_2(1)$ and $x_2(N)$. The value of n, which is related to the grid spacing, is more conveniently determined by defining the parameter Λ as

$$\Lambda = \frac{x_2(N) - x_2(N-1)}{x_2(2) - x_2(1)} \tag{5.54}$$

which specifies the ratio of the last to the first grid spacing. The value of n is related to Λ by

$$\Lambda = \frac{e^{Nn} - e^{(N-1)n}}{e^{2n} - e^{n}} \tag{5.55}$$

The computations in this report were performed with 50 cross-stream grid lines based on a Λ value of 6.47 which was chosen as a compromise between core storage and accuracy.

The streamwise grid spacing was chosen on the basis of storage economy. Since streamwise spacing gradients are relatively weak and since the interest concentrates in the fully developed region where there are no streamwise gradients, a relatively coarse uniform stream-wise grid of 40 nodes was chosen.

The starting conditions for the k-ϵ model computations were uniform velocity, pressure, k and $\epsilon_{(k)}$ fields of near zero value. The starting conditions of the PTASM model computations were the converged k-ϵ solution in the same geometry.

The k-ϵ model computations reached a convergence level of 0.1% in 425 iterations at a rate of 2.96 seconds per iteration on a CDC Cybar 175 computer. The PTASM model computations, beginning with the k-ϵ solution, achieved a convergence level of 3 significant figures for the

field variables $\overline{U}_1$, $\overline{U}_2$, k and $\epsilon_{(k)}$ while $\overline{P}$ had only converged to 1 significant figure in 250 iterations at a rate of 4.15 seconds per iteration. This slow convergence was due to the effects of the normal turbulent stresses on the cross-stream pressure gradient. When the normal stress was combined with pressure, since $\frac{\partial}{\partial x_2}(\overline{P} - \rho\overline{u_2^2}) = 0$ for fully developed channel flow, convergence of all field variables was achieved to 3 significant figures in 202 iterations.

5.5 Boundary Conditions and Equations

5.5.1 Mean Momentum Equation in the Streamwise Direction

5.5.1a Inlet Conditions

The $\overline{U}_1$ velocity was specified to be a uniform profile of 0.973 ms^{-1} at the inlet. The $\overline{U}_1$ equation of section 5.3.1 was then used for these boundary elements.

5.5.1b Top and Bottom Channel Walls

The $\overline{U}_1$ velocity on the top and bottom walls of the channel was specified to be zero. The $\overline{U}_1$ equation of Section 5.3.1 was however modified for use in these boundary elements so that the shear stress would be accurately represented. The shear stress is calculated from the experimentally verified relation (Warnica, 1981; Sha and Launder, 1979)

$$\tau_{(w)} = -\mu \frac{\overline{U}_{1(P)}}{X_{2(P)}} \quad \text{(when the near wall point is inside the viscous sublayer)} \quad (5.56)$$

$$\tau_{(w)} = \frac{-\rho C_{(\mu)}^{1/4} k_{(P)}^{1/2} \mathcal{K} \overline{U}_{1(P)}}{\ln\left(E \rho k_{(P)}^{1/2} C_{(\mu)}^{1/4} X_{2(P)}/\mu\right)} \quad \text{(when the near wall point is outside the viscous sublayer)} \quad (5.57)$$

where the subscript p denotes that the value is taken to be at the near wall point.

The constants $C_{(\mu)}$, κ, and E are 0.09, 0.4187 and 9.793, respectively. The value of κ plays an important role in the calculations since $\varepsilon_{(w)}$ is directly proportional to it. The value of κ has been suggested by different experimenters to vary from 0.342 to 0.4187(Byrne, Hatton and Marriott,1970).

5.5.1c Outlet Conditions

The momentum equation for the velocity at the outlet boundary has been modified to take advantage of its locally parabolic character. The momentum equation is generally of the form (Warnica,1981; Patanker,1980).

$$(a_{(E)} + a_{(W)} + a_{(N)} + a_{(S)} - Sp * V_{(P)})\,\bar{U}_{1(P)} = a_{(E)}\bar{U}_{1(E)} + a_{(W)}\bar{U}_{1(W)} + a_{(N)}\bar{U}_{1(N)} + a_{(S)}\bar{U}_{1(S)} + A_{(e)} + Su * V_{(P)} \qquad (5.58)$$

Because recirculation is not observed at the outflow of a fully developed channel, the $a_{(E)}$ coefficient is set to zero to ensure that $U_{1(P)}$ is independent of $U_{1(E)}$. Also, since the $\bar{U}_2$ velocity is zero the $a_{(S)}$ and $a_{(N)}$ coefficients consist only of diffusion which is ignored. Equation (5.48) therefore becomes

$$\bar{U}_{1(P)} = \bar{U}_{1(W)} + \frac{A_{(e)}}{a_{(W)}}\left(\bar{P}_{(W)} - \bar{P}_{(e)}\right) \qquad (5.59)$$

5.5.2 Mean Momentum Equation in the Transverse Direction

The $\overline{U}_2$ velocity specified at the inlet, outlet, the top and bottom walls was zero. The $\overline{U}_2$ equation of section 5.3.2 was used for these boundary elements.

5.5.3 Pressure Correction Equation

The pressure correction equation at the boundaries is formulated by substitution of the velocities at the boundary control volumes into the continuity equation. Therefore the boundary equation for the pressure correction follows directly from the velocity boundary conditions. The following equations are modifications of the standard pressure correction equation (Warnica,1981).

(a) Inlet

$$\left(A_{(e)}d_{(e)} + A_{(n)}d_{(n)} + A_{(s)}d_{(s)}\right)\overline{P}'_{(P)}$$

$$= A_{(n)}d_{(n)}\overline{P}'_{(N)} + A_{(s)}d_{(s)}\overline{P}'_{(S)} + A_{(e)}d_{(e)}\overline{P}'_{(E)} \qquad (5.60)$$

$$-\left(\overline{U}^{*}_{1(e)}A_{(e)} - \overline{U}_{1(w)}A_{(w)} + \overline{U}^{*}_{2(n)}A_{(n)} - \overline{U}^{*}_{2(s)}A_{(s)}\right)$$

(b) Outlet

$$\left(\frac{A^{2}_{(e)}d_{(e)}}{a_{(w)}} + A_{(n)}d_{(n)} + A_{(s)}d_{(s)}\right)\overline{P}'_{(P)}$$

$$= A_{(n)}d_{(n)}\overline{P}'_{(N)} + A_{(s)}d_{(s)}\overline{P}'_{(S)} \qquad (5.61)$$

$$-\left[\frac{A^{2}_{(e)}}{a_{(w)}}\left(\overline{P}^{*}_{(P)} - \overline{P}_{(E)}\right) + \overline{U}^{*}_{2(n)}A_{(n)} + \overline{U}^{*}_{2(s)}A_{(s)}\right]$$

(c) Top Wall

$$(A_{(e)}d_{(e)} + A_{(n)}d_{(n)} + A_{(s)}d_{(s)})\,\bar{P}^{\Delta}_{(P)}$$

$$= A_{(e)}d_{(e)}\,\bar{P}^{\Delta}_{(E)} + A_{(w)}d_{(w)}\,\bar{P}^{\Delta}_{(W)} + A_{(s)}d_{(s)}\,\bar{P}^{\Delta}_{(S)} \qquad (5.62)$$

$$- (\bar{U}^{*}_{1(e)}A_{(e)} - \bar{U}^{*}_{1(w)}A_{(w)} + \bar{U}_{2(n)}A_{(n)} - \bar{U}^{*}_{2(s)}A_{(s)})$$

(d) Bottom Wall

$$(A_{(e)}d_{(e)} + A_{(w)}d_{(w)} + A_{(n)}d_{(n)})\,\bar{P}^{\Delta}_{(P)} = A_{(e)}d_{(e)}\,\bar{P}^{\Delta}_{(E)}$$

$$+ A_{(w)}d_{(w)}\,\bar{P}^{\Delta}_{(W)} + A_{(n)}d_{(n)}\,\bar{P}^{\Delta}_{(N)} \qquad (5.63)$$

$$- (\bar{U}^{*}_{1(e)}A_{(e)} - \bar{U}^{*}_{1(w)}A_{(w)} + \bar{U}^{*}_{2(n)}A_{(n)} - \bar{U}_{2(s)}A_{(s)})$$

The star indicates the value calculated at the last iteration and d is the coefficient of pressure in the velocity equation.

5.5.4 Boundary Conditions for Pressure

Since the velocity is specified at the top and bottom walls and the inlet, it is not a function of pressure at these points. Only at the outflow the boundary velocity becomes a function of pressure gradient and for this reason the pressure needs to be specified here. This is achieved by the common proceedure (Raithby and Schneider, 1979) by subtracting the pressure correction at top corner of the outlet from all the pressure corrections including the point where pressure is to be specified. This results in a specified pressure at this point which is equal to the initial pressure guess while all other points are corrected by an amount relative to the pressure correction at the specified point.

5.5.5 Mean Turbulent Kinetic Energy Equation

5.5.5a Inlet Condition

The inlet value of k was specified to be $4 \times 10^{-4} m^2 s^{-2}$. The specific value used here is not of great importance because we are interested in the fully developed region which should be independent of the inlet conditions. The k equation of Section 5.3.3 was used for calculations at these boundary elements.

5.5.5b Top and Bottom Walls

The value of turbulent kinetic energy at the top and bottom walls is zero. For calculations in these boundary elements it is necessary to modify the k equation of Section 5.3.3 so that the production and dissipation of k are accurately represented. The following relations are used (Warnica,1981; Sha and Launder,1979):

$$P_{(k)} = \tau_{(w)} \bar{U}_{1(p)} / (x_{2(p)} \rho)$$

$$\epsilon_{(k)} = \rho C_{(\mu)} k_{(p)}^2 / \mu$$

(when the near wall point is within the viscous region) (5.64)

$$P_{(k)} = \tau_{(w)} \bar{U}_{1(p)} / (x_{2(p)} \rho)$$

$$\epsilon_{(k)} = \frac{C_\mu^{3/4} k_{(p)}^{3/2}}{\kappa x_{2(p)}} \ln \left(E \rho k_{(p)}^{1/2} C_\mu^{1/4} x_{2(p)} / \mu \right)$$

(when the near wall point is outside the viscous region) (5.65)

5.5.5c Outlet Conditions

The turbulent kinetic energy equation at the outlet boundary control volume is of the form

$$(a_{(W)} + a_{(N)} + a_{(S)} - Sp * V_{(P)})\, k_{(P)} = a_{(N)} k_{(N)} + a_{(S)} k_{(S)} + a_{(W)} k_{(W)} + Su * V_{(P)} \qquad (5.66)$$

Because of the locally parabolic nature of the outlet the $a_{(E)}$ coefficient was set to zero.

5.5.6 Mean Turbulent Kinetic Energy Dissipation Equation

5.5.6a Inlet Conditions

As with the turbulent kinetic energy the inlet conditions of $\epsilon_{(K)}$ are not important since we are primarily interested in the fully developed region. The value of $\epsilon_{(K)}$ at the inlet was specified to be 3×10^{-5} $m^2 s^{-3}$ and the $\epsilon_{(K)}$ equation was used for the computations.

5.5.6b Top and Bottom Walls

The calculation of $\epsilon_{(K)}$ at these boundary elements does not use the equation, but the relation

$$\epsilon_{(K)} = \frac{k^{3/2}}{\ell} \qquad (5.67)$$

where ℓ is the dissipation length scale. This relation can be derived by studying the energy transfer through the various eddy sizes of turbulence (Townsend, 1976). It has further been established experimentally (Townsend, 1976) that $\ell = 2.5 y_1$ where y_1 is the distance from the wall.

5.5.6c Outlet Conditions

At the outlet, the locally parabolic character of the outflow is exploited and the equation for $\epsilon_{(k)}$ becomes

$$\left(a_{(w)} + a_{(n)} + a_{(s)} - S_P + V_{(p)}\right) \epsilon_{(k)(p)} = a_{(w)}\epsilon_{(k)(w)} + a_{(n)}\epsilon_{(k)(n)} + a_{(s)}\epsilon_{(k)(s)} + Su * V_{(p)} \quad (5.68)$$

since $a_{(E)}$ is set to zero.

5.6 Comparison with Experimental Results and Discussion

The aims of this comparison were

a) to establish the ability of the PTASM to predict the mean velocity and the components of the Reynolds Stress ,

b) to evaluate the effect of a near wall correction formula (Shir,1973 ; Launder, Reece and Rodi,1976),

c) to establish the ability of k-ϵ model to predict the mean velocity and the components of the Reynolds stress tensor, and

d) to compare the predictive capabilities of the Reynolds Stress Model Closure (Lauder, Reece and Rodi,1976) and the PTASM,

Two sets of data were used for purposes of comparison; Laufer (1951) and Comte-Bellot (1965). Results from the two experimental investigations are shown in Figures 13, 14 and 15. The experiments of Laufer and Comte-Bellot were performed at Reynolds numbers of approximately 57,000. The data pertaining to the turbulence quantities differ by as much as 20% in some locations, a difference which can be only partially attributed to geometrical dfferences. The Laufer and Compte-Bellot geometries had aspect ratios of 12 and 13.3 and lengths 7 and 12 m respectively.

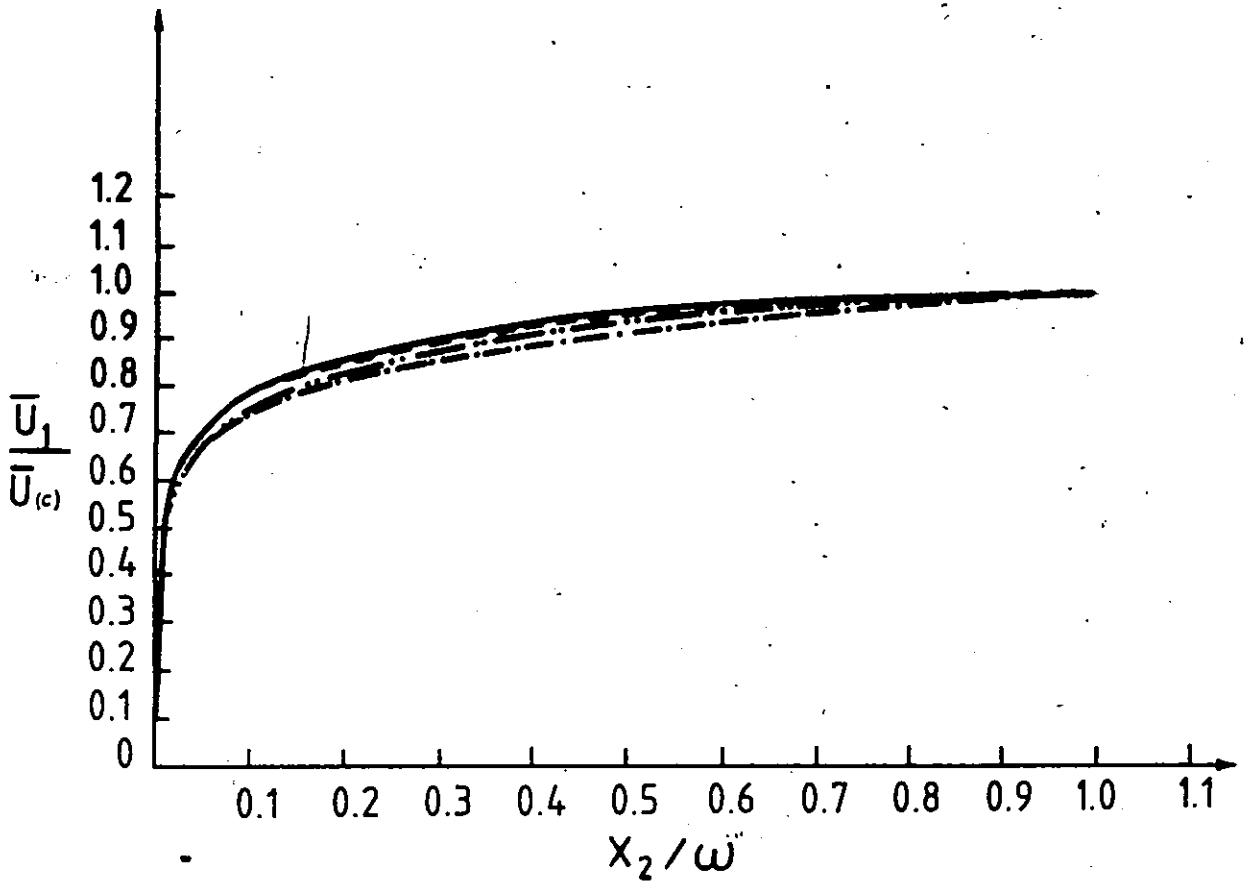

FIGURE 13: Mean Velocity Profile for Fully Developed Channel Flow; --- Laufer Data, — . — Comte-Bellot Data, — .. — k-ε Model, — PTASM.

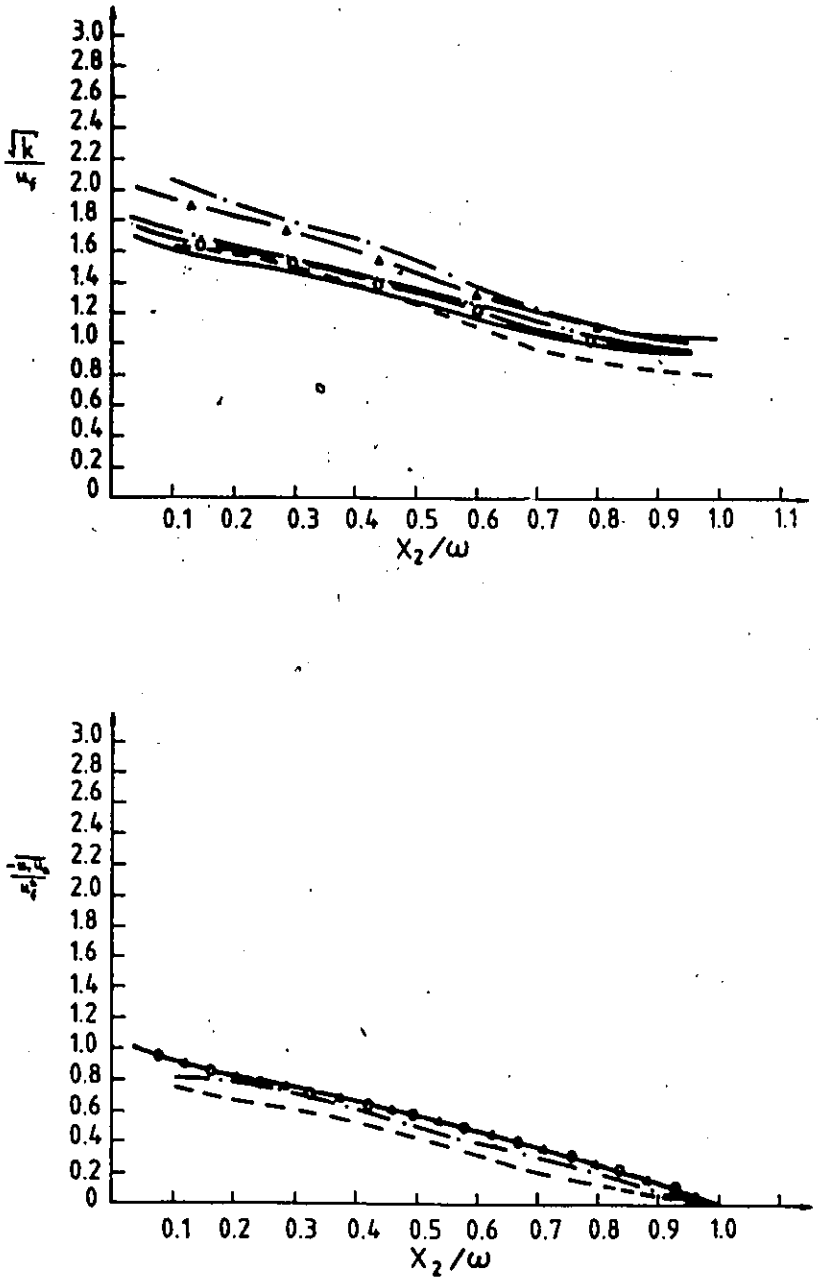

FIGURE 14: Turbulent Kinetic Energy and Shear Stress Distributions for Fully Developed Channel Flow: — O — PTASM with Lander, et al. wall correction, — Δ — PTASM with Shir wall correction, — □ — RSM, — PTASM, ---- Laufer data, — .— Comte-Bellot Data, —..— $k^{\frac{3}{2}}\varepsilon$ Model

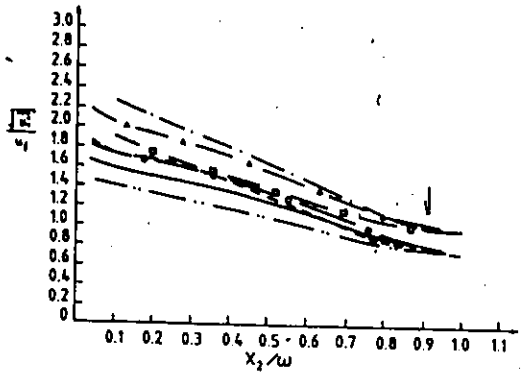

(a)

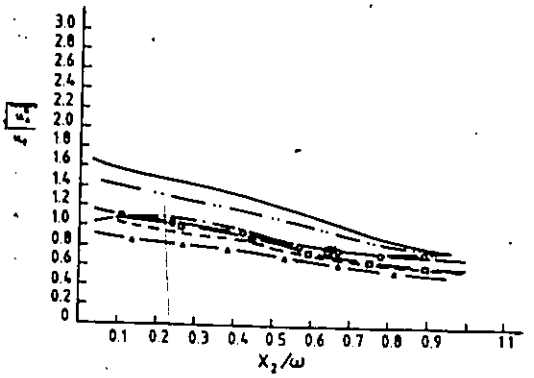

(b)

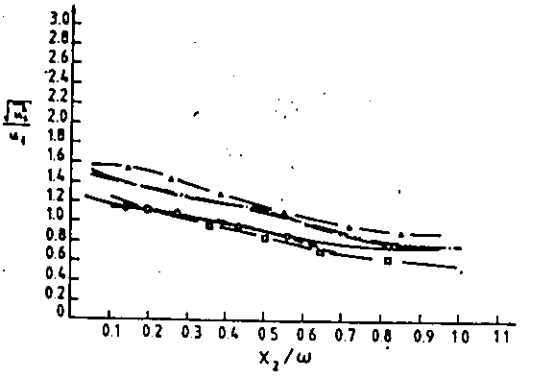

(c)

FIGURE 15: Turbulent Normal Stress Distribution in Fully Developed Channel Flow, (a) Streamwise Component, b) Transverse Component, and (c) Cross-Stream Component; Symbols as in Figure 14

5.6.1 PTASM Predictions

(a) The predicted mean velocity field is flatter than Laufer's data, but the deviation is only about 1%. The predicted flat shape of the mean velocity profile may be due to the stress strain relation of the PTASM. For large strains such as in the near wall region, the dimensionless eddy viscosity becomes small which probably results in a flatter mean profile.

(b) The level of k is predicted fairly well over most of the channel with the exception of the channel center where it is overpredicted; this is paradoxical because the turbulent shear stress, which is responsible for the production of k and $\epsilon_{(k)}$, is overpredicted everywhere in the channel.

(c) The turbulent shear stress $-\overline{u_1 u_2}/u^2_{(f)}$ is overpredicted all across the channel because it is proportional to $\overline{u_2^2}$ and it is everywhere overpredicted.

(d) The turbulent normal stress $\sqrt{\overline{u_3^2}}/u_{(f)}$ is underpredicted near the wall and is always on the wrong side of k in comparison to the data of Laufer. The $\sqrt{\overline{u_2^2}}/u_{(f)}$ and $\sqrt{\overline{u_3^2}}/u_{(f)}$ normal stresses are asssumed equal by the model while the measurements show a systematic difference which becomes more pronounced as the wall is approached. The cause of these poor predictions is that the effect of the wall on the pressure redistribution term has not been accounted for.

(e) The three normal stresses are predicted to be equal at the center of the channel while both sets of data indicate that they are not

equal. This discrepancy is also attributed to an improper modelling of the pressure-strain correlation since there is no production by the mean shear at the channel center.

5.6.2 Effect of Near Wall Correction Formula

In an attempt to account for the discrepancies between the measured and predicted turbulence fields, two wall correction models to the pressure-strain redistribution terms were investigated; the model of Shir (1973), equation (3.16), and the model of Launder, Reece and Rodi (1976), equation (3.15). The predictions obtained with both these correction models are compared to the data.

5.6.2a The Shir Near Wall Correction Formula

(a) The level of $\sqrt{k}/u_{(f)}$ has been overpredicted by as much as 20% near the wall where the correction is greatest; this is surprising because the correction suppressed $\overline{u_1 u_2}$ which is responsible for the production of k. This paradoxical effect is probably caused by a change in the mean velocity profile which also contributes to the production of k.

(b) This near wall correction has simulated all the correct effects, having increased $\sqrt{\overline{u_1^2}}/u_{(f)}$ and $\sqrt{\overline{u_3^2}}/u_{(f)}$ while decreasing $\sqrt{\overline{u_2^2}}/u_{(f)}$ and $\overline{u_1 u_2}/u_{(f)}^2$. This was done by transferring energy from $\overline{u_2^2}$ to $\overline{u_1^2}$ and $\overline{u_3^2}$. The resulting predictions are not as close to the measurements of Laufer as they were before the correction because the amount of energy transferred was too large.

5.6.2b The Launder, Reece and Rodi Near Wall Correction Formula

(a) The level of $\sqrt{k}/u_{(f)}$ was increased slightly due to the wall correction of the PTASM; again it is believed that this increase in turbulent production is due to a change in the mean velocity field which is caused by a decrease in $-\overline{u_1 u_2}$.

(b) In the region close to the wall, this wall correction formula has caused an increase in the predictions $\sqrt{\overline{u_1^2}}/u_{(f)}$ and $\sqrt{\overline{u_2^2}}/u_{(f)}$ and a decrease in $\sqrt{\overline{u_2^2}}/u_{(f)}$ and $\overline{u_1 u_2}/u^2_{(f)}$. These changes have somewhat improved the correspondence with the data.

(c) At the center of the channel this wall correction has not separated $\sqrt{\overline{u_1^2}}/u_{(f)}$ from $\sqrt{\overline{u_2^2}}/u_{(f)}$ and $\sqrt{\overline{u_3^2}}/u_{(f)}$

This failure must be directly related to the PTASM assumption because the same wall correction was succesful in this respect when used in conjunction with the full Reynolds Stress model (Launder, Reece and Rodi, 1976).

5.6.3 k-ϵ Model Predictions

(a) The normalized mean velocity is slightly lower than the data of Laufer, but by less than 5%, which can be considered as an acceptable approximation.

(b) The level of $\sqrt{k}/u_{(f)}$ is predicted to be larger than the measurements at the center of the channel. This overprediction is probably due to the fact that the k-ϵ model is unable to account for a change in the relative magnitudes of the normal stresses.

(c) The predicted level of $\overline{u_1 u_2}/u^2_{(f)}$ is larger than that measured by Laufer throughout the channel cross-section and especially at the channel wall. This may be partially explained

by the k-ϵ model stress strain relationship which remains linear even at very high levels of strain.

(d) The k-ϵ model predicts equal values of $\sqrt{\overline{u_1^2}}/u_{(f)}$, $\sqrt{\overline{u_2^2}}/u_{(f)}$ and $\sqrt{\overline{u_3^2}}/u_{(f)}$ all across the channel in clear contradiction of both sets of data.

5.6.4 Full Reynolds Stress Closure Predictions

This section compares the predictions of the PTASM (with wall correction) to the RSM (with wall correction) predictions carried out by Launder, Reece and Rodi (1976). The two turbulence models are identical with the exception that the former has eliminated the transport of the components of the Reynolds Stress Tensor by using the proportional transport approximation and the latter has calculated these terms exactly. The RSM closure has been solved with an equilibrium logarithmic wall function, however. Although not explicitly stated, it appears that Launder, Reece and Rodi (1976) have performed their computations using R=57,000 and u_f=0.038 ms^{-1} corresponding to the Comte-Bellot (1965) experiments.

The RSM gives fair predictions of $\sqrt{\overline{u_1^2}}/u_{(f)}$, $\sqrt{\overline{u_2^2}}/u_{(f)}$ and $\sqrt{\overline{u_3^2}}/u_{(f)}$, are distinct and agree fairly well with the data of Comte-Bellot (1965) throughout the channel. The failure of the PTASM to predict this behaviour is attributed to the failure of the wall correction even though both the RSM and PTASM use the same wall correction. The reason that the PTASM prediction of equal normal stresses, even at the center of the channel where there is no mean shear is that the proportional transport assumption causes the turbulent portion of the near wall correction to be cancelled out.

5.7 Closure

The Proportional Transport Algebraic Stress Model (PTASM) gives good predictions of both the mean velocity field and the Reynolds stress, normalized respectively by $U_{(c)}$ and $u_{(f)}$. However, it must be remembered that the values of $U_{(c)}$ and $u_{(f)}$ are different in the predictions and data, so that the predicted dimensional values differ from the experimental ones. A change in the wall functions (which would alter the value of the solutions for $U_{(c)}$ and $u_{(f)}$) could possibly reduce such differences, but this possibility has not been explored.

The PTASM gives better predictions of the normal Reynolds stress than the k-ϵ model does. However, PTASM predictions of the mean velocity profile, the turbulent kinetic energy level, and the turbulent shear stress (away from the wall) are only slightly better than those of the k-ϵ model. The reason for this is that $\bar{U}$, and k are determined by $\overline{u_1 u_2}$ which in the k-ϵ model is independent of $\sqrt{\overline{u_1^2}}$, $\sqrt{\overline{u_2^2}}$, and $\sqrt{\overline{u_3^2}}$.

The wall correction formula of Shir was found to increase differences between predicted and measured values of Reynolds stresses. The wall correction formula of Launder, Reece and Rodi (1976) improved the predictions in the regions of high mean shear strain rate but not to a sufficient degree to justify its use considering the required computational effort.

The PTASM model predictions compared well with the Reynolds Stress Closure model predictions except in the center of the channel where the mean shear strain is negligible. In this region, the PTASM model

predictions wrongly tended toward an isotropic state of turbulence. This effect can be traced to the pressure strain correlation model which is hampered by the proportional transport assumption.

CHAPTER VI

TWO-DIMENSIONAL TUBE FILLED CHANNEL FLOW

6.1 Introduction

Section 3.4 proposes a set of mean field equations and a turbulence closure suitable for porous medium. The associated volume averaging procedure introduced 3 unknown terms $F_{(1)i}$, $F_{(2)}$ and $F_{(3)}$, and three unknown constants $c_{(\mu)}$, $c_{(16)}$ and $c_{(18)}$.

This chapter summarizes currently available relations for $F_{(1)i}$ and $F_{(2)}$ while proposing a relation for $F_{(3)}$. Predictions using $F_{(1)i}$ and $F_{(2)}$ are made for isothermal flow in a tube filled channel. This relatively simple geometry provides a good test for the accuracy of the proposed turbulence model. Experimental data are reviewed and used to evaluate the predicted solution of the turbulence model equation.

6.2 Formulation of Relations for the Effects of the Tubes

6.2.1 Mean Momentum Transfer to the Tubes

The term $F_{(1)i}$ of equation (3.109) for mean momentum represents the transport of mean momentum to the tube walls. A more convenient expression for this term is

$$F_{(1)i} = \frac{f}{|\Delta x_i|} \frac{\rho}{2} |\bar{U}_i| \bar{U}_i \qquad (6.1)$$

where f is an empirical factor, different for flow parallel (Daugherty, 1977) and flow perpendicular (Butterworth, 1979) to the tubes. In this chapter only cross-flow relations are used.

The technique for evaluating this term in cross-flow is to measure the mean kinetic pressure drop across a large number of tube banks in developed isothermal one-dimensional flow. The basis of the method can be seen by simplifying the mean momentum equation for this flow. With all volume-averaged velocity and turbulence parameter gradients being zero, the equation is simplified into

$$\frac{d}{dx_i}\bar{P} = F_{(i)i} \qquad (6.2)$$

This establishes a relation between $F_{(i)i}$ and the mean kinetic pressure.

The Butterworth (1979) correlation for triangular or rotated triangular and square or rotated square tube patterns at high flow rates will be used in this investigation

$$F_{(i)i} = -\frac{4f}{d}\Phi^2\frac{\rho}{2}\bar{U}_i^2 \qquad (6.3)$$

where $$f = 0.5\,\frac{d^2 d_{(H)}}{(p-d)^3}\,R^{-0.267}$$

d and p are the diameter and pitch of the tube bundle, $d_{(H)}$ is twice

the ratio of the liquid volume per unit length to wetted surface area; R is Reynolds number based on tube diameter.

6.2.2 Mean Heat Transfer to the Tubes

The $F_{(2)}$ term in equation (3.110) for the mean temperature represents the heat transfer between the tubes and the shell side fluid. This is customarily calculated using the formula

$$F_{(2)} = h A \left(\underline{T} - \underline{\overline{T}}_{(tube)} \right) \qquad (6.4)$$

where A is the heat transfer area. Empirical expressions for h are available and are different for flow parallel (Sparrow, 1961) and flow perpendicular (Zukauskus, 1978) to the tubes.

6.2.3 Generation of Turbulence by the Tubes

The $F_{(3)}$ term in equation (3.108) for the mean turbulent kinetic energy could depend on the levels of k, $|\underline{\overline{U}}_i|$ and $(\rho - d)$, while the dependence on $|\underline{\overline{U}}_i|$ indicates an additional dependence on ρ and μ. Using the Buckingham P_1 Theorem (Douglas, 1969) and choosing ρ, $|\underline{\overline{U}}_i|$ and $(\rho - d)$ as primary variables $F_{(3)}$ may be expressed as

$$\frac{(\rho - d) F_{(3)}}{|\underline{\overline{U}}_i|^3} = b \left[\frac{k}{|\underline{\overline{U}}_i|^2} \right]^m \left[\frac{\rho |\underline{\overline{U}}_i| (\rho - d)}{\mu} \right]^n \qquad (6.5)$$

where m, n and b are unknown constants which could be evaluated

experimentally. However, if m and n were small, as in a fully developed turbulent flow,

$$F_{(3)} = b \frac{|\bar{U}_i|^3}{(r-d)} \tag{6.6}$$

This analysis will not be pursued any further because of a lack of relevant experimental results. It does, however, indicate the dependence of $F_{(3)}$ on Reynolds number, the turbulence intensity, the velocity and the gap spacing.

It is generally accepted that mean kinetic energy is transformed into turbulent kinetic energy, which, in turn, is dissipated into thermal energy of the fluid. The equations governing these quantities for an incompressible fluid are

$$\frac{\partial}{\partial t}(\rho + \frac{\partial}{\partial x_j}(\rho \bar{U}_j) = \frac{\partial}{\partial x_j}\{[-\bar{P}\delta_{ij} + \mu(\frac{\partial}{\partial x_j}\bar{U}_i + \frac{\partial}{\partial x_i}\bar{U}_j) - \rho\overline{u_i u_j}]\bar{U}_i\} + \rho\overline{u_i u_j}\frac{\partial}{\partial x_j}\bar{U}_i - \mu\frac{\partial}{\partial x_j}\bar{U}_i(\frac{\partial}{\partial x_j}\bar{U}_i + \frac{\partial}{\partial x_i}\bar{U}_j) \tag{6.7}$$

$$\frac{\partial}{\partial t}\overline{\rho} + \frac{\partial}{\partial x_j}(\overline{\rho}\bar{U}_j) = \frac{\partial}{\partial x_j}\{\overline{[-p\delta_{ij} + \mu(\frac{\partial u_i}{\partial x_j} + \frac{\partial u_j}{\partial x_i})]} - \overline{\rho u_i u_j/2}]u_i\} - \rho\overline{u_i u_j}\frac{\partial}{\partial x_j}\bar{U}_i - \mu\overline{\frac{\partial u_i}{\partial x_j}(\frac{\partial u_i}{\partial x_j} + \frac{\partial u_j}{\partial x_i})} \tag{6.8}$$

$$\frac{\partial}{\partial t}\mathcal{E} + \frac{\partial}{\partial x_j}(\mathcal{E}\bar{U}_j) = \frac{\partial}{\partial x_j}(-\rho\overline{u_j\theta} + \kappa\frac{\partial}{\partial x_j}\bar{T}) + \mu\frac{\partial}{\partial x_j}\bar{U}_i(\frac{\partial}{\partial x_j}\bar{U}_i + \frac{\partial}{\partial x_i}\bar{U}_j) + \overline{\mu\frac{\partial u_i}{\partial x_j}(\frac{\partial u_i}{\partial x_j} + \frac{\partial u_j}{\partial x_i})} \tag{6.9}$$

where:

$$\mathcal{K} \equiv \tfrac{1}{2}\rho \bar{U}_i \bar{U}_i$$

$$\mathcal{T} \equiv \tfrac{1}{2}\rho \overline{u_i u_i}$$

$$\mathcal{E} \equiv \text{molecular kinetic energy}$$

Mean kinetic energy is lost by two mechanisms, one producing turbulence and one directly increasing the thermal energy level. The viscous sink of the turbulent kinetic energy equation is a source of thermal energy. The unknown term $F_{(3)}$ is the turbulent sink of the mean kinetic energy equation. Integrating equation (6.7) for the mean turbulent kinetic energy over the hypothetical volume of Figure 4 gives the expression

$$\frac{\partial}{\partial t}\underline{\mathcal{K}} + \frac{\partial}{\partial x_j}(\underline{\mathcal{K}\bar{U}_j}) = \frac{\partial}{\partial x_j}\Big\{\underline{\Big[-\bar{P}\delta_{ij} + \mu\Big(\frac{\partial}{\partial x_j}\bar{U}_i + \frac{\partial}{\partial x_i}\bar{U}_j\Big) - \rho\,\overline{u_i u_j}\Big]\bar{U}_i}\Big\} - \int_{V_{(f)}} \mu\Big(\frac{\partial}{\partial x_j}\bar{U}_i + \frac{\partial}{\partial x_i}\bar{U}_j\Big)\frac{\partial}{\partial x_j}\bar{U}_i\, dV + \int_{V_{(f)}} \rho\,\overline{u_i u_j}\frac{\partial}{\partial x_j}\bar{U}_i\, dV \qquad (6.10)$$

To obtain this equation the relation between average of a gradient and gradient of an average has been used (equation 3.98). The flow in Figure 4 is steady and therefore the local time derivative may be ignored. The convective term may be changed into a surface integral by Gauss's theorem and equation (3.98) because

$$\frac{\partial}{\partial x_j}\left(\mathcal{K}\bar{U}_j\right) = \int_{S_{(f)}} \mathcal{K}\bar{U}_j n_j\, ds \qquad (6.11)$$

If the volume-averaged mean kinetic energy is further assumed to be homogeneous, its spatial derivatives can be ignored. Thus, equation (6.10) is simplified for the flow of Figure 4 into

$$\frac{\partial}{\partial x_j}\left\{\left[-\bar{P}\delta_{ij}+\mu\left(\frac{\partial}{\partial x_j}\bar{U}_i+\frac{\partial}{\partial x_i}\bar{U}_j\right)-\rho\overline{u_i u_j}\right]\bar{U}_i\right\}$$
$$=\int_{V(f)}\mu\left(\frac{\partial}{\partial x_j}\bar{U}_i+\frac{\partial}{\partial x_i}\bar{U}_j\right)\frac{\partial}{\partial x_j}\bar{U}_i\,dV \qquad (6.12)$$
$$+\int_{V(f)}-\rho\overline{u_i u_j}\frac{\partial}{\partial x_j}\bar{U}_i\,dV$$

The term on the left hand side may be transformed into a surface integral as

$$\int_{S(ff)}\left[-\bar{P}\delta_{ij}+\mu\left(\frac{\partial}{\partial x_j}\bar{U}_i+\frac{\partial}{\partial x_i}\bar{U}_j\right)-\rho\overline{u_i u_j}\right]\bar{U}_i n_j\,ds$$
$$=\int_{V(f)}\mu\left(\frac{\partial}{\partial x_j}\bar{U}_i+\frac{\partial}{\partial x_i}\bar{U}_j\right)\frac{\partial}{\partial x_j}\bar{U}_i\,dV \qquad (6.13)$$
$$+\int_{V(f)}-\rho\overline{u_i u_j}\frac{\partial}{\partial x_j}\bar{U}_i\,dV$$

The above expression represents the balance between the rate at which work is done on the flow volume and the rate at which thermal and turbulent energy are created internally. In a flow of the type shown in Figure 4, it is generally assumed that the viscous and turbulent stresses are small in comparison with the normal pressure stress (Slattery,1981).

Then, equation (6.13) becomes

$$\int_{S(f)} -\overline{P}\,\overline{U}_i n_i\, ds = \int_{V(f)} \mu \left(\frac{\partial}{\partial x_j}\overline{U}_i + \frac{\partial}{\partial x_i}\overline{U}_j\right)\frac{\partial}{\partial x_j}\overline{U}_i\, dV + \int_{V(f)} -\rho\overline{u_i u_j}\frac{\partial}{\partial x_j}\overline{U}_i\, dV \qquad (6.14)$$

If U_j is assumed constant over the surface integral of equation (6.14) and the divergence of the mean flow is ignored, this equation is simplified into

$$-\overline{U}_1\frac{\partial}{\partial x_1}\overline{P} = \int_{V(f)} \mu \left(\frac{\partial}{\partial x_j}\overline{U}_i + \frac{\partial}{\partial x_i}\overline{U}_j\right)\frac{\partial}{\partial x_j}\overline{U}_i\, dV + \int_{V(f)} -\rho\overline{u_i u_j}\frac{\partial}{\partial x_j}\overline{U}_i\, dV \qquad (6.15)$$

The rate of transfer of mean kinetic energy into turbulent kinetic energy is much greater than viscous disspation rate since the turbulent stress is larger than the viscous stress. Ignoring the viscous term, equation (6.17) becomes

$$\overline{U}_1\frac{\partial}{\partial x_1}\overline{P} = \int_{V(f)} -\rho\overline{u_i u_j}\frac{\partial}{\partial x_j}\overline{U}_i\, dV \qquad (6.16)$$

Combining equations (6.3) and (6.16) one gets

$$\underline{\bar{U}}_i F_{(3)i} = \int_{V_{(1)}} -\rho \overline{u_i u_j} \frac{\partial}{\partial x_j} \bar{U}_i \, dV \tag{6.17}$$

Thus, the unknown turbulent kinetic energy production $F_{(3)}$ may be expressed in terms of the empirically known mean momentum transfer to the tubes, $F_{(1)i}$, as

$$F_{(3)} = \underline{\bar{U}}_i F_{(1)i} \tag{6.18}$$

for the simple flow of Figure 4. This relationship must be generalized to the case where the direction of the flow is arbitrary.

The mean kinetic energy equation can be derived by taking the inner product of the mean momentum equation and the mean velocity vector. An equation for the volume average mean kinetic energy equation may be formed in a similar manner by using equation (3.105) for the volume averaged mean momentum and the volume averaged mean velocity vector $\underline{\bar{U}}_i$. The result is

$$\frac{\partial}{\partial t}\left(\underline{\rho}\right) + \frac{\partial}{\partial x_j}\left(\underline{\rho}\,\underline{\bar{U}}_j\right) = \frac{\partial}{\partial x_j}\left[\left(-\underline{\bar{P}}\,\delta_{ij} - \rho\,\underline{\overline{u_i u_j}}\right)\underline{\bar{U}}_i\right] + F_{(1)i}\,\underline{\bar{U}}_i \tag{6.19}$$

If the viscous stresses are ignored and the mean density and mean velocity are assumed constant over the surface of the averaging volume, equation (6.10) would become

$$\frac{\partial}{\partial t}\underline{\rho} + \frac{\partial}{\partial x_j}\left(\underline{\rho}\,\underline{\bar{U}_j}\right) = \frac{\partial}{\partial x_j}\left[\left(-\underline{\bar{P}}\,\delta_{ij} - \rho\,\underline{\overline{u_i u_j}}\right)\underline{\bar{U}_i}\right]$$

$$+ \frac{1}{V_{(s)}}\int_{V_{(s)}} \rho\,\overline{u_i u_j}\,\frac{\partial}{\partial x_j}\,\bar{U}_i\,dV \qquad (6.20)$$

Subtracting equation (6.20) from equation (6.19) one gets

$$F_{(1)\,i}\,\underline{\bar{U}_i} = -\frac{1}{V_{(s)}}\int_{V_{(s)}} \rho\,\overline{u_i u_j}\,\frac{\partial}{\partial x_j}\,\bar{U}_i\,dV \qquad (6.21)$$

and therefore,

$$F_{(s)} = -F_{(1)\,i}\,\underline{\bar{U}_i} \qquad (6.22)$$

which is the general expression for arbitrary flow direction.

The empirical correlation $F_{(1)\,i}$ is measured as the average pressure drop over a large number of tube rows. The previous dimensional analysis gave a possible expression of the form

$$\frac{(R-d)\,F_{(s)}}{|\underline{\bar{U}_i}|^2} = b\left[\frac{k}{|\underline{\bar{U}_i}|^2}\right]^m \left[\frac{\rho\,|\underline{\bar{U}_i}|\,(R-d)}{\mu}\right]^n \qquad (6.23)$$

The turbulence intensity is bound to affect the mean velocity gradients and hence the level of $F_{(3)}$. The turbulence intensity will change across the tube bundle and, as a result, the production will not be only a function of volume averaged mean velocity as indicated by equation (6.22). Without this dependence on $k/|\overline{\underline{U}_i}|^2$, $F_{(3)}$ will be constant in the streamwise direction of the tube filled channel because the volume average velocity is constant and this may induce some error. This effect has been ignored in this analysis with the hope that it is not very important.

6.3 Experimental Results

6.3.1 Data of Currie

Currie (1983) has investigated a 356 mm long, 114 mm wide and 115 mm deep duct of which 210 mm of length was filled with tubes of 12.6 mm diameter, arranged in a isosceles triangular pattern of 19.1 mm pitch. The Reynolds number based on the tube diameter and free stream velocity was 8410, while the tube bundle liquid to total volume ratio was 0.635. A laser-Doppler anemometer was used and all measurements were made in the gap between tubes. Only two components of the mean turbulent kinetic energy were measured; thus, the total mean turbulent kinetic energy can be estimated only within a factor of about 1.2 because of the uncertainty in the magnitude of the third component. The turbulent kinetic energy in the gap will be estimated by the formula

$$k_{(gap)} = \frac{3}{4}\left(\overline{u_1^2} + \overline{u_2^2}\right) \qquad (6.24)$$

which is based on the assumption that the $\overline{u_3^2}$ component is equal to the average of $\overline{u_1^2}$ and $\overline{u_2^2}$. In addition, the turbulent kinetic energy of the gap must be related to the volume average level. Some relation between these parameters is indicated in the local measurements of the velocity and one component of the turbulent kinetic energy by Martin, Elphick and Gollish (1983). The results in Figure 16 indicate a relation of the form $k_{(gap)}/\underline{k} \approx 0.10$. This involves a large degree of uncertainty and as a result the size of k must be used only as an order of magnitude estimate. However, it is assumed that this ratio of $k_{(gap)}$ to $\underline{k}$ is sufficiently constant throughout the bundle, so that the shape of the $\underline{k}$ curve may be used for comparison with the numerical predictions.

The cross-stream variation of $\underline{k}$ and $\overline{U}_1$ was moderate across the width of the duct. In addition, there was little streamwise variation of $\overline{U}_1$ in the bundle and $\overline{U}_2$ and $\overline{U}_3$ are near zero on the average. The estimated streamwise variation of $\underline{k}$ are shown in Figure 17.

6.3.2 Data of Fitzpatrick and Donaldson

The geometry investigated by Fitzpatrick and Donaldson (1980) was a 800 mm long, 209 mm wide and 150 mm deep duct, of which 400 mm of lenth was filled with 6.35 mm deameter tubes arranged in a rectangular pattern with a longitudinal and transverse pitch of 12.5 and 11.11 mm. The Reynolds number based on the tube diameter and free stream velocity was 3860 while the tube bundles fluid to total volume ratio was 0.77. The measurements were made in air using a hot wire anemometer. Measurements of the streamwise component of turbulent kinetic energy were made for successive streamwise stations half row apart along the

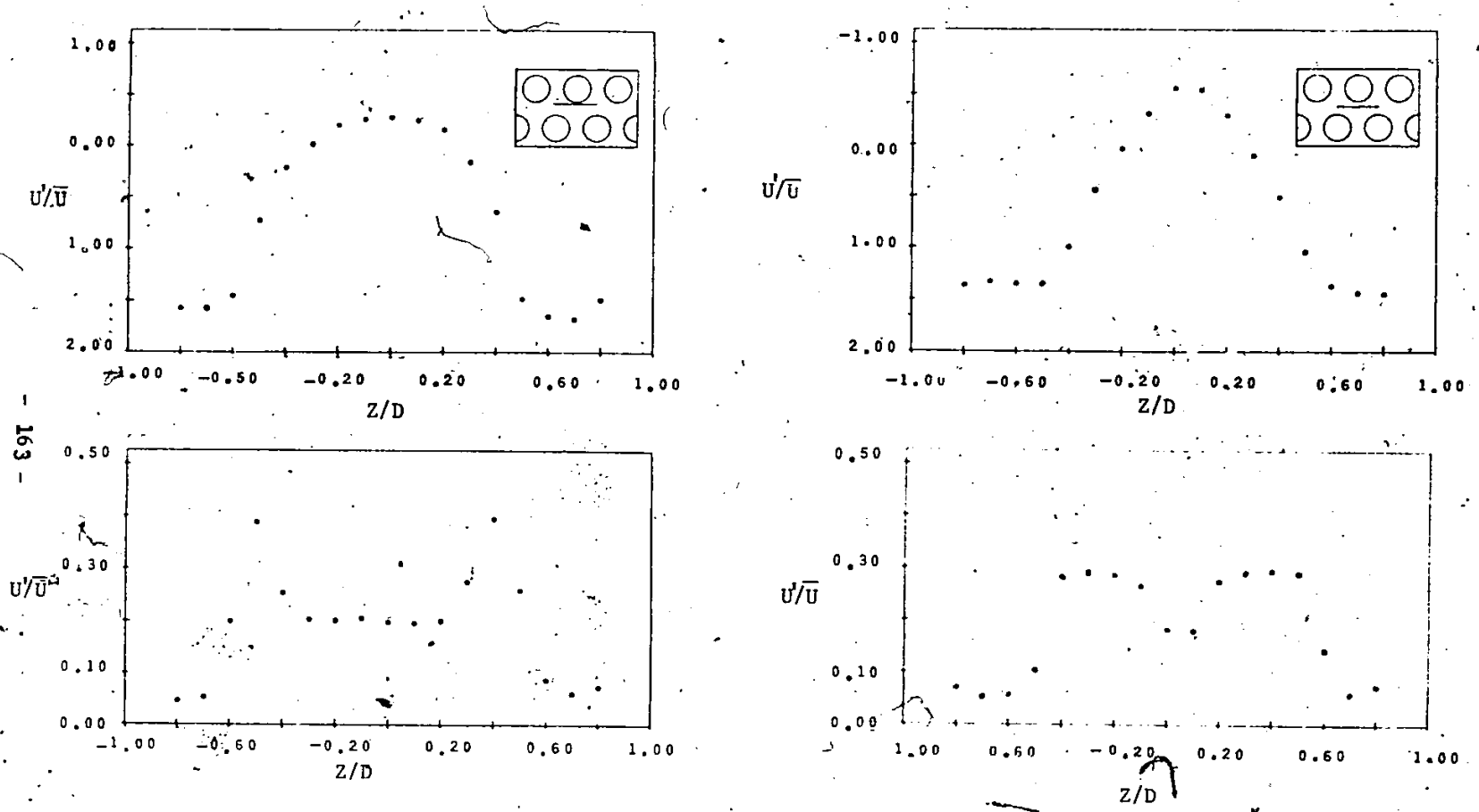

FIGURE 16: Local Variation of Mean Velocity and its Standard Deviation in a Tube Bundle from Martin, Elphick and Gollish, (1983).

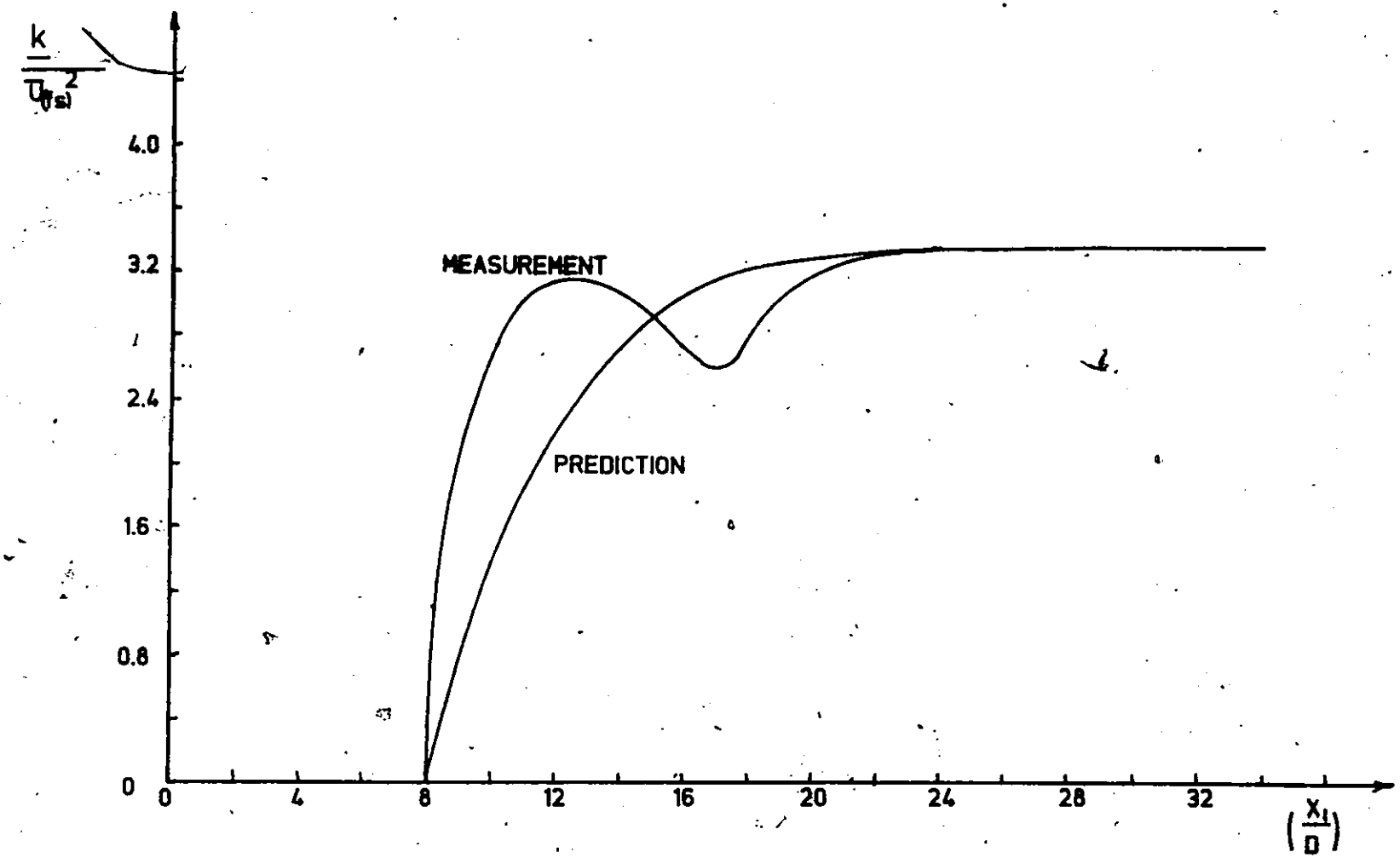

FIGURE 17: Streamwise Development of Volume Averaged Turbulent Kinetic Energy in a Tube Bundle with a Triangular Tube Array; Measurements by Currie (1983)

channel centreline. As a result, every second measurement was in the gap between tubes. This experiment used a square tube array, hence the relationship between $k_{(gap)}$ and the intrinsic volume average $\underline{k}$, which was used in Section 6.3.1, may not be directly applied. The authors made no local measurements and, as a result, the $\underline{k}$ values cannot be estimated. It is likely, however, that the values of $\underline{k}$ exceed those of $k_{(gap)}$. In the absence of better estimates, the relation $\underline{k} = 10\ k_{(gap)}$ will be used in this section also.

The level of $\underline{k}/U^2_{(gap)}$ estimated from the measurements in this paper is shown in Figure 18. It is not clear from the report whether the measured turbulence intensity is the sum of the three components or just the streamwise component or an estimate based on the streamwise component.

6.4 Governing Equations

The gap level of measured mean turbulent kinetic energy varies only slightly in the cross-stream direction near the centerline. This indicates that the diffusion effects of turbulence parameters in this region would be much smaller than production effects. In addition, the only volume-averaged mean velocity component (streamwise) has little cross-stream or time variation. These facts simplify the $\underline{k}$ and $\underline{\epsilon}_{(k)}$ equations for the tube filled region to

$$\underline{U}_1 \frac{d}{dx_1} k = F_{(s)} - \underline{\epsilon}_{(k)} \qquad (6.25)$$

$$\underline{U}_1 \frac{d}{dx_1} \underline{\epsilon}_{(k)} = C_{(1\epsilon)}\, \underline{\epsilon}_{(k)}\, \underline{k}^{-1} F_{(s)} - C_{(2\epsilon)}\, \underline{\epsilon}^2_{(k)}\, \underline{k}^{-1} \qquad (6.26)$$

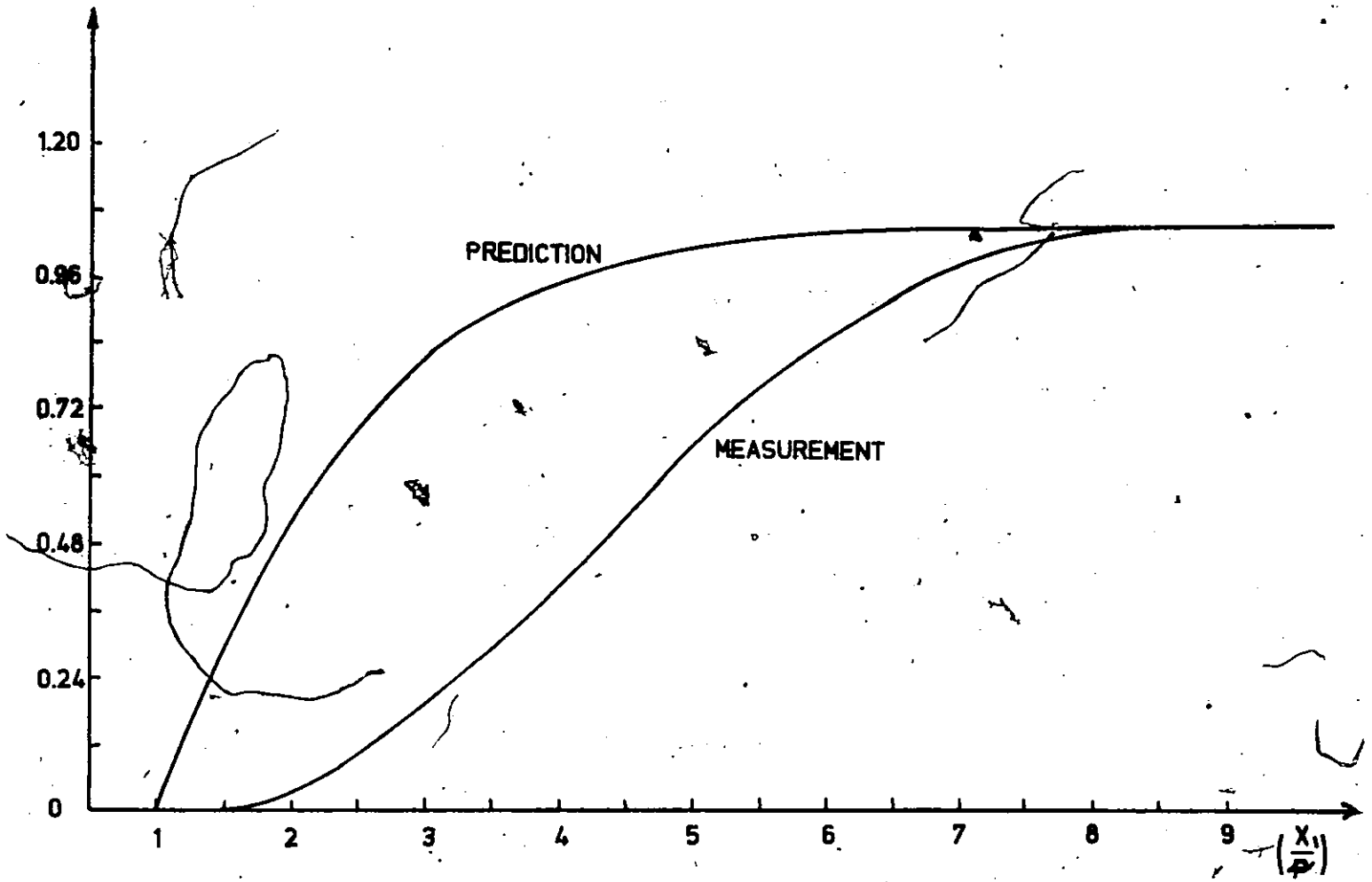

FIGURE 18: Streamwise Development of Volume Average Turbulent Kinetic Energy in a Tube Bundle with a Square Tube Array, Measurements by Fitzpatrick and Donaldson (1975)

These equations are similar to the equations describing the nearly homogeneous shear flow described in Chapter 4 with the following exceptions: the variables are volume averages and the turbulent production is constant for the tube-filled channel flow. As a result an expression analogous to the one in Chapter 4 for the turbulent kinetic energy may also be employed here.

$$\underline{U}_1 \frac{d}{dx_1} \underline{k} = F_{(3)} - \underline{k}^{\underline{c}_{(16)}} / \underline{\ell} \qquad (6.27)$$

$$\underline{\ell} = \underline{\ell}_{(0)} + (\underline{c}_{(18)} - \underline{c}_{(16)}) \int \underline{k}^{\underline{c}_{(16)}-1} \underline{U}_1^{-1} dx_1 \qquad (6.28)$$

This is an integro-differential equation and cannot be solved directly. However, it does permit some insight to the simultaneous solution of equations (6.25) and (6.26). Since the integral $\int \underline{k}^{\underline{c}_{(16)}-1} dx_1$ is always positive, $\underline{\ell}$ increases as x_1 increases if $\underline{c}_{(18)} > \underline{c}_{(16)}$ and decreases as x_1 increases if $\underline{c}_{(16)} < \underline{c}_{(18)}$.

The constants $c_{(16)}$ and $c_{(18)}$ of the standard $k-\epsilon$ model were replaced by $\underline{c}_{(16)}$ and $\underline{c}_{(18)}$ after the volume averaging procedure, in order to account for the non-uniformity of k, $\epsilon_{(k)}$ and $P_{(k)}$ in the averaging volume. However, in view of the severe non-uniformity of k (Figure 16) the constants $\underline{c}_{(16)}$ and $\underline{c}_{(18)}$ may deviate significantly from the usual $c_{(16)}$ and $c_{(18)}$ values of 1.44 and 1.92 respectively.

If $\underline{c}_{(16)} = \underline{c}_{(18)}$ then equation (6.28) becomes $\underline{\ell} = \underline{\ell}_{(0)}$ and equation (6.27) reduces to the first order differential equation

$$\underline{U}_1 \frac{d}{dx_1} \underline{k} = F_{(3)} - \underline{k}^{\underline{c}_{(16)}} / \underline{\ell}_{(0)} \qquad (6.29)$$

which has the asymptotic solution

$$\underline{k} = \left(\underline{\ell}_{(o)} F_{(3)} \right)^{\frac{1}{\underline{c}_{(4)}}} \qquad (6.30)$$

If $\underline{\ell}$ or $\underline{\ell}_o$ is to be regarded as a length scale, $\underline{L}$, then dimensional homogeneity requires that $\underline{c}_{(6)} = 3/2$. Although the general equation (6.27) does not have a known exact solution, it permits relatively simple solutions for two limiting cases:

i) When $(x - x_o)$ is very small, the integral

$$(\underline{c}_{(8)} - \underline{c}_{(4)}) \int \underline{k}^{\underline{c}_{(4)}-1} / \underline{\bar{U}}_1 \, dx_1$$

is also very small and, as a result, equation (6.27) becomes approximately equal to equation (6.29). In this case, $\underline{\ell}_o$ is the "dissipation length scale" at the intial position.

ii) When $(x - x_o)$ is very large the integral

$$(\underline{c}_{(8)} - \underline{c}_{(4)}) \int \underline{k}^{\underline{c}_{(4)}-1} / \underline{\bar{U}}_1 \, dx_1$$

is very large and equation (6.27) becomes approximately equal to

$$\underline{\bar{U}}_1 \frac{d}{dx_1} \underline{k} = F_{(3)} - \underline{k}^{\underline{c}_{(4)}} / (\underline{c}_{(8)} - \underline{c}_{(4)}) \int \underline{k}^{\underline{c}_{(4)}-1} / \underline{\bar{U}}_1 \, dx_1 \qquad (6.31)$$

For the latter case a power solution is possible. Assuming that $\underline{k} = b x_1^n$ and substituting this into equation (6.3), one gets the relation

$$\underline{U}_1 \, n \, b \, x_1^{n-1} = F_{(8)} - \frac{b^{n\underline{c}_{(16)}} \, x^{n\underline{c}_{(16)}} \, \underline{U}_1 \left[n \left(\underline{c}_{(16)} - 1 \right) + 1 \right]}{\left(\underline{c}_{(18)} - \underline{c}_{(16)} \right) b^{\underline{c}_{(16)} - 1} \, x_1^{n(\underline{c}_{(16)} - 1) + 1}} \qquad (6.32)$$

which is satisfied when

$$b = \left(1 - \frac{\underline{c}_{(16)}}{\underline{c}_{(18)}} \right) \frac{F_{(8)}}{\underline{U}_1} \quad \text{and} \quad n = 1 \qquad (6.33)$$

The range of validity of the linear solution depends on the initial conditions of $\underline{k}$ and $\underline{\epsilon}_{(k)}$ (since $\underline{L}_{(0)} = \frac{k_{(0)}^{\underline{c}_{(16)}}}{\underline{\epsilon}_{(k)(0)}} \neq 0$) at the entrance of the bundle. If, however, it is satisfied at one position, it must also be satisfied at all downstream positions. This makes an asymptopic solution of $\underline{k}$ impossible unless $\underline{c}_{(16)} = \underline{c}_{(18)}$.

The data in Figures 17 and 18 both show that $\underline{k}$ has an asymptopic behaviour, and, as a result, $\underline{c}_{(16)}$ must equal $\underline{c}_{(18)}$ in this region. In addition, since $dk/dx_1 = 0$, equation (6.27) with $\underline{c}_{(16)} = 3/2$ simplifies to

$$\underline{L}_{(\infty)} = \underline{k}_{(\infty)}^{3/2} / F_{(8)} \qquad (6.34)$$

which could be used to determine the value of the length scale although it is hoped that further experimental data will allow $\underline{L}_{(\infty)}$ to be correlated to the tube bundle geometry which would allow $\underline{k}_{(\infty)}$ to be determined from equation (6.34).

If $\underline{c}_{(16)}$ is assumed to equal $\underline{c}_{(18)}$ even before the asymptotic region, then the length scale $L_{(\infty)}$ must also apply outside this region and the governing equation for the entire bundle would be

$$\underline{U}_1 \frac{d}{dx_1} \underline{k} = F_{(3)} - \underline{k}^{3/2} / L_{(\infty)} \qquad (6.35)$$

This would then be solved using the initial conditions for $\underline{k}$. Its accuracy will depend on the difference between $\underline{L}_{(0)}$ and $\underline{L}_{(\infty)}$ near the entrance. The assumption that $\underline{c}_{(16)} \triangleq \underline{c}_{(18)}$ everywhere is equivalent to the assumption that local $\underline{k}$ and $\epsilon_{(k)}$ profiles are everywhere similar.

6.5 Solution of the Equations

6.5.1 One-Dimensional Calculations

Equation (6.35) has been solved using the Runge-Kutta technique for the experimental conditions described by Currie (1983) and by Fitzpatrick and Donaldson (1975). The $F_{(3)}$ values were calculated from equations (6.3). These solutions were found by forward integration from the beginning of the bundle using the value of $\underline{k}$ at this point as an initial condition.

The calculations compare well with the data of Currie (Figure 17), but are unable to predict the measured undulations, the largest of which occurs at $x/d = 17$.

The calculations show much poorer agreement with the high Reynolds number data of Fitzpatrick and Donaldson (Figure 18), especially in the initial part.

6.5.2 Two-Dimensional Calculations

Two sets of equations were solved within the channel. Outside of the tube bundle, the k-ϵ model was used in conjunction with the mean momentum and mean mass conservation equations for the open region.

Within the tube bundle, the modified volume averaged k-ϵ model, mean momentum and mean mass conservation equations were solved. The empirical functions used, $F_{(1)i}$ and $F_{(3)}$, were the ones described by equations (6.3) and (6.18). Density and molecular viscosity were kept constant during these calculations.

At the interface between the tube-free and tube-filled regions the solutions were assumed to be continuous. The geometry modelled was that of Currie (1983); the long extension following the bundle was not present in the experimental rig but it was introduced in the calculations in order to permit a fully developed channel flow before the exit and, thus, the requirement of no stramwise velocity gradient could be applied as an exit boundary condition. The grid used for the present calculations is shown in Figure 19. The numerical discretization scheme and solution procedure used here are identical to those used in the channel flow analysis of Chapter 5.

The equation and boundary conditions used in the present calculations were identical to those used in the 2-D channel of Section 5 with the exception that the velocity, turbulent kinetic energy and turbulent kinetic energy dissipation rate at the inlet used here were chosen to comply with corresponding measurements as follows $0.35\ ms^{-1}$, $0.114 \times 10^{-3}\ m^2s^{-2}$ and $17.33 \times 10^{-3}\ m^2s^{-2}$ and $17.33 \times 10^{-6}\ m^{2-3}$ respectively.

The calculated mean velocity and turbulent kinetic energy (Figure

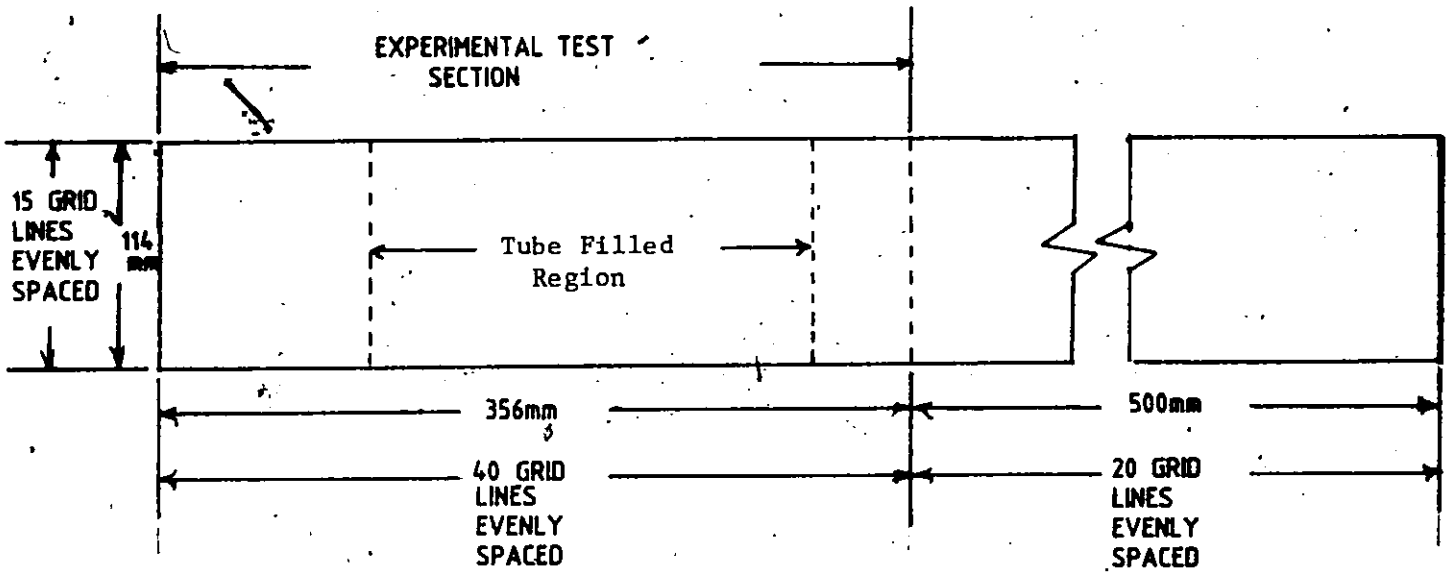

FIGURE 19: Computational Grid for the Tube Filled Channel

20) were fairly uniform in the cross-stream direction, in agreement with the measurements indicated. Figure 20 shows predicted pressure within ±10% of the measured overall pressure drop. Figure 20 shows that when the coefficients $c_{(16)}$ and $c_{(18)}$ were 1.44 and 1.92, respectively k became a linear function of x with a slope of 1.87. This is very close to the linear relation (6.33) which for $(c_{(16)}/c_{(18)})$ = 0.75 gives a linear function with a slope of 1.86. Making the assumption that $c_{(16)} = c_{(18)} = 1.5$ throughout the region and thus allowing $l = l_{(0)}$ results in a very inadequate level of k which does not reach an asymptote but continues to grow linearly with a slope of 0.31. This is contrary to what is expected from a dimensional analysis. The cause of this effect is attributed to additional production of turbulent kinetic energy at the wall which has been accounted for in this two-dimensional analysis. When $\epsilon_{(k)}$ is specified as $k^{3/2}/l$ where l = 0.069 the solution is very similar to the 1-D prediction (see Figure 17).

The apparent leveling off of k in Figure 20 is actually an end-effect resulting from a gradual change of the $V_{(f)}$ to V. The linear growth would continue if the bundle were extended.

6.6 Discussion

The data of Currie (1983) and Fitzpatrick and Donaldson (1980) both have a region where k reaches a constant value. However, the two experimental configurations are very different, having triangular and square tube arrays respectively. Figures 17 and 18 show that k increases faster in the triangular tube array than in the square tube array. The triangular array causes more violent deformation and a

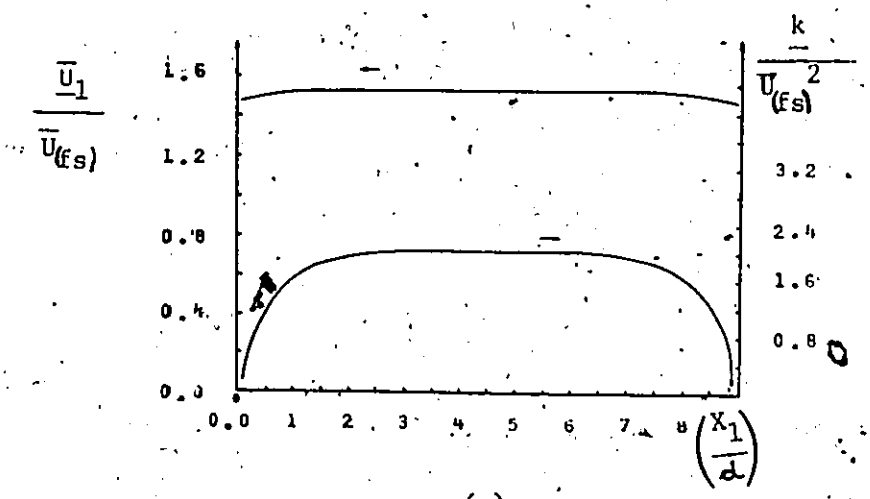

(a)

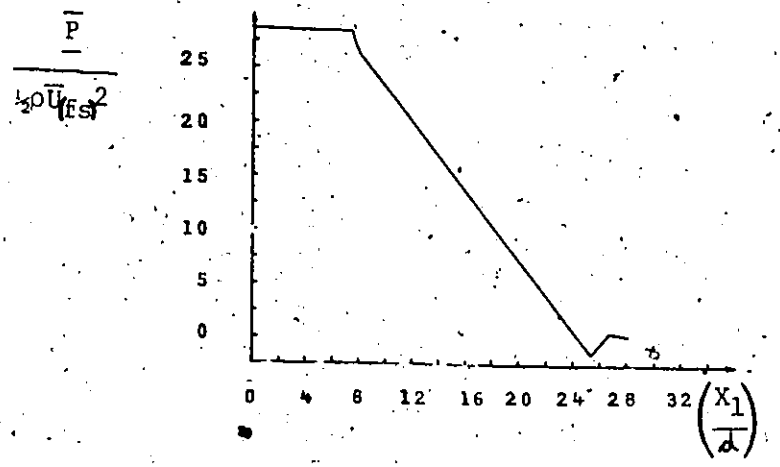

(b)

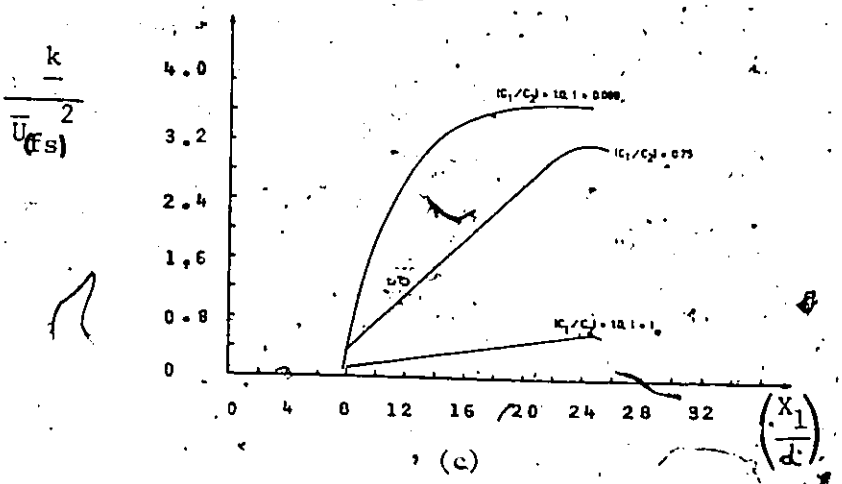

(c)

FIGURE 20: Two-Dimensional Calculations in Tube Filled Channel Flow
a) Transverse Distribution of Streamwise Velocity and Turbulent Kinetic Energy, b) Streamwise Variation of Pressure, c) Streamwise Development of Turbulent Kinetic Energy.

faster adjustment of the free-stream length scale. The square tube array has a lag of one-half row before any significant development of $\underline{k}$ takes place which results in a non-uniformity in the production of $\underline{k}$ at the entrance. Another difference is in the location of a local minimum in $\underline{k}$ which is present in the lower Reynolds number data of Fitzpatrick and Donaldson (1980), but tends to disappear as Reynolds number increases. A similar minimum appears in the data of Currie, but it is much more pronounced and occurs after $\underline{k}$ is nearly developed. The cause of these minima is not known with any certainty, but the fact that, in one case, the minimum diminishes with increasing Reynolds number, implies that it may be due to a transition of the flow to a fully turbulent regime, which affects the production rate, $F_{(3)}$.

The increase of $\underline{k}$ in the square tube array is much milder than that in the triangular tube array. A possible cause of this may be that the convection rate in the square tube array is much higher, since the slope of $\underline{k}$ $d\underline{k}/dx_1$, is proportional to the convection rate. It is possible that the convection rate may be closer to the gap velocity rather than to the volume average velocity which was used. This deficiency may be inherent in the application of the porous medium concept to tube bundles.

The length scale was evaluated using the volume average convection rate, since accurate measurements of length scale are not available. For illustrative purposes, $\underline{k}$ has been re-calculated for the Fitzpatrick and Donaldson data using a larger value of $\underline{k}$ which is equivalent to increasing the convection rate (Figure 21). It can be seen that the discrepancy between prediction and measurement diminishes compared to that in Figure 18.

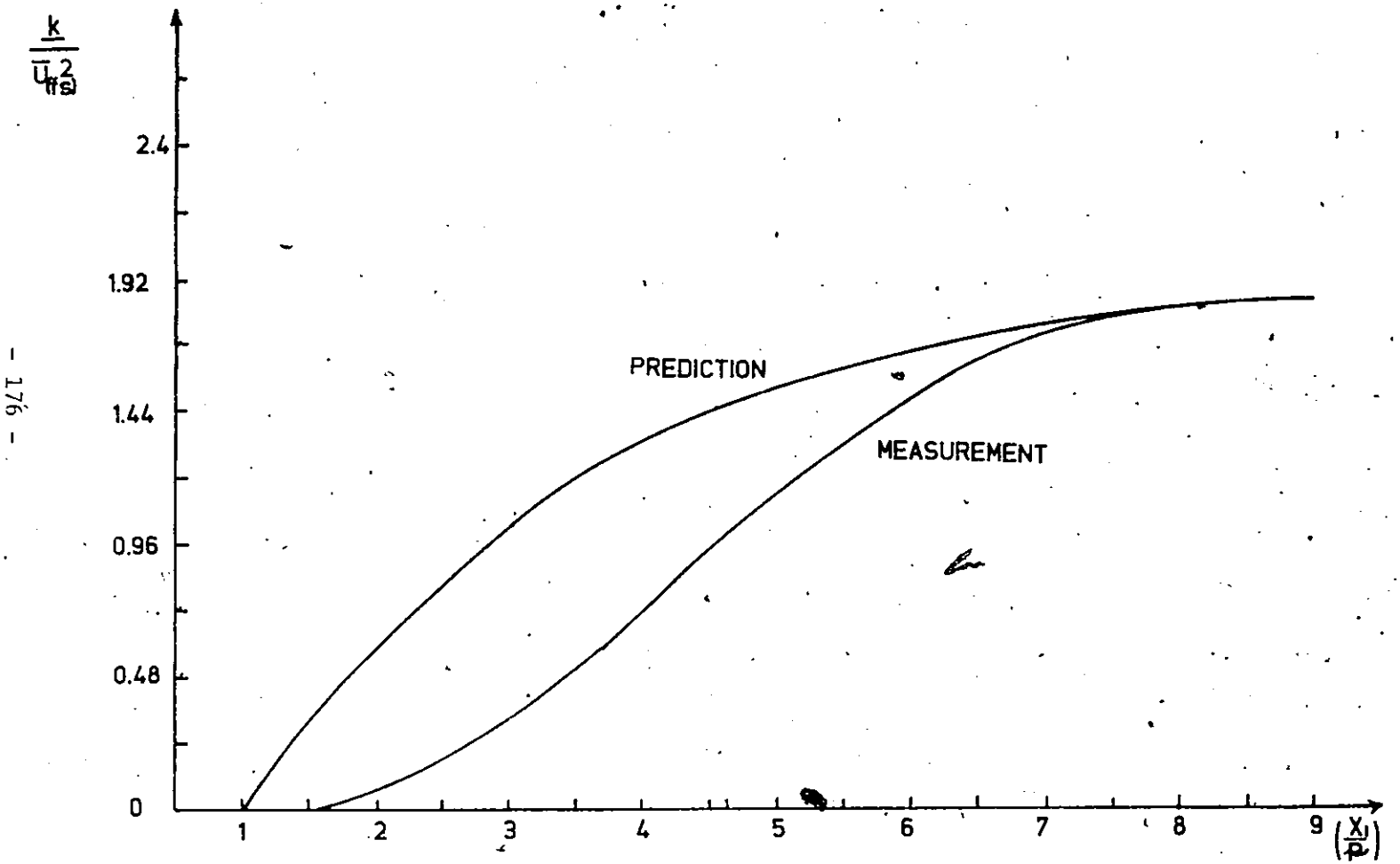

FIGURE 21: Streamwise Development of Volume Average Turbulent Kinetic Energy in a Tube Bundle with a Square Tube Array and High Convection Rate; Measurements from Fitzpatrick and Donaldson (1980)

The levels of $\underline{k}/\overline{U}_1^2$ as estimated from $k_{(gap)}$, are different for the two experiments although the Reynolds numbers are similar. In view of the differences in geometry and possible error in calculating $\underline{k}$ from $k_{(gap)}$, meaningful comparisons between the two sets of data and the model seem unlikely.

The solution of equation (6.35) approaches asymptotically the measured values as a result of the proper choice for $L_{(\infty)}$, since adequate data for $\underline{L}_{(\infty)}$ are unavailable. This equation requires that the length scale immediately adjusts to $\underline{L}_{(\infty)}$ on entering the bundle. The agreement is better near the asymptotic values and, especially in the case of the Fitzpatrick and Donaldson (1980) results, poor near the entry; this error may be partly due to the constant length scale assumption and the use of constant production of $\underline{k}$. The values of $\underline{L}_{(\infty)}$ calculated from $\underline{k}_{(\infty)}$ and equation (6.34), were 69 mm and 17 mm for the triangular and square tube arrays, respectively.

The parameter $\underline{\ell}$ is the volume average dissipation length scale. Experiments have shown that the local value of ℓ is about 0.94 times the integral length scale (Townsend, 1976). In bundles, the integral length scale cannot be greater than the largest dimension which is bound by solid tube surfaces. This maximum is about 19 mm and 12 mm for the triangular and square tube arrays, respectively. The values of $\underline{L}_{(\infty)}$ used in the calculations were larger than the above maxima, but not by an order of magnitude. When accurate measurements of $\underline{k}$ and become available, and the dependence of $\underline{L}_{(\infty)}$ on the tube geometry is determined, then equation (6.25) could provide a turbulence model for the fully developed flow in a tube bank. The general equation

(6.17) also possesses this ability, by allowing $\underline{c}_{(16)}$ and $\underline{c}_{(18)}$ to vary with x_1 to predict the development of $\underline{k}$ up to the asymptotic range. This would allow predictive capability for $\underline{k}$, $\underline{\epsilon}_{(k)}$ and hence $\mu_{(t)}$ and $\Gamma_{(t)}$ throughout the tube bundle.

6.7 Closure

The calculated pressure drop over the channel length agrees well with the measured pressure drop. This finding supports the use of the numerical methods and pressure drop correlations.

A turbulence model with the potential capability to predict turbulent kinetic energy levels in tube bundles has been presented. Its success, however, cannot be evaluated mainly because of the large uncertainty present in estimating the volume average mean turbulent kinetic energy and length scale. Additional data must be provided before further progress in establishing a valid turbulence model can be made.

CHAPTER VII

TWO-DIMENSIONAL RECIRCULATING FLOWS

7.1 Introduction

Chapters IV, V and VI have considered flows whose streamlines were rectilinear and in which upstream boundary conditions were sufficient for the solution of the governing equations. Flows of this type are classified as rectilinear parabolic. In this chapter, flows with curved streamlines, which require specification of boundary conditions over the entire boundary are considered. These flows are classified as recirculating elliptic.

This curvature has a very important effect on the statistical structure of the turbulence parameters. It has been experimentally observed by several investigators (for example, Castro and Bradshaw, 1976; Gilles, Johnston, Kays and Moffat, 1980; Guitton and Newman, 1977) that a concave flow generally suppresses the turbulence field while a convex one amplifies it.

The purpose of this chapter is to determine whether the effects of mean streamline curvature on turbulence can be predicted by turbulence models. Earlier studies of this problem include tests of the RSM (Gibson and Rodi, 1981) and three modified forms of the k-ϵ model (Rodi and Scheuerer, 1983), one of which was very similar to the PTASM, using data in a curved mixing layer (Castro and Bradshaw, 1976).

The present work is a test of k-ε model and the PTASM in the model heat exchanger of Figure 22. The resulting equations are fully elliptic, and retain all components of the mean fluid deformation tensor.

7.2 The Dependence of Streamline Curvature on Vorticity

The curvature parameter of a line in a plane is defined as (Protter and Morrey,1977).

$$\psi = \frac{d^2 x_2 / dx_1^2}{\left[1 + \left(\frac{dx_2}{dx_1}\right)^2\right]^{3/2}} \tag{7.1}$$

The inverse of this is the local radius of curvature. The curve is called convex when $\psi > 0$ and concave when $\psi < 0$.

The slope of a mean streamline is, by definition

$$\frac{dx_2}{dx_1} = \frac{\bar{U}_2}{\bar{U}_1} \tag{7.2}$$

so that the streamline curvature is expressed as

$$\psi_{(s1)} = \frac{\frac{\bar{U}_2}{\bar{U}_1}\left[-\frac{\partial}{\partial x_1}\bar{U}_1 - \frac{\bar{U}_2}{\bar{U}_1}\frac{\partial}{\partial x_2}\bar{U}_1 + \frac{\bar{U}_1}{\bar{U}_2}\frac{\partial}{\partial x_1}\bar{U}_2 + \frac{\partial}{\partial x_2}\bar{U}_2\right]}{\left[1 + \left(\frac{\bar{U}_2}{\bar{U}_1}\right)^2\right]^{3/2}} \tag{7.3}$$

in cartesian components.

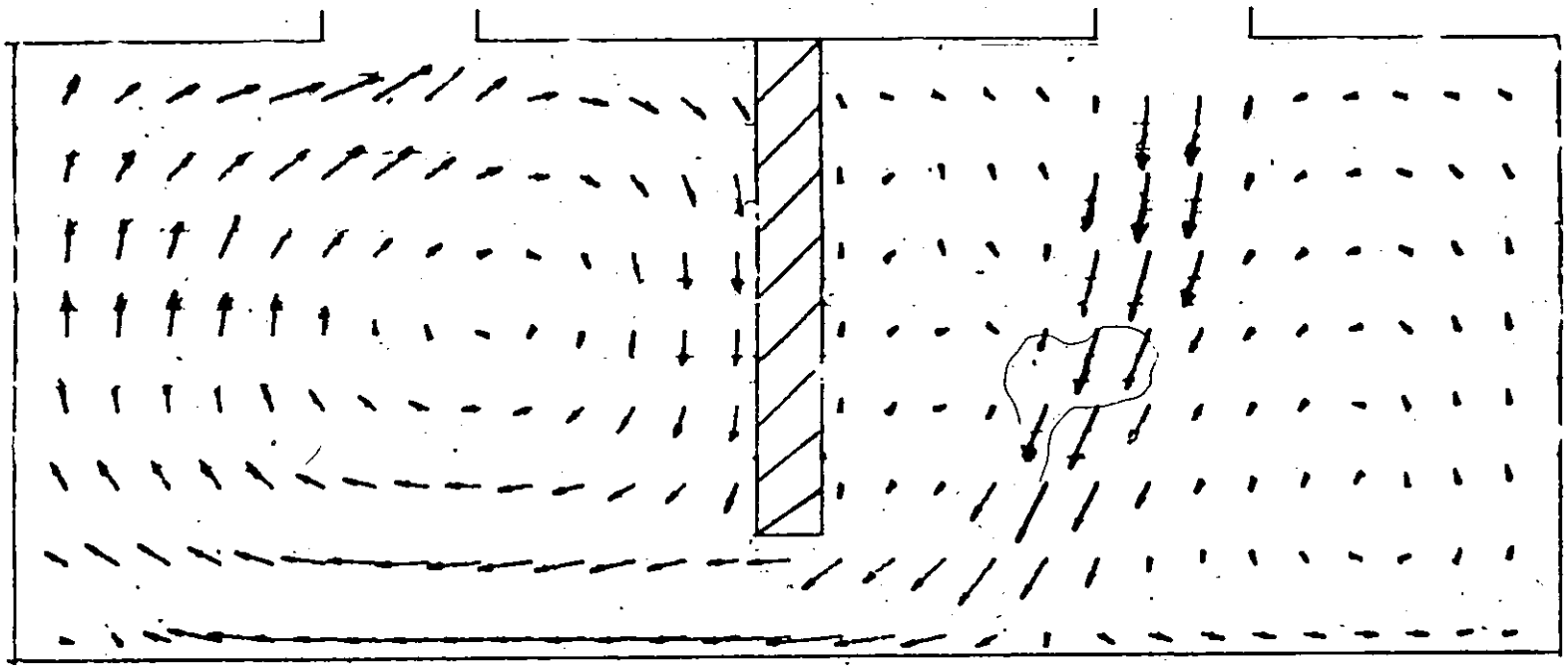

FIGURE 22: Mean Velocity Measurements in a Model Heat Exchanger, Elphick and Martin, 1982.

When $\psi_{(s)} \neq 0$ the fluid particles are, on the average, travelling along curved trajectories. However, momentum is conserved along straight lines and curved flows require additional inertial forces to maintain them. The Reynolds stresses are inertial forces resulting from the decomposition of the instantaneous acceleration of the fluid (see section 3.1) and hence will certainly be affected by streamline curvature.

The mean vorticity of the flow represents the average rate of rotation of an individual fluid particle. For a two-dimensional plane flow, the only non-zero vorticity component in curvilinear components tangent and normal to the mean streamlines (intrinsic coordinates; Serrin, 1959) is

$$\overline{\Omega}_{12} = \frac{1}{2}\left(\frac{2v}{2n} - \psi_{(s)}\, v\right) \tag{7.4}$$

where $v = (\bar{U}_i \bar{U}_i)^{\frac{1}{2}}$ and n is the coordinate normal to the streamline. The mean strain rate in intrinsic coordinates is

$$\overline{S}_{12} = \frac{1}{2}\left(\frac{2v}{2n} + \psi_{(s)}\, v\right) \tag{7.5}$$

Subtracting equation (7.4) from equation (7.5) gives a relation between vorticity, mean strain rate and curvatures as

$$\psi_{(s)} = \frac{\overline{S}_{12} - \overline{\Omega}_{12}}{v} \tag{7.6}$$

In plane shear flow, the vorticity and strain have equal magnitudes and opposite signs, and hence $\gamma_{(s)} = 0$. When $\bar{\Omega}_{12} \neq 0$ and $\bar{S}_{12} = 0$, this is rigid body rotation; and when $\bar{\Omega}_{12} = 0$ and $\bar{S}_{12} \neq 0$, the mean flow has a potential. In these latter two cases, streamline curvature is caused by the vorticity and strain respectively. Equation (7.5) shows that if Reynolds stresses depend on mean curvature, then they also depend on mean strain and mean vorticity.

In order to explore this issue, the EASM, PTASM and IEASM models have been expressed in terms of vorticity and strain instead of the mean velocity gradient

EASM

$$\overline{u_i u_j} = \frac{2}{3} k \delta_{ij} - \left(\frac{1-c_{(1)}}{c_{(2)}}\right) \frac{k}{\epsilon} \left[\left(\overline{u_i u_k} \delta_{mj} + \overline{u_j u_k} \delta_{mi} \right) \left(\bar{S}_{mk} + \bar{\Omega}_{mk} \right) - \frac{2}{3} \left(\overline{u_m u_k} \bar{S}_{mk} \right) \delta_{ij} \right] \tag{7.7}$$

PTASM

$$\overline{u_i u_j} = \frac{2}{3} k \delta_{ij} - (1-c_{(1)}) \frac{k}{\epsilon} \left[\frac{\left(\overline{u_i u_k} \delta_{mj} + \overline{u_j u_k} \delta_{mi} \right)\left(\bar{S}_{mk} + \bar{\Omega}_{mk} \right)}{- \left(\overline{u_m u_k} \bar{S}_{mk} \right) / \epsilon_{(x)} +} \right. \tag{7.8}$$

$$\left. \frac{- \frac{2}{3} \left(\overline{u_m u_k} \bar{S}_{mk} \right) \delta_{ij}}{c_{(2)} - 1} \right]$$

k-ε model

$$\overline{u_i u_j} = \frac{2}{3} k \delta_{ij} - 2 c_{(\mu)} \frac{k^2}{\epsilon} \bar{S}_{ij} \tag{7.9}$$

This demonstrates that the EASM and the PTASM provide expressions for $\overline{u_i u_j}$ in which both the strain and vorticity appear explicitly while the k- ϵ model provides only a strain dependent expression. The k- ϵ model has been found to work well in nearly parallel shear flows (Launder and Spalding, 1974) but poorly in plane flows with streamline curvature (Gibson and Rodi, 1981). Modification of the k-ϵ model that account for curvature dependence have been suggested by Launder, Priddin and Sharma (1977) and by Hanjalic, Launder and Sindir (1982). Both the plane shear layer and the curved shear layer are rotational and a model prediction of the first but not the second flow would expose the model's inability to accomodate curvature effects. Some caution is necessary when considering the plane shear layer, where mean vorticity and shear-strain are equal; the k-ϵ model dependence on vorticity and strain rate maybe confused. This problem does not arise in the curved shear layer, where shear and vorticity are unequal.

7.3 Previous Tests on a Curved Mixing Layer

The experimental investigation of a concave mixing layer by Castro and Bradshaw (1976) (Figure 23) is particularly useful because it is not subject to the complicating wall effect which is present in curved boundary flows. The measurements show clearly (Figure 24) that curvature suppresses the turbulent kinetic energy and the shear-stress along the center streamline, the latter more significantly.

Calculations for the mixing layer of Castro and Bradshaw have been performed by Gibson and Rodi (1981) using the RSM and by Rodi and Scheuerer (1983) using the k-ϵ model and a simplified version of the

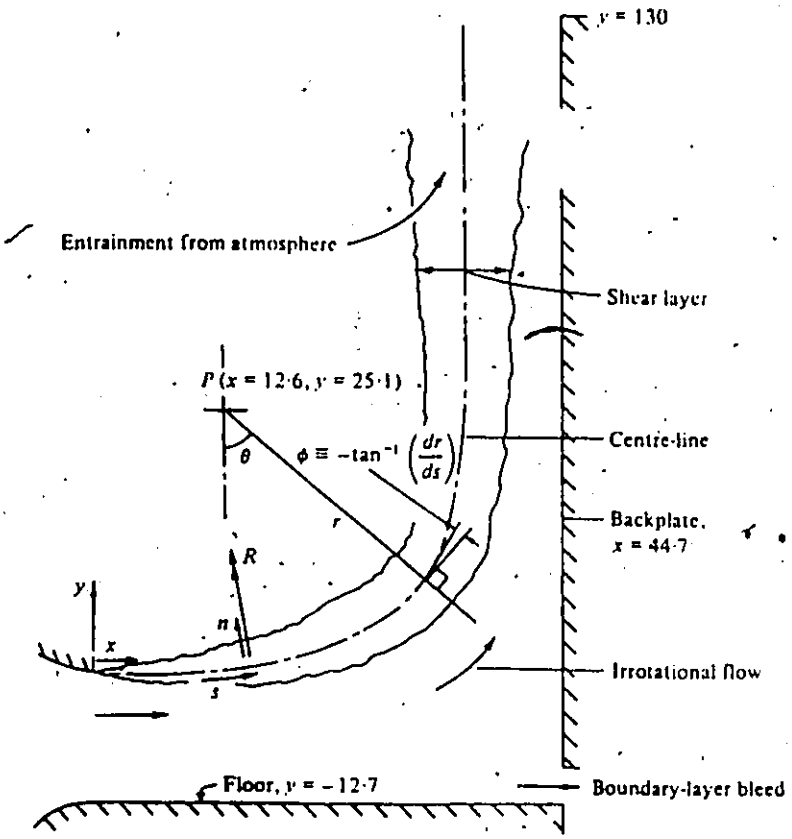

FIGURE 23: Curved Mixing Layer of Castro and Bradshaw (1976)

PTASM. All of these calculations were performed using parabolic equations which were expressed in terms of the coordinate directions normal and parallel to the measured streamlines.

As shown in Figure 24, all three models predict the turbulent kinetic energy reasonably well. Predictions of shear stress are fair with the RSM and PTASM, but relatively poor with the k-ϵ model. It is important to note that the two investigations used slightly different values of $c_{(16)}$ and $c_{(18)}$ (1.45 and 1.90 versus 1.44 and 1.92) which may be partially responsible for the discrepancy between solutions.

As mentioned earlier, the curved mixing layer is a flow where strain rate and vorticity are not equal. The fact that the RSM and PTASM correctly take this into account in calculating the normal components and shear stress is certainly an important factor in their success. The success of the PTASM is very surprising because this model is based on the assumption that $\overline{u_i u_j}/k$ is constant along the mean streamlines (Section 3.3), a condition which is certainly not satisfied in this flow. A possible explanation is that the strain rate is high enough for the level of $\overline{u_i u_j}/k$ to be independent of initial conditions everywhere in the flow (see discussion in Chapter IV).

A comparison of the three models predictions indicates that the PTASM should be preferable for application to recirculating flows. Its predictions are significantly superior to those of the k-ϵ model, and comparable with the RSM, however, is considerably more complicated.

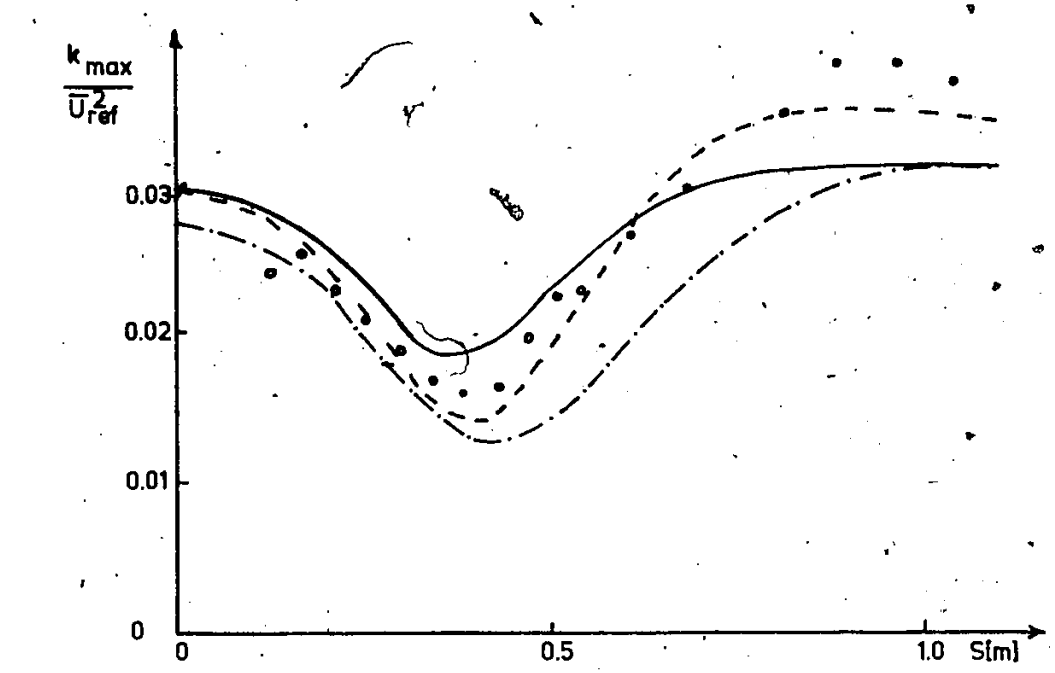

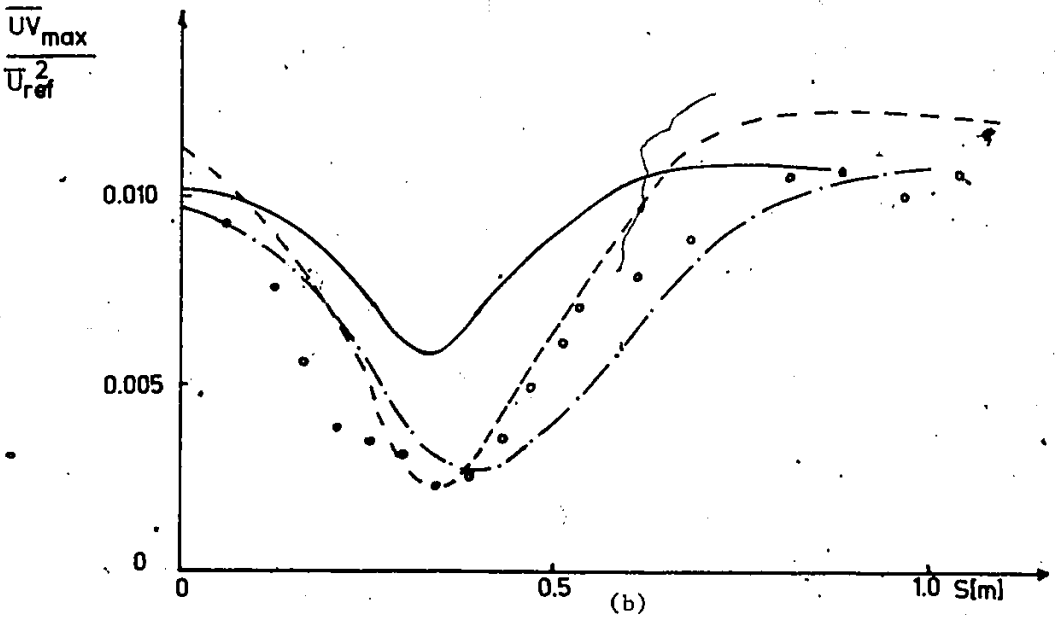

(b)

FIGURE 24: Streamwise Development of Turbulent Kinetic Energy and Shear Stress in a Curved Mixing Layer; o Data of Castro and Bradshaw (1976) —k-ε model, --- PTASM (Rodi and Scheuerer, 1983), —.— RSM (Gibson and Rodi, 1981).

7.4 Applications of the k-ε Model and PTASM to Fully Elliptic Flow

7.4.1 Previous Work

The RSM, from which the PTASM is derived, has been applied by Pope and Whitelaw (1976) to the recirculating flow behind bluff bodies. The mean streamlines have not published but such flows usually involve significant curvature. No problems caused by the turbulence model were reported in obtaining a solution.

No applications of the general PTASM model are known, but simplified PTASM and EASM have been applied by Gooray, Watkins and Aung (1983) and Leschziner and Rodi (1981) respectively to recirculating flows. In both studies the isotropic turbulent viscosity of the k-ε model has been replaced by the ratio of the turbulent shear-stress to the mean shear strain as predicted by the PTASM or EASM. The model for the shear stress was based on the thin shear flow approximation (Bradshaw, 1973) along the streamlines. Such models are useful when the shear stress alone is of interest since they cannot estimate the normal stresses and since most recirculating flows are predominantly influenced by the shear stress .

This approach provides a turbulent viscosity which depends on the vorticity and strain of the mean flow and hence provides a useful alternative to the more complicated RSM and PTASM models. The first study reported no difficulties in obtaining convergence, while the second one reported the prediction of negative turbulent viscosities. Although negative turbulent viscosities have been observed in asymmetric flows (Hanjalic and Launder, 1972) such cases cannot be predicted by either the PTASM or EASM. Leschziner and Rodi replace

negative viscosities by a small positive value.

7.4.2 Present Calculations

This section applies the PTASM and the IEASM (k-ϵ version) to a fully elliptic flow, which exhibits divergence, convergence and curvature of the mean streamlines, conditions which are met in heat exchangers.

The flow geometry, shown in Figure 25, represents a simplified two-dimensional heat exchanger. The cross-section corresponding roughly to that in the experimental set-up of Elphick and Martin (1982). Unfortunately, the experiment had a low aspect ratio, 0.3:1, and lacked sufficient two dimensionality for comprison with turbulence estimates. The mean velocity measurements are shown in Figure 22.

The normal and tangential velocity and k and at the solid walls were treated in the same manner as the top and bottom channel walls in Chapter V. Within the baffle the mean velocity was set to zero by setting $Sp = 10^{30}$ in both momentum equations (see Chapter V).

The mean streamwise velocity at the inlet was set equal to the experimental value 0.854 ms^{-1} while the mean tangential velocity at the inlet was specified to be zero. The inlet conditions of k and were 1.32×10^{-2} m^2s^{-2} and 7.66×10^{-3} m^2s^{-3}. The outlet velocity was also set to 0.854 ms^{-1} since the inlet and outlet have the same area. The transverse outlet mean velocity was to zero. Due to the parabolic nature of the k and $\epsilon_{(N)}$ equations, these quantities do not have to be specified at the outlet. The north coefficients $a_{(N)}$ were set to

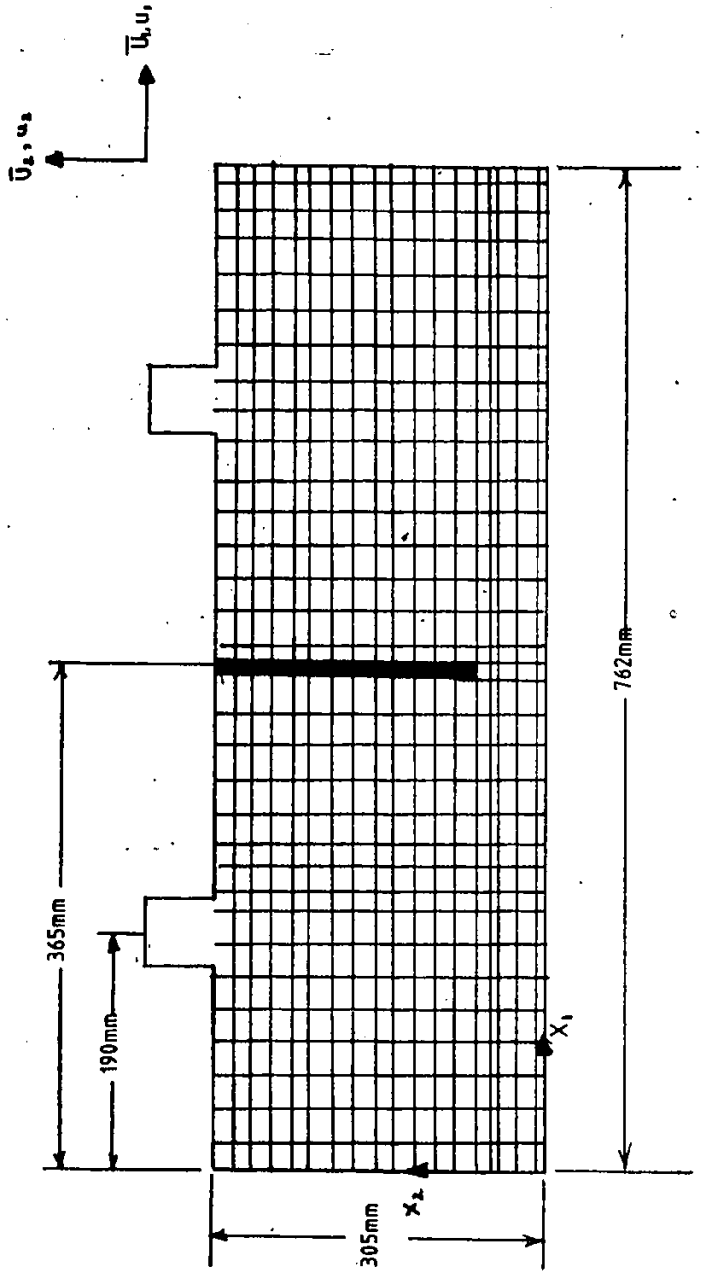

FIGURE 25: Computational Grid for the Model Heat Exchanger

zero as in the turbulent channel flow in Section 5.5.

Using the k-ε model, the solutions converged within 0.1% of the current solutions after 150 iterations, each of which required 0.96 s. The mean velocity field is illustrated by a vector plot and the turbulent kinetic energy by isolines in Figures 26 and 27.

Using the PTASM, the solution did not converge. A close investigation showed that, during the iteration procedure, negative values of turbulent kinetic energy were calculated at some points and the solution wandered indefinitely. This issue will be discussed further in the next section.

7.5 On the Relizability of Turbulence Models

Negative kinetic energy is physically meaningless, and for a model to be useful it must not allow such solutions. In practice, solutions must be achieved by iterative procedures and hence it is necessary for unrealistic values to be excluded even at intermediate steps for arbitrary realistic initial levels of turbulent kinetic energy, turbulent kinetic energy dissipation rate and mean velocity.

Schumann (1977) has formulated the following conditions for the realizability of a turbulence model

$$\overline{u_i u_j} \geq 0 \qquad \text{for} \quad i = j \tag{7.10}$$

$$\left| \overline{u_i u_j} \right| \leq \left(\overline{u_i^2}\, \overline{u_j^2} \right)^{1/2} \qquad \text{for } i \neq j \tag{7.11}$$

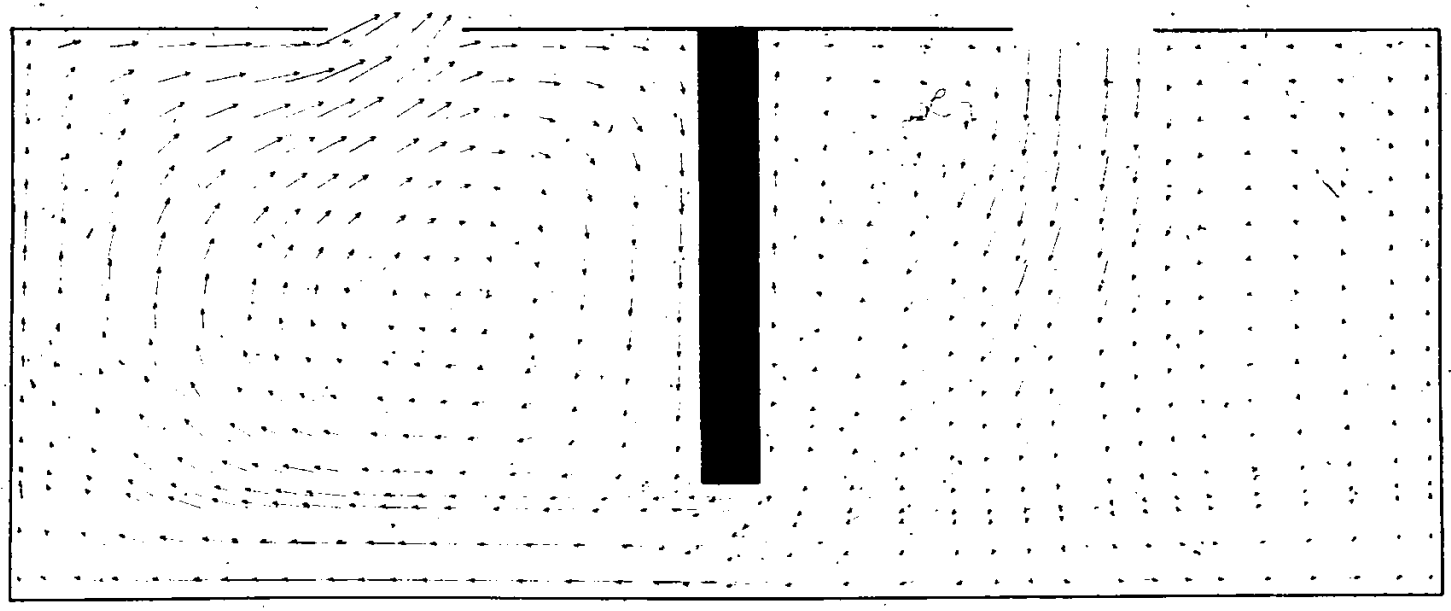

FIGURE 26: k-ε Model Predictions of Mean Velocity for the Model Heat Exchanger

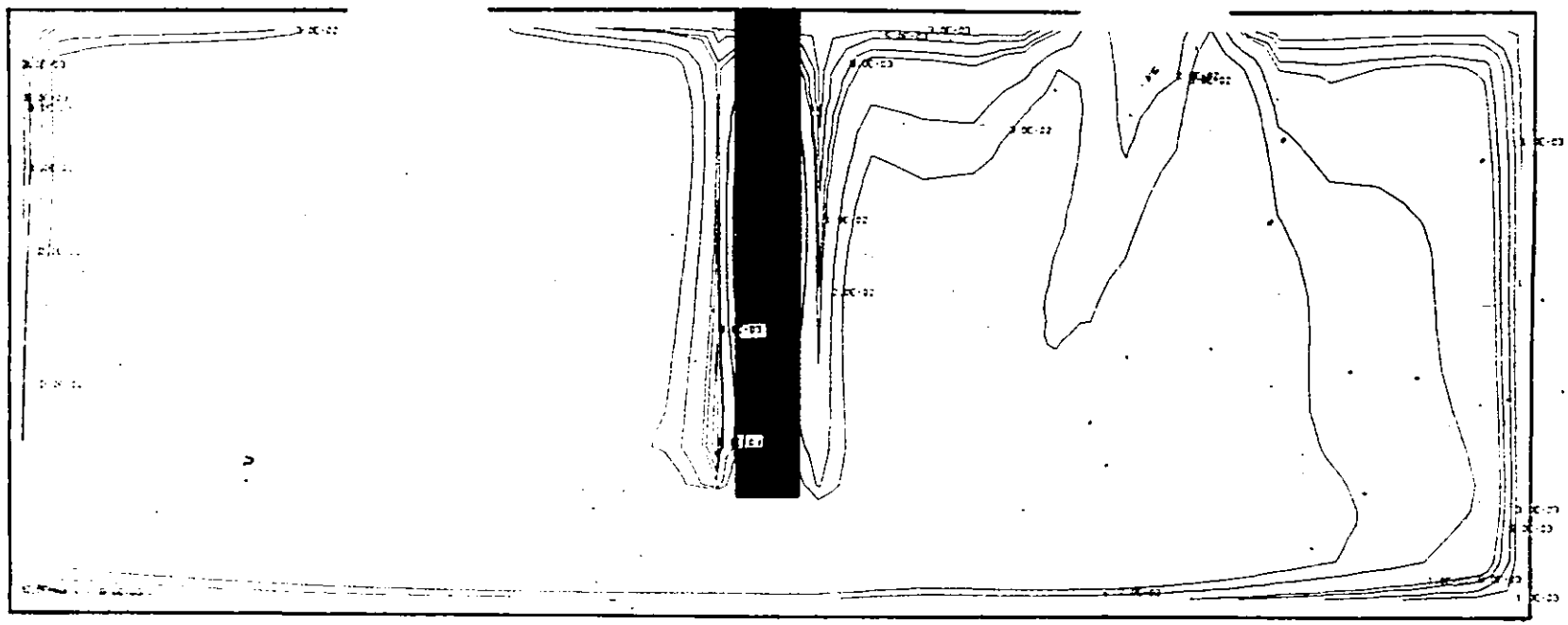

FIGURE 27: k-ε Model Prediction of Turbulent Kinetic Energy for the Model Heat Exchanger

$$\left| \overline{u_i u_j} \right| \geq 0 \qquad (7.12)$$

In addition, all derivatives of $\overline{u_i^2}$ must be zero when $\overline{u_i^2}$ is zero, to avoid negative values of $\overline{u_i^2}$ at subsequent times or positions. Schumann (1977) demonstrates that the exact transport equation for $\overline{u_i u_j}$ satisfies these conditions.

Applying the conditions (7.10), (7.11) and (7.12) to the RSM, Schumann (1977) concludes that this model is not realizable. For example, when $\overline{u_1^2} = 0$ and $d\overline{u_i^2}/dt = 0$, one gets

$$P_{11} - c_{(1)}\left(P_{11} - \tfrac{2}{3} P_{(k)}\right) - c_{(2)} \frac{\epsilon_{(k)}}{k}\left(\overline{u_i^2} - \tfrac{2}{3} k\right) + D_{11} - \tfrac{2}{3} \epsilon_{(k)} \neq 0 \qquad (7.13)$$

This may be seen by expanding the expression in terms of the mean velocity and $\overline{u_i u_j}$ in 2 dimensions, for simplicity, as

$$\begin{aligned} &-2\left(1-c_{(1)}\right)\left(\overline{u_1^2}\frac{\partial}{\partial x_1}\bar{U}_1 + \overline{u_1 u_2}\frac{\partial}{\partial x_2}\bar{U}_1\right) - \tfrac{2}{3} c_{(1)}\left(\overline{u_1^2}\frac{\partial}{\partial x_1}\bar{U}_1\right. \\ &+ \overline{u_1 u_2}\frac{\partial}{\partial x_2}\bar{U}_1 + \overline{u_1 u_2}\frac{\partial}{\partial x_1}\bar{U}_2 + \left.\overline{u_2^2}\frac{\partial}{\partial x_2}\bar{U}_2\right) - c_{(2)}\frac{\epsilon_{(k)}}{k}\left(\overline{u_i^2} - \tfrac{2}{3}k\right) \\ &+ c_{(1)}\frac{\partial}{\partial x_1}\left(\frac{k}{\epsilon_{(k)}}\overline{u_1^2}\frac{\partial}{\partial x_1}\overline{u_i^2} + \frac{k}{\epsilon_{(k)}}\frac{\partial}{\partial x_2}\overline{u_1^2}\right) \\ &+ c_{(1)}\frac{\partial}{\partial x_2}\left(\frac{k}{\epsilon_{(k)}}\overline{u_1 u_2}\frac{\partial}{\partial x_1}\overline{u_i^2} + \frac{k}{\epsilon_{(k)}}\overline{u_1 u_2}\frac{\partial}{\partial x_2}\overline{u_i^2}\right) \\ &- \tfrac{2}{3}\epsilon_{(k)} \neq 0 \end{aligned} \qquad (7.14)$$

When $\overline{u_1^2} = 0$, it follows from condition (7.10) that $\overline{u_1 u_2} = 0$; in addition there is the requirement that all derivatives of $\overline{u_1^2}$ must be

zero. These constraints reduce equation (7.14) to

$$-\frac{2}{3} c_{(1)} \overline{u_2^2} \frac{\partial}{\partial x_2} \bar{U}_2 + D_{11} \neq 0 \qquad (7.15)$$

which is not necessarily zero for arbitrary values of $\overline{u_i u_j}$ and $\partial \bar{U}_2 / \partial x_2$. This finding is relevant because the PTASM was derived from the RSM using the realizable constraint

$$\frac{d}{dt} \overline{u_i u_j} = \frac{\overline{u_i u_j}}{k} \frac{d}{dt} k \qquad (7.16)$$

Any non-realizability of the PTASM may be traced to the non-realizability of the RSM. To examine the conditions under which the PTASM may be non-realizable, the recirculating flow of Figure 22 will be separated into two regions.

(i) The converging and diverging flow regions, where

$$\left(\frac{\partial}{\partial x_1} \bar{U}_1\right)_{(\vec{q}_{(0)}, t_{(0)})} = b \qquad \left(\frac{\partial}{\partial x_2} \bar{U}_1\right)_{(\vec{q}_{(0)}, t_{(0)})} = 0$$

$$\left(\frac{\partial}{\partial x_1} \bar{U}_2\right)_{(\vec{q}_{(0)}, t_{(0)})} = 0 \qquad \left(\frac{\partial}{\partial x_2} \bar{U}_2\right)_{(\vec{q}_{(0)}, t_{(0)})} = -b \qquad (7.17)$$

(ii) The general shear flows, where

$$\left(\frac{\partial}{\partial x_1} \bar{U}_1\right)_{(\vec{q}_{(0)}, t_{(0)})} = 0 \qquad \left(\frac{\partial}{\partial x_2} \bar{U}_1\right)_{(\vec{q}_{(0)}, t_{(0)})} = m$$

$$\left(\frac{\partial}{\partial x_1} \bar{U}_2\right)_{(\vec{q}_{(0)}, t_{(0)})} = n \qquad \left(\frac{\partial}{\partial x_2} \bar{U}_2\right)_{(\vec{q}_{(0)}, t_{(0)})} = 0 \qquad (7.18)$$

As a further simplification, it will be assumed that the mean velocity gradients are correct throughout the flow and not just at the point $(\vec{q}_{(0)}, t_{(0)})$. The corresponding equations for the mean velocity are

(i) $\bar{U}_1 = b x_1 \quad , \bar{U}_2 = -b x_2$ (7.19)

(ii) $\bar{U}_1 = m x_2 \quad , \bar{U}_2 = n x_1$ (7.20)

The mean streamlines for these flows are

$$x_1 x_2 = \text{constant} \tag{7.21}$$

$$\frac{x_1^2}{\left(-\frac{m}{2}\right)} + \frac{x_2^2}{\left(\frac{n}{2}\right)} = \text{constant} \tag{7.22}$$

The solutions of these equations is illustrated in Figure 28.

The corresponding expressions for the PTASM are as follows

$$\frac{\overline{u_1^2}}{k} = \frac{2}{3}\left[\frac{-\left[3(1-c_{(1)})\overline{u_1^2} + c_1(\overline{u_1^2} - \overline{u_2^2})\right]b + (c_{(1)}-1)\epsilon_{(k)}}{-(\overline{u_1^2} - \overline{u_2^2})b + (c_{(1)}-1)\epsilon_{(k)}}\right] \tag{7.23}$$

$$\overline{u_1 u_2} = 0 \tag{7.24}$$

$$\frac{\overline{u_2^2}}{k} = \frac{2}{3}\left[\frac{-\left[-3(1-c_{(1)})\overline{u_2^2} + c_{(1)}(\overline{u_1^2} - \overline{u_2^2})\right]b + (c_{(1)}-1)\epsilon_{(k)}}{-(\overline{u_1^2} - \overline{u_2^2})b + (c_{(1)}-1)\epsilon_{(k)}}\right] \tag{7.25}$$

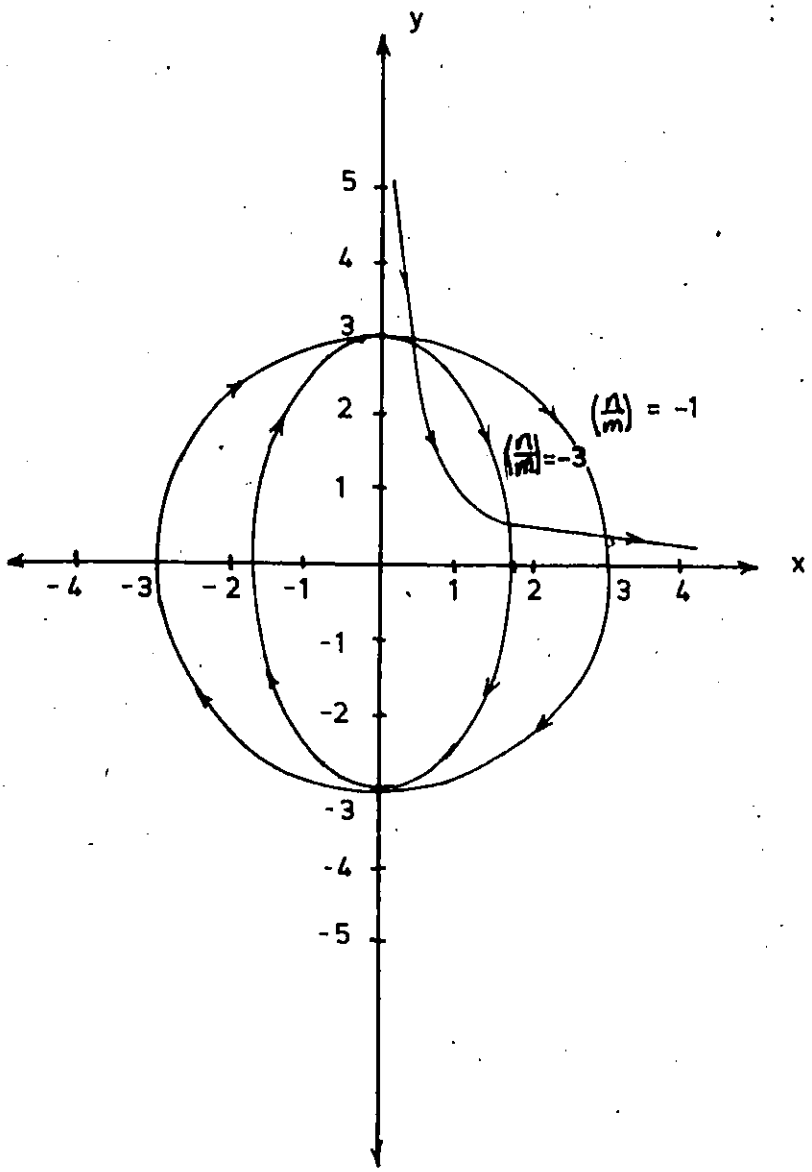

FIGURE 28: Mean Streamlines for Converging and Shear Flows

Equations (7.22) and (7.24) are both quadratic with bilinear and linear terms. When a is large and hence $(c_{(2)}-1)\epsilon_{(k)}$ is negligible, equations (7.22) and (7.25) become

$$\frac{\overline{u_1^2}}{k} = \left[\frac{2(1-c_{(1)})\,\overline{u_1^2} + \frac{2}{3}c_{(1)}(\overline{u_1^2}-\overline{u_2^2})}{\overline{u_1^2}-\overline{u_2^2}}\right] \qquad (7.26)$$

$$\frac{\overline{u_2^2}}{k} = \left[\frac{-2(1-c_{(1)})\,\overline{u_2^2} + \frac{2}{3}c_{(1)}(\overline{u_1^2}-\overline{u_2^2})}{\overline{u_1^2}-\overline{u_2^2}}\right] \qquad (7.27)$$

Inspection of these equations shows that $\overline{u_1^2}$ must equal $\overline{u_2^2}$ since exchanging $\overline{u_1^2}$ to $\overline{u_2^2}$ and vice-versa in one equation results in the other equation. Then equation (3.26) reduces to

$$2(1-c_{(1)})\,\overline{u_2^2} = 0 \qquad (7.28)$$

which is realizable. However, equations (7.26) and (7.27) cannot be solved by an iterative procedure because they are identical and this will cause the solution to wander indefinitely. The implication for equations (7.23) and (7.25) is that as "b" increases, they approach equations (7.26) and (7.27) and the solution becomes more difficult to find.

For the second flow, whose velocity is described by equations (7.18),

$$\frac{\overline{u_1^2}}{k} = \frac{2}{3}\left[\frac{-\left[(6-4c_{(1)})m + c_{(1)}n\right]\overline{u_1u_2} + (c_{(1)}-1)\epsilon_{(k)}}{-(m+n)\,\overline{u_1u_2} + (c_{(1)}-1)\epsilon_{(k)}}\right] \qquad (7.29)$$

$$(\overline{u_1u_2})^2 + \left[-(c_{(1)}-1)\epsilon_{(k)}/(m+n) - \tfrac{2}{5}c_1 k\right]\overline{u_1u_2} + \left[-(1-c_{(1)})\right.$$

$$\left. k(\overline{u_1^2}m + \overline{u_2^2}n) + \tfrac{2}{3}(c_{(2)}-1)k\epsilon_{(k)}\right]/(m+n) = 0 \qquad (7.30)$$

$$\frac{\overline{\mu_2^2}}{k} = \frac{2}{3}\left[\frac{-[(3-2c_{(1)})n + c_1 m]\overline{u_1u_2} + (c_{(2)}-1)\epsilon_{(k)}}{-(m+n)\overline{u_1u_2} + (c_{(2)}-1)\epsilon_{(k)}}\right] \qquad (7.31)$$

Equations (7.28) and (7.30) pocess negative values for $\overline{u_1^2}$ and $\overline{u_2^2}$ when $(m+n)(\overline{u_1u_2})$ is of roughly the same magnitude as $(c_{(2)}-1)\epsilon_{(k)}$ since the numerator and denominator may have opposite signs. When m and n are large and hence $(c_{(2)}-1)$ is negligible, equations (7.29) and (7.31) reduce to

$$\frac{\overline{u_1^2}}{k} = \frac{2}{3}\,\frac{(6-4c_{(1)})(m/n) + c_{(1)}}{m/n + 1} \qquad (7.32)$$

and

$$\frac{\overline{u_2^2}}{k} = \frac{2}{3}\,\frac{(3-2c_{(1)}) + c_{(1)}m/n}{m/n + 1} \qquad (7.33)$$

which are independent of $\overline{u_1u_2}$. With the commonly used value $c_{(1)} = 0.6$, equations (7.32) and (7.33) become

$$\frac{\overline{u_1^2}}{k} = 2.4\,\frac{m/n + 0.1667}{m/n + 1} \qquad (7.34)$$

and

$$\frac{\overline{u_2^2}}{k} = 1.2\,\frac{m/n + 3}{m/n + 1} \qquad (7.35)$$

If $-1 < (m/n) < -0.1667$, then $\overline{u_1^2}$ is negative. When $-3 < (m/n) < -1$, $\overline{u_2^2}$ is negative. Such conditions are inevitable during the solution of a recirculating flow.

It is interesting to note that, if $(m/n) \ll -1$ then equations (7.32) and (7.33) give realizable results. This condition is satisfied by plane shear flows such as the ones in Chapters IV and V. The above examples of recirculating flows demonstrate that the PTASM may not yield realizable results. In the general case, when all gradient components may be nonzero, the chance for non-realizable solutions is likely to increase.

7.6 Numerical Diffusion

In recirculating flows, the mean streamlines are inevitably misaligned with the computational grid lines. In such flows it is well known that the hybrid differencing scheme outlined in Chapter V leads to considerable error in the calculation of field variables (for example see Patankar,1980) because the convected quantity at a point is not based on the true upstream value but rather on an average of the neighbouring points which are upstream and along the computational grid lines. This error is proportional to the gradients of the field variable and it is often regarded as artificial or numerical diffusion. In the spirit of this analogy, a numerical viscosity for this type of error has been estimated by de Vahl Davis and Mallinsen (1976) as

$$\nu_{(n)} = \frac{|\bar{U}_i| \, \Delta x_1 \, \Delta x_2 \sin 2\alpha}{4(\Delta x_2 \sin^3\alpha + \Delta x_1 \cos^3\alpha)} \qquad (7.36)$$

where α is the angle between the mean streamline and either

computational grid line. It can be seen from equation (7.36) that, when $\alpha = 0$ as in a plane shear flow, $\nu_{(n)}$ is zero, while $\nu_{(n)}$ is maximum when $\alpha = 45°$.

The purpose of turbulence modelling in the recirculating regions is to predict the level of cross streamline transport of flow variables. Even if the turbulence parameters could be accurately calculated, their effect on the mean field would be overpowered by this numerical error. The calculation of the turbulent parameters is also affected by the numerical diffusion indirectly because the latter results in reduced values of the mean velocity gradients.

The ratio of $\nu_{(n)}/\nu_{(t)}$ ($\nu_{(t)}$ is the eddy viscosity) has been calculated using the k-ϵ computations shown in Figures 26 and 27. As shown in Figure 29, $\nu_{(n)}/\nu_{(t)}$ often exceeds 2.0. Equation (7.36) shows that if one wishes to reduce this ratio to , say, 0.1 one would have to reduce both Δx_1 and Δx_2 by a factor of 20, for the upwind scheme, which would increase the number of points in this region by a factor of 400; in such cases, the 2n -order accurate central difference scheme would have been more practica.. Hence, grid-independent solutions can only be obtained if diffusion is not a very important means of transport and a turbulence model is unnecessary. This difficulty has been realized by Leshiezer and Rodi (1981), Gooray, Watkins and Aung (1983), and Thompson and Wilks (1982), who have tested higher order differencing schemes in recirculating flows, which are free of numerical diffusion. Such schemes include the Quick scheme of Leonard (1977) and the Skew Upwind Scheme of Raithby (1976).

Leshiezer and Rodi (1981) have reported significant improvement in the solutions of recirculating flows with the use of the higher order

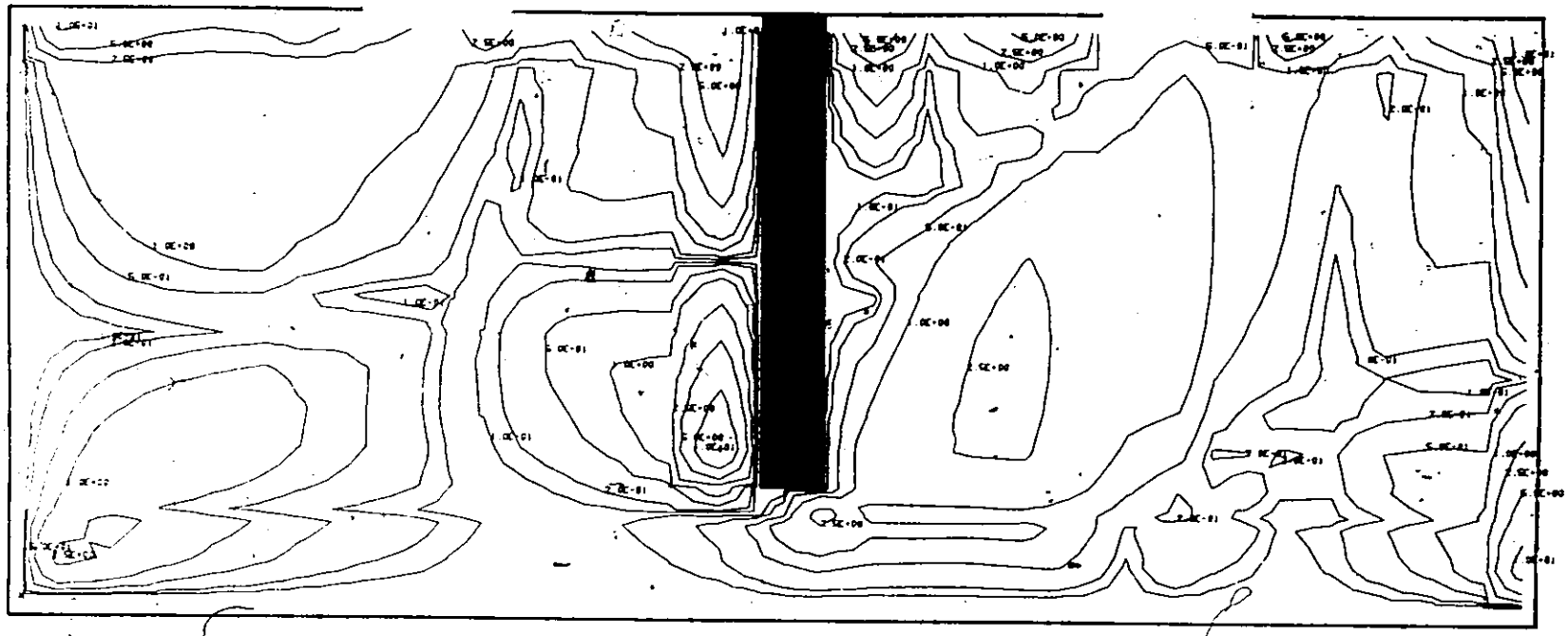

FIGURE 29: Ratio of Numerical to Turbulent Viscosity for the Model Heat Exchanger Flow

differencing schemes. Surprisingly they also reported that a curvature modification for the k-ϵ model reduced the accuracy of the calculations based on the upwind scheme while improving those based on the higher order schemes.

7.7 Discussion

The inability of the PTASM to provide solutions in general recirculating flows is disappointing because its application to the curved mixing layer of Castro and Bradshaw (1976) showed great potential. In contrast, it was found that in plane shear flow the non-realizability of the PTASM model did not present a problem and solutions were achieved.

From the point of view of a streamline coordinate system, many flows are shear flows. It is possible, however, that when expressed in intrinsic curvilinear coordinates, the PTASM is also realizable, as in a plane shear flow. For instance, consider Rodi's (1983) simplified equations for $\overline{u^2}$, $\overline{uv}$ and $\overline{v^2}$

$$\frac{\overline{u^2}}{k} = \frac{2}{3} + \frac{4}{3}\,\frac{(1-c_{(1)})\,P_{(k)}}{P_{(k)} + (c_{(2)}-1)\epsilon_{(k)}}\left[\frac{\frac{2}{2n}\bar{U} + 2\bar{U}/r}{\frac{2}{2n}\bar{U} - \bar{U}/r}\right] \qquad (7.37)$$

$$\frac{\overline{uv}}{k} = -\frac{1-c_{(1)}}{P_{(k)} + (c_{(2)}-1)\epsilon_{(k)}}\left[\frac{\overline{v^2}}{k}\,\frac{2}{2n}\bar{U} - \left(\frac{2\overline{u^2}}{k} - \frac{\overline{v^2}}{k}\right)\frac{\bar{U}}{r}\right] \qquad (7.38)$$

$$\frac{\overline{v^2}}{k} = \frac{2}{3} - \frac{2}{3}\frac{(1-c_{(1)})P_{(k)}}{P_{(k)}+(c_{(2)}-1)\epsilon_{(k)}}\left[\frac{\frac{\partial}{\partial n}\bar{U}+5\bar{U}/r}{\frac{\partial}{\partial n}\bar{U}-\bar{U}/r}\right] \quad (7.39)$$

where $P_{(k)} = -uv(\partial\bar{U}/\partial n - \bar{U}/r)$, $\bar{U}$ and u are the mean and fluctuating velocities tangent to the streamlines, v is the fluctuating velocity normal to the streamlines, r is the local radius of curvature, and n is the coordinate normal to the streamlines. Equation (7.37) is non-realizable for sufficiently large values of $(\bar{U}/r\ /\partial\bar{U}/\partial n)$, but the flow in which it was used lacked the proper conditions to expose this fault. Thus it seems surprising and encouraging that Gooray et al (1983), who also used equations (7.37), (7.38), (7.39) in their investigation of a backward facing step flow did not encounter this problem. Although this simplified PTASM neglects the effect of streamline divergence and gives improper predictions for the normal stresses, its predictions for the shear stress is better than the standard $k-\epsilon$ model, and therefore it deserves further tests in other recirculating flows. A possible solution to this problem appears to be the modification of the RSM and PTASM so that they are realizable. A related technique, suggested by Schumann (1977), is to isolate the terms responsible for the non-realizable behaviour and multiply them by a factor which is unity when the term is realizable and zero when it is not. This would in fact introduce a new model which would require new constants and verification; furthermore, such modifications would be entirely formalistic and cannot be justified by physical arguments.

7.8 Closure

If the turbulence structure of a recirculating flow is an important factor in the mean flow, then the use of a higher order differencing scheme which avoids numerical diffusion errors is necessary since the use of the hybrid scheme will easily mask the effects of improved turbulence models.

There is evidence (Rodi, 1981), that the simplifed EASM with enforced realizability is capable of better predictions of some recirculating flows than the k-ϵ model. The current method for enforcing this realizability is to replace the non-realizable values with arbitrary realizable ones. The simplified PTASM of Rodi and Scheuerer (1983) pocesses similar non-realizability, but its occurrence has not been reported. This alternative should be investigated further.

The full PTASM model shows potential for recirculating flows with convergence, divergence and shear, provided that it is modified to become realizable. This would require a re-modelling of several terms in the Reynolds stress transport equation.

CHAPTER VIII

SUMMARY AND CONCLUSIONS

In fully developed uniformly sheared turbulence, the ratio of Reynolds shear-stress to turbulent kinetic energy becomes constant and all the turbulence models studied can be made to work by adjusting the appropriate constants. However, in the developing regions of such flows, none of the tested models is adequate because they can not account for the initial conditions of the shear stress. In heat exchangers, regions which have approximately plane uniform shear are unlikely to be extensive and, unless the strain rate is exceedingly high, the initial conditions will be important. Hence, none of these models is likely to be applicable to this type of flow.

The channel flow has a considerable variation of strain rate, which emphasizes the differences between the stress-strain rate relationships of the k-ε model and PTASM. Comparison between predictions of these models indicates that the PTASM gives a more accurate relationship between shear-stress and strain rate.

The channel investigation offered an opportunity to evaluate the models' ability to account for the wall's effect on the turbulence. The

channel wall influences the normal components of Reynolds stress in the entire channel, although the shear stress is influenced substantially only within a distance from the wall equal to one sixth of the channel height. In practical computations of heat exchanger flows, the wall function method will very likely be sufficiently accurate for most the tube-free region and hence the use of a near-wall correction is probably not necessary.

Analysis of the tube-filled channel has demonstrated that the production of turbulent kinetic energy in a tube filled region must account for the local velocity gradients around the tubes. This additional production is well accounted for by the volume averaged velocity times the volume averaged pressure gradient. The turbulence level in this region will approach an asymptoptic level and hence a constant volume average dissipation length scale must be used for the predictions.

The analysis of recirculating flow has demonstrated that a curvature-dependent version of the PTASM is necessary for the accurate prediction of Reynolds shear-stress in flows with streamline curvature. It has also been shown that the model does not provide realistic solutions under more complicated conditions such as in a fully elliptic heat exchanger flow. Currently, the best developed turbulence model for application to the open regions is the k-ε model, although its predictions must be taken qualitatively and used in combination with the standard wall function technique for the near wall regions.

The turbulence model is not the only factor contributing to the inaccuracy of the analysis. In fact, careful testing of turbulence modelling should be done after the problems of numerical

diffusion, proper dimensionality of the calculation procedure, and pressure and heat transfer correlations for the tube bundle have been adequately addressed. The second problem generates particular concern. Typical heat exchangers have exceedingly complicated boundaries including several expansions and contractions. Because vorticity can be generated and reoriented by the fluid strain, it is very unlikely that the flow in such geometries could be treated as one - or two-dimensional. Nevertheless, two-dimensional calculations might be attractive, since they are much more economic than three-dimensional one. In three-dimensional flows, a considerable amount of turbulence production will be taking place in planes other than the one in which calculations are being performed. Even a perfect model of turbulence cannot provide accurate answers without accurate specification of the turbulence production.

For quantitative predictions of the mean velocity and temperature, accurate description of turbulence is important, even for simple, "classical" flows such as free and wall jets, wakes and expansions. The flow in a heat exchanger is a combination of such simpler flows and hence the accuracy of the total calculation must be dependent on the turbulence characteristics. However, when "sensitive" regions do not exist, turbulence effects may be unimportant.

CHAPTER IX

RECOMMENDATIONS FOR FURTHER WORK

An experimental evaluation of the volume average turbulent kinetic energy and integral length scale for different tube arrays is necessary to complete the k-ε turbulence model for porous media. Measurements of cross stream diffusion are also necessary to evaluate the coefficients of diffusion for this model.

To allow proper validation of a turbulence model for recirculating flow, measurements of turbulent kinetic energy and turbulent shear stress must be obtained in geometries which have a sufficient aspect ratio to be considered as two-dimensional. Currently the best candidate turbulence model for a recirculating flow is the simplified PTASM of Gooray, Watkins and Aung (1983) and its performance should be investigated further.

There is evidence to indicate that the mean velocity profiles of many confined flows of engineering importance are not strongly dependent on the turbulent shear-stress (Boyle and Colay, 1983). In forced convection heat exchangers, heat transfer is usually calculated on the basis of the mean velocity distribution so knowledge of the effect of turbulence on heat transport is necessary. The identification of which types of flows are insensitive to turbulent shear-stress should be made.

REFERENCES

Aris, R. (1962) "Vectors, tensors and the basic equations of fluid mechanics" Prentice-Hall Inc., Englewood Cliffs N.J.

Aupoix, B. and Cousteix, J. (1982) "Subgrid scale model for isotropic turbulence", La Recherche Aerospatiale, no. 1982-4, pp. 1-10.

Aupoix, B.; Consteix, J. and Liandrat, J. (1983) "Effects of rotation on isotropic turbulence", 4th Symposium on Turbulent Shear Flows, Karlsruhe, pp. 9.7-9.12.

Batchelor, G.K. and Townsend, A.A. (1948) "Decay of turbulence in the final period", Proc. Roy. Soc. of London, vol. A-194, no. 1039, pp. 527-543.

Batchelor, G.K. and Proudman, I. (1952) "The effect of rapid distortion of a fluid in turbulent motion", Quart. Journ. Mech and Applied Math, vol. 7, part 1, pp. 83-103.

Bergles, G.; Gosman, A.D. and Launder, B.E. (1978) "The turbulent jet in a cross-section at low injection rates: a three-dimensional numerical treatment", Numerical Heat Transfer, vol. 1, pp. 217-242.

Boussinesq, J. (1877) Mem. Pres. Div. Savants Acad. Sci. Paris, vol. 123, p. 46.

Boussinesq, J. (1903) "Theorie analytique de la chaleur", vol. 2, p. 154.

Boyle, D.R. and Golay, M.W. (1983) "Measurement of a recirculating, two-dimensional, turbulent flow and comparison to turbulence model predictions. 1: Steady state case", J. of fluids Eng., vol. 105, pp. 439-446.

Bradshaw, P. (1968) "The analogy between streamline curvature and bouyancy in turbulent shear flow", J. Fluid Mech., vol. 36, part 1, pp. 177-191.

Bradshaw, P. (1973) "Effect of streamwise curvature on turbulent flows", AGARDograph no. 169.

Butterworth, D. (1979) "The correlation of crossflow pressure drop data by means of the permeability concept", United Kingdom Atomic Energy Authority, Harwell, AERE-R9435.

Byrne, B.J.; Hatton, A.P. and Morriott, P.G. (1970) "Turbulent flow and heat transfer in the entrance region of a parallel wall passage", Inst. Mech. Eng. Proceedings, vol. 184, part 1, no. 39, pp. 1130-1143.

Castro, I.P. and Bradshaw, P. (1976) "The turbulence structure of a highly curved mixing layer", J. Fluid Mech., vol. 73, part 2, pp. 265-304

Champagne, F.H.; Harris, V.G. and Corrsin, S. (1969) "Experiments on nearly homogeneous turbulent shear flow", J. Fluid Mech., vol. 41, part 1, pp. 81-139.

Chieng, C.C. and Launder, B.E. (1980) "On the calculation of turbulent heat transport downstream from an abrupt expansion", ASME HTD, vol. 13, pp. 9-20.

Chou, P.Y. (1945) "On velocity correlations and the solutions of the equations of turbulent fluctuation", Quart. J. of Appl. Math., vol. 3, pp. 38-54.

Compte-Bellot, G. (1965) "Ecoulement turbulent entre deux parois parallèles", Publications Scientifiques du Ministère de L'au, No. 419.

Corrsin, S. (1951) "The decay of isotropic temperature fluctuations in an isotropic turbulence", J. Aeronautical Sci., vol. 18, no. 6, pp. 417-423.

Corrsin, S. (1974) "Limitations of gradient transport models in random walks and in turbulence", Adv. Geophys., vol. 18a, pp. 25-60.

Crow, S.C. (1968) "Viscoelastic properties of fine grained incompressible turbulence", J. Fluid Mech., vol. 33, part 1, pp. 1-20.

Currie, I.G. (1983) "Flow measurements around heat exchanger tubes and scaling strips", Laser Dopler Anemometry Laboratory, Univ. of Toronto.

Daly, B.J. and Harlow, H.H. (1970) "Transport equations in turbulence", Phys. of Fluids, vol. 13, no. 11, pp. 2634-2649.

Daugherty, R.L. (1977) "Fluid mechanics with engineering applications", McGraw-Hill, NY, 7th Ed.

de Vahl Davis, G. and Mallinson, G.D. (1976) "An evaluation of upwind and central difference approximations by a study of recirculating flow", Computer and Fluids, vol. 4, pp. 29-43.

Deardorff, J.W. (1970) "A numerical study of three-dimensional turbulent channel flow at large reynolds number", J. Fluid Mech., vol. 41, part 2, pp. 454-480.

Donaldson, C. DuP.; Sullivan, R.D. and Rosenbaum, H. (1972) "A theoretical study of the generation of atmospheric clear air turbulence", AIAA J., vol. 10, no. 2, pp. 162-170.

Douglas, J.F. (1969) "An introduction to dimensional analysis for engineers", Pitman, London.

Dryden, H.L. (1943) "A review of the statistical theory of turbulence", Quart. Appl. Math., vol. 1, no. 1, pp. 7-42.

Elphick, I.G. and Martin, W.W. (1982) "Flow distribution measurements in a model heat exchanger, PHASE #1", Laser Dopler Anemometry Laboratory, Univ. of Toronto.

Eskinazi, S. and Erian, F.F. (1969) "Energy reversal in turbulent flows", Phys. of Fluids, vol. 12, no. 10, pp. 1988-1998.

Euler, L. (1755) "Principes généraux du mouvement des fluides", Hist. Acad. Berlin.

Farmer, C.L. (1982) "A survey of turbulence models with particular reference to dense gas dispersion", United Kingdom, Atomic Energy Authority, Warrington.

Fitzpatrick, J.A. and Donaldson, I.S. (1980) "Row depth effects on turbulence spectra and acoustic vibrations in tube banks", J. of Sound and Vibration, vol. 73, part 2, pp. 225-237.

Gibson, M.M. (1978) "An algebraic stress and heat flux model for turbulent shear flow with streamline curvature", Int. J. Heat Mass Transfer, vol. 21, pp. 1609-1617.

Gibson, M.M. and Launder, B.E. (1976) "On the calculation of horizontal, turbulent free shear flows under gravitational influence", J. of Heat Transfer, Feb., pp. 81-87.

Gibson, M.M. and Launder, B.E. (1978) "Ground effects on pressure fluctuations in the atmospheric boundary layer", J. Fluid Mech., vol. 86, part 3, pp. 491-511.

Gibson, M.M. and Rodi, W. (1981) "A Reynolds-stress closure model of turbulence applied to the calculation of a highly curved mixing layer", J. Fluid Mech., vol. 103, pp. 161-182.

Gibson, M.M., Jones, W.P. and Yonnis B.A. (1981) "Calculation of turbulent boundary layers on curved surfaces", Phys. Fluids, vol. 24, no. 3, pp. 386-395.

Gillis, J.C.: Johnston, J.P.: Kays, M.M. and Moffat, R.J. (1980), Stanford Univ. Dept. of Mech. Eng. Thermosciences Division Report no. HMT-31.

Gooray, A.M., Watkins, C.B., and Aung, W. (1983) "Improvement to the k-ϵ model for calculations of turbulent recirculating flow", 4th Symposium on Turbulent Shear Flows, Karlsruhe, pp. 18.26-18.31.

Guitton, D.E. and Newman, B.G. (1977) "Self preserving turbulent wall jets over convex surfaces", J. Fluid Mech., vol. 81, pp. 155.

Hanjalic, K. and Launder, B.E. (1972) "Fully developed asymmetric flow in a plane channel", J. Fluid Mech., vol. 51, part 2, pp. 301-335.

Hanjalic, K. and Launder, B.E. (1972) "A Reynolds stress model of turbulence and its application to thin shear flows", J. Fluid Mech., vol. 52, pp. 609-638.

Hanjalic, K.; Launder, B.E. and Sindir, M. (1982), see Rodi and Scheuerer 1983.

Harlow, F.H. and Nakayama, P.I. (1968) "Transport of turbulence energy decay rate", Los Alamos Sci. Lab. of the Univ. of California, LA-3854, UC-34, Physics TID-4500, Appendix C.

Hinze, J.O. (1975) "Turbulence", 2nd Edition, McGraw-Hill, N.Y.

Irwin, H.P.A.H. (1975) "Measurements in blown boundary layers and their prediction by Reynolds stress modelling", Ph.D. thesis, Dept. of Mech. Eng., Univ. of McGill.

Irwin, H.P.A.H. and Smith, P.A. (1975) "Prediction of the effect of streamline curvature on turbulence", Phys. Fluids, vol. 18, no. 6, pp. 624-630.

Jones, W.P. and Launder, B.E. (1973) "The calculation of low Reynolds number phenomena with a two equation model of turbulence", Int. J. of Heat Mass Transfer, vol. 16, p. 1189.

Karnik, U. (1983) "Experiments on uniformly sheared turbulence", MASc Thesis, Univ. of Ottawa.

Karnik, U. and Tavoularis, S. (1983) "The asymptotic development of nearly homogeneous turbulent shear flow", Fourth Symposium on Turbulent Shear Flows, Karlsruhe, pp. 14.18-14.23.

Kim, J. (1983) "The effect of rotation on turbulence structure", 4th Symposium on Turbulent Shear Flows, Karlsruhe, pp. 6.14-6.19.

Kolmogorov, A.N. (1941) "The local structure of turbulence in incompressible viscous fluid for very large Reynolds number", Dokl. Acad. Nauk. SSSR, vol. 30, no. 4, pp. 299-303.

Kolmolgorov, A.N. (1941) "Decay of isotropic turbulence in an incompressible viscous liquid", Dokl. Acad. Nauk SSSR, vol. 31, no. 6, pp. 538-541.

Kolmogorov, A.N. (1942) "Equations of turbulent motion of an incompressible fluid", Izvestia Akad. Nauk SSSR, Seria fizicheska vol. 1, no. 1-2, pp. 56-58.

Ladyzhenskaya, O.A. (1963) "The mathematical theory of viscous incompressible flow", Gordon and Breach, New York.

Laufer, J. (1951) "Investigation of turbulent flow in a two-dimensional channel", National Advisory Committee for Aeronautics, Report 1053.

Laufer, J. (1983) "Deterministic and stochastic aspects of turbulence", J. of Applied Mech., vol. 50, p. 1079.

Launder, B.E. (1971) "An improved algebraic modelling of the Reynolds stresses", Imperical College of Science and Technology, TM/TN/A9.

Launder, B.E. (1974) "On the effects of a gravitational field on the turbulent transport of heat and momentum", J. Fluid Mech., vol. 67, part 3, pp. 569-581.

Launder, B.E. (1975) "On the effects of a gravitational field on the transport of heat and momentum", J. Fluid Mech., vol. 67, pp. 569-581.

Launder, B.E. and Spalding, D.B. (1972) "Mathematical models of turbulence", Academic Press, N.Y.

Launder, B.E. and Ying, W.M. (1973) "Prediction of flow and heat transfer in ducts of square cross-section", Proc. Inst. Mech. Eng., vol. 187, pp. 455-461.

Launder, B.E. and Spalding, D.B. (1974) "Numerical computation of turbulent flows", Computer Methods in Applied Mechanics and Engineering, pp. 269-289.

Launder, B.E.; Reece, G.J., and Rodi, W. (1976) "Progress in the development of a Reynolds stress turbulence closure", J. Fluid Mech., vol. 68, pp. 537-566.

Launder, B.E. and Samaraweera, D.S.A. (1979) "Application of a second-moment turbulence closure to heat and mass transport in thin shear flows - I. two-dimensional transport", Int. J. Heat Mass Transfer, vol. 22, pp. 1631-1643.

Leschziner, M.A. and Rodi, W. (1981) "Calculation of annular and twin parallel jets using various discretization schemes and turbulence model Variations", J. Fluids Eng. vol. 103, pp. 352-360.

Leslie, D.C. (1980) "Analysis of a strongly sheared, nearby homogeneous turbulent shear flow", J. Fluid Mech., vol. 98, part 2, pp. 435-448.

Lin, C.C. (1948) "Note on the law of decay of isotropic turbulence", Proc. Nat. Acad. Sci., USA, vol. 34, no. 4, pp. 230-233.

Lumley, J.L. (1970) "Towards a turbulent constituent relation", J. Fluid Mech. vol. 41, part 2, pp.413-434.

Lumley, J.L. (1978) "Computational modeling of turbulent flows", Advances in Applied Mechanics, vol. 18, Academic Press, N.Y., pp. 123-176.

Lumley, J.L. (1980) "Second order modeling of turbulent flows", Prediction Methods for Turbulent Flows, Ed. Kollman, Hemisphere Publ. Company, Washington, pp. 2-31.

Lumley, J.L. (1983) "Turbulence modeling", J. of Applied Mech. vol. 50, p. 1097.

Lumley, J.L. and Newman, G.R. (1977) "The return to isotropy of homogeneous turbulence", J. Fluid Mech., vol. 82, part 1, pp. 161-178.

Martin, W.W.; Elphick, I.G.; and Gollish, S. (1983) "Flow distribution measurements in a model of a heat exchanger", Engineering Applications of Laser Velocimetry, Ed. Coleman and Pfund, Book no. H00230.

Mellor, G.L. and Herring, H.J. (1973) "A survey of the mean turbulent field closure models", AIAA Journal, vol. 11, no. 5, pp. 590-599.

Moin, P.; Mansour, N.M.; Reynolds, W.C. and Ferziger, J.H. (1978) "Large eddy simulation of turbulent shear flows", Sixth Int. Conf. on Numerical Methods in Fluid Dynamics, Ed. H. Cabannes, M. Holt and V. Rusanov.

Moin, P. and Kim, J. (1982). "Numerical investigation of turbulent channel flow", J. Fluid Mech., vol. 118, pp. 341-377.

Mollo-Christensen, E. (1971) "Physics of turbulent flow", AIAA Journal, vol. 9, no. 7, pp. 1217-1228.

Monin, A.S. and Yaglom, A.M., (1981) "Statistical fluid mechanics: mechanics of turbulence", vol. 2, M.I.T. Press, Cambridge, Massachusetts.

Mulhearn, P.J. and Luxton, R.E. (1975) "The development of turbulence structure in a unform shear flow", J. Fluid Mech., vol. 68, p.577.

Naot, D.; Shavit, A. and Wolfshtein, M. (1970) "Interactions between components of the turbulent velocity correlation tensor due to pressure fluctuations", Israel J. of Tech., vol. 8, no. 3, pp. 259-269.

Naot, D.; Shavit, A. and Wolfshtein, M. (1973) "Two-point correlation model and the redistribution of reynolds stresses", Phys. Fluids, vol. 16, no. 6, pp. 738-743.

Naot, D.; Shavit, A. and Wolfstein, M. (1974) "Numerical calculation of Reynolds stresses in a square duct with secondary flow", Warme-und Stoffubertragrung 7, pp. 151-161.

Navier (1822) "Mem. de l'Academie", Vol. 6, p. 389.

Orzag, and Patterson (1972) "Numerical simulation of three-dimensional homogeneous isotropic turbulence", Phys. Rev. Lett., vol. 28, pp.76-79.

Owen, P.R. (1965) "Buffeting excitation of boiler tube vibration", J. Mech. Eng. Sci., vol. 7, no. 4, pp. 431-439.

Patankar, S.V. and Spalding, D.B. (1970) "Heat and mass transfer in boundary layers", 2nd Ed., Interest Books, London.

Patankar, S.V. and Spalding, D.B. (1974) "A calculation proceedure for the transient and steady-state behavior of shell-and-tube heat exchangers", Heat Exchangers: Afgan, N.H. and Schlunder, E.U., McGraw-Hill, N.Y.

Patankar, S.V. (1980) "Numerical heat transfer and fluid flow", Hemisphere Publishing Company, Washington, McGraw-Hill, New York.

Pope, S.B. and Whitelaw, J.H. (1976) "The calculation of near wake flows", J. Fluid Mech. vol. 73, part 1, pp.9-32.

Prandtl, L. (1925) "Report on investigation into developed turbulence", Zeitschrift fur angeWandte Math. and Mech., vol. 5, no. 2, pp. 316-139.

Prandtl, L. (1945) "Uber ein neues formelsystem fur die ausgebildete turbulenz", Nach. Akad. Wiss. Gottingen Math Phys., p.6.

Protter, M.H. and Morrey, C.B. (1977) "Calculus with analytic geometry: a first course", 3rd ed., Addison-Wesley, Reading Massachusetts.

Raithby, G.D. (1976) "Skew upstram differencing schemes for problems involving fluid flow", Comp. Meth. in Appl. Mech. and Eng., vol. 9, pp. 153-164.

Raithby, G.D. and Schneider, G.E. (1979) "Numerical solution of problems in incompressible fluid flow: Treatment of the velocity-pressure coupling", Numerical Heat Transfer, vol.2, pp. 417-440.

Reynolds, O. (1883) "An experimental investigation of the circumstances which determine whether the motion of water shall be direct or sinuous and the law of resistance in parallel channels", Phil. Trans. Roy. Soc. London, vol. 174, pp. 935-982.

Reynolds, O. (1894) "On the dynamical theory of incompressible viscous fluids and the determination of the criterion", Phil. Trans. Royal Society of London, vol. 186, pp. 123-161.

Richardson (1926) "Atmospheric diffusion on a distance neighbour graph", Proc. Roy. Soc., vol. A-110, no. 756, pp. 709-737.

Rodi, W. (1971) "On the equation governing the rate of turbulent energy dissipation", Imperial College London, TM/TN/A/14.

Rodi, W. (1976) "A new algebraic relation for calculating the Reynolds stress", ZAMM 56, T219-T221.

Rodi, W. (1980) "Turbulence models for environmental problems", Prediction Methods for Turbulent Flows, Ed. Kollman, Hemisphere Publ. Company, Washington, pp. 259-349.

Rodi, W. and Ljuboja, M. (1980) "Calculation of turbulent wall jets with an algebraic Reynolds stress model", J. of Fluids Eng., Trans. ASME, vol. 102, pp. 350-356.

Rodi, W. and Scheuerer, G. (1983) "Calculation of curved shear layers with two-equation models", Phys. Fluids, vol. 26, no. 6, pp. 1422-1436.

Rogallo, R.S. (1981) "Numerical experiments in homogeneous turbulence", NASA Tech. Mem. 81315.

Rogallo, R.S. and Moin, P. (1984) "Numerical simulation of turbulent flows", Ann. Review Fluid Mech., vol. 16, pp. 99-137.

Rose, W.G. (1966) "Results of an attempt to generate a homogeneous turbulent shear flow", J. Fluid Mech., vol. 25, p. 97.

Rose, W.G. (1970) "Interaction of grid turbulence with a uniform shear flow", J. Fluid Mech., vol. 44, p. 767.

Rotta, J. (1951) "Statistische theorie nichthomogener turbulenz", Zeitschrift fur Phys., vol. 129, pp. 547-572.

Schumann, U. and Herring, J.R. (1976) "Axisymmetric homogeneous turbulence: a comparison of direct spectral simulations with the direct interaction approximation", J. Fluid Mech., vol. 76, part 4, pp. 755-782.

Schumann, U. (1977) "Realizability of Reynolds stress turbulence models", Physics of Fluids, vol. 20, no. 5, pp. 721-725.

Schumann, U. and Patterson, S.G. (1978) "Numerical study of the return of axisymmetric turbulence to isotropy". J. Fluid Mech., vol. 88, part 4, pp. 711-735.

Serrin, J. (1959) "Mathematical principles of classical fluid mechanics". Encyclopedia of Physics, Vol. VIII/1, Fluid Mechanics I, Springer-Verlag, Berlin.

Sha, W.T. and Launder, B.E. (1979) "A general model for turbulent momentum and heat transport in liquid metals", Argonne National Laboratory, Report ANL-77-78, Argonne, Illinois.

Shir, C.C. (1973) "A preliminary numerical study of atmospheric turbulent flow in the idealized planetary boundary layer", Journal of the Atmospheric Sciences, vol. 30, pp. 1327-1339.

Slattery, J.C. (1981) "Momentum, energy, and mass transfer in continua, 2nd Ed., Krieger publishing Company, Huntington, New York.

Spalding, D.B. (1969) "The prediction of two-dimensional steady turbulent flows", Imperial College, Heat Transfer Section Report, EF/TN/A/16.

Spalding, D.B. (1982) "Turbulence models: A lecture course", Imperial College, London.

Spalding, D.B. (1982) "A two equation model of turbulence", VDI - Forschungsheft 549, "Stromunstechnische and Thermodynamische Probleme'.

Spalding, D.B. and Launder, B.E. (1974) "The numerical computation of turbulent flows", Comp. Meth. in Appl. Mech. and Eng., vol. 3, pp. 269-289.

Sparrow, E.M. et. al. (1961) "Heat transfer to longitudinal laminar flow between cylinders", J. Heat Transfer, vol. 83, pp. 415-432.

Speziale, C.G. (1979) "Invariance of turbulent closure models", Phys. Fluids, vol. 26, no. 6.

St. Venant, J.C.B. (1843) C. R. Acad. Sci., p. 77.

Stokes, G. (1845) Trans. Cambridge Phil. Soc. vol. 8, p. 287, Papers 1, pp. 75-129.

Tavoularis, S. (1984) "Asymptotic laws for transversely homogeneous shear flows", private communication.

Tavoularis, S. and Corrsin, S. (1980) "Experiments in nearly homogeneous turbulent shear flow with a uniform mean temperature gradient", J. Fluid Mech., vol. 104, p. 311.

Taylor, G.I. (1921) "Diffusion by continuous movements", Proc. London Math. Soc., vol. 2, no. 20, pp. 196-211.

Taylor, G.I. (1935) "Statistical theory of turbulence", Proc. Roy. Soc., vol. A-151, no. 874, pp. 421-464.

Taylor, G.I. (1970) "Some early ideas about turbulence", J. Fluid Mech., vol. 41, part 1, pp. 3-11.

Tennekes, H. and Lumley, J.L. (1972) "A first course in turbulence", MIT Press, Cambridge Massachusetts.

Thompson, C.P. and Wilks, N.S. (1982) "Experiments with higher order finite difference formulae", United Kingdom Atomic Energy Authority, Harwell, AERE-R-10493.

Townsend, A.A. (1954) "The uniform distortion of homogeneous turbulence", Quart. J. Mech. and Applied Math., vol. 7, part 1, pp. 104-127.

Townsend, A.A. (1970) "Entrainment and the structure of turbulent flow", J. Fluid Mech., vol. 41, part 1, pp. 13-46.

Townsend, A.A. (1976) "The structure of turbulent shear flow", Cambridge University Press, 2nd Edition, London.

Townsend, A.A. (1980) "The response of sheared turbulence to additional distortion", J. Fluid Mech., vol. 81, part 1, pp. 171-191.

Von Karman, T. and Howarth, L. (1938) "On the statistical theory of isotropic turbulence", Proc. Roy. Soc., vol. A-164, no. 917, pp. 192-215.

Von Karman, T. (1948) "Progress in the statistical theory of turbulence", Presented at the Heat Transfer and Fluid Mechanics Institute, Los Angeles, California.

Von Karman, T. and Lin, C.A. (1949) "On the concept of similarity in the theory of isotropic turbulence", Rev. Mod. Phys., vol. 21, no. 3, pp. 516-519.

Warnica, W.D. (1981) "Mathematical modelling and prediction of turbulent recirculating flow", Chalk River Nuclear Laboratorie Report no. 2198, Chalk River Ontario Canada.

Whitaker, S. (1976) "Elementary heat transfer analysis", Pergamon Press Inc., N.Y.

Wood, P.E. and Leal, L.G. (1983) "Similarity solutions of free shear flows with mean reynolds stress turbulence models", Numerical Heat Transfer, vol. 6, pp. 235-244.

Zukauskas, A. and Ulinskas, R. (1978) "Some aspects of heat transfer from banks of tubes in cross-flow for the low reynolds number range", 6th Int. Heat Transfer Conference, Toronto, paper HX-10, vol. 4.